SPECIATION AND MEASUREMENT OF ALUMINIUM IN ENVIRONMENTAL SYSTEMS

A thesis submitted in partial fulfilment of the requirements for the degree of

DOCTOR OF PHILOSOPHY IN CHEMISTRY

at the

University of Canterbury

by

Martin L. Adams

1999

ABSTRACT

Aluminium speciation is of importance, as certain Al species are toxic to algae, fish and plants. The work within this thesis is directed towards the development and application of analytical methods to determine aluminium speciation in environmental systems. Significant changes to soil properties in New Zealand have occurred as a result of land management practices. This work contributes to the knowledge of soil aluminium chemistry by developing and applying techniques which enable changes to the concentrations of toxic Al species in soil solution to be quantified.

An established technique for Al fractionation, using oxine-derivatised Fractogel, was applied to environmental situations in which Al is of importance. Detailed investigations of the aluminium speciation in soil solutions from a range of sites were performed. A pAl – pH curve was constructed from measurements of 'free Al' concentrations in soil solutions. The possible mechanisms controlling Al^{3+} concentrations in soil solution, including an Al - fulvic acid binding curve are discussed.

The impact of land use change from grassland to conifer forest on the Al concentrations in soils and soil solutions was examined, and the effects of afforestation on soil chemistry quantified. The Al speciation in a sequence of high country pastoral soils was also studied. Complementary experiments such as root elongation bio-toxicity studies and aluminium complexation-capacity determinations were performed to provide information on the impacts of soil acidification.

In a study of relevance to the water treatment industry, a series of Al complexation capacity titrations were carried out to compare the Al-binding interactions between a commercially-available synthetic flocculant (polyacrylamide) and those of a natural polymeric flocculant (sodium alginate).

Fundamental method development studies were performed. The application of oxine-derivatised Fractogel to the fractionation of Fe^{II} and Fe^{III} was examined. The ability of the resin to sequester Fe^{II} and/or Fe^{III} from organic complexes was investigated. The developed protocol allowed quantification of Fe^{II} by using a simple flow injection analysis (FIA) manifold. The addition of a line containing a reducing agent to the manifold allowed an on-line reduction of Fe^{III}, and hence total Fe (Fe^{II} + Fe^{III}) to be determined.

The development of a new Al^{3+} fractionation protocol is also described. The method involves a short reaction (*ca.* 1.1 s) between a sample and an iminodiacetate controlled-pore glass resin in an FIA manifold. The performance of the resin was tested to determine whether Al was sequestered from organic complexes, from samples of high ionic strength or from Al-hydroxy polymer solutions. Samples of humic waters and soil extracts were analysed, and the results compared with those obtained by established methods.

The equilibrium reactions between aluminium(III) and two known plant exudates, caffeic and chlorogenic acids, have been studied by potentiometric and spectrophotometric titrations in aqueous solution (I = 0.10 M KCl, 25.0°C), and the stability constants determined.

ACKNOWLEDGEMENTS

I sincerely thank my supervisor Professor Kip Powell for his ongoing help and support throughout the course of this work. I also gratefully thank my associate supervisor Dr Jan Gregor for all her enthusiasm, and interest during this project.

I thank a number of people for their helpful collaboration during this work. Dr Murray Davis and Dr Peter McIntosh provided guidance for soil sampling and shared their ideas concerning the experimental results. Thank you also to Dr Alison Downard, Dr David Hawke and Dr Nils Nilsson for their practical help and interesting discussions. The assistance of members from the technical staff of this department is gratefully acknowledged; especially Archna Tandon, John Davis, Alistair Duff, Sandy Ferguson, Wayne Mackay and Bruce Reid.

I thank the Chemistry Department, the Institute of Environmental Science and Research Ltd (ESR) and the New Zealand Foundation for Research, Science and Technology (contracts UOC315 and UOC609) for financial support during this work. I also acknowledge funding from the Evans Fund, the Royal Society of New Zealand (Canterbury Branch) and Fernz Chemicals, for their respective contributions towards conference expenses.

Finally, thanks to my family and friends who have all provided varying ratios of help, support, entertainment, distraction, and company over the years.

CONTENTS

CHAPTER ONE: INTRODUCTION

CHAPTER TWO: MATERIALS AND METHODS

CHAPTER FOUR: ALUMINIUM SPECIATION IN SOUTH ISLAND HIGH COUNTRY SOILS

Section A: Aluminium speciation in an altitude sequence of high country soils

Section B: Aluminium speciation in hieracium-infested high country soils

CHAPTER SIX: EFFECTS OF AGEING SOIL AND SOIL SOLUTION SAMPLES BEFORE ANALYSIS

CHAPTER SEVEN: INTERACTION OF ALUMINIUM WITH POLYELECTROLYTE FLOCCULANTS

CHAPTER NINE: IMINODIACETATE CHELATING RESIN: APPLICATION TO ALUMINIUM ANALYSIS

CHAPTER TEN: SOLUTION EQUILIBRIUM STUDIES

CHAPTER ELEVEN: CONCLUSION

APPENDICES

REFERENCES

CHAPTER 1

INTRODUCTION

1.1 ALUMINIUM SOLUTION CHEMISTRY

1.1.1 Aluminium hydrolysis

(*i*) *Monomeric aluminium species*

Aluminium exists in aqueous solution as an octahedrally-coordinated ion, surrounded by 6 water molecules: $Al(H_2O)_6^{3+}$. Due to the combination of the high positive charge of the trivalent ion and the small ionic radius of Al^{3+}, the surrounding water molecules form a strong primary hydration sphere around the central Al^{3+}. The rate of exchange of the coordinated inner-sphere water with bulk water is relatively slow (k_{H_2O} *ca.* 10^0 s^{-1}), two orders of magnitude lower than that for Fe^{3+} (Cotton and Wilkinson 1988). The $Al(H_2O)_6^{3+}$ ion undergoes hydrolysis in solutions above *ca.* pH 3.5, as protons are lost from the coordinated water molecules to the bulk solvent (Equation 1.1).

$$Al(H_2O)_6^{3+} + H_2O \rightleftharpoons Al(H_2O)_5(OH)^{2+} + H_3O^+ \qquad (1.1)$$

This reaction, and the subsequent hydrolysis reactions of monomeric aluminium are presented below (waters of hydration have been omitted for simplicity), with the relevant thermodynamic hydrolysis constants (Nordstrom and May 1996).

$$Al^{3+} + H_2O \rightleftharpoons Al(OH)^{2+} + H^+ \qquad \log^*K_1 = -5.00$$

$$Al^{3+} + 2H_2O \rightleftharpoons Al(OH)_2^+ + 2H^+ \qquad \log^*\beta_2 = -10.1$$

$$Al^{3+} + 3H_2O \rightleftharpoons Al(OH)_3 + 3H^+ \qquad \log^*\beta_3 = -16.8$$

$$Al^{3+} + 4H_2O \rightleftharpoons Al(OH)_4^- + 4H^+ \qquad \log^*\beta_4 = -22.99$$

where $\beta_x\,(K_x) = \dfrac{\{Al(OH)_x^{(3-x)+}\}\{H^+\}^x}{\{Al^{3+}\}}$, and $\{\}$ indicates ionic activity.

The hydrolysis constants indicate that for solutions having pH >5.0, hydroxy-aluminium species dominate. With increasing pH, the coordination around the central Al^{3+} ion changes from an octahedral to a tetrahedral environment. ^{27}Al NMR clearly indicates the change in coordination state that occurs upon increasing solution pH. In acidic solution, a single narrow resonance at 0 ppm is observed, corresponding to the octahedral $Al(H_2O)_6^{3+}$ ion (Figure 1.1).

As base is added to the solution, the line-width for the Al^{3+} peak is observed to increase and the integrated area decreases. The broadening of this peak has been shown to be caused by a fast proton exchange with the species $Al(OH)(H_2O)_5^{2+}$ (Öhman and Edlund 1996). In alkaline solution, at high amounts of added base (>3 added OH^- per Al^{3+}), a new resonance peak appears at *ca.* 80 ppm which remains invariant up to high pH. This peak has been uniformly assigned to the tetrahedrally-coordinated aluminate ion $Al(OH)_4^-$ (Öhman and Edlund 1996).

(*ii*) *Polymeric aluminium species*

A large number of soluble polymeric aluminium species (of general formula $[Al_x(OH)_y^{(3x-y)+}]$), have been proposed to exist in solutions of pH 5.0 to *ca.* 7.0. The majority of these aluminium species have had structures proposed on the basis of indirect evidence, using (often conflicting) data obtained from a wide variety of experimental techniques and conditions. Slow reaction kinetics, and interference from transient and permanent aluminium precipitation have also added to experimental difficulties (Baes and Mesmer 1976). This conflicting experimental evidence has resulted in much discussion in the literature and caused definitive differentiation of the polymeric species to be problematic.

In more recent years, the direct analytical technique of ^{27}Al NMR has provided much valuable information on the existence of polymeric species in solution. A large amount of evidence suggests that two species, $Al_2(\mu\text{-}OH)_2(H_2O)_8^{4+}$ and $AlO_4Al_{12}(OH)_{24}(H_2O)_{12}^{7+}$ (commonly referred to as the 'Al_{13}' polymer), are widely present in hydrolysed solutions prepared at varying Al^{3+} concentrations and from a variety of Al^{3+} salts (Bertsch and Parker 1996). A broad resonance at 4.0 ppm, slightly downfield from the mononuclear $Al(H_2O)_6^{3+}$ peak at 0 ppm, has been assigned to the $Al_2(OH)_2^{4+}$ species (Figure 1.1).

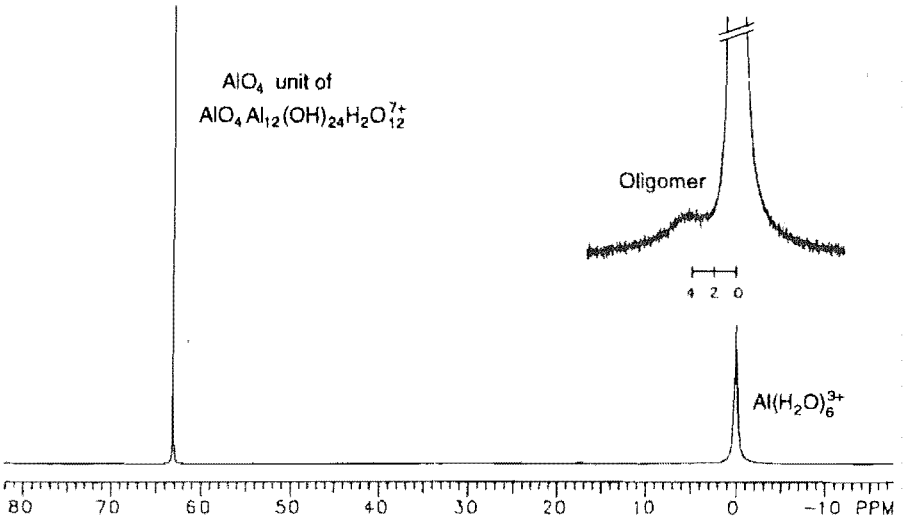

Figure 1.1. ^{27}NMR spectrum generated at 78.2 MHz and 25°C for a 0.05 M Al solution having a OH:Al molar ratio of 2.25. Resonances associated with $Al(H_2O)_6^{3+}$ (at 0 ppm), the oligomer (at ~4 ppm), and the AlO_4 unit of the Al_{13} species (at ~63 ppm) are clearly visible (from Bertsch and Parker 1996).

The Al_{13} species ($AlO_4Al_{12}(OH)_{24}(H_2O)_{12}^{7+}$) is proposed to consist of a tetrahedrally-coordinated central AlO_4, surrounded by 12 octahedrally-coordinated Al atoms, joined together by common edges and vertices (Figure 1.2). A sharp resonance is observed downfield (*ca.* 62.5 ppm) in the ^{27}Al NMR spectrum (Figure 1.1), which is attributed to the highly symmetrical environment of the central tetrahedrally-coordinated Al.

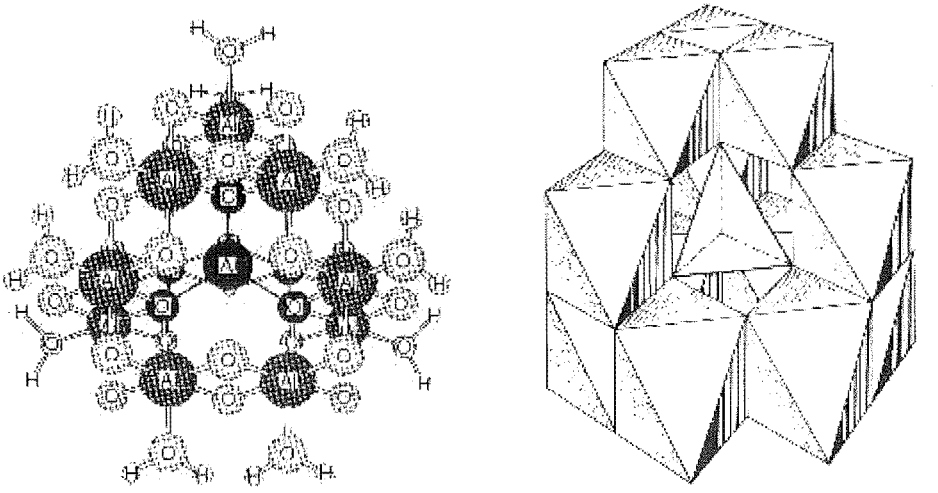

Figure 1.2. Ball and stick and polyhedral representations of the $AlO_4Al_{12}(OH)_{24}(H_2O)_{12}^{7+}$ tridecameric (Al_{13}) polynuclear species (from Bertsch and Parker (1996) and Baes and Mesmer (1976), respectively).

A very broad resonance at *ca.* 12 ppm downfield is also observed at high field strengths, and has been assigned to the remaining 12 octahedrally-coordinated Al. However indirect evidence, coupled with Al mass balance calculations, still suggests the existence of further polymeric species that are not observed by ^{27}Al NMR (Bertsch and Parker 1996). The Al_{13} polymer is metastable in solution, and divergent views exist in the literature as to the precise nature of the chemical aggregation and subsequent precipitation of solid-phase aluminium hydroxide (gibbsite [α-$Al(OH)_3$] or bayerite [γ-$Al(OH)_3$]) that occurs on ageing. The reader is referred to the article by Bertsch and Parker (1996) for a comprehensive discussion of the current understanding of aqueous polynuclear aluminium species. It is clear that the task of identifying polymeric Al species and their formation/decomposition pathways is far from being resolved.

1.1.2 Aluminium complexation

(i) Inorganic complexation

The Al^{3+} ion is a typical example of a Lewis acid and a 'hard' metal, and hence prefers to bind to 'hard' donors such as oxygen and fluoride. The major inorganic ligands which complex aluminium are F^-, H_2O, OH^-, PO_4^{3-} and SO_4^{2-} (Nordstrom and May 1996). It has been observed by ^{27}Al NMR that practically no change in chemical shift values is observed for acidic aluminium solutions containing perchlorate, chloride, bromide, iodide or nitrate ions, implying that the formation of contact ion-pairs with these anions is negligible (Öhman and Edlund 1996).

In natural systems both F^- and SO_4^{2-} may bind Al^{3+} to a significant extent (log K_1 = 7.0 and 3.5 respectively, (Nordstrom and May 1996)). Fluoride has a strong affinity for Al^{3+} under acidic conditions, and with an increasing F^- concentration, will replace coordinated H_2O or OH^- ligands in a stepwise fashion until all octahedral binding positions around the Al^{3+} ion are occupied (*i.e.* AlF_6^{3-}). However, fluoride concentrations in natural systems are typically low relative to the Al^{3+} concentration, and hence at pH values below 5.5, low ligand-number complexes predominate (*e.g.* AlF^{2+}, AlF_2^+) (Driscoll and Postek 1996). At higher pH, OH^- competes effectively with F^- for Al^{3+}, and hence $Al(OH)_4^-$ will predominate in alkaline conditions.

The sulfate anion also complexes aluminium under acidic conditions, but with Al forms considerably weaker complexes than F^-. At low SO_4^{2-} concentrations, $AlSO_4^+$ is the predominant complex formed, while at higher SO_4^{2-} concentrations the species $Al(SO_4)_2^-$ also

forms. Due to the low stability of aluminium sulfate complexes, they are typically only found in natural systems which are subject to acidic deposition and thus contain high concentrations of SO_4^{2-} and low pH (Driscoll and Postek 1996). There are few reliable stability constants published for soluble Al-phosphate complexes. These systems are difficult to characterise due to the low solubility of many Al-phosphate species (Nordstrom and May 1996). However, the very low PO_4^{3-} concentrations that typically exist in natural waters means the formation of Al-phosphate complexes can generally be regarded as negligible.

(ii) Organic complexation

Aluminium binds strongly to both low and high-molecular weight organic species, and specifically to oxygen-containing functional groups *e.g.* carboxylate, phenolic, enolic or alcoholic groups (Vance *et al.* 1996). Aluminium complexation to these functional groups generally increases significantly with increasing pH, as binding competition by protons decreases. Naturally occurring organic species which contain such functional groups therefore play an important role in the solubility and speciation of Al in both soils and natural waters (Driscoll *et al.* 1985; Lundström 1993).

However, the diverse nature of organic matter that occurs in natural samples often presents difficulties in quantifying the concentrations of individual organic species present. Low-molecular weight organic species are structurally well-defined and include compounds such as simple aliphatic carboxylic acids, hydroxamate siderophores, phenols, phenolic acids and sugar acids (Vance *et al.* 1996). These species are generally produced either as a result of microbial or plant excretion, or through the chemical decomposition of biological materials. Numerous examples exist in the literature of studies investigating the complexation of aluminium to these types of compounds (*e.g.* references within Nordstrom and May 1996). Such studies are highly relevant due to the prevalence of such organic compounds in natural systems.

High-molecular weight organic species, including fulvic and humic acids, are an extremely heterogenous and structurally ill-defined group of compounds. These species are operationally-defined on the basis of solubility: fulvic acids are soluble in both acid and base, whereas humic acids are soluble in base, but are precipitated by acid. Fulvic acids are typically of lower molecular mass than humic acids, but contain a relatively greater number of functional groups (by mass) (McLaren and Cameron 1996; Vance *et al.* 1996). Both fulvic and humic acids are ubiquitous in natural systems and, in terms of both functional groups and

binding strengths, contain a wide range of potential aluminium binding sites. Attempts to thermodynamically model the interactions between Al and organic matter are difficult due to the range of binding sites, and also the polyelectrolyte nature of the humic substances. Any model of an Al-organic system requires compensation for changes in humic substance configuration, inter- and intra-molecular electrostatic repulsions, and aggregation, with changing solution properties (*e.g.* pH and ionic strength) (Vance *et al.* 1996). Through their ability to strongly bind aluminium in solution, organic species play an important role in the environmental chemistry of aluminium.

1.2 ALUMINIUM IN THE ENVIRONMENT

1.2.1 Aluminium in soils

Aluminium is the most abundant metal in the earth's crust (Baes and Mesmer 1976). The predominant pool of aluminium at the surface of the earth is found in sediment, soil and rock, where the trivalent aluminium ion occurs as a component of a variety of crystalline aluminosilicates, oxyhydroxide and non-silicate containing minerals (Driscoll and Postek 1996; McLaren and Cameron 1996). In this form, aluminium is usually regarded as being unavailable (*i.e.* unreactive) for chemical and biological reactions.

However, crystalline minerals are subject to decomposition through chemical and physical weathering, the mechanisms of which may be enhanced by carbonic acid, various soluble organic acids and strong acids (acid rain) (Driscoll and Postek 1996). As a result of such weathering, a fraction of the previously immobile aluminium is released and subsequently becomes more available for various biogeochemical processes. A schematic representation of the chemical pathways that link pools of Al in the environment is given in Figure 1.3.

During the weathering process, a large amount of aluminium may be released into the soil from parent materials that contain aluminium. This aluminium can subsequently take part in a variety of reactions. Each reaction or process provides a 'sink' for the aluminium released during mineral dissolution, and hence may be regarded as potentially controlling the amount of Al in soil solution. In acidic soils, Al^{3+} (and H^{+}) will occupy a high proportion of the available cation exchange sites on the negatively charged soil and colloid surfaces (McLaren and Cameron 1996). This creates a large exchangeable 'reservoir' of Al that may be rapidly mobilised into soil solution. The associated loss of the basic cations (*i.e.* Ca^{2+}, Mg^{2+}, K^{+} and

Na^+) by leaching has a large deleterious effect on the buffering capacity and base saturation of the soil.

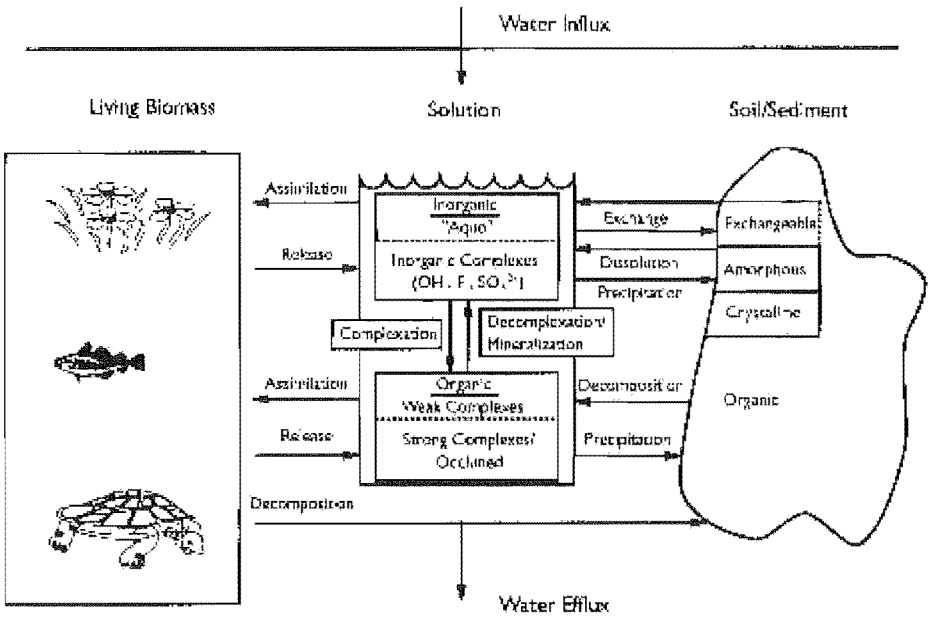

Figure 1.3. A schematic representation of the Al cycle. Within the environment Al can exist in pools of living biomass, solution or solid phase matter. Many transfers link the individual pools and regulate Al concentrations (from Driscoll and Postek 1996).

Aluminium may also combine with soluble silicic acid, $Si(OH)_4$, at near-neutral pH to form a range of precipitated short-range order aluminosilicate minerals (*e.g.* allophane, halloysite, kaolinite and imogolite) (Lindsay and Walthall 1996; McLaren and Cameron 1996). Browne and Driscoll (1992) proposed that as the precipitation kinetics of such minerals are slow, soluble Al-Si complexes may form as intermediates in the precipitation and dissolution reactions of solid-phase aluminosilicate minerals. Using a fluorescence probe technique, they found Al-Si complexes accounted for up to 95% of the total inorganic mononuclear Al in natural waters.

Other workers have also indicated the potential for soluble (hydroxy-)Al-Si complexes to form in solution (Chappell and Birchall 1988; Exley and Birchall 1992). However, many environmental models do not include aqueous aluminosilicate species, for the simple reason that reliable thermodynamic data are not available for such species (Browne and Driscoll 1992). Given the median concentration of dissolved Si in surface waters is *ca.* 250 μM (Stumm and Morgan 1996), Si-Al complexes may prove to be of significance in future environmental models.

Organic acids also play an important role in the weathering of aluminium-containing minerals. The formation of stable, soluble aluminium organic complexes facilitates the chemical weathering that occurs at mineral surfaces. Much surface-adsorbed Al is bound strongly at clay and mineral surfaces or by insoluble humic complexes and has slow exchange kinetics. The ability of organic complexes to maintain Al^{3+} in solution also contributes to transport of Al^{3+} into lower soil horizons in a profile, and from catchment areas into streams and lakes.

There is strong evidence that in acidic soils, an organic phase controls the concentration of aluminium in soil solution (Bloom 1979; Walker *et al.* 1990; Mulder and Stein 1994; Powell and Hawke 1995). The formation of podzols is frequently given as an example of the role that Al-organic complexes play in soil formation processes. Podzols are acid soils with low base saturation, typically formed under forested sites in cool humid climates (Wilson 1986). These soils typically have organic-rich upper soil layers (O and A horizons), underlain by a bleached eluvial (E) horizon, from which substantially more Al^{3+} and Fe^{3+} has been lost than silicon. Below the E horizon is a dark-coloured illuvial (B) horizon, in which Al, Fe and/or organic matter is accumulated (Hewitt 1992; Vance *et al.* 1996).

There has been debate as to the actual mechanism of podzolisation. The traditional theory of podzolisation suggests that Al^{3+} and Fe^{3+} are transported as soluble organic complexes down from the O, A and E horizons into the B horizon. The organic acids primarily originate from decomposing forest litter and foliage leachates (Lundstrom 1993). Precipitation of these complexes occurs in the B horizon as a result of metal saturation, organic polymerisation, and/or changes in ionic composition or pH (Vance *et al.* 1996). Aluminium-organic complexes may also precipitate as further complexation processes and/or microbial oxidation increases the Al to organic-carbon ratio of these species, hence reducing their solubility (Driscoll and Postek 1996). However, an alternative theory proposed by Farmer (1982), Anderson *et al.* (1982) and Farmer *et al.* (1983) suggests that soluble alumino-silicate sols (imogolite and allophane) are the primary mechanism of aluminium transportation through the soil profile. Soluble organic colloids are subsequently precipitated on the previously deposited imogolite and allophane in the B horizon (Vance *et al.* 1996).

In environments that contain negligible amounts of either organic ligands or $Si(OH)_4$, aluminium may also be precipitated as a mineral phase, either as an oxide (boehmite and diaspore - AlOOH) or hydroxide species (amorphous, bayerite, gibbsite or norstrandite - $Al(OH)_3$) (Lindsay and Walthall 1996). This process is likely to be favoured in soils where

the pH is *ca.* 6.0 to 6.5, the region of minimal Al solubility. Where soil sulfate concentrations are high, hydroxy-sulfate minerals may also form (alunite – $KAl_3(SO_4)_2(OH)_6$, basaluminite – $Al_4(OH)_{10}SO_4.5H_2O$ or jurbanite - $AlSO_4(OH).5H_2O$) (Lindsay and Walthall 1996).

1.2.2 Aluminium mobilisation and transport

As noted above, the largest pool of aluminium in the lithosphere is contained in sediment, soil and rock, and is commonly associated with aluminosilicate minerals. However, the rate of aluminium weathering (and subsequent availability for biogeochemical processes) from these materials is very slow. Therefore, although soils and sediments may ultimately control aqueous concentrations of aluminium, it is more probable that aluminium measured in aqueous systems is derived from more labile sources such as soil exchange sites, dissolution from $Al(OH)_3$ mineral phases or from decomposition/mineralisation of organic-Al species (Driscoll and Postek 1996). Nevertheless, the concentration of aluminium is relatively low in most natural waters, due to the low solubility of aluminium minerals at circumneutral pH values, and the typically low concentrations of organic complexing ligands. Stumm and Morgan (1996) report a median Al^{3+} concentration of 0.4 μM for terrestrial waters.

Al^{3+} is solubilised and transported into aqueous solution from solid-phase sources by several mechanisms. The role of organic acids in transporting Al^{3+} through soil profiles into B soil horizons has been discussed above, in relation to the podzolisation process. The compositions and concentrations of the various aluminium species that occur in soil solutions or waters are dependent upon both the hydrological pathways taken by water percolating through soils, and the chemical nature of the parent material(s) through which this water passes. As the solubility of aluminium increases markedly with decreasing soil pH, the natural or anthropogenic acidification of soil and waters has a large effect on Al^{3+} mobilisation. However, the natural buffering of soils or waters can concurrently reduce the magnitude of any pH changes caused by acidification processes. The nature of the mineral phase that is dissolving, soil cation exchange reactions and ligand complexation reactions are all important factors that contribute to natural buffering processes.

CO_2-induced acidity has also been proposed to have an important role in mobilising Al^{3+}, promoted by the elevated partial pressures of CO_2 that occur within soil, which causes the formation, and subsequent proton dissociation of H_2CO_3 (Reuss and Johnson 1985; Driscoll and Postek 1996). For example, the soil atmosphere of New Zealand pastoral soils commonly contains 70 to 140 times the atmospheric concentration of CO_2 (Parfitt *et al.* 1997). At

pH > 5.0, carbonic acid may be the dominant proton donor source for chemical weathering. HCO_3^-, as a mobile counterion, also regulates the transport of many metals (Driscoll and Postek 1996; Dahlgren *et al.* 1997). Several authors have discussed the potential changes in soil solution speciation that can occur as a result of pH changes caused by the degassing of extracted soil solutions (Suarez 1987; Zabowski and Sletten 1991; Dahlgren *et al.* 1997).

Anthropogenic sources of acidification came to public prominence during the mid- and late-1980s, when long-term inputs of 'acid rain' were identified as causing significant changes to soil and aquatic ecosystems, primarily in regions of Europe and eastern North America. The effect of atmospheric deposition of strong acids (*e.g.* H_2SO_4 and HNO_3) was particularly pronounced in catchment areas where shallow, acidic soils characterised by low base saturations were underlain by chemically resistant igneous or metamorphic bedrocks (*e.g.* granite, gneiss and quartzite) (Driscoll and Postek 1996).

Neutralisation of such strong acids may be accomplished within soil systems by the exchange of cations (Ca^{2+}, Mg^{2+}, Na^+, K^+ and NH_4^+). However, if these processes are limited, and the rate of strong acid inputs exceeds the consumption of protons by soil weathering, the H^+ may mobilise Al^{3+} from soil exchange sites or previously precipitated species and transport it from soil solution into surface waters. Interrelating factors such as climate, elevation, slope, temperature, vegetation and the nature of the soil organic matter have also been shown to affect the mobilisation rate of Al^{3+} and soil development processes in areas subject to acidic deposition.

At a site subject to strong acid inputs, Cronan and Schofield (1979) found high concentrations of aluminium in soil solutions from every soil horizon. This result was in contrast to the normal podzolisation process where concentrations of soluble Al are negligible in the B horizon and below. They proposed that the inputs of strong acids from atmospheric deposition facilitated the transport of Al through the soil horizon and therefore, potentially, from the soil solution into surface waters. Driscoll *et al.* (1985) noted the transport of significant quantities of dissolved inorganic Al from a forested Spodosol B_s horizon. The aluminium was not retained in lower B horizons, but rather was transported into catchment waters.

Wilson (1986) reviewed the relative effects of organic and mineral acids on the weathering of various minerals. Complexing organic acids (*e.g.* citric, oxalic and tartaric acids) were

observed to extract two to three times more aluminium than did mineral acids (HCl and H_2SO_4). The complexing acids also completely broke down the mineral structure, whereas the mineral acids induced the formation of secondary acid clay minerals such as hydroxy-aluminium interlayered vermiculites. However, the mineral acids were capable of depleting exchangeable cations much more rapidly than the complexing acids. Wilson (1986) concluded that if the rapid replacement of exchangeable soil cations was not compensated for by an increased rate of production of basic cations from weathering of minerals, the formation of unstable acid clays could occur. The subsequent decomposition of these clays would result in soils of greater acidity, that could release significant amounts of ionic aluminium.

Concentrations of aluminium in streams subject to acidic deposition have been shown to vary both spatially (Johnson 1979; Rosseland *et al.* 1992) and temporally (Campbell *et al.* 1992). Johnson (1979) observed that neutralisation of acidity from acid rain was substantially accomplished in the upper soil horizons, and H^+ and Al^{3+} concentrations successively decreased at sites downstream of the catchment area.

In Europe and North America, 'pulsed' increases in acidification and aluminium concentrations have been observed, and are generally associated with autumn rainfall and spring snowmelt events. One reason proposed for elevated Al^{3+} concentrations at times of high rainfall, is that the input of water at these times exceeds the capacity of the lower soil horizons to transmit the water flow. As a result, excess water 'washes' through upper soil horizons, resulting in stream water that is low in pH and concentrations of basic cations, high in concentrations of dissolved organic carbon and Al species, and is typically highly undersaturated with respect to mineral-phase solubilities (Campbell *et al.* 1992; Driscoll and Postek 1996). During snowmelt, large quantities of mineral acids that have accumulated in the snowpack are also released, and may also contribute to the further acidification of the soil solution (Driscoll *et al.* 1985).

1.3 ALUMINIUM TOXICITY

Soluble aluminium species are the most chemically and biologically available forms of aluminium, but comprise only a small fraction of the total Al present in the environment. There is no known biochemical pathway for which aluminium is essential as a trace element. In contrast, adverse impacts of aluminium have been documented for a wide range of organisms. There is still debate as to the aluminium species responsible for biological

toxicity. The complicated solution chemistry of Al, with several species co-existing, often means individual species cannot be investigated in isolation. Experimental collinearity among Al species can also cause problems. In addition, it is likely that the formation of the Al_{13} polymeric species in solution has often not been considered by authors, leading to the possible incorrect attribution of toxicity to other species (Kinraide 1991).

1.3.1 Plants

The physiological symptoms of aluminium toxicity in plants are pronounced. Toxicity commonly leads to a reduction in root elongation and branching, root tip dieback and root thickening and increased brittleness. With prolonged exposure to Al treatments, plants may exhibit further symptoms such as yellowing or browning of the roots, wilting, loss of apical dominance, reduced crop yields, and reduced Ca and Mg concentrations in roots and shoots (Russell 1988; Rosseland *et al.* 1990). Although the Al^{3+} ion has commonly been regarded as the primary toxic species, a number of studies have shown that the activities (as opposed to concentrations) of the 'free' monomeric Al species ($[Al^{3+}] + [Al(OH)^{2+}] + [Al(OH)_2^+] + [Al(OH)_3] + [Al(OH)_4^-]$) provide better indicators of stress on root or whole plant growth than the activity of Al^{3+} alone.

Experiments to determine the toxicity of aluminium are complicated by the fact that there are often large variations in toxicity among both plant species and cultivars, and that the Al tolerance for a particular species may be dependent on the growth parameter measured (Rosseland *et al.* 1990; Mookherji *et al.* 1991; Shann and Bertsch 1993). Wright and Wright (1987) correlated phytotoxicity toward subterranean clover (*Trifolium subterraneum* L.) with the sum of the activities of the free Al^{3+} ion and the positively charged monomeric species $AlOH^{2+}$, $Al(OH)_2^+$, and $AlSO_4^+$ in soil solution. Alva *et al.* (1986) established a similar correlation and also looked at the beneficial effects of increased levels of calcium on root elongation in solution culture experiments. They demonstrated that the ameliorative effects of increased calcium levels were more than just the result of increased ionic strength leading to a decrease in aluminium activity (and hence toxicity). This reinforced several other studies of root systems, in which the levels of calcium in and around membrane interfaces had been shown to be beneficial for healthy root growth beyond simply ameliorating a hypothesised Ca-deficiency or by reduction of Al activity (Baker 1988).

Parker *et al.* (1988) used wheat (*Triticum aestivum*) to indicate that, in the absence of polynuclear aluminium-hydroxy species, Al^{3+} activity was the best single indicator of root

growth stress in hydroponic solution (given that cation amelioration was also considered). Unlike the two studies above, the sum of mononuclear species activities was not found to be a reliable predictor of root growth. It was also clear that when present, polymeric aluminium hydroxy species were as toxic to plants as Al^{3+}.

In a second study, Parker *et al.* (1989) investigated the root elongation of soybean (*Glycine max* L. cv. Stafford) and two wheat cultivars (*Triticum aestivum* L. cvs. Tyler and Seneca) in the presence of a polymeric aluminium fraction (dominantly comprised of the Al_{13} polymer). The soybean and both wheat cultivars were found to be more sensitive to the polymeric aluminium species than to mononuclear Al^{3+}; minimum root growth was observed when the concentration of the polymeric species reached *ca.* 3 μM [Al]. Interestingly, although the two wheat cultivars exhibited a differential tolerance to Al^{3+}, their response to the polymeric aluminium species was identical, suggesting there may be physiological differences in the mechanism of mono- and polynuclear Al toxicity. Other workers such as Wagatsuma and Kaneko (1987) and Shann and Bertsch (1993) observed similar reductions in root growth and plant mineral content when aluminium polymeric species were present.

The case against the toxicity of inorganic Al fluoride and sulfate complexes is good. Cameron *et al.* (1986) investigated the effects of Al and its F^- and SO_4^{2-} complexes on the root elongation of barley (*Hordeum vulgare)* in nutrient solutions. The root elongation of barley seedlings was found to correlate with Al^{3+} concentrations, but not with total soluble Al or Al complexed to F^- or SO_4^{2-}. Further references to similar studies are found in the review article by Kinraide (1991).

Organically-bound Al is also considered to be non-toxic. The addition of organic matter (straw *etc.*) to soils high in soluble aluminium, results in a decrease in toxicity symptoms. Hue *et al.* (1986) illustrated this by investigating the detoxifying abilities of short chain carboxylic acids (citric, salicylic *etc.*) on cotton (*Gossypium hirsutum* L.) taproots. The aluminium detoxifying capacities were observed to be highly correlated with the relative positions of the OH and COOH groups. Positions that favoured the formation of stable 5 or 6 membered ring structures bound with aluminium had the greatest detoxifying capacities. The excretion of Al-complexing low molecular-weight organic acids by plants has been proposed as a primary defence mechanism for Al-tolerant plants which grow in acidic soils (Rosseland *et al.* 1990; Miyasaka *et al.* 1991; Delhaize and Ryan 1995).

A range of chemical mechanisms have been suggested through which aluminium may cause toxicity (Rosseland *et al.* 1990; Delhaize and Ryan 1995). Al may bind directly to proteins and pectic residues in cell walls, competing with, or displacing other cations (especially Ca) from critical sites. This will reduce the membrane potential in cell walls and inhibit nutrient transport from the soil solution through cell membranes. If Al passes through the cell membrane into the cell cytoplasm, it has the potential to bind to, and inhibit the activity of, a range of biochemically important ligands (*e.g.* the Ca-binding protein calmodulin, numerous enzymes involved in cation uptake, tubulin, ATP, and/or GTP). Al may also have the ability to inhibit DNA synthesis in cell nuclei by binding to DNA phosphate groups.

1.3.2 Aquatic species

Freshwater acidification and the associated increases in soluble aluminium concentrations have been reported as having adverse impacts on a range of aquatic invertebrate and vertebrate species. In the presence of high Al concentrations, a diverse range of invertebrate populations have been observed to decline (*e.g.* zoo-plankton, mayfly nymphs, chironomids, stoneflies and caddis larvae). However, the exact mechanisms by which Al affects such invertebrate species are largely unknown (Rosseland *et al.* 1990).

More is known about the toxicological impacts of aluminium on fish in acidic freshwaters. Fish exposed to acidic Al-rich water typically accumulate Al on the gill surface and excrete increased mucus in the gills. Aluminium precipitation in the gills has been proposed to be due to both the negative charge of the gill mucus, and the higher pH which occurs at the interface between the mucus surface and water as a result of gill NH_3/NH_4^+ exchange. Increased mucus layers result in increased diffusion distances for oxygen and carbon dioxide exchange between water and blood, leading to increased respiratory (hyperventilation) and metabolic (heart rate) stress (Rosseland *et al.* 1990; Poléo *et al.* 1997). Increases in heart rate have also been linked to fish attempting to restore homeostasis and reduce iono-regulatory disturbances, for in addition to H^+, Al^{3+} causes an increased outflux, and decreased influx of plasma ions (Na^+ and Cl^-). Further factors such as water temperature, ionic strength, organic matter content and species of fish are also important parameters in toxicity studies (Poléo *et al.* 1997).

Numerous studies have correlated Al toxicity to fish with concentrations of monomeric or 'labile' Al in acidic freshwaters (*e.g.* references within Rosseland *et al.* 1990). However, several more recent studies (*e.g.* Rosseland *et al.* 1992; Poléo *et al.* 1994; Witters 1998) have reported the natural formation of soluble polynuclear aluminium species, which have been

also shown to cause acute toxicity towards fish. These studies investigated the water chemistry at the confluence of rivers with different pH values, such as may occur at the intersection of a limed tributary with an acidic tributary. Greater toxicity was observed for Atlantic salmon (*Salmo salar* L.) and brown trout (*Salmo trutta* L.) in mixing zones slightly downstream of the confluence points (pH 4.8-6.5) than in the acidic tributaries alone (pH 4.8). The osmoregulatory failure, increased ventilation frequency, and rapid formation of gill lesions that occurred in these zones was ascribed to the formation of toxic polymeric aluminium species. Verbost *et al.* (1995) have demonstrated that a short exposure to an artificial mixing zone followed by a stay in water downstream of this zone, as may occur in nature, was still detrimental to migrating trout. However, none of these studies attempted to positively identify the Al_{13} hydroxy-polymer (by ^{27}Al NMR) as a component of the 'soluble high-molecular weight polymeric aluminium species'.

1.3.3 Human

There is compelling, but little conclusive evidence, relating Al intake to human medical conditions. Al can bind to a wide range of biochemically important chemicals, including small organic ligands (*e.g.* maltol, lactate, citrate and oxalate), amines, RNA and DNA (at phosphate sites), and to a wide range of proteins (calmodulin, transferrin, and nucleoside di- and tri-phosphates (*e.g.* ADP, ATP, GDP and GTP)) (Nelson 1996; Powell and Heath 1996). Berthon (1996) has published a comprehensive review discussing aluminium speciation studies in relation to aluminium metabolism and toxicity.

An unambiguous causative effect of abnormal Al intake has only been established for two disorders, dialysis dementia and iron-adequate microcytic anaemia (Corain *et al.* 1996). Dialysis dementia (DD) was first identified in the 1970s, with the realisation that the accumulation of aluminium in patients using renal dialysis was causing toxic effects. Typical patient symptoms included a progressive onset of dementia, motor abnormalities, and speech difficulties. This syndrome was initially attributed to direct contamination of the dialysate with residual amounts of aluminium from alum-treated tapwater. However, even after purification of dialysis water, symptoms still persisted in many patients, including those not on dialysis. A secondary cause of dialysis dementia was subsequently identified as medication containing high concentrations of Al-containing phosphate binders, which were orally admitted to all uraemic patients at the time. This subsequently brought to light the somewhat overlooked premise that gastrointestinal absorption of aluminium was potentially an important source of aluminium (Berthon 1996).

Modern dialysis prevention strategies have greatly reduced the occurrence of dialysis dementia. Extensive research has since been performed, investigating potential sources and concentrations of dietary and occupational aluminium intake (*e.g.* Rajwanshi *et al.* 1997; Benke *et al.* 1998). Animal experiments have shown that the administration of Al can cause behavioural and/or motor disturbances even at Al concentrations that do not cause overt signs of ill health (Rosseland *et al.* 1990). As Al neurotoxicity is often associated with a prolonged exposure to a relatively low concentration of Al, it is possible that long-lived species such as humans may be most vulnerable to such exposures.

A possible link between aluminium and Alzheimer's disease was first proposed when significantly elevated concentrations of Al were found in selected brain areas of patients, specifically in the senile plaques and neurofibrillary tangles that are characteristic of this disease. Symptoms of Alzheimer's disease include progressive memory loss, learning impairment and reduced motor and speech functions. No single cause for the onset of Alzheimer's disease has been identified, although a genetic predisposition to the disease seems likely for some sufferers.

Early epidemiological evidence linked Alzheimer's disease to regions where water supplies were alum-treated, and suggested that the residual amounts of Al in drinking water may be more readily taken up by the body than Al in food (Birchall and Chappell 1989; Martyn *et al.* 1989). However, a recent CSIRO study (CAAC 1998) found less than 2% of daily dietary intake of aluminium comes from water and there is no difference between the bioavailability of aluminium in alum-treated drinking water and that from dietary sources. Although it is still unclear whether aluminium accumulation is a symptom or a cause of Alzheimer's disease, Al has nevertheless been found to directly cause aggregation (albeit by a still-unknown mechanism) of β-amyloid, the major component of senile plaques. Similarly, Al has further been shown to have the ability to induce the neurofibrillary tangles by causing conformational changes to neurofilament molecules, leading to subsequent aggregations (Berthon 1996).

Al has also been proposed as being a plausible explanation for the high incidences of amyothropic lateral sclerosis (ALS) and Parkinsonism-dementia in some indigenous populations of the western Pacific. These areas are characterised by red soils deficient in Ca and Mg, but rich in Al and Fe. The spinal cord and brain Al concentration of study subjects suffering from these diseases was reportedly comparable to those from other human and animal studies where Al was associated with disorders in the central nervous system (Ganrot 1986). Incidences of such diseases have dramatically declined over the past decades, possibly linked to population changes in diet and lifestyle.

1.4 ANALYTICAL METHODS FOR ALUMINIUM SPECIATION

1.4.1 Total aluminium determination

A range of analytical techniques have been used for the quantitative determination of aluminium. Viable methods of analysis must have the ability to detect aluminium at the low concentrations found in natural systems (typically < 5.0 μM). Common techniques used include flame and graphite-furnace atomic absorption spectrometry, ICP emission spectrometry, ICP-MS, reaction of Al with an organic spectrophotometric or fluorometric reagent, gas and liquid chromatography, fluoride ion selective electrode and neutron activation analysis. While any one of these techniques may prove to be adequate for a specific situation, generally each also has several limitations. For example, atomic absorption methods are frequently hampered by the formation of Al refractory compounds and sample matrix interference, spectrophotometric UV-VIS methods may be prone to interference from the presence of other metals (*e.g.* Fe^{3+}) and competing organic ligands, and both ICP-MS and neutron activation analysis while offering excellent analytical sensitivities, require specialised equipment and have high running costs.

1.4.2 Aluminium speciation

Knowledge of aluminium speciation is of importance in soil chemistry, as ion-activity product calculations (such as those used to determine whether precipitation and mineral formation are feasible) generally require estimated concentrations of the monomeric inorganic Al^{3+} ion. Aluminium speciation is also important because the different chemical forms of aluminium are of varying bioavailability, reactivity and toxicity. Toxicity is commonly correlated with the sum of the 'free', or 'labile' and/or polymeric forms of Al, and hence a method for the measurement of these fractions in soil solutions and natural waters is clearly desirable.

One approach used for determining the speciation of natural samples is to calculate the equilibrium concentrations of species, using complexation and redox equilibrium constants and the experimentally determined total component concentrations. However, this approach has several difficulties. Databases of stability constants are still by no means complete, although more comprehensive collections are nowadays available (*e.g.* Pettit and Powell 1997). However, stability constants may still require corrections (or approximations) for changes in ionic strength and temperature.

Furthermore, in addition to kinetic factors, the need to identify all significant chemical components present in a sample, together with the adsorption, polymerisation and heterogeneous processes which also occur in nature, limits the ultimate success of

computational equilibrium procedures (Campanella *et al.* 1996; Powell 1998). Such computational equilibrium approaches may nevertheless be very helpful, and for example, are essential for determining the species composition in synthetic solutions, used in experimentally validating new analytical methods. For these reasons, the determination of specific aluminium species is commonly performed experimentally, using a variety of separation techniques and/or detection methods.

As discussed above, the free Al^{3+} ion, $Al(OH)^{2+}$ and hydroxy-polymeric species are regarded as being of greatest toxicity towards plants and fish. It would therefore be ideal if an analytical method was able to fractionate and quantify these species as one 'toxic-Al' fraction. However, due to the varying molecular charge, reactivity and size of these species, this is difficult to achieve.

^{27}Al NMR offers the most potential as a future direct method of analysis for Al species. At present however, this method suffers from two major drawbacks. Species identification often proves difficult, and the detection limits obtained with the technique are still very high relative to the concentrations of Al species that typically exist in environmental samples (MacFall *et al.* 1995). The lack of an adequate direct method for the analysis of Al^{3+} has seen the development of many methods that use indirect fractionation procedures to determine fractions of soluble aluminium that are commonly termed *'free'* or *'labile'* Al. Such fractions commonly include the Al^{3+}, $Al(OH)^{2+}$ and $Al(OH)_2^+$ species, and possibly aluminium fluoride and sulfate complexes. The actual fractionation of species may either occur at the time of detection, or as a preliminary process prior to detection.

One major problem with the developed analytical speciation methods is that comparison of results between methods is often difficult. This arises because virtually all methodologies are operationally defined in some respect. Furthermore, it is important that new methods are validated in some way. This may be done, for example, by using model Al-ligand solutions for which the equilibrium species composition has been calculated using a computer speciation program and reliable stability constants (Clarke *et al.* 1992). Often such experimental validation is overlooked. It is therefore usually unclear as to exactly what aluminium species are determined for a given analysis method, or even whether a single species has been quantitatively captured or reacted before analysis occurs.

Complications also arise due to the partitioning of aluminium between solid particulate matter and aqueous species. Aluminium determinations described in the literature have been made using a range of digestion and filtering procedures. Most researchers filter samples before analysis, typically using 0.025, 0.1 or 0.45 μm filter-pore sizes, in an effort to distinguish between particulate and soluble Al species. As particulate matter exists in a continuum of sizes however, results can show a strong dependence on filter-pore size (Menzies *et al.* 1991; Bloom and Erich 1996). Generally the larger the filter-pore size, the higher the concentration of aluminium determined in the sample.

In techniques which involve a separation/fractionation of species either chemically (by preferential reaction with, for example, a colorimetric reagent) or physically (*e.g.* by capture on an ion-exchange resin), it is necessary that the separation step be sufficiently fast so as to avoid re-equilibration of the system.

Many authors have compared the results from a number of different speciation methods, commonly finding each method detects slightly different forms of aluminium (*e.g.* LaZerte 1984; Lalande and Hendershot 1986; Hodges 1987; Berggren 1989; Kerven *et al.* 1989*a* and 1989*b*; Simpson *et al.* 1997). As a comprehensive discussion and comparison of the various analytical methodologies for determining aluminium is beyond the scope of this introduction, interested readers are directed to the extensive reviews that exist on this subject (Bloom and Erich 1996; Clarke *et al.* 1996). Although a range of analytical approaches have been used to determine aluminium speciation, the methods generally fall into one of the following categories.

(i) Reaction rates with complexing agents

Many older methods in the literature attempted the analysis of labile inorganic monomeric Al (Al^{3+}, $Al(OH)^{2+}$ and $Al(OH)_2^{+}$) through a 'selective' reaction between the labile Al species and a spectrophotometric/fluorimetric reagent. These methods were commonly overly aggressive towards organically-bound Al, (or the elapsed experimental time was too long) causing sample re-equilibration, the subsequent release of Al from non-toxic organic complexes (and/or particulate matter) and an over-estimation of the inorganic monomeric Al. Such problems led to the development of kinetically-based methodologies.

These kinetic techniques attempt to exploit the slow dissociation kinetics of Al complexes by using a rapid or limited reaction time between the sample and complexing ligand to minimise

sample equilibrium changes, and therefore minimise any potential redistribution of aluminium between different species. A 'reactive' Al fraction is commonly determined, which may include the monomeric inorganic Al species, in addition to some labile organic species. Commonly selected complexing reagents include aluminon (*e.g.* Alva *et al.* 1989; Kerven *et al.* 1989*a*;) ferron (*e.g.* Hodges 1987; Alva *et al.* 1989; Jallah and Smyth 1998), morin (*e.g.* Ahmed and Hossan 1995; Browne *et al.* 1990), oxine (*e.g.* Barnes 1975; Hodges 1987; Kozûh 1996; Dixon 1998) and pyrocatechol violet (*e.g.* Røyset 1986; Bartlett *et al.* 1987; Henshaw and Lewis 1988; Quintela *et al.* 1993).

These methods have the advantage of measuring the labile rapidly-reacting aluminium fraction directly, as opposed to Driscoll's method (see below) where the labile Al is calculated by difference. However, as with Driscoll's method, these techniques remain operationally defined, with the concentration of 'reactive' Al measured being dependent upon the complexing reagent used, its concentration, and the contact time between the reagent and the sample.

Barnes (1975) presented an early method based upon a kinetic discrimination, which involved a short reaction (*ca.* 30 s) between an aluminium sample and oxine (8-hydroxyquinoline). The resulting aluminium trioxinate complex was extracted at pH 8.3 into methyl isobutyl ketone and detected spectrophotometrically. This operationally defined fraction of aluminium was termed *dissolved and readily reactive species of aluminium.* This method was claimed to be able to detect as little as 74 nM Al in samples. The Barnes technique has been refined by many authors (*e.g.* Bloom *et al.* 1978; LaZerte 1984; Lalande and Hendershot 1986), by using various extraction times and solvents, and varying extraction pH in efforts to improve selectivity and precision.

Analytical techniques based on flow injection analysis (FIA) offer many advantages over conventional batch analysis methods. Short (and reproducible) contact times between a sample and reagent are easily obtained, helping to minimise any shift in chemical equilibria during the speciation measurement. This, and other advantages of performing chemical speciation by FIA are described by Campanella *et al.* (1996).

Clarke *et al.* (1992) used a flow injection analysis method to allow a short (2.3 s) reaction time between an aluminium sample and oxine, before extraction into a chloroform phase (5.1 s), separation and spectrophotometric detection occurred. The detection limit for this technique is 185 nM. However, even with an effective total contact time of *ca.* 7.4 seconds, it

is possible a small, but significant amount of sample re-equilibration will occur. Simpson *et al.* (1997) noted two other potential problems with this method, namely the relatively high oxine concentration (1.4 mM) used during the 2.3 s reaction time could be overly aggressive towards organically-bound aluminium, and secondly, the removal of interfering Fe^{3+} (by hydroxylamine reduction and complexation with 1,10-phenanthroline) causes a sudden increase in the number of potential aluminium-binding sites on organic matter that could thus further disrupt the sample equilibrium. Nevertheless, Clarke *et al.* (1992) achieved good agreement between analytical results and the equilibrium-calculated compositions for synthetic samples.

Hawke and Powell (1994) used a rapid direct reaction (*ca.* 7 s) between Al^{3+} and the colorimetric reagent chrome azurol S (CAS) in an FIA manifold. The short reaction time ensured that only the most labile aluminium species underwent significant reaction. Al was quantified by the spectrophotometric measurement of a rapidly-forming reaction intermediate at an isosbestic point. The detection limit for this technique was 60 nM. Subsequent work applied this method to the analysis of 'reactive Al' and aluminium complexation capacities in soil solutions and natural waters (Hawke and Powell 1995; Powell and Hawke 1995; Hawke *et al.* 1996; Powell *et al.* 1997).

(*ii*) *Ion-exchange and chelating resins*

An alternative approach to the direct kinetic-based methodologies is the selective capture of various aluminium species on ion-exchange or derivatised chelating resins, with detection occurring after an elution step. Such techniques have become increasingly popular in recent years, due to both their analytical selectivity and the ease with which they may be automated *e.g.* through incorporation of micro-columns into flow injection analysis manifolds. Changes in the elemental and species selectivity of chelating resins are possible by varying the adsorbent or derivatised chelating reagent. These methods commonly involve separate fractionation and detection steps, with the target analyte species initially being sequestered by the resin, before a subsequent elution and detection step.

Several advantages are offered by such techniques over alternative speciation methodologies. An important advantage obtained by using columns containing a resin is the benefit of sample preconcentration. If a large sample volume is passed over a resin and the targeted Al species captured, removal of the captured species with a smaller volume of eluent before analysis can greatly improve sensitivity. The use of a resin also allows the analyte to be separated from the

sample matrix, which eliminates potential matrix-interference problems during the detection process (Powell 1998).

Driscoll (1984) published an important method (commonly referred to as 'Driscoll's method'; Figure 1.4) which has subsequently been widely used for field work and as a basis for other methods (*e.g.* Sullivan and Seip 1986; Backes and Tipping 1987; Berggren 1989; Kerven *et al.* 1989*a*). This method involves division of a sample into three fractions, and analysis of the first two fractions with and without prior acidification, using the 30 s rapid-oxine method of Barnes (1975). These two fractions are called *acid reactive* and *total monomeric aluminium*, respectively. The third fraction is passed through a column containing a strong cation-exchange resin, which retains the labile, positively charged inorganic monomeric aluminium species, while organically-bound aluminium (assumed to be anionic and non-labile) passes through. This fraction is subsequently analysed to give *non-labile monomeric aluminium*, and by subtraction of this fraction from the *total monomeric aluminium* fraction, the concentration of *labile monomeric aluminium* is obtained.

Several inherent disadvantages exist with Driscoll's method. Firstly, the *labile monomeric aluminium* fraction is calculated as the difference between two measurements, one of which (the *non-labile monomeric aluminium*) is operationally defined. In addition, with the experimental time-scale used, there is the potential for sample re-equilibration to occur, with Al being sequestered from organic complexes. Indeed, Driscoll (1984) did observe some removal of Al from organic-Al complexes by the cation-exchange resin, the degree of removal being dependent upon sample flow rate through the column.

Other authors (*e.g.* Berggren 1989; Dahlgren and Ugolini 1989; Kerven 1989*a*) also noted the dissociation of organic Al complexes when samples were passed over strong cation-exchange resins. Driscoll (1984) also did not investigate the fate of cationic polymeric Al species in his analysis method. Such species may either be captured on the cation exchange resin, or pass through as part of the *non-labile monomeric aluminium* fraction.

Many authors have determined 'reactive' Al fractions by using chelating resins. Reagents that are capable of binding Al strongly are, typically, covalently-bonded onto solid/gel matrix supports. By rapidly (and reproducibly) passing a sample over such resins, only the most labile Al species are captured. The captured fraction is subsequently eluted (typically using a strong mineral acid) and quantified using an established analysis method. Hirayama *et al.*

(1994) used PTFE-coated CAS-immobilised silica gel to determine the fraction of soluble and suspended Al species in natural waters. Other authors have also used CAS-loaded resins to separate and preconcentrate total Al from other trace metals within a sample (Jones and Schwedt 1989; Molina-Diaz *et al.* 1993; Molodovan and Vlădescu 1996).

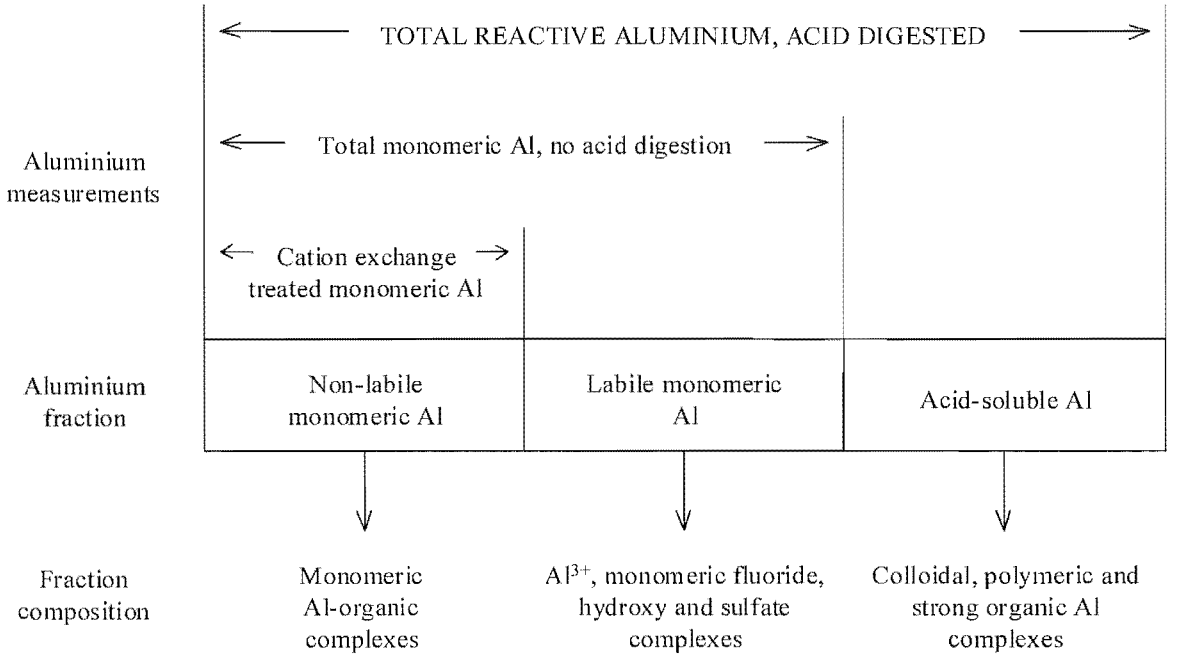

Figure 1.4. A schematic representation of the aluminium fractionation procedure of Driscoll (1984).

The sulphonated azo dye Chromotrope 2B has also been used to preconcentrate Al before analysis (Pesavento *et al.* 1989; Martín-Esteban *et al.* 1995). The latter authors reported detection limits for their technique of 370 nM and 3.7 nM, using FAAS and ICP-MS detection respectively. Using ICP-AES detection, the detection limit was 10.4 nM. Pesavento *et al.* (1998*a* and 1998*b*) used equilibrium calculations to determine the Al speciation in fresh and drinking water samples after capturing various fractions of Al on a strong anion-exchange resin AG1X8 and the iminodiacetate chelating resin Chelex 100.

Simpson *et al.* (1997) used a micro-column containing oxine-derivatised Fractogel in a flow injection analysis method to obtain a kinetically-based fractionation of Al species. This technique was used extensively in this thesis work, and is described in detail below (Section 1.4.3). A large number of chelating resins containing a variety of functional groups and immobilised on a range of solid supports have been used to preconcentrate samples and to remove matrix interferences when analysing total Al and other trace metals by sensitive techniques such as ICP-MS (Bilba *et al.* 1998). Examples of specific immobilised ligands used for these purposes include oxine (8-hydroxyquinoline) (Hill 1974; Landing 1986;

Simpson *et al.* 1997) and other colorimetric reagents (Singh and Dhingra 1992; Saxena *et al.* 1994), iminodiacetate (Bloxham 1994; Nelms *et al.* 1996; Taylor *et al.* 1996; Yuchi *et al.* 1997), hydroximate (Ahuja *et al.* 1996), and EDTA-type ligands (Burba *et al.* 1994). Several workers have also performed comparative studies and investigated chelating resins containing a range of functional groups (Rao 1995; Mahmoud 1996).

Davison and Zhang (1994) have recently introduced a novel technique for determining labile species based on diffusive gradients in thin films (DGT). An *in-situ* sampling device is used, containing an ion-exchange resin separated from the sample solution by an ion-permeable polyacrylamide hydrogel. A diffusion layer forms at the outer surface of the gel and a concentration gradient is generated within the gel, as ion transport is limited by diffusion processes. The only species measured are those which react directly with the binding agent or those that are in labile equilibrium with the reacting species within an effective measurement time determined by the diffusion layer thickness.

The DGT technique can potentially be used to detect any metal or organic species that is able to diffuse through a gel layer and react with an immobilised reagent in the backing layer. The method has been applied to the quantification of trace metals in freshwater and marine systems and also to the determination of vertical concentration profiles of trace metals in sediment pore waters (Zhang and Davison 1995).

(iii) Dialysis and ultrafiltration

Dialysis membranes (typically 1-55 nm pore diameters) and ultrafiltration membranes (typically 1-15 nm pore diameters) have been used to achieve size exclusion of soluble Al species from both colloidal aluminium, and aluminium bound to large organic molecules such as fulvic and humic acids (*e.g.* Benes and Stennes 1974; LaZerte 1984; Berggren 1989; Gregor *et al.* 1996). It is likely that dialysis often does not completely separate inorganic monomeric aluminium species from aluminium bound to low-molecular-weight organic species such as oxalate and citrate. For instance, LaZerte (1984) found up to 12% of organic matter in lake and stream waters passed through a dialysis membrane.

A further difficulty with dialysis techniques is that a lengthy sampling equilibration period (*ca.* 24 hours) is required before analysis, allowing ample time for aluminium species within the sample to re-equilibrate. Bloom and Erich (1996) also note the potential of the sample pH to change as a result of CO_2 degassing or through sample dilution. This could lead to a loss of

aluminium if the sample is in equilibrium with solid-phase Al. Further difficulties with dialysis techniques have been discussed by Florence and Batley (1980).

(*iv*) *Fluoride ion-selective electrode*

Aluminium is the only metal that binds significantly to fluoride, and hence it is possible to calculate the activity of $\{Al^{3+}\}$ indirectly, by knowledge of the total and free activity of fluoride $\{F^-\}$, and the total aluminium concentration. Although a long time may be required to reach a steady potential, stable readings from a fluoride ion-selective electrode (ISE) may be obtained in solutions containing as little as 10^{-8} M aluminium (Bloom and Erich 1996).

The major advantage of $\{Al^{3+}\}$ determination by fluoride ISE is that minimal, if any, disturbance occurs to the sample equilibrium during measurement. However, LaZerte (1984) found for samples of higher pH (>5.5), where hydroxide competes strongly with fluoride for aluminium, small errors in the measurement of F^- activity could lead to large errors (± 70%) in the calculated aluminium concentrations.

A further source of error for ISE methods is that fluoride or aluminium-fluoride complexes may bind to either aluminosilicate minerals or organic matter that is present within a sample. Driscoll (1984) used a fluoride ISE to compare analytical results from surface water samples with results obtained using his cation exchange method. Agreement between the two methods was good, but organic monomeric aluminium calculated from the fluoride ISE was generally greater than the *non-labile monomeric aluminium* obtained by the resin procedure.

1.4.3 Oxine-derivatised Fractogel for aluminium analysis

Concentrations of 'reactive' or 'free' aluminium were generally determined in this work using the method of Simpson *et al.* (1997). This kinetic-based flow injection analysis technique involves a 1.3 s contact time between an injected sample aliquot (600 or 250 µL) and oxine-derivatised Fractogel contained in a polycarbonate micro-column. In this method, 'free Al' ($[Al^{3+}] + [Al(OH)^{2+}] + [Al(OH)_2^+] + [Al(OH)_3] + [Al(OH)_4^-]) + [AlF^{2+}]$) is (pre)concentrated on the resin as the sample flows through the micro-column (22 µL internal volume).

'Organic-bound' Al does not react with the gel and is immediately measured down-line in the effluent by spectrophotometric analysis with chrome azurol S (CAS) (Hawke and Powell 1994; Hawke *et al.* 1996). 'Organic-bound Al' is an operationally-defined fraction as it refers only to the Al in moderately-labile complexes from which Al can be sequestered by CAS in

the 30 s reaction time in the FIA manifold. It is not the total organically-bound Al fraction. It is only about 30% of that measured in 30 s by the more aggressive reagent pyrocatechol violet (PCV), as noted by Powell (1998).

The captured 'free Al' is subsequently eluted from the resin with 0.03 M NaOH, before being buffered to pH 5.0 and measured spectrophotometrically down-line using CAS. This method also has the ability to determine polymeric Al-hydroxy species (*e.g.* $Al_{13}(OH)_{24}(H_2O)_{12}^{7+}$). These species are quantitatively retained by the column, but are not desorbed during the time-scale of the 0.03 M NaOH elution step. However, they may be quantified using a 2 min stopped-flow elution protocol with 0.2 M NaOH. Further experimental details of this method are described in Chapter 2 (Section 2.2.7).

The method has been experimentally validated using synthetic aluminium-ligand solutions (for which the species composition was known from solution equilibrium calculations). These experiments indicated that the oxine-derivatised Fractogel does not significantly sequester aluminium from citrate, oxalate or malonate complexes. Nevertheless, it is likely that Al in very labile organic complexes will be sequestered by the column and quantified as part of the 'free Al' fraction. The 1:1 aluminium fluoride complex AlF^{2+} is also retained on the Fractogel and similarly will be quantified as 'free Al'.

A common problem with complexing agents used for the spectrophotometric determination of Al^{3+} is interference arising from the presence of Fe^{3+}. Although Fe^{3+} can be masked by reduction to Fe^{2+} with ascorbic acid, and subsequently complexed with 2,2'-bipyridine or 1-10 phenanthroline, this increases sample dilution and can cause changes in Al speciation to occur. Although Fe^{3+} is retained by the oxine-derivatised Fractogel, it is not eluted with the 0.03 M NaOH eluent, and hence does not interfere in the downline aluminium chemistry (Simpson *et al.* 1997). The stopped-flow cleaning procedure with 0.2 M NaOH does remove Fe^{3+} from the resin, but the eluted Fe^{3+} is not detected by the CAS reagent. Simpson *et al.* (1997) proposed this was due to the formation of a colloidal precipitate of $Fe(OH)_3$, produced as the eluted $Fe(OH)_4^-$ merges with the pH 5.0 acetate buffer. As the colloidal $Fe(OH)_3$ is too stable to be dissolved by the CAS, it is not detected.

1.5 SCOPE OF THIS WORK

This research has been based around the environmental solution chemistry of aluminium. Chapter 3 discusses some general studies in soil aluminium chemistry, including the calculation of soil solution $[Al^{3+}]$ from experimentally-determined concentrations of 'free Al' ($[Al^{3+}] + [Al(OH)^{2+}] + [Al(OH)_2^{+}] + [Al(OH)_3] + [Al(OH)_4^{-}] + [AlF^{2+}]$). Historical and contemporary data were combined, using soil solution data from a variety of sites, encompassing a range of New Zealand soils and vegetation types. The control of Al^{3+} solubility was proposed to be due to an $Al(OH)_3$ solid phase at pH >5.6, and by soil organic matter at pH <5.0, respectively. This interpretation was supported by data from a pH-dependent Al - fulvic acid binding curve, for which the calculated values of log $[Al^{3+}]$ followed the same curvilinear relationship as a plot of $\log[Al^{3+}]$ *vs.* pH calculated for the soil solutions.

Chapters 4 and 5 discuss the application of existing flow injection analysis (FIA) methodologies to determine the speciation of aluminium in soil solutions. These techniques were applied to several detailed investigations of environmental situations where current or historical land management practices have caused soil acidification and elevated concentrations of potentially bio-toxic forms of aluminium to occur. A detailed study of the aluminium speciation in a series of high-country pastoral soils from the South Island, New Zealand was performed (Chapter 4).

The impact of land use change, from grassland to conifer forest, on aluminium speciation in soils and soil solutions was also examined. The aluminium chemistry of soils from grassland was compared to that from adjoining 15-19 year old forest stands at three contrasting pairs of sites in the South Island, New Zealand (Chapter 5). In addition to performing a range of Al measurements, further complementary experiments such as root elongation bio-toxicity studies and aluminium complexation-capacity determinations were carried out to provide information on the impacts of soil acidification. Chapter 6 presents the results from a study investigating the effects of sample ageing on soil and soil solution aluminium concentrations.

Chapter 7 discusses the determination of aluminium speciation in a situation of relevance to the water treatment industry. This study compared the aluminium binding properties of a commercially available anionic flocculant to those of alginate, a naturally-derived, anionic, non-toxic flocculant. The aim of this work was to determine whether fundamental binding differences occurred between aluminium and the two contrasting polyelectrolytes.

Chapters 8 and 9 describe the development of new flow injection analysis techniques to determine the speciation of iron and aluminium in natural samples. The speciation of iron in humic waters was also examined, using a micro-column containing oxine-derivatised Fractogel. A simple FIA manifold enabled quantification of Fe^{2+}, while the addition of an extra line to the manifold allowed the sum of the concentrations of Fe^{2+} and Fe^{3+} species to be determined. The concentration of Fe^{3+} was calculated by difference. The ability of Fe^{3+} complexes to undergo photo-reduction in the presence of fulvic and humic acids to produce Fe^{2+} was investigated. A commercially available iminodiacetate chelating-resin was contained in a micro-column, and used to achieve a kinetically-based fractionation between reactive 'free Al' species ($[Al^{3+}] + [Al(OH)^{2+}] + [Al(OH)_2^{+}]$) and non-toxic organically-bound Al.

Chapter 10 discusses the fundamental complexation chemistry of aluminium and two naturally-occurring organic acid ligands (caffeic and chlorogenic acids), which was investigated using potentiometric and spectrophotometric titration techniques. Stability constants for these systems were determined from the resulting data.

The development of appropriate analytical methods, which target the toxic 'free Al' species, is necessary for acquiring knowledge of the role of aluminium in soils. This work describes the development of such analytical protocols, and their application to determine the concentrations of toxic soil solution 'free Al' in a number of New Zealand soils. The data obtained from these studies provides information on the effects of soil acidification on aluminium speciation in soils, and hence also indicates how soil fertility may be maintained or improved by suitable land management practices.

CHAPTER 2

MATERIALS AND METHODS

2.1 MATERIALS

2.1.1 Water

All stock and working solutions were prepared using water from a Milli-Q® (Millipore) water purification system, in which distilled water was sequentially passed through a Super-C carbon cartridge, Ion-ex anion and cation exchange cartridges, an Organex-Q cartridge and finally a Millipak® 0.22 μm pore size filter. Triply distilled water (TDW) was used to prepare non-analytical solutions, and for cleaning and rinsing of glassware.

2.1.2 Volumetric equipment

All glassware was a minimum of B standard. Glass and plasticware containers for solution storage or preparation were cleaned before use by immersion in an acid-bath (10% HNO_3, *ca.* 24 hours), followed by repeated rinsing and filling with TDW. Pipettes used for quantitative work (*e.g.* solution equilibria experiments) were calibrated by weighing volumes of TDW delivered at a known temperature. Published density data (Dean 1992) were used to convert the weight of water dispensed into a volume. Micropipettes (10-100 μL, 100-1000 μL, Eppendorf) were similarly calibrated.

2.1.3 Flow injection analysis equipment

Specific details of flow injection analysis (FIA) manifolds are given in the relevant chapters. A general description of the FIA equipment used is provided here.

FIA solutions were pumped with a 4-channel Alitea XV (Sweden) peristaltic pump, using Tygon® (Ismatec, Switzerland) pump tubing of various diameters. Manifolds were constructed from microline™ tubing (0.51 mm i.d. Cole-Parmer). Connections between sections of microline tubing were effected using *ca.* 2 cm lengths of either silicon tubing (1.3 mm i.d. Pharmacia LKB) or Tygon® tubing (1.09 mm i.d. Ismatec, Switzerland). Solutions were merged at confluence points using 30°/30° glass mixers, as recommended by Clark *et al.*

(1989) for optimal mixing. Small 'mixing reactors' were placed in buffer and reagent lines, and after the confluence merging zones to enhance mixing and to absorb pulses from the FIA pump and injection valve. The reactors were prepared following the method of Hawke *et al.* (1996), by connecting *ca.* 20 mm lengths of silicone tubing (1.3 mm i.d. Pharmacia LKB) with short segments of microline (0.51 mm i.d. Cole-Parmer), to give small 'mixing reactors' with an internal volume of *ca.* 20 μL.

Two types of injection valve were used for FIA work: (*i*) a Rheodyne 5020 (6-port) with 0.80 mm i.d. injection loops and (*ii*) a VALCO valve (CHEMINERT, C12-3110EH) (10-port) with twin 0.76 mm i.d. injection loops, controlled by a VICI actuator. The injection valve was connected to allow filling of the elution loop while the sample loop was 'in-line'. The injection loops of both valves were Teflon® and were connected with Activon (OM2301, Omnifit) two-way Teflon-tube couplers. Threaded Teflon-tube end fittings and grippers (OM2110, OM2310, Omnifit) were used to connect microline tubing to the injection valves and to micro-columns. FIA scans were recorded using a GBC 918 UV/VIS spectrophotometer, with peak height determined using the software (GBC) supplied with the instrument. Baseline subtraction was performed manually when necessary.

(*i*) *Micro-columns*

Micro-columns were constructed from transparent polycarbonate (acid and alkali resistant), with a 22 μL internal volume (7 mm by 2 mm i.d.) (Simpson *et al.* 1997). The columns were packed wet with Prosep resin or oxine-derivatised Fractogel and connected to the FIA system with the threaded Teflon-tube end fittings and grippers described above. To retain the fine resin material within the column, a circular disk of fine nylon mesh (50 μm) was placed between the resin and the connectors.

(*ii*) *Prosep resin*

A commercially available iminodiacetate-derivatised controlled pore glass chelating resin (PROSEP® Chelating-1) was obtained from Bioprocessing, Consett, Co Durham, England.

(*iii*) *Oxine-derivatised Fractogel*

Several batches of oxine (8-hydroxyquinoline)-derivatised Fractogel were prepared following the method of Landing *et al.* (1986). The Fractogel-TSK polymer substrate consists of intertwined vinyl polymer agglomerates, which allow high mechanical and chemical stability, high porosity, and high hydrophilicity, due to the presence of ether linkages and hydroxyl

groups. The Fractogel polymer exhibits no cation exchange capacity and does not concentrate dissolved organic species such as fulvic and humic acids (Landing *et al.* 1986).

(*a*) *Reagents*

Reagents used in the preparation of the oxine-derivatised Fractogel included: Fractogel TSK Toyopearl HW-40C (50-100 μm), oxine (BDH AnalaR), *p*-nitrobenzoyl chloride (Merck GPR), CH_2Cl_2 (BDH HiPerSolv for HPLC), Et_3N (BDH GPR), $Na_2S_2O_4$ (Hopkin & Williams GPR), $NaNO_2$ (Hopkin & Williams AnalaR), ethanol (May & Baker AnalaR), acetone (BDH AnalaR), acetic acid (Ajax AnalaR), NaOH (BDH AnalaR) and HCl (BDH AnalaR). Milli-Q water was used for rinsing of products, and used for the preparation of all solutions.

(*b*) *Description of Derivatisation Method*

Resin Preparation: All glassware was cleaned and oven-dried before use. 5 g of Fractogel resin slurry was rinsed 4 times in 100 mL water to remove traces of the NaN_3 preservative. After allowing to settle for 20 minutes, the resin was collected in a sintered glass filter (porosity 3) and rinsed with: (*i*) 2 times 50 mL 1 M NaOH, (*ii*) 3 times 50 mL H_2O, (*iii*) 2 times 50 mL 1 M HCl, (*iv*) 3 times 50 mL H_2O, (*v*) 2 times 50 mL ethanol, (*vi*) 2 times 50 mL acetone and (*vii*) 2 times 50 mL CH_2Cl_2. After drying under suction for 20 minutes, the resin was transferred to an oven (40°C) for 2 hours.

Immobilisation Procedure: After drying, 1 g of resin was placed in a solution containing 20 mL CH_2Cl_2, 1.05 mL Et_3N and 0.425 g *p*-nitrobenzoyl chloride, and stirred at 40°C (oilbath) for 12 hours. The resulting benzoylated product was collected in a sintered glass filter (3) and rinsed with 2 times 100 mL CH_2Cl_2 and then 2 times 100 mL H_2O, to rehydrate the resin. The nitro group was subsequently reduced by stirring the resin in a solution containing 1 g $Na_2S_2O_4$ in 21 mL H_2O, for 3 hours at room temperature. The product was filtered and rinsed with 2 times 100 mL H_2O. Diazotisation of this material was achieved by adding the resin to an ice-cold solution of 1 g $NaNO_2$ in 20 mL 0.2 M acetic acid, with periodic stirring for 45 minutes. The yellow product was filtered and rinsed with 3 times 50 mL ice-cold H_2O. The phenyl-azo coupling was achieved by adding the product to 0.2 g oxine in 10 mL of 95% ethanol, with periodic stirring for 45 minutes, resulting in the formation of the dark-red oxine-derivatised Fractogel.

Cleaning and Storage: The final product was filtered and rinsed with: (*i*) 2 times 50 mL 0.5 M NaOH, (*ii*) 3 times 50 mL H_2O, (*iii*) 2 times 50 mL 1 M HCl, and (*iv*) 3 times 50 mL

H_2O. The resin was stored as a slurry in milli-Q water; 'fines' were decanted after a final settling period.

2.1.4 Buffers

(i) Electrode calibration buffers

Two primary reference National Institute of Standards and Technology (NIST) phthalate and phosphate buffers were used to calibrate pH electrodes before use. Electrode calibration for potentiometric titrations was more careful, and is described in Section 10.2.9. Buffers were prepared according to the method of Vogel (1961).

(i) 0.05 M Phthalate Buffer: (pH 4.01, 25°C): 10.21 g of potassium hydrogen phthalate ($KOOC.C_6H_4.COOH$) (dried at 110°C) was dissolved in 1 L of milli-Q water.

(ii) 0.025 M Phosphate Buffer: (pH 6.86, 25°C): 3.40 g of potassium di-hydrogen phosphate (KH_2PO_4) and 3.55 g of di-sodium hydrogen orthophosphate (Na_2HPO_4) (both dried at 110°C) were dissolved in 1 L of milli-Q water.

Buffer solutions were stored in plastic and refrigerated when not in use. Solutions were replaced every 6 to 8 weeks, or earlier if deterioration was apparent.

(ii) General buffers

Acetic acid (Ajax AnalaR), anhydrous sodium acetate (BDH AnalaR) and MES [2-(N-morpholino)ethanesulfonic acid] (Sigma 99.5%) were used as buffers in spectrophotometric FIA manifolds, aluminium complexation capacity titrations and in preparing solutions to a required pH. All were used as supplied, without further purification.

A total ionic strength adjustment buffer (TISAB) was used when determining fluoride concentrations in soil solutions by ion-selective electrode. The buffer contained 0.05 M acetic acid (Ajax AnalaR), 0.05 M anhydrous sodium acetate (BDH AnalaR), 0.05 M EDTA (Merck pro analysis) and 1 M KCl (BDH AnalaR).

2.1.5 Metal stock solutions

Al^{3+} stock solutions were prepared from aluminium chloride $AlCl_3.6H_2O$ (Puratronic 99.9995%, Alfa). To prevent hydrolysis, sufficient standardised HCl (BDH AnalaR) was added in order that the final solutions had pH < 2.0. The Al stock was standardised gravimetrically as the oxinate, following the method of Vogel (1961) (Appendix I). Fe^{3+} stock solutions (*ca.* 2 mM) were prepared by dissolving ammonium ferric sulfate $NH_4Fe(SO_4)_2.12H_2O$ (BDH AnalaR) in 0.4 M HNO_3 (BDH AnalaR). Fe^{2+} stock solutions (also *ca.* 2 mM) were prepared by dissolving di-ammonium ferrous sulfate $(NH_4)_2Fe(SO_4)_2.6H_2O$ (BDH AnalaR) in 0.4 M HNO_3 (BDH AnalaR). Acidified (*ca.* 1 mM HCl (BDH AnalaR)) stock solutions of other metals were also prepared from the following reagents: $CoCl_2.6H_2O$, $CrCl_3.6H_2O$, $CuCl_2.2H_2O$, $NiCl_2.2H_2O$, $Pb(NO_3)_2$ (all BDH AnalaR), $MnSO_4.4H_2O$ (Hopkin & Williams AnalaR) and $ZnCl_2$ (Riedel-deHaën p.A.). Metal solutions were stored at room temperature.

2.1.6 Ligands

All ligands were used as supplied, without further purification, unless stated otherwise. The colorimetric reagents pyrocatechol violet (PCV) (Aldrich) and chrome azurol S (CAS) (60% pure, Aldrich) were used for the spectrophotometric determination of Al. 2,2'-bipyridyl (BDH AnalaR) and 1,10-phenanthroline hydrate (BDH AnalaR and Serva p.A.) were used for spectrophotometric determination of Fe^{2+}.

Sodium alginate (BDH) had previously been purified by precipitation and dialysis to remove potential contaminant metal ions (Gregor *et al.* 1996). A commercially available anionic polyacrylamide-based flocculant Crystalfloc B610 PWG (IChem Ltd.), was used as supplied.

The sample of fulvic acid used had previously been isolated from International Humic Substance Society (IHSS) reference peat by the acid pyrophosphate - XAD-7 method (Gregor and Powell 1986) (elemental analysis: C 49.3%, H 3.7%, N 2.3%, Al 0.01% and Fe 0.05%; total ash content 0.2%; weight *per* mole of titratable carboxyl groups = 137; Gregor 1987). Acidified (pH < 2.5) stock solutions of citric acid (BDH AnalaR), malonic acid (Riedel-deHaën pure), oxalic acid (Fisons AnalaR) and tartaric acid (BDH AnalaR) were prepared for model ligand studies. Diluted ligand solutions were subsequently spiked with Al^{3+}, Fe^{3+} or Fe^{2+} and buffered to the desired pH in 0.01 M acetate buffer. Solutions were equilibrated at least 24 hours before analysis.

2.2 METHODS

2.2.1 Soil sampling protocol

Site-specific sampling details are given in the relevant chapters. The general protocol for soil sampling is described here.

Soils were sampled by pooling cores of replicate samples, taken either at random or following replicate transects at sample sites. Tussock bases and large roots that lay on transect lines were avoided. Overlying vegetation matter was removed to expose the mineral soil before sampling. Small roots, other vegetation matter, and stones within soil cores were removed by hand, either at the time of sampling, or later, in the laboratory. Samples were stored in sealed plastic bags in an insulated chest for transit, then refrigerated at 4°C upon arrival at the laboratory.

2.2.2 Soil pH measurement

(*i*) *Field pH measurement*

A slurry was made in the field by stirring *ca.* 10 g soil with 25 mL TDW. The stirred soil slurry was allowed to settle for 5 minutes, before the soil pH was measured by using a portable Lutron pH206 meter and Radiometer pHC2451 combination glass – calomel electrode fitted with an annular ring liquid junction.

(*ii*) *Laboratory pH measurement*

Soil pH was measured in the laboratory on both field-moist and air-dried soil samples (30°C, Clayson fan oven). Soil slurries were prepared using 10 g soil and 25 mL TDW (soil:water ratio of 1.0:2.5 (Blakemore *et al.* 1987)). Slurries were stirred vigorously with a magnetic stirrer (5 minutes) and left to settle overnight. pH values were measured using the same meter and electrode as above, with the liquid junction in the supernatant and the glass bulb in the sediment. The pH meter was calibrated against National Institute of Standards and Technology (NIST) phthalate and phosphate buffers before use.

2.2.3 Soil solution extraction

Soil solution was extracted by centrifugation, generally within 24 hours of soil sampling, using a method similar to that described by Reynolds (1984). All centrifugation and filtration equipment was acid-washed before use. Soils that were too dry for soil solution extraction were moistened prior to centrifugation. Typically 10-15% TDW (by weight) was added to a sub-sample of soil. Moistened soils were stored in plastic bags and refrigerated for a *ca.* 24 hour equilibration period, before subsequent extraction of the soil solution.

Teflon soil solution extraction tubes (internal dimensions 90 mm length by 20 mm diameter, 1 mm hole at bottom) were fabricated in the Department of Chemistry's mechanical workshop, University of Canterbury. Soil was firmly pressed into the extraction tubes, which were then placed into Becton Dickinson Labware polypropylene FALCON® 2070 50 mL centrifuge tubes and capped. Three to six tubes of approximately equal weight were centrifuged for *ca.* 30 min at 3000 r.p.m. (relative centrifugal force (RCF) = 1100 g) using a BTL bench centrifuge at room temperature. The extracted soil solution was transferred to a syringe and membrane filtered (0.025 μm cellulose nitrate, Schleicher & Schuell) into a 15 mL centrifuge tube (FALCON® 2096) using a manual press.

Membrane filters were soaked in TDW before use. Earlier work (Adams *et al.* 1996) indicated that these cellulose nitrate membranes appear to contain a basic trace impurity, which causes the observed pH of a 0.1 mmol L^{-1} phthalate solution, after filtering, to increase from pH 5.0 to 5.2. Soaking the membranes in TDW prior to use, appears to remove the impurity.

2.2.4 Soil solution analyses

Soil solutions were analysed as soon as possible after extraction. Solutions that were not analysed within 3 hours of extraction were kept refrigerated, but allowed to return to room temperature before analysis. All soil solutions were analysed within 24 hours of extraction.

(i) pH measurements

Soil solution pH was measured on the fresh soil solution extract using a Russell CMAWL/4/5/S7 micro-combination electrode with a PHM64 pH meter (Radiometer, Copenhagen), calibrated against NIST phthalate and phosphate buffers.

(ii) Natural organic matter

The concentration of fulvic and humic substances in soil solution was estimated by measurement of the UV absorbance at 250 nm (A_{250}) using a GBC UV/VIS 918 spectrophotometer (1 cm quartz cell), and application of the molar absorptivity coefficient (ε_{250} = 0.030 $(cm.mg/L)^{-1}$ at pH 4.7 (buffered by 2.5 mM acetate)) for a sample of fulvic acid previously isolated from International Humic Substance Society (IHSS) reference peat by the acid pyrophosphate - XAD-7 method (Gregor and Powell 1986). This measurement of soluble organic matter will not include those organic species that are UV-transparent and which may be expected to exist in soil solutions *e.g.* low molecular weight organic acids.

(iii) Fluoride

Concentrations of fluoride in soil solution were determined using a Radiometer ISEC241F combined ion-selective electrode, with a PHM64 pH meter (Radiometer, Copenhagen). Total fluoride was determined after the addition of a total ionic strength adjustment buffer (TISAB), using a sample:buffer ratio of 5:1.

(iv) Ion chromatography

A Dionex DX-100 ion chromatograph and Dionex 4400 data integrator were used to determine soil solution concentrations of Ca^{2+}, Mg^{2+}, K^+ and Na^+. An Ionpac® CG12A guard column and Ionpac® CS12A analytical column were used, and were cleaned before use according to the manufacturer's instructions. 25 µL samples were injected into 11 mM H_2SO_4 (Fisons AnalaR) eluent (1.0 mL/min flow rate). Eluent and standards were prepared using freshly generated Milli-Q® water. The cation self-regenerating suppressor (CSRS-1) was used with a current setting of 500 mA. The resulting integrated peak areas from the chromatogram were automatically calculated and printed by the data integrator.

2.2.5 Analyses of natural waters

(i) Sampling

Natural water samples were collected in acid-washed, TDW rinsed polyethylene bottles. The bottles were rinsed repeatedly with the water about to be sampled, before being filled with water taken from below the surface. Samples were refrigerated (4°C) on return to the laboratory. Prior to analysis, subsamples of water were filtered (0.025 µm cellulose nitrate, Schleicher & Schuell) and allowed to return to room temperature before analysis.

(ii) pH measurement

The pH of natural water samples was determined using a Russell CMAWL/4/5/S7 micro-combination electrode with a PHM64 pH meter (Radiometer, Copenhagen). Due to the typical low ionic strength of natural waters, the electrode was calibrated against diluted NIST buffers (0.01 M phthalate buffer, pH 4.117 at 25°C; 0.0025 M phosphate buffer, pH 7.068 at 25°C) (Covington *et al.* 1983).

(iii) Natural organic matter

The concentration of fulvic and humic substances in filtered water samples was estimated by measurement of the UV absorbance at 250 nm (A_{250}), using a GBC UV/VIS 918 spectrophotometer (1 cm quartz cell).

2.2.6 Commercial analyses

Elemental microanalysis of ligands was performed at the Campbell Microanalytical Laboratory, University of Otago, New Zealand. Plasma emission spectroscopy was used to determine total concentrations of a number of elements (Al, Ca, Fe, K, Mg, Na, P and S) in soil solutions. These analyses were performed at the ICP facility located at AgResearch Grasslands Research Centre, Palmerston North, New Zealand. For a number of soil solutions, total organic carbon (TOC) measurements were obtained from the Institute of Environmental Science and Research Ltd. (ESR), Christchurch Science Centre and from the Wellington Science Centre, New Zealand. Glassware for TOC samples was cleaned in chromic acid for 24 hours before use. For selected soils, acidity and exchangeable cation analyses were performed by the New Zealand Forest Research Institute, Rotorua, New Zealand.

2.2.7 Aluminium analyses

(i) Determination of total Al

Total aluminium was determined using a GBC 908 electrothermal atomic absorption spectrometer. This was fitted with a GF3000 graphite furnace workhead/power supply, and a PAL3000 autosampler. Measurements were made with the GBC Ultra-pulse continuum source background correction system switched on. Absorbance was monitored at 309.5 nm (lamp current 5 mA; slit width 0.5 nm). ETAAS analyses were performed using the furnace protocol described in Table 2.1, with argon (BOC Gases, Christchurch) used for the inert gas supply. Samples and standards were prepared in 1% HNO_3.

Table 2.1. Furnace control program for ETAAS analyses.

Step	Final temp. (°C)	Ramp time (s)	Hold time (s)	Inert gas	Read
1. Drying	90	0.1	1.0	Yes	No
2. Drying	120	20.0	5.0	Yes	No
3. Drying	150	5.0	5.0	Yes	No
4. Pyrolysis	1100	20.0	5.0	Yes	No
5. Cooling	200	5.0	2.0	Yes	No
6. Cooling	200	2.0	5.0	No	No
7. Atomisation	2500	1.2	2.0	No	Yes
8. Clean	2600	1.0	2.0	Yes	No

(ii) Determination of total reactive Al

Total reactive Al was determined on acidified soil solution (pH 2.0, 24 hours) by a 30 s reaction with the colorimetric reagent pyrocatechol violet, (PCV), in a flow injection analysis manifold (Røyset 1986).

(iii) Determination of 'free Al' and 'organic-bound-Al'

As discussed in the Introduction (Section 1.4.3), concentrations of 'free' and 'organic-bound' Al were determined in samples by using the method of Simpson *et al.* (1997). A brief discussion of the methodology of this technique is presented here. Further experimental details and method validation may be found in Simpson *et al.* (1997). The FIA manifold for this technique is depicted in (Figure 2.1).

The micro-column containing oxine-derivatised Fractogel was cleaned daily before use, by performing several stopped-flow elutions (2 min, 0.2 M NaOH), followed by successive injections of 1 M HCl across the column. In addition, the direction of flow through the column was reversed daily to help avoid a build-up in back-pressure due to compaction of the Fractogel. A second micro-column (15 x 2.5 mm) (not shown in Figure 2.1) containing Chelex 100 resin was placed between the pump and the sample injection valve as a precaution against the accumulation of trace impurities from the carrier reagent onto the Fractogel.

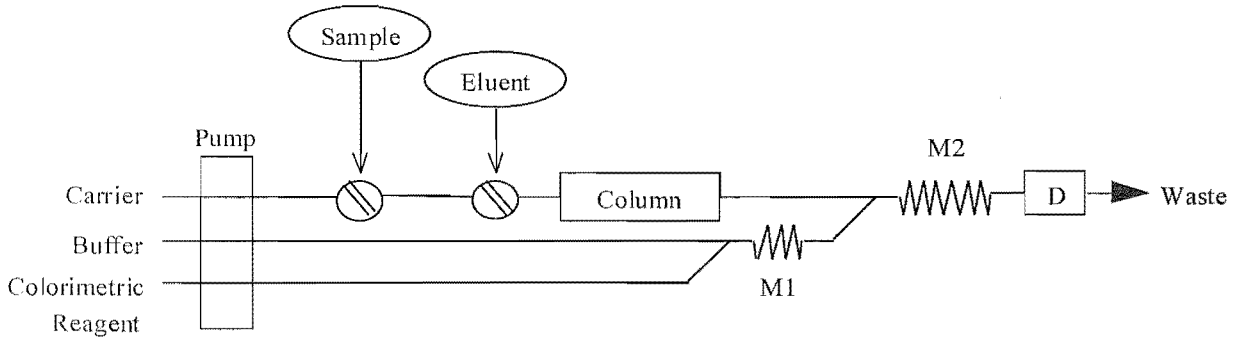

Figure 2.1. Flow injection analysis manifold for the analysis of 'free Al' and 'organic-bound Al' using a 22 μL micro-column containing oxine-derivatised Fractogel. Carrier solution = 0.05 M sodium acetate/0.05 M NaCl, pH 5.0 (ENE-10; 0.95 mm i.d. pump tube; 1.0 mL/min); Buffer = 2 M sodium acetate (ENE-04; 0.44 mm i.d. pump tube; 0.21 mL/min), pH 5.3; Colorimetric reagent = 2 mM CAS (ENE-01; 0.19 mm i.d. pump tube; 0.04 mL/min); Eluent = 0.03 M NaOH in 0.07 M NaCl; Pump speed = 40 r.p.m; D = UV/VIS detector (545 nm); Sample injection loop = 650 or 250 μL, Elution injection loop = 250 μL. Mixing loop M1 is 80 cm in length, M2 is 300 cm.

Aluminium standards and samples were injected into the carrier line using a 650 μL sample loop. A smaller 250 μL sample loop was used for samples from aluminium complexation capacity titrations and natural samples of high Al concentration, allowing an extension of the linear working range from ca. 20 μM to *ca.* 40 μM Al. 'Free' Al captured on the column was eluted as the aluminate ion ($Al(OH)_4^-$), using 250 μL of 0.03 M NaOH/0.07 M NaCl. This alkali/aluminate plug was subsequently reacted with CAS and buffered to pH 5.0 with 2 M acetate buffer at the merging zone. The method has a detection limit (2σ) for 'free Al' of 70 nM, a linear working range of *ca.* 0.2-25 μM and a relative RSD of 7% and 1% at 0.5 and 16 μM, respectively. Samples containing natural or model organic ligands exhibited an additional peak corresponding to a fraction of moderately-labile 'organic-bound' Al that is not captured by the resin (Figure 2.2). This peak appeared immediately after passage of the sample across the column and prior to elution of the captured 'free Al'. This peak is broader than elution peaks, due to the chromatographing of Al-ligand complexes along the column and increased dispersion of the sample plug as it passes through the column.

Quantifying this 'organic-bound' Al fraction required a separate calibration protocol. Aluminate standards were prepared by diluting the Al^{3+} stock solution in 0.03 M NaOH. Due to the high pH of these standards, the Al was not able to be sequestered by the column, and consequently experienced the same amount of dispersion through the column as that undergone by a sample. The plug of aluminate was subsequently buffered and quantified

downline as per normal, to give a linear calibration curve (unless specified otherwise, peak height was used for measurement purposes).

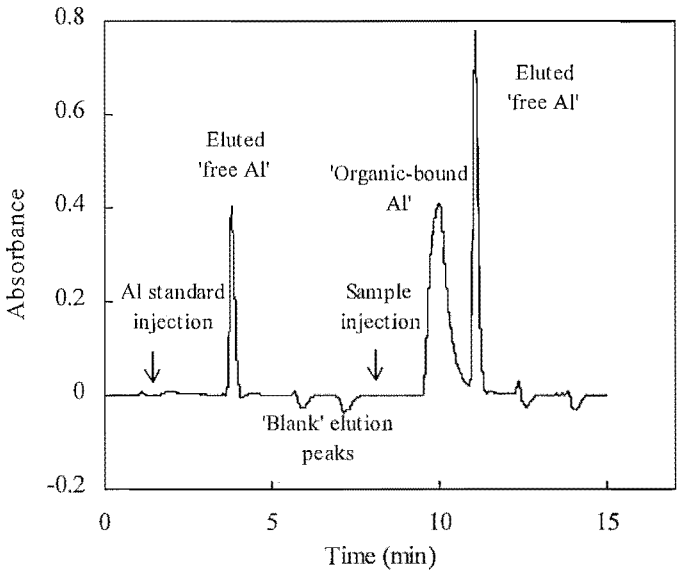

Figure 2.2. A scan showing the signals obtained from injections of a 5 μM Al^{3+} standard and a soil solution sample, using the oxine-derivatised Fractogel method.

The presence of polymeric hydroxy-aluminium species (*e.g.* $Al_{13}(OH)_{32}^{7+}$) was detected using a stopped-flow elution protocol. These species are retained by the column, but only a minor amount is eluted using the 0.03 M NaOH/0.07 M NaCl eluent. Quantitative removal and subsequent detection of polymeric species was achieved using 0.2 M NaOH (65 μL) with the carrier flow stopped for 2 minutes, in a 'stopped-flow' elution protocol.

2.2.8 Aluminium complexation capacity experiments

Aluminium complexation capacity (Al-CC) titrations were performed at 25 ± 0.1°C in a magnetically-stirred, water-jacketed cell. pH was measured with a Russell SWR757 glass and CR5 calomel electrode pair that had been calibrated as an $[H^+]$ probe (Section 10.2.9). Sufficient KCl (BDH AnalaR) was added to the titration solution to give a final concentration of 0.05 M. Titrations performed at pH 4.20, 4.70, 5.10 and 5.50 were buffered using 0.005 M acetic acid (Ajax AnalaR). Titrations at pH 6.50 were performed in the presence of 0.005 M MES buffer (Sigma).

For Al-CC titrations of fulvic acid and polyelectrolyte samples, a sufficient volume of stock fulvic acid, alginate or polyacrylamide was added to the titration cell to give the desired ligand concentration. Due to the impracticality of extracting sufficient quantities of soil

solution, Al-CC titrations were performed on diluted soil solutions (4 or 7 mL soil solution in a total cell volume of 40-60 mL).

Al-CC titrations involved the incremental addition of standardised Al^{3+} to the titration cell using a Gilmont micrometer syringe. When necessary, cell pH was adjusted during titrations by the addition of a small volume of *ca.* 1 M KOH (BDH AnalaR) using a second Gilmont micrometer syringe. The solution was stirred and mixed for 5 minutes, before a sample (2 to 5 mL) was withdrawn into a plastic syringe (Terumo, Japan). Samples were kept at 25°C for approximately 1-3 hours for equilibration, before 'free Al' and 'organic-bound Al' were analysed as described above. The 'free Al' values increased linearly for values of 'Total added [Al(III)]' in excess of the complexation capacity; Al-CC was derived from the intercept of the regression line through these data and the 'Total added [Al(III)]' axis. This intercept represents the limiting value of the Al binding capacity of soluble organic matter under excess metal conditions (Hawke *et al.* 1996).

2.2.9 Speciation calculations

The computer program SOLGASWATER (Eriksson, 1979) was used to perform speciation calculations. Relevant complexation, hydrolysis and protonation constants were selected from literature sources or from the IUPAC Stability Constants Database (Pettit and Powell, 1997). In instances where stability constants at a particular ionic strength were unavailable, the Davies Equation (Appendix II) was used to adjust selected constants to the desired ionic strength.

Selected stability constants for various H^+-Al^{3+}-ligand systems are given in the relevant chapters. Unless noted otherwise, the aluminium hydrolysis constants used for speciation calculations are those reported by Brown *et al.* (1985), obtained by numerical refinement of potentiometric data (25°C; 0.1 M $NaNO_3$). The hydrolysis constant for the species $Al(OH)_3$ was taken from Baes and Mesmer (1976). The hydrolysis constant for the formation of $Al(OH)_4^-$ was calculated by the method of Millero and Schreiber (1982) from the thermodynamic constants of Palmer and Wesolowski (1992) (assuming $\gamma(Al(OH)_4^-) = \gamma(OH^-)$).

Table 2.2. Hydrolysis constants ($\beta_{p,q}$) for aluminium used in this work (25°C). The $\beta_{p,q}$ values are defined according to the reaction $pH^+ + qAl^{3+} \rightleftharpoons Al_q(OH)_p^{(-p+3q)+}$.

Species	$\beta_{p,q}$	Log $\beta_{p,q}$
$Al(OH)^{2+}$	(-1,1)	-5.33
$Al(OH)_2^+$	(-2,1)	-10.91
$Al(OH)_3$	(-3,1)	-15.60
$Al_3(OH)_4^{5+}$	(-4,3)	-13.13
$Al_{13}(OH)_{32}^{7+}$	(-32,13)	-107.41
$Al(OH)_4^-$	(-4,1)	-23.30
K_w	(-1,0)	-13.79

2.2.10 Calculation of $[Al^{3+}]$

Concentrations of $[Al^{3+}]$ in soil solution were calculated in a two step process. Firstly $[AlF^{2+}]$, which is sequestered by the oxine-derivatised Fractogel, was subtracted from the measured 'free Al' to give the sum of the monomeric aluminium-hydroxy species concentrations. Secondly, $[Al^{3+}]$ was calculated from this value, by using the computer speciation program SOLGASWATER (Eriksson 1979). No correction was made for complexation of Al^{3+} by sulfate.

As noted above, AlF^{2+} is sequestered by the oxine-derivatised Fractogel and included as part of the 'free Al' measurement. AlF_2^+ and other aluminium fluoride complexes of higher coordination number are not sequestered. High soil solution concentrations of fluoride were almost exclusively found in pastoral soils with a known history of fertiliser application. In soils from exotic or indigenous forested areas, and for non-fertilised pastoral soils, the concentrations of fluoride in soil solution were generally low, and hence calculated concentrations of AlF^{2+} were negligible.

Thermodynamic aluminium-fluoride stability constants (I = 0.000 M, 25°C) (Nordstrom and May 1989), were adjusted to I = 0.005 M using the Davies equation, and to 10°C using the van't Hoff equation, and the enthalpies for aluminium fluoride complex formation (Nordstrom and May 1989). These calculations gave the following derived constants: $K_1 = 6.76$; log $*\beta_2 =$

12.29. Thermodynamic aluminium hydrolysis constants (Nordstrom and May 1989) were also adjusted to I = 0.005 M using the Davies equation, and to 10°C using the temperature-dependence equations for log *K published by Nordstrom and May (1989). The following derived constants were used: log $*K_t(Al^{3+})$ = -5.57; log $*\beta_2$ = -11.4; log $*\beta_3$ = -18.7; log $*\beta_4$ = -24.5. The ionic strength selected (I = 0.005 M) is typical of soil solutions from New Zealand topsoils (Edmeades *et al.* 1985), while the temperature correction to 10°C reflected approximate soil temperatures.

Using a derived mass-balance relationship (Appendix II), the soil solution pH and the measured concentrations of 'free Al' and total fluoride, the concentration of AlF^{2+} present in soil solution was calculated. This value was subtracted from the concentration of 'free Al', to give the sum of the monomeric aluminium hydroxy species concentrations ($[Al^{3+}]$ + $[Al(OH)^{2+}]$ + $[Al(OH)_2^+]$ + $[Al(OH_3)]$ + $[Al(OH)_4^-]$), which was used for the subsequent SOLGASWATER solution equilibrium calculations to determine the concentration of $[Al^{3+}]$ in soil solution.

The solubility line for gibbsite ($Al(OH)_3$) was calculated (Appendix II) using log $*K_{s0}$ (gibbsite) = 8.79, which was derived from the data of Palmer and Wesolowski (1992), after extrapolation to 10°C and to an ionic strength of 0.005 M. Temperature dependence data for log $*K_{s0}$ (amorphous $Al(OH)_3$) are not available, and therefore the value of log $*K_{s0}$ for 25°C (Stumm and Morgan 1981) was adjusted to 10°C by subtracting the correction calculated for log $*K_{s0}$ of gibbsite, to give log $*K_{s0}$ (amorphous $Al(OH)_3$) = 11.9.

2.2.11 Lucerne root elongation studies

Seeds of lucerne (*Medicago sativa* cv Wairau) were germinated for 72 h on damp filter paper in a growth chamber (16 h light, 8 h dark at 22.5°C), before being planted into pots containing 100 g of soil (field moist soil plus 10-15% TDW added by weight, equilibrated in the growth chamber for 72 h). Five seedlings were planted per pot, with three replicate pots per soil. The pots were placed in the growth chamber for a further 5 days, after which the seedlings were carefully removed and root length measured by ruler. The significance of differences in root elongation was established using paired *t*-tests.

2.2.12 Statistical analyses

Statistical analyses were performed using the statistical tools within Microsoft® Excel 97.

CHAPTER 3

GENERAL STUDIES OF SOIL ALUMINIUM CHEMISTRY

This chapter discusses the results of two sections of work concerning soil aluminium chemistry. The first section discusses the calculation of soil solution [Al^{3+}] concentrations from the experimentally-determined concentrations of 'free Al'. The mechanisms controlling soil solution Al^{3+} concentrations are discussed and related to results from a pH-dependent Al - fulvic acid binding curve. The second section discusses the interpretation of results obtained from a fulvic acid-aluminium complexation capacity titration.

SECTION A: THE RELATIONSHIP BETWEEN SOIL SOLUTION pH AND Al^{3+} CONCENTRATIONS IN A RANGE OF SOUTH ISLAND, NEW ZEALAND SOILS

3.1 INTRODUCTION

The toxicity of inorganic monomeric Al to plants and fish is well known and is discussed in Section 1.3 of this work. Equally well known is the low solubility of Al^{3+} at circumneutral pH (log K_{s0} (gibbsite) = -34.3; I = 0.0 M; Palmer and Wesolowski 1992). Simple calculations using this solubility product qualitatively explain the low concentrations of Al^{3+} in soil solution and natural waters, despite the high crustal abundance of Al. However, there is strong evidence, particularly at pH <5.0, that the monomeric Al concentration in soil solution is controlled by soil organic matter, rather than by hydroxide minerals (Mulder and Stein 1994). Several such studies are discussed below.

David and Driscoll (1984) found O horizon soil solutions from two forested sites were highly undersaturated with respect to a variety of evaluated mineral equilibria, with the soil solution aluminium activity appearing to be regulated by the dissociation of aluminium-organic complexes. In contrast, concentrations of aluminium in soil leachates from E and B horizons

(containing high DOC concentrations) while also generally indicating undersaturation with respect to $Al(OH)_3$ solid phases, were closer to the calculated solubility of a kaolinite solid phase. In a similar study, Driscoll *et al.* (1985) found that soil solutions from forested, acidic surface horizons (O and E) were highly undersaturated with respect to natural gibbsite, but approached saturation in the deeper horizons (of higher pH).

Walker *et al.* (1990) conducted a study to determine the influence of organic matter on the solubility of Al in organic soil horizons. Results showed that the equilibrium solubility of Al was dependent on solution pH, and the degree to which the organic matter was saturated with Al. No difference was noted when soils from different regions were compared, suggesting that the determination of aqueous Al concentrations in organic horizons could be achieved with a simple model. In an earlier paper Cronan *et al.* (1986) had also shown that the dissolved Al concentration in soils at pH <5.0 was dependent upon the Al loading of the organic matter.

Takahashi *et al.* (1995) found contrasting results for the A horizons of a series of soil samples. Non-allophanic Andosol and Spodosol samples displayed pAl *vs.* pH slopes of 2.0-2.4, considerably lower than those of the common $Al(OH)_3$ phases. In contrast, an allophanic Andosol sample had a slope of 2.9 and a solubility virtually equal to that of gibbsite. Quantification of the soil Al pools indicated that Al-humus complexes were the primary source of dissolved Al.

Heinrichs *et al.* (1996) found contrasting log $[Al^{3+}]$ *vs.* pH relationships in soil samples from a forested, acid sensitive region. The Al concentrations in soil solution from topsoil (2 to 4% organic carbon) indicated significant undersaturation with respect to Al-containing mineral phases. This supports a hypothesis that in acid soils, complexation by (solid phase) organic matter controls Al solubility, even in mineral soil horizons that are relatively low in organic carbon. At greater depths (30 to 180 cm) soils were oversaturated with respect to a crystalline gibbsite controlling phase, indicative of a 'natural' disordered $Al(OH)_3$ solid phase. Lawrence and David (1997) also found that the log $[Al^{3+}]$ *vs.* pH relationship was different for different soil horizons at the same site.

Many previous studies have not attempted to differentiate between operationally-defined concentrations of 'reactive Al' and $[Al^{3+}]$ *per se*. Earlier studies from this group used a rapid (7 s) FIA technique (Hawke and Powell 1994) to determine a 'reactive Al' fraction. This

method detected a small proportion of labile organic Al in addition to the inorganic monomeric Al species (Hawke and Powell 1994; Hawke *et al.* 1996). Simpson *et al.* (1997) analysed 16 water and soil solution samples using both analytical methods. The subsequent correlation obtained between the two methods allows the earlier 'reactive Al' results obtained from the 7 s FIA technique to be adjusted, giving a concentration of 'free Al' ($[Al^{3+}]$ + $[Al(OH)^{2+}]$ + $[Al(OH)_2^{+}]$ + $[AlF^{2+}]$) that is comparable to that obtained directly from the oxine-derivatised Fractogel method.

The aim of this study was to establish an $[Al^{3+}]$ *vs.* pH relationship for a series of soils from sites with contrasting vegetation (forest, pasture, or pasture reverting to forest), so that the phase(s) that controls Al solubility might be determined. In particular, the hypothesis that the same log $[Al^{3+}]$ *vs.* pH relationship (which links soil solution $[Al^{3+}]$ and soil solution pH), holds regardless of soil type and vegetation was tested. Results for seven soil types (determined by the oxine-derivatised Fractogel method) are combined with those from seven previously studied sites (determined by the 7 s FIA method). The results are compared with those for a previously-determined Al-fulvic acid binding curve.

3.2 MATERIALS AND METHODS

3.2.1 Sampling

Sites were chosen to cover a range of vegetation types and soil types (Figure 3.1, Table 3.1). Twelve of the fourteen sites had previously been sampled between December 1995 and February 1996. The two remaining sites (Cragieburn and Longslip) were sampled during March and May 1996. Samples were collected following the protocol described in Section 2.2.1, with 10-20 soil cores (0-7.5 or 0-10 cm, respectively) from each sampling site pooled, stored in sealed plastic bags in an insulated container for transport to the laboratory, and then refrigerated at 4°C.

3.2.2 Soil solution analyses

Soil solutions were extracted and filtered within 48 hours of sampling as described in Section 2.2.3. Soil solution pH and the concentration of total fluoride in soil solutions were determined as described in Section 2.2.4.

Table 3.1. Description of soil sampling sites.

Site	pH range	Soil type[A]	Vegetation
Craigieburn[B]	4.9 - 5.9	Allophanic Brown Soil	Indigenous forest + Tussock grasses + Shrub
Edendale[B]	5.0 - 7.0	Firm Brown Soil	Exotic pasture + Indigenous forest
Grey Valley[B]	4.1 - 4.7	Firm and Acid Brown Soils	Indigenous forest
Hinewai[B, C]	3.6 - 5.7	Typic Firm Brown Soil	Regenerating forest[B] + Indigenous forest[C]
Invermay[B]	5.8 - 6.6	Fragic Pallic Soil	Exotic pasture
Longslip[B]	5.9 - 7.6	Brown and Recent Soils	Exotic pasture
Telford[B]	6.0 - 6.2	Perch-Gley Pallic Soil	Exotic pasture + Indigenous forest
Bealey Spur[C]	2.7 - 4.1	Typic Orthic Podzol	Indigenous forest
Broken River[C]	4.1 - 5.1	Typic Orthic Brown Soil	Indigenous forest
Riccarton Bush[C]	4.7 - 5.5	Typic Orthic Gley Soil	Indigenous forest
Maher Creek[D]	3.9 - 4.6	Acidic Orthic Brown Soil	Indigenous forest
Punakaiki[D]	3.6 - 4.7	Acidic Orthic Brown Soil	Indigenous forest
Tekapo[E]	4.3 - 5.8	Immature Pallic Soil	Exotic pasture

[A] New Zealand Soil Classification (Hewitt 1993).

[B] Previously unpublished data.

[C] Powell and Hawke (1995).

[D] Hawke and Powell (1995).

[E] Powell *et al.* (1997).

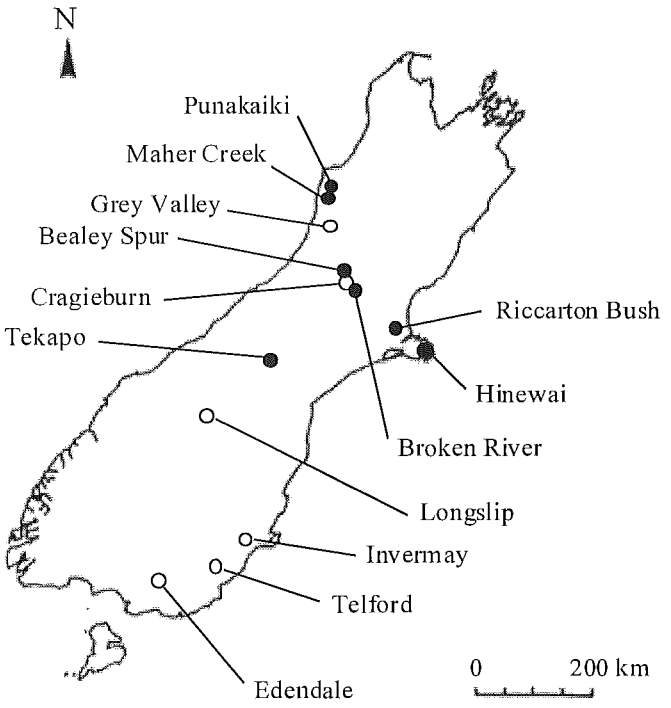

Figure 3.1. Soil sampling locations (○ indicate sites where soil solution was analysed using the oxine-derivatised Fractogel method; ● indicate soil solutions analysed using the 7 s FIA method.

'Free Al' was measured using either the oxine-derivatised resin Fractogel method (described in Section 2.2.7), or by the rapid chrome azurol S (CAS) method of Hawke and Powell (1994). The latter method involves a rapid direct reaction (*ca.* 7 s) between Al^{3+} and the colorimetric reagent CAS in a flow injection analysis (FIA) manifold. The short reaction time ensures that only the most labile aluminium species are able to react before detection occurs. Al is quantified by the spectrophotometric measurement of a rapidly-forming reaction intermediate, using an isosbestic point.

3.2.3 Combination of results from different studies

As noted above, results from studies using two aluminium analytical methodologies have been combined. The earlier studies (Hawke and Powell 1995; Powell and Hawke 1995; Powell *et al.* 1997) used the rapid (7 s) FIA method of Hawke and Powell (1994) (Al_{7s}). Later studies used the oxine-derivatised Fractogel resin method (Al_{resin}). A correlation (Figure 3.2) based on the data of Simpson *et al.* (1997) established the relationship between the different fractions of 'free Al' as measured by the two protocols: $Al_{resin} = 0.89\ Al_{7s}$ ($r^2 = 0.88$, n = 16). This relationship was used to convert the Al_{7s} values to the resin-based definition of 'free Al', before calculation of $[Al^{3+}]$.

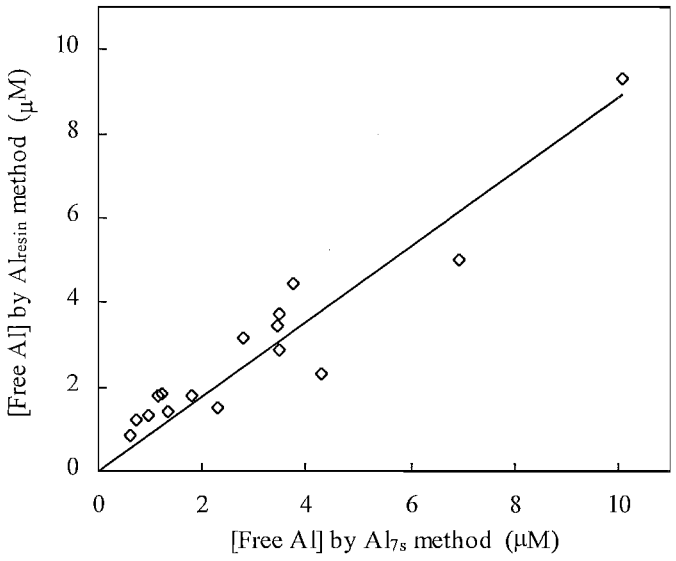

Figure 3.2. Data from Simpson *et al.* (1997) showing the correlation between the 1.3 s oxine-derivatised resin method and the rapid 7 s FIA method of Hawke and Powell (1994). The least-squares regression line has slope of 0.89 ($r^2 = 0.88$, n = 16).

The Al-fulvic acid (FA) binding curve experiment was taken from Hawke *et al.* (1996). The fulvic acid was isolated from International Humic Substance Society (IHSS) reference peat by the acid pyrophosphate-XAD-7 method (Gregor and Powell 1986). A fulvic acid concentration of 17 mg L^{-1} and 9 μM Al in 0.05 M KNO_3 electrolyte (60 mL) was used. Aliquots (1 mL) were removed from the experimental solution throughout the pH range 2.5-7.0 and 'free Al' was subsequently determined by the Al_{7s} method. The obtained values of 'free Al' (Al_{7s}) were converted to Al_{resin} using the relationship above.

3.2.4 Calculation of $[Al^{3+}]$

Concentrations of $[Al^{3+}]$ in soil solution were calculated using the computer speciation program SOLGASWATER (Eriksson 1979). This used the sum of the monomeric aluminium hydroxy species concentrations ($[Al^{3+}] + [Al(OH)^{2+}] + [Al(OH)_2^+] + [Al(OH_3)] + [Al(OH)_4^-]$), that was obtained by subtracting the calculated concentration of AlF^{2+} from the measured concentration of 'free Al' (as described in Section 2.2.10). Thermodynamic stability constants for aluminium hydrolysis and for aluminium fluoride complexation were adjusted to an ionic strength of 0.005 M (typical for soil solutions from New Zealand topsoils (Edmeades *et al.* 1985)) and to a temperature of 10°C (which reflects approximate soil temperatures) (Section 2.2.10). No correction was made for complexation of Al^{3+} by sulfate. Aluminium sulfate complexes are of low stability, and are typically found only in areas subject to acidic deposition, where pH is low and the SO_4^{2-} concentration is high (Driscoll and Postek 1996).

3.3 RESULTS

Results of soil solution 'free Al' analyses that were obtained using the rapid 7 s FIA method may be found in the following papers: Hawke and Powell (1995), Powell and Hawke (1995) and Powell *et al.* (1997). The previously unpublished results (Nilsson and Adams) for soil solution pH and 'free Al' analyses, obtained using the oxine-derivatised Fractogel method, are given in Table 3.2. A table containing results for soil solution pH, 'free Al' and fluoride measurements for all sites is given in Appendix III. For sites where fluoride measurements were not performed, the total [F] used to calculate [AlF^{2+}] in soil solution was obtained using averaged results from neighbouring sites, or estimated using results obtained for similar sites. These sites are marked by (*) in Appendix (III).

The plot of log [Al^{3+}] *vs.* pH (Figure 3.3) shows that the calculated [Al^{3+}] spanned 8 orders of magnitude, from 10^{-4} to 10^{-12} M, over the pH range 2.67-7.62. All data fitted the same curve, with no patterns attributable to variation in vegetation or soil type. An outlier (at log [Al^{3+}] = -4.42, pH = 4.13) was from indigenous forest in the Grey Valley. Other samples from this site fitted the overall trend well. Although low pH data were predominantly from forested sites and high pH data were predominantly from pasture sites, there was significant overlap. Results from forest sites were in the pH range 2.67 to 6.00 while pasture sites were in the pH range 4.33 to 7.62.

Samples from two sites, Longslip (pH range 5.88-7.62) and Invermay (pH range 5.78-6.57), included soils from liming experiments. At Longslip, both limed and unlimed areas were sampled. All results from these sites, despite having widely different total [F^-], fitted the trend established for other sites (Figure 3.3). This indicates that the [Al^{3+}] has reached a steady state within the elapsed time following lime application.

While the samples were mostly from A horizons, samples from B, Oa and E horizons were also analysed. The wide geographic extent of sampling also ensured that soils came from a range of parent materials including alluvium, basalt, glacial till and loess. There was no discernible deviation from the overall trend in Figure 3.3 that could be ascribed to a soil effect.

Table 3.2. Previously unpublished analytical data obtained using the oxine-derivatised Fractogel method.

Site	pH	Free Al (μM)	Site	pH	Free Al (μM)
Cragieburn	5.93	2.8	Invermay	5.78	2.3
	5.59	1.0		6.00	1.5
	4.85	3.7		6.57	0.40
	5.18	1.6		6.08	1.3
Edendale	5.02	4.2		6.51	0.38
	6.99	0.19	Longslip	7.12	0.48
	5.78	0.88		7.47	0.50
	5.34	2.2		7.62	1.0
Grey Valley	4.36	4.3		7.07	0.56
	4.67	3.2		7.44	0.87
	4.59	4.6		7.12	0.96
	4.13	40.2		6.09	0.52
	4.59	3.2		6.16	0.40
Hinewai	5.37	0.86		6.25	0.43
	5.40	1.2		5.96	0.51
	5.56	1.3		5.93	0.75
	5.63	1.8		6.20	0.31
	4.93	4.5		5.88	0.71
	5.71	1.8	Telford	6.00	1.4
				6.18	1.2

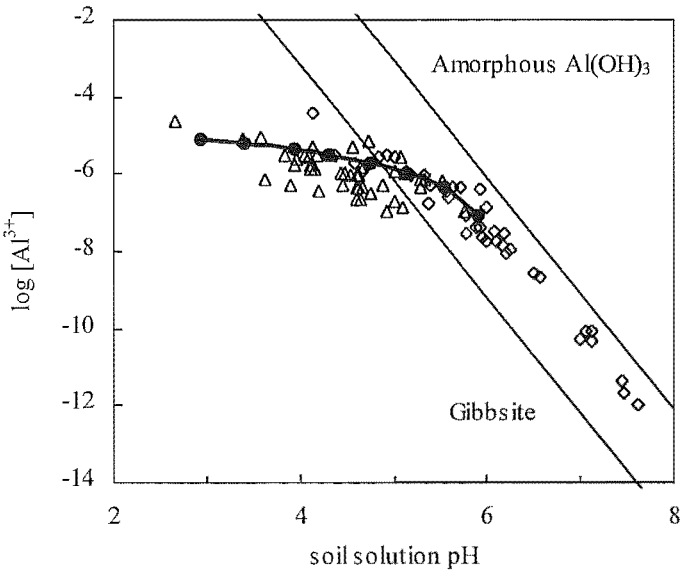

Figure 3.3. Relationship between log $[Al^{3+}]$ and soil solution pH (◇ data obtained using the 1.3 s oxine-derivatised resin method; △ data obtained using the rapid 7 s FIA method of Hawke and Powell (1994)). The solid curve shows data (●) for binding of Al to a soil fulvic acid (from Hawke *et al.* 1996) converted to log $[Al^{3+}]$ as explained in the text. The solubility line for gibbsite was calculated using log $*K_{s0}$ = 8.79, that for amorphous $Al(OH)_3$ was calculated using log $*K_{s0}$ = 11.9.

3.4 DISCUSSION

3.4.1 Effect of pH on solubility

While there was no discernible vegetation or horizon effect, the plot of log $[Al^{3+}]$ *vs.* pH (Figure 3.3) showed two distinct regions. At pH >5.7, the data were consistent with $[Al^{3+}]$ solubility control by an $Al(OH)_3$ solid phase (slope = -2.7, r^2 = 0.96). At pH <5.0, the slope was much lower (-0.59, r^2 = 0.26), indicative of solubility control by a different phase.

The general consensus for solubility control in acid soils is that an organic phase is involved (Cronan *et al.* 1986; Walker *et al.* 1990; Mulder and Stein 1994; Powell and Hawke 1995). This hypothesis was evaluated by reference to an aluminium fulvic acid binding curve (9 μM Al^{3+}, 17 mg/L fulvic acid; Figure 4 from Hawke *et al.* 1996). The 'free Al' data for this curve were converted to $[Al^{3+}]$ as described above, using the established correlation between Al_{7s} and Al_{resin}, and the adjusted Al^{3+} hydrolysis constants. The results (solid curve Figure 3.3) show that the pH - log $[Al^{3+}]$ data for fulvic acid closely follow the soil data over the available pH range (3.0-6.0). This comparison used a fulvic acid binding curve, but in organic soils the distribution of Al^{3+} between soil solution and the solid phase will be controlled by both fulvic

acids and the less soluble humic acids. At any given pH, the binding curve shown is valid for only one aluminium and fulvic acid concentration. In soils, where concentrations of soluble aluminium and organic acids will increase as pH decreases, the apparent position of a binding curve could well lie slightly lower (for ligands having a higher affinity for Al than the sample of fulvic acid used), or higher, than the curve given in Figure 3.3.

At pH >5.6, the data in Figure 3.3 indicate equilibrium with a phase for which the dissolution reaction in acid media consumes $3H^+$ per Al^{3+}. This condition is met by gibbsite, kaolinite, imogolite, halloysite, amorphous $Al(OH)_3$ and hydroxy-aluminous interlayers of 2:1 layer silicates. The very slow equilibration rate of kaolinite and of 2:1 layer silicates (Dahlgren and Ugolini 1989) indicates that these are probably not the phases that control $[Al^{3+}]$. Microcrystalline gibbsite, amorphous $Al(OH)_3$ and hydroxy-aluminous interlayers seem the most likely, both from their equilibration rates and $*K_{s0}$ values. The data in Figure 3.3 also indicate that at pH <5.0, soil solutions were under-saturated with respect to solid phases such as gibbsite and amorphous $Al(OH)_3$. It can be inferred that, given adequate time for equilibration, and an excess of organic matter, these phases may not co-exist with humic and fulvic acids at pH <5.0.

The pH range for the fulvic acid binding curve (Figure 3.3) includes the low pH end of the region considered to be controlled by $Al(OH)_3$ solubility. 'Binding' of Al at pH *ca.* 6 could be *via* fulvic acid adsorption onto an $Al(OH)_3$ colloid rather than fulvic acid binding *per se* in homogeneous solution. Colloidal $Al(OH)_3$ does not react with the reagent CAS in the time scale of the kinetic FIA technique used to determine the binding curve, and would not be determined as 'free Al'.

It should be noted that the pH of a soil solution and that of the parent soil will not be the same. Work from this group has consistently indicated that freshly extracted soil solutions have a pH *ca.* 0.4 above the value measured for a field-moist soil slurry (1.0:2.5 soil:H_2O ratio) and *ca.* 0.7 pH above that measured for an air-dried soil (Adams *et al.* 1996; Chapter 4, Chapter 5). Thus in Figure 3.3 the 'break point' in the data at pH *ca.* 5.6 should be interpreted as a soil pH of *ca.* 5.2 (field moist) or *ca.* 4.9 (air dried).

3.4.2 Sources of random error

The soil data in Figure 3.3 show a degree of scatter. Data from all sampling sites showed intra-site scatter, indicating that at least some of the scatter is real. Cronan *et al.* (1986) showed that Al solubility varied as a function of the degree of Al saturation on the organic matter. These workers noted that the greater the degree of saturation, the greater the resulting Al activity at a given pH. Much of the scatter observed in Figure 3.3 may therefore be due to different degrees of Al saturation on the organic matter. In addition, there are four potential sources of analytical error (*i*) Al analyses, (*ii*) fluoride analyses, (*iii*) pH analyses, and (*iv*) assumptions made in the speciation calculations. The RSD of the oxine-derivatised Fractogel method for 'free Al' was estimated by Simpson *et al.* (1997) to be 1% at 16 μM and 7% at 0.3 μM. Uncertainty associated with this level of precision is negligible compared with the scatter shown in Figure 3.3. At low concentrations of total fluoride in soil solution (< *ca.* 5 μM), the performance of the fluoride ion-selective electrode is likely to be relatively poor, resulting in low accuracy for calculated concentrations of $[AlF^{2+}]$. This will certainly have contributed to the observed scatter in Figure 3.3.

For measurements of pH at the low ionic strengths typical of freshwaters and soil solution, a precision of the order of ± 0.02 pH can be achieved by using carefully maintained, top-quality electrodes (Davison 1990). In practice though, this level of precision is unlikely to be attained, and a precision of ± 0.1 pH (± 25% in $[H^+]$) is perhaps more realistic. This level of precision would contribute to the scatter in Figure 3.3 at pH >5.0, but does not account for the scatter at lower pH.

No account was taken of the site-specific effects of temperature and ionic strength on the Al^{3+} hydrolysis, and aluminium fluoride stability constants. The stability constants used in calculations were valid for 10°C and I = 0.005 M. Ionic strength measurements were not made for any site, but ionic strengths in the New Zealand topsoils sampled by Edmeades *et al.* (1985) were reported in the range 0.003-0.016 M, with a typical value of 0.005 M. Temperature measurements were made only at the forest sites reported by Powell and Hawke (1995) and at the Longslip sites. Both temperature and ionic strength effects on equilibrium constants can significantly affect speciation calculations (Hawke and Hunter 1992). However, temperature and ionic strength measurements could be misleading, because of (*i*) kinetic effects arising from the need to wet some soils before soil solution extraction (Edmeades *et al.* 1985), (*ii*) decreases in ionic strength due to CO_2 degassing (Dahlgren *et al.* 1997) and (*iii*) soil re-equilibration during sample processing (*e.g.* the centrifuging of soil samples at room

temperature after storage at 4°C). During the storage time (albeit short) prior to soil solution extraction, the changes in soil temperature, and CO_2 degassing could also promote slow changes that involve complexation or dissolution.

Notwithstanding the lack of actual measurements and the difficulty in obtaining reliable values for ionic strengths, some idea of the size of potential effects can be gained. The sampling carried out by Powell and Hawke (1995) was in winter at moderate elevations, with soil temperatures in the range 3 to 7°C. At Longslip, soil temperatures were in the range 6-10°C. In contrast, the sampling carried out by Powell *et al.* (1997) was in summer at a location where soil temperatures were closer to 15°C.

Using the temperature-dependence equations given by Nordstrom and May (1989), the equilibrium constant values at 0.005 M ionic strength and 3°C (15°C) are log $*K_1$ = -5.78 (-5.42), log $*\beta_2$ = -11.9 (-11.0), log $*\beta_3$ = -19.5 (-18.2) and log $*\beta_4$ = -25.4 (-23.9). At pH 6.00 and 1.0 μM total 'free Al', the effect of this temperature difference is to change the value of log $[Al^{3+}]$ from –6.60 (3°C) to –7.22 (15°C). At 10°C a change in ionic strength from 0.000 to 0.005 M decreases the stability constants by 0.13 to 0.2 log units. With the preceding example and a temperature of 10°C, the value of log $[Al^{3+}]$ changes from -7.07 (0.000 M) to -6.91 (0.005 M). Overall, therefore, the magnitude of temperature and ionic strength effects on stability constants may account for much of the scatter observed in Figure 3.3.

3.4.3 Sources of systematic error

The accuracy of the data plotted in Figure 3.3 must be considered. In particular, the relationship at pH >5.6 may be subject to a systematic error. As plotted, the data fall between the solubility lines for amorphous $Al(OH)_3$ and gibbsite. Errors arising from the slow re-equilibration between solution and solid phase Al will move the data toward the gibbsite solubility line. Furthermore, if the FIA-chelating resin technique of Simpson *et al.* (1997) over-estimates free Al (by sequestering some Al from labile organic complexes), then correction of the data would also move the points toward the gibbsite solubility line. However, the method validation experiments carried out by Simpson *et al.* (1997) using malonate, oxalate and citrate as model ligands, suggest that any sequestering of Al from organic-bound complexes is minor.

Another potential source of systematic error is pH measurement. Dahlgren *et al.* (1997) noted the loss of CO_2 from soil after sampling and during centrifugation. Provided the soil solution is in contact with the soil the pH change arising from degassing of soils is insignificant. However, CO_2 loss from the extracted soil solution can be significant and may have contributed to the observed increase in pH. Microbial oxidation of organic matter in the extracted soil solution is also a potential source of pH error. This effect is likely to be insignificant given (*i*) immediate analysis after soil solution extraction, and (*ii*) membrane filtration (0.025 μm) that would essentially sterilise the solution.

3.4.4 Polymeric Al hydroxy species

The possible presence of polymeric Al species (*e.g.* $Al_{13}(OH)_{32}^{7+}$ - 'Al_{13}') in the measured 'free Al' was discounted. Simpson *et al.* (1997) established that negligible amounts of Al_{13} captured on the resin were eluted by each injection of 0.03 M NaOH, and therefore are not quantified as part of the 'free Al' fraction. However, the question of whether this species actually exists in soil and/or soil solution is contentious.

Only one published report claims the presence of Al_{13} (detected by ^{27}Al NMR) in soil samples (Hunter and Ross 1991). However, subsequent NMR investigations (by the same authors) performed on a large number of soil samples (including the original sites where Al_{13} was detected) failed to reveal any further indications of its presence (Bertsch and Parker 1996). Hiradate *et al.* (1998) used ^{27}Al NMR in an unsuccessful attempt to detect Al_{13} in 1 M KCl soil extracts from seven soils. They concluded that either Al_{13} is not formed in the soils, or it is strongly adsorbed to mineral surfaces or solid-phase organic matter. However, the pH of their soil extracts ranged from 3.0 to 4.2, and it is unlikely that the Al_{13} polymer would persist in such acidic solutions.

Furrer *et al.* (1992) simulated natural conditions by passing acidic Al solutions over granulated marble. Over two-thirds of the monomeric Al was converted to polynuclear Al_{13} (measured by ^{27}Al NMR spectroscopy), suggesting that Al_{13} formation may be possible in nature if the total Al concentration is sufficiently high. In addition, several recent studies (Rosseland *et al.* 1992; Poléo *et al.* 1994; Witters 1998) have attributed increased fish toxicity observed at the confluence of acidic rivers with limed tributaries, to the formation of soluble polynuclear aluminium species. However, no study has attempted to identify the proposed Al polymeric species.

3.5 CONCLUSION

Concentrations of $[Al^{3+}]$ were calculated in soil solutions from concentrations of the experimentally-determined monomeric 'free Al' species ($[Al^{3+}] + [Al(OH)^{2+}] + [Al(OH)_2^+] + [Al(OH_3)] + [Al(OH)_4^-] + [AlF^{2+}]$). Soil solution samples came from 13 sites encompassing a range of New Zealand soils (Brown, Gley, Pallic, Podzol and Recent Soils), and vegetation types (pasture, shrub lands and indigenous and exotic forest). The resultant data ($n = 85$) covered the pH range 2.7-7.6, and showed a single curvilinear relationship between log $[Al^{3+}]$ and pH, indicating that the same phase(s) are controlling Al solubility, regardless of vegetation or soil type. Two solubility controls are consistent with the data: soil organic matter at pH <5.0, and a solid $Al(OH)_3$ phase at pH >5.6.

Support for organic control of $[Al^{3+}]$ in acid soils comes from the high correlation between the soil data and $[Al^{3+}]$ calculated from the fulvic acid – Al^{3+} binding curve. Organic control of $[Al^{3+}]$ in acid soil decreases plant exposure to Al toxicity that would otherwise occur if $[Al^{3+}]$ was controlled by $Al(OH)_3$ solubility. Organic ligands arise from litter decomposition and are therefore part of the natural acidifying (and soil impoverishment) process. They have also been shown to arise from direct exudation by root systems (*e.g.* Makepeace *et al.* 1985; Jones and Kochian 1996), and such processes can be interpreted as an adaptive strategy on the part of the particular plant species or community. The results imply that natural organic matter generated from litter decomposition controls $[Al^{3+}]$ at pH <5.0, but leave open the question of additional plant protection against Al toxicity at higher pH by exudation of Al^{3+}-complexing ligands.

SECTION B: ALUMINIUM COMPLEXATION CAPACITY TITRATION OF A SOIL FULVIC ACID

3.6 INTRODUCTION

The complexation capacity of a material represents the limiting value of the Al binding capacity of the soluble organic species, under excess (forcing) metal conditions (Hawke *et al.* 1996). Values of the complexation capacity of a ligand are generally pH dependent, for as the pH is decreased, metal binding strength decreases as proton competition becomes increasingly important.

The determination of complexation capacity (CC) measurements has conventionally been performed using voltammetric (ASV) or potentiometric (ISE) methods. The major difference between these two methodologies is that ASV measurements are kinetically based and result in an operationally defined CC, dependent upon the thickness of the diffusion layer at the electrode surface. In contrast, results from ISE methods produce an equilibrium CC value, which may (in principle) be used in relevant metal-ligand equilibrium calculations. However, potentiometric methods using ion-selective electrodes commonly suffer from poor sensitivity, and may overestimate the (equilibrium) value of the complexation capacity due to the formation of ion-pairs (*e.g.* with chloride (Hawke *et al.* 1996)).

A range of graphical methods have been used to determine the complexation capacity of a material from experimental titration data (*e.g.* see discussion within Hawke *et al.* 1996). The method used for this work uses a simple linearisation procedure, taking the *x*-intercept of a line fitted through the final 'free Al' data points of the titration, in excess of the aluminium complexation capacity (Al-CC) value. This method assumes that binding is due to the presence of strong ligands only, and so may underestimate the true Al-CC. The resulting operational Al-CC value is defined as the maximum amount of Al that remains bound to the soluble organic material, and which is not sequestered during the *ca.* 1.1 s contact time with the oxine-derivatised Fractogel.

This section describes an Al-CC titration for a standard fulvic acid sample. The same protocols were used for performing Al-CC titrations for soil solutions - work described in later chapters.

3.7 MATERIALS AND METHODS

The aluminium complexation capacity (Al-CC) titration was performed following the protocol described in Section 2.2.8. The sample of fulvic acid had previously been isolated from International Humic Substance Society (IHSS) reference peat by the acid pyrophosphate-XAD-7 method (Gregor and Powell 1986). Chemical characterisation data for this sample of fulvic acid is given in Section 2.1.6.

The Al-CC determination involved the incremental addition of Al^{3+} (0-*ca.*55 μM) to a solution containing 17 mg/L fulvic acid, buffered to a pH of 4.7 (0.005 M acetate buffer, 0.05 M KCl). Total cell volume was 150 mL. After the addition of an increment of Al, the solution was equilibrated for 3 minutes before a sample aliquot (5 mL) was withdrawn from the cell. Aliquots removed from the titration were equilibrated for a further *ca.* 120 min before 'free Al' and organic-bound Al' were analysed using the oxine-derivatised Fractogel method (described in Section 2.2.7.2). The analysis did not require the entire 5 mL sample, and the remaining volume for half the samples was refrigerated, and re-analysed after a further equilibration period of 24 hr. This established whether the samples had reached equilibrium in the *ca.* 120 min before the initial analysis. The refrigerated samples were allowed to warm to room temperature before analysis.

A 'blank' Al-CC titration was performed in the presence of 0.05 M acetate buffer and 0.05 M KCl, (but in the absence of fulvic acid), to determine whether weak Al-acetate complex formation might potentially interfere in the Al-CC titrations.

3.8 RESULTS AND DISCUSSION

The aluminium complexation capacity curve obtained for the sample of fulvic acid is given in Figure 3.4. Data are also shown for the concentrations of 'free Al' obtained from the 'blank' acetate titration (×). A line fitted through these points has a zero intercept and a slope of 0.99 (r^2 = 1.00), following the predicted theoretical values. As neither measurable concentrations of 'organic bound Al' nor an Al-CC intercept were observed for this 'blank' titration, it is inferred that acetate has a negligible effect on Al-CC titrations.

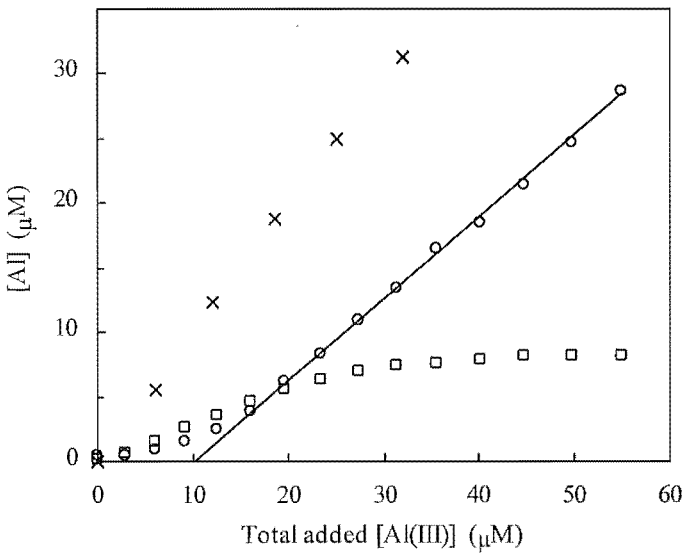

Figure 3.4. Aluminium complexation capacity curve for a fulvic acid sample (pH 4.7, 0.005 M acetate buffer, 0.05 M KCl). The slope of the fitted line is 0.64, r^2 = 1.00. (○ 'free Al'; □ 'organic-bound Al'; × 'blank' Al-CC titration).

Extrapolation of a fitted line through the 'free Al' data in excess of the complexation capacity, gives an intercept (Al-CC) with the *x*-axis of 10.1 μM, corresponding to a binding capacity (at pH 4.7) of 16.0 mg Al/g fulvic acid (594 μM Al/g fulvic acid). Given the weight *per* mole of titratable carboxyl groups for this fulvic acid has previously been determined as 137 (Gregor 1987), the theoretical complexation capacity for this fulvic acid is 197 mg Al/g COOH equivalent, assuming 1:1 complexation between aluminium and carboxyl sites. The intercept of 10.1 μM represents the sum of the non-labile (inert) and moderately-labile 'organic-bound Al' fractions. The 'organic-bound' Al concentrations, which represent an operationally-defined 'moderately-labile' fraction of aluminium, reach a plateau at a concentration of *ca.* 8 μM Al, representing a gradual saturation of these 'moderately-labile' binding sites with aluminium. This plateau of 8 μM Al is reached after the addition of *ca.* 40 μM aluminium, indicating that these 'moderately-labile' sites do not strongly bind Al. Interestingly, the slope through the 'free Al' datum points in excess of the Al-CC has a considerably smaller slope (slope = 0.64) than the theoretical slope of 1.0. Smaller slopes than the theoretical have been reported previously for Al-CC titrations (Powell and Hawke 1995; Hawke *et al.* 1996). The smaller slope indicates the difficulty in fully saturating the fulvic acid with Al. There is a gradual saturation of complexation sites of varying stability and lability (Powell 1998).

Results from the samples that were analysed after an equilibration period of 24 hours are compared with those analysed after 120 min equilibration in Figure 3.5. Results from the two

experiments are in excellent agreement, confirming that an initial period of *ca.* 120 min was sufficient for the added aluminium and fulvic acid to reach equilibrium.

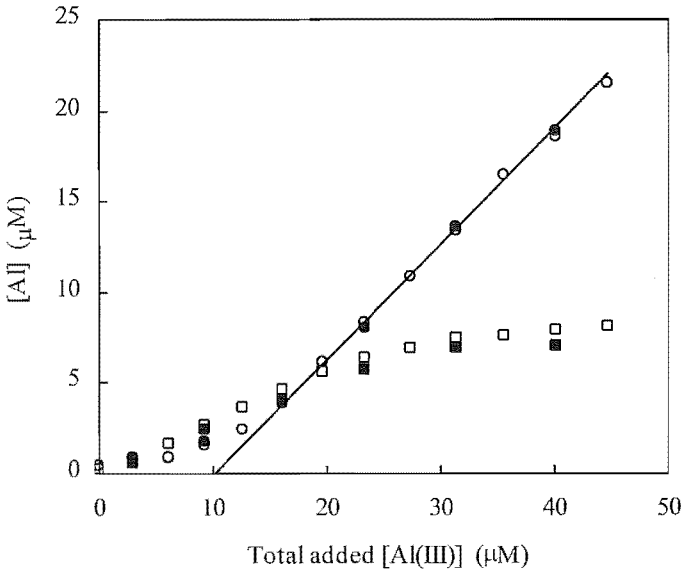

Figure 3.5. Aluminium complexation capacity titration curve showing comparison between concentrations of 'free Al' (○) and 'organic-bound Al' (□) in samples that (*i*) - (open symbols) had been analysed after *ca.* 120 min equilibration time and, (*ii*) - (filled symbols) were analysed after a further 24 hours equilibration time.

3.9 CONCLUSION

The aim of this work was to use the oxine-derivatised Fractogel method to obtain a complexation capacity curve for a soil-extracted fulvic acid sample. The Al-CC for a 17 mg/L solution of fulvic acid was found to be 10.1 μM Al (594 μM Al/g fulvic acid) at pH 4.7. 'Moderately-labile' aluminium complexation sites accounted for *ca.* 80% of the total fulvic acid binding sites, the remaining *ca.* 20% of complexation sites were non-labile (strongly-complexing).

Operationally, the presence of 0.005 M acetate buffer was found to have no measurable effect on the complexation capacity titrations. No difference was found between the concentrations of 'free Al' and 'organic-bound Al' for Al-CC samples equilibrated for *ca.* 120 min and those equilibrated for 24 hours, indicating that a *ca.* 120 min period was sufficient to attain equilibrium.

CHAPTER 4

ALUMINIUM SPECIATION IN SOUTH ISLAND HIGH COUNTRY SOILS

This chapter is in two sections. The first section discusses an investigation of aluminium speciation in soil solutions obtained from an altitude sequence of high country pastoral soils in South Canterbury, New Zealand. A second section reports the results of a study investigating *Hieracium* growth in high country pastoral soils and the associated soil solution aluminium speciation.

SECTION A: ALUMINIUM SPECIATION IN AN ALTITUDE SEQUENCE OF HIGH COUNTRY SOILS

4.1 INTRODUCTION

The long-term sustainability of pastoral farming on seasonally dry high country soils is dependent on achieving a balance between nutrient inputs and nutrient losses, at minimal cost. Despite the often low productivity of such soils, O'Connor and Harris (1991) suggested that 150 years of high country pastoralism has caused significant losses of N, P, K and S. They argued that nutrient removal and transfer under grazing pastoralism and from leaching losses could exceed the rate of supply of nutrients by weathering. This view has been confirmed by later studies (*e.g.* McIntosh 1997). Legume-based pastures can be established on these soils if adequate S and P are provided (McIntosh *et al.* 1985).

To detect long-term soil changes, a soil monitoring network consisting of 38 sites was established in 1978 on steeplands at 730 to 1250 m on Longslip Station, South Canterbury. In 1979 the area was over-sown with clover and grasses and S(28%)-fortified superphosphate was applied at approximately 100 kg/ha.year between 1979 and 1992. The pre-trial topsoil pH at the study site (mean 5.8; 0-7.5 cm) was ideal for legume growth, but acidification was expected from the regular application of elemental S, the release of H^+ by legumes and the

greater dry matter production and return of organic matter to the soil. The impact of acidification could be significant, considering the medium to low percentage base saturation range of these soils.

Since 1978, topsoils (0-7.5 cm) have indeed become more acid, and average topsoil $pH_{(H_2O)}$ has decreased. McIntosh *et al.* (1994*a*, 1994*b*) noted that from 1978 to 1992 the average pH (1:3 soil:water ratio) of air-dried topsoil (n = 38) decreased from 5.79 to 5.40 (*ca.* 0.03 pH per year). This decrease was consistent with the amount of dry matter (DM) produced and the application rate of elemental S (McIntosh *et al.* 1985). By 1996, topsoil pH had fallen to 5.25. A larger pH decrease has been observed at the higher sampling sites. In a recent study Ruth *et al.* (1998) found soil pH was generally lower, and extractable (0.01 M $CaCl_2$) aluminium concentrations higher, on hilltops than in base-of-slope locations for acid soils in a Victorian (Australia) catchment area. Findings of decreased pH at sites of higher altitude can be rationalised on the basis of exchangeable cation leaching exceeding the rate of weathering in the high altitude soils. Although New Zealand high country soils are generally only weakly leached (McIntosh *et al.* 1994*b*), there is nevertheless a net removal of exchangeable cations from soil colloids at the higher sites (replaced by H^+ and Al^{3+}), whereas at lower altitudes cation leaching and plant-induced weathering are more in balance.

Such acidification at the Longslip site, if continued, has the potential to reduce legume production by release of Al^{3+} from exchange sites and into soil solution. Liming would probably be required if the soil pH fell to 5.0, but even with increased productivity (to around 6 tonne DM/ha), it is probably not economical to apply lime to such soils (McIntosh *et al.* 1994*b*). Other changes observed (0-7.5 cm soil depth) included a significant increase in soil C (from 3.3 to 5.5%), a 13% decrease in %N for shady slopes and a 26% increase for sunny slopes (McIntosh *et al.* 1994*b*). The increase in percentage soil carbon from 3.3% is of particular significance. For soil organic matter a figure of 2.5% C is critical. Below this threshold, there are problems with soil structure (leading to increased rates of topsoil loss from rain and wind erosion) and with seed germination.

This investigation reports the results of a detailed analysis of the aluminium chemistry of soil solutions from an altitude sequence (730-1190 m) of South Canterbury high country soils. The oxine-derivatised Fractogel method of Simpson *et al.* (1997) was used to obtain concentrations for 'free Al' ($[Al^{3+}] + [Al(OH)^{2+}] + [Al(OH)_2^+] + [AlF^{2+}]$), and the 'organic-bound Al' fraction. The Al-complexation capacities (Al-CC) of the soil solutions were also

determined, to establish the capacity of soluble organic substances to mask potential aluminium toxicity. Lucerne (*Medicago sativa* cv Wairau) root elongation experiments were used to determine whether the existing concentrations of soil aluminium were sufficiently high to inhibit root length elongation.

4.2 MATERIALS AND METHODS

4.2.1 Site description

The sampling site was a steep spur with a strong aspect contrast (north-west *vs.* south-east) on Longslip Station, south of the Ahuriri River, on the western margin of the Mackenzie basin, South Canterbury, New Zealand (Figure 4.1). Sampling was performed at 6 sites representing sunny and shady aspects at three altitudes (1190, 945, 730 m).

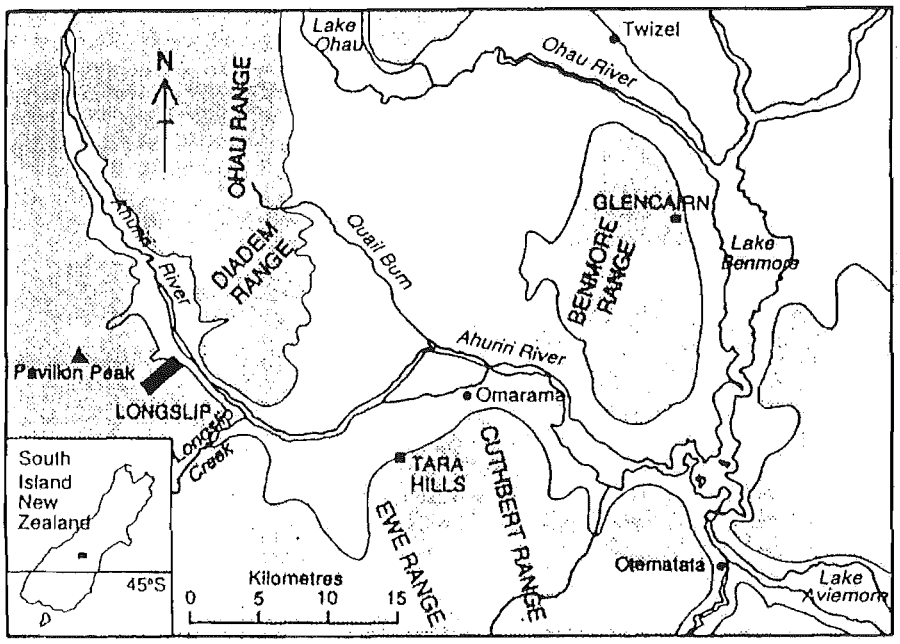

Figure 4.1. Location map showing the southern Mackenzie and Upper Waitaki basins (from McIntosh *et al.* 1994*b*).

The soils were classified as yellow-brown earths (shady slopes and altitudes above 1000 m) and yellow-grey earths (sunny slopes below about 1000 m) (McIntosh *et al.* 1981). These soils are now classified as Typic Orthic Brown Soils and Typic Immature Pallic Soils, respectively, in the New Zealand Soil Classification (Hewitt 1993). The site receives approximately 700-1000 mm annual rainfall. The history of fertiliser application is described above; the site is grazed by merino at relatively low stocking rates. Vegetation at the

sampling sites was dominated by the native species *Chionochloa rigida* (narrow-leaved snow tussock), *Poa cita* (silver tussock), and *Raoulia australis* (scabweed), as well as various introduced grasses and clovers *Anthoxanthum odoratum* (sweet vernal), *Agrostis capillaris* (browntop) and *Trifolium repens* (white clover), and the invasive weed *Hieracium pilosella* (mouse-ear hawkweed) (McIntosh *et al.* 1994*b*). Areas of bare ground were also noticeable, especially at the two sites of highest elevation.

4.2.2 Soil sampling

At each of the six sampling sites, 20 one inch soil cores (0-7.5 cm) were taken from replicate transects and pooled. Upper mid-slope sites (not near-ridge sites) were selected for sampling, reducing the risk of sampling at stock-camp sites. Samples were stored in an insulated chest for transit, then refrigerated in the laboratory at 4°C before analysis.

4.2.3 Soil pH and temperature measurement

Soil pH was measured in the field, and later in the laboratory on both field-moist and air-dried soil samples, as described in Section 2.2.2. The temperature of soil samples (0-7.5 cm) was determined at time of sampling using an ATC temperature probe attached to the Lutron pH206 meter.

4.2.4 Soil solution analyses

Field-moist soils were wetted with TDW to an additional 15% moisture (by weight) and equilibrated for 12 h at 4°C. Soil solutions were extracted and filtered (0.025 μm) within 24 h of field sampling, as described in Section 2.2.3. Soil solution pH was measured using the method described in Section 2.2.4. The concentration of fulvic and humic substances in soil solution was estimated by measurement of the UV absorbance at 250 nm (A_{250}) using a GBC UV/VIS 918 spectrophotometer, and application of the molar absorptivity coefficient (ε_{250} = 0.030 $(cm.mg/L)^{-1}$ at pH 4.7) for a sample of fulvic acid previously isolated from International Humic Substance Society (IHSS) reference peat by the acid pyrophosphate - XAD-7 method (Gregor and Powell 1986). The concentration of fluoride in soil solutions was determined using a Radiometer ISEC241F ion-selective electrode, after addition of an acetate/EDTA total ionic strength adjustment buffer (TISAB).

4.2.5 Aluminium analyses

Total reactive Al was determined using the method of Røyset (1986), on the acidified soil solution (pH 2.0, 24 h) using a 30 s reaction with pyrocatechol violet, (PCV), as described in Section 2.2.7. 'Free' and 'organic-bound' Al were determined immediately on the freshly extracted soil solution by the method of Simpson *et al.* (1997) (Section 2.2.7). Concentrations of $[Al^{3+}]$ in soil solution were calculated using the computer speciation program SOLGASWATER (Eriksson 1979), from the sum of the monomeric aluminium hydroxy species concentrations ($[Al^{3+}] + [Al(OH)^{2+}] + [Al(OH)_2^{+}] + [Al(OH_3)] + [Al(OH)_4^{-}]$), obtained by subtraction of the calculated concentration of AlF^{2+} from the measured concentration of 'free Al' as described in Section 2.2.10. No correction was made for complexation of Al^{3+} by sulfate. Aluminium sulfate complexes are of low stability and typically form only in natural areas subject to acidic deposition, where pH is low and the concentration of SO_4^{2-} high (Driscoll and Postek 1996).

Al complexation capacity (Al-CC) measurements were made on fresh soil solutions (7.0 mL soil solution diluted to 40 mL; pH 4.7 and 5.1) extracted from soils used for lucerne root elongation studies (8 days incubation at 22°C). These soils had been stored field-moist for 4 weeks at 4°C before their use in the lucerne study. The Al-CC titrations were performed according to the method described in Section 2.2.8.

4.2.6 Lucerne root elongation study

Six subsamples of the Longslip soils (field moist soil plus 10% TDW added by weight, equilibrated in growth chamber for 72 h) were used for root elongation studies. The protocol for the lucerne (*Medicago sativa* cv Wairau) root elongation experiments is described in Section 2.2.11.

4.3 RESULTS

Both soil slurry and soil solution pH values are relevant parameters to a discussion of soil chemistry (Table 4.1). The results indicate that for all sites the pH values for air-dried soil samples are in the range 5.2-5.6. The average pH across the 6 sites (5.35), is 0.08 lower than that measured for the same six sites in 1992, but this difference is not significant ($P<0.24$). There was no clear trend in pH values with change in elevation or with aspect.

Table 4.1. Site and pH data for Longslip soil samples

Altitude		Soil temp. (°C)	Field pH (±0.04)[A]	Laboratory pH Moist (±0.04)[A]	Laboratory pH Air-dry (±0.04)[A]	Soil solution pH (± 0.03)[A]
1190 m	Sunny	7.9	5.52	5.36	5.13	6.09
	Shady	7.2	6.14	5.85	5.61	6.16
945 m	Sunny	9.5	5.50	5.82	5.55	6.25
	Shady	6.5	5.18	5.57	5.18	5.96
730 m	Sunny	10.1	5.36	5.47	5.17	5.93
	Shady	8.8	5.71	5.71	5.48	6.20

[A] Error associated with instrumental precision (1 s.d.).

The analytical results for soil solution pH, A_{250}, total reactive Al, 'free Al', 'organic-bound Al' and log $[Al^{3+}]$ at the six sites (2 aspects at 3 elevations) are given in Table 4.2. As these Longslip soils have a known history of fertiliser application, before calculation of log $[Al^{3+}]$ (described in Section 2.2.10), the concentration of total fluoride in soil solution was determined, and the subsequent calculated concentration of AlF^{2+} in each soil solution subtracted from the measured concentration of 'free Al' to give the sum of the monomeric aluminium-hydroxy species concentrations ($[Al^{3+}] + [Al(OH)^{2+}] + [Al(OH)_2^+] + [Al(OH_3)] + [Al(OH)_4^-]$). Due to limited soil solution volumes, fluoride concentrations were measured for only two of the six samples (1190 m sunny 3.9 μM; 1190 m shady 2.7 μM). The mean of these two measurements (3.3 μM) was used as an estimate of the fluoride concentration in the four remaining soil solutions. No correction was made for complexation of Al^{3+} by sulfate, even though these soils have had previous applications of S-enriched fertiliser. The stability of aluminium sulfate complexes is very low relative to aluminium fluoride complexes. Solution equilibrium modelling calculations indicated that at the pH, Al^{3+} and fluoride concentrations of these soils, formation of aluminium sulfate complexes would be negligible.

Al-CC values were measured for each of the six sites (2 aspects at 3 elevations) at two pH values (pH 5.1 and 4.7); the results are given in Table 4.3. Experimental results from a typical complexation capacity curve are given in Figure 4.2.

Table 4.2. Analytical results for soil solutions from Longslip sites

Altitude	Aspect	pH	A_{250}	Free Al (μM)	Org. Al (μM)	PCV Al (μM)	Calculated log $[Al^{3+}]$
		(± 0.03)[A]	(± 0.003)[A]	(± 0.04)[A]	(± 0.04)[A]	(± 0.08)[A]	
1190 m	Sunny	6.09	0.350	0.52	1.2	2.7	-7.34
	Shady	6.16	0.231	0.40	0.67	2.1	-7.58
945 m	Sunny	6.25	1.074	0.43	2.6	7.6	-7.72
	Shady	5.96	0.377	0.51	1.3	3.5	-7.15
730 m	Sunny	5.93	0.903	0.75	3.4	7.9	-6.93
	Shady	6.20	0.350	0.31	0.99	4.5	-7.77

[A] Error associated with instrumental and method precision (1 s.d.).

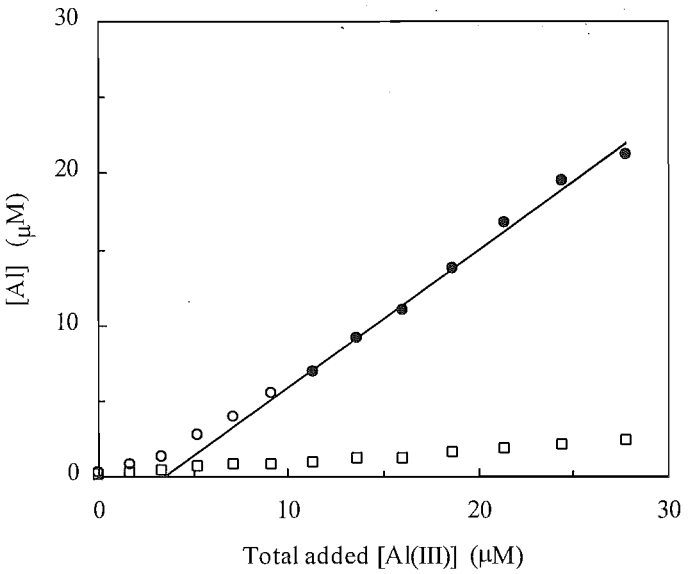

Figure 4.2. Al-CC titration curve at pH 5.1 (for shady site at 1190 m). The volume of soil solution was 7.0 mL made up to 40 mL (final composition 0.05 M KCl, 0.005 M acetate buffer). Filled symbols indicate datum points used to fit the line (r^2 = 1.00) to calculate the complexation capacity of the diluted soil solution (○ 'free Al'; □ 'organic-bound' Al).

Results from the *M. sativa* root elongation experiments are given in Table 4.3. The root elongation experiments were performed using soil samples that had been stored field-moist at 4°C for 4 weeks. Soil solutions were analysed after removal of the *M. sativa* seedlings. This revealed that, in general, the stored soils had higher concentrations of 'free Al', and lower soil solution pH and A_{250} (Table 4.3) than the fresh soils (Table 4.2). Despite the higher concentrations of 'free Al' observed for these soils, the root elongation results did not significantly correlate with the toxic 'free Al' measured in the extracted soil solutions. Furthermore, no significant correlation with soil solution pH was observed. The lack of significance calculated between the soils is in part attributable to the high standard deviations obtained for the data, relative to the value of the mean.

4.4 DISCUSSION

4.4.1 Soil solution chemistry in relation to elevation and aspect

The pH results (Table 4.1) indicate general trends that have been reported before. The average pH measured on wet samples in the field (5.57) and in the lab (5.63) is higher than that for air-dried samples: ΔpH = 0.22 (P<0.11) and 0.28 (P<0.02), respectively. This trend was also noted by Adams *et al.* (1996) for a series of lowland yellow-brown earths and yellow-grey earths under indigenous forest and pastures. Courchesne *et al.* (1995) observed a significant relationship between the pH decrease on drying of forest soils and their total organic carbon. From this it could be inferred that the higher acidity in air-dried samples results from oxidation of organic matter, producing carboxylic acid functional groups. Bartlett and James (1980) also note the process of drying soil tends to increase the surface acidity of soil and increase the solubility and oxidisability of soil organic matter.

The average pH measured for soil solutions (6.10) was *ca.* 0.6 pH above that for moist soil samples. Dahlgren *et al.* (1997) noted the significant loss of CO_2 during the extraction of soil solution by centrifugation. Provided the soil solution is in equilibrium with the soil this degassing should not affect soil or soil solution pH, but any loss from the extracted solution may lead to an increase in pH. In soil slurries, a further uncertainty arises from the effect of soil colloids on the liquid junction potential of the pH reference electrode (Adams *et al.* 1996); this has been termed the suspension effect (Sumner 1994). These colloids could not contribute to the soil solution pH as they are removed in the 0.025 μm filtration. The soil solution pH is pertinent to the Al speciation measurements and calculations.

Table 4.3. Analytical results for soil solutions used in root elongation and Al-CC experiments.

	Aspect	pH	Free Al (μM)	Org. Al (μM)	Mean root length (σ)	A_{250}	Estimated [FA][A]	Al-CC_{calc}[B] (μM)	Al-CC_{meas}[C] (μM)	
		(± 0.03)[D]	(± 0.04)[D]	(± 0.04)[D]	(mm)	(± 0.003)[D]	(mg/L)	pH 4.7	pH 4.7	pH 5.1
1190 m	sunny	6.21	0.80	1.8	42 (6)	0.589	19.6	11.6	20.7	36.4
	shady	5.81	0.75	1.0	51 (17)	0.289	9.6	5.7	12.8	19.2
945 m	sunny	5.09	1.5	2.2	51 (17)	0.555	18.5	11.0	21.4	32.5
	shady	5.01	2.1	1.6	40 (14)	0.289	9.6	5.7	10.3	17.4
730 m	sunny	5.47	0.65	1.5	26 (5)	0.503	16.8	10.0	19.0	27.3
	shady	5.26	1.4	0.65	44 (11)	0.241	8.0	4.7	8.6	14.9

[A] [FA], estimated fulvic acid concentration, see Materials and Methods.

[B] Al-CC_{calc}, calculated using estimated soil solution [FA] and the previously determined Al-CC of an isolated soil fulvic acid.

[C] Al-CC_{meas}, determined by titration.

[D] Error associated with instrumental and method precision (1 s.d.).

For all soil solutions, the concentrations of 'free Al' (0.31 to 0.75 μM) (Table 4.2), were well below any reported thresholds for $\{Al^{3+}\}$-induced suppression of growth by legumes or pasture grasses (Edmeades *et al.* 1991; Wheeler *et al.* 1992), (where $\{Al^{3+}\}$ refers to the activity of $Al(H_2O)_6^{3+}$). These authors reported that respective values of 3-5 $\times 10^{-6}$ and *ca.* 10 $\times 10^{-6}$ in $\{Al^{3+}\}$ were required to reduce plant total dry matter (TDM) by 50%. These activities are equivalent to 'free Al' concentrations of around 6-10 μM and 20 μM, respectively.

Although root elongation inhibition may be expected before a 50% reduction in TDM occurs, the concentrations of 'free Al' observed in this work are nevertheless still likely to be below any $\{Al^{3+}\}$ toxicity threshold. The concentrations of 'organic-bound Al' are also low. 'Organic-bound Al' correlates positively with the estimation of humic substances as given by A_{250} values ($r^2 = 0.86$) (Figure 4.3). At all elevations the concentration of 'organic-bound Al' is higher on the sunny aspects than on the shady. This reflects the higher input of organic matter (and the associated increase in organic C) observed on the sunny aspects than on the shady aspects since fertilisation began (McIntosh *et al.* 1994*b*).

The calculated values for log $[Al^{3+}]$, after adjustment of the concentrations of 'free Al' for the presence of AlF^{2+}, are given in Table 4.2. Figure 4.4 presents the results for the calculated soil solution concentrations of $[Al^{3+}]$, with and without adjustment of the 'free Al' concentrations for the presence of AlF^{2+}. With no adjustment, the calculated values for log $[Al^{3+}]$ in the soil solutions were in the range –6.93 to –7.77, and correlated strongly with soil solution pH ($r^2 = 0.95$). Adjustment of the soil solution 'free Al' concentrations for the presence of AlF^{2+} reduced the calculated concentrations of log $[Al^{3+}]$ by a mean value of 0.35 log units. The corrected values for log $[Al^{3+}]$ were also strongly correlated to soil solution pH ($r^2 = 0.89$). In both cases, the values for log $[Al^{3+}]$ fell between the calculated solubility lines for gibbsite and amorphous $Al(OH)_3$, consistent with control of soil solution $[Al^{3+}]$ by a solid $Al(OH)_3$ mineral phase in this pH range.

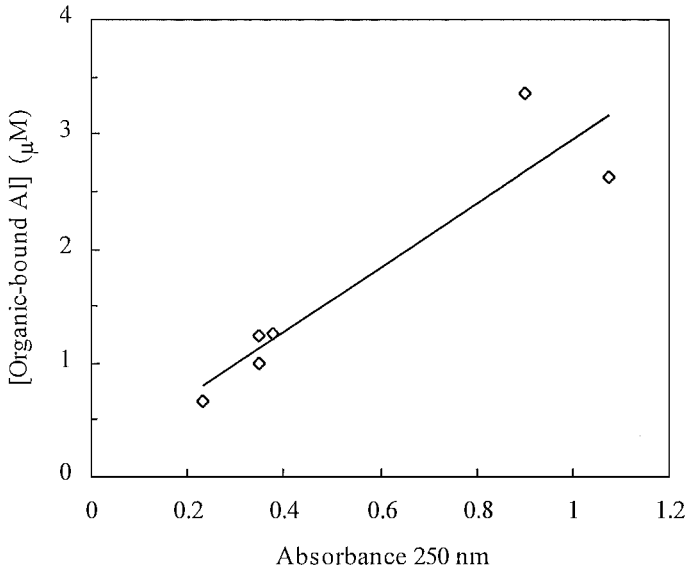

Figure 4.3. Correlation between soil solution UV absorbance at 250 nm and the determined concentration of 'organic-bound Al' for the Longslip samples.

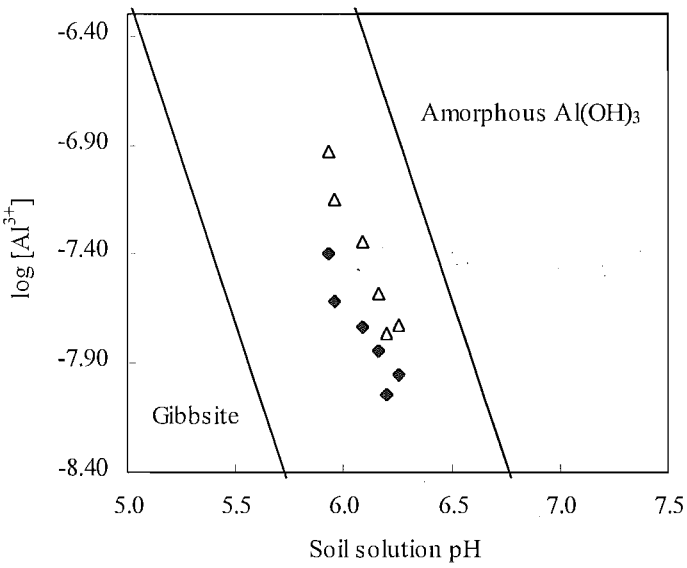

Figure 4.4. Relationship between log $[Al^{3+}]$ and soil solution pH. The solubility lines shown for gibbsite and amorphous $Al(OH)_3$ were calculated using log $*K_{s0}$ = 8.79 and log $*K_{s0}$ = 11.9, respectively. (△ before adjustment of 'free Al' for the presence of AlF^{2+}; ◆ after adjustment for the presence of AlF^{2+}).

4.4.2 Aluminium complexation capacities

Al-CC values were measured for each of the six sites (2 aspects at 3 elevations) at two pH values (pH 5.1 and 4.7); the results are given in Table 4.3. The Al-CC measures the capacity of the humic substances and other natural organic matter (NOM) species in soil solution to bind Al in non-labile and slowly-labile forms. In any soil solution sample, part of the total metal complexation capacity of the humic substance is already satisfied by Al^{3+} (and Fe^{3+}) in the soil solution. Therefore the Al-CC measurement gives the non-utilised or available capacity. At each pH the Al-CC was higher for soils from sunny aspects, commensurate with their higher A_{250} values. The factorial difference in Al-CC between sunny and shady sites was approximately 1.9. A similar factor was observed for the A_{250} values (2.0 ± 0.1). It follows that the Al-CC values correlate strongly with A_{250} values (r^2 = 0.96 and 0.97 at pH 4.7 and pH 5.1, respectively (Figure 4.5).

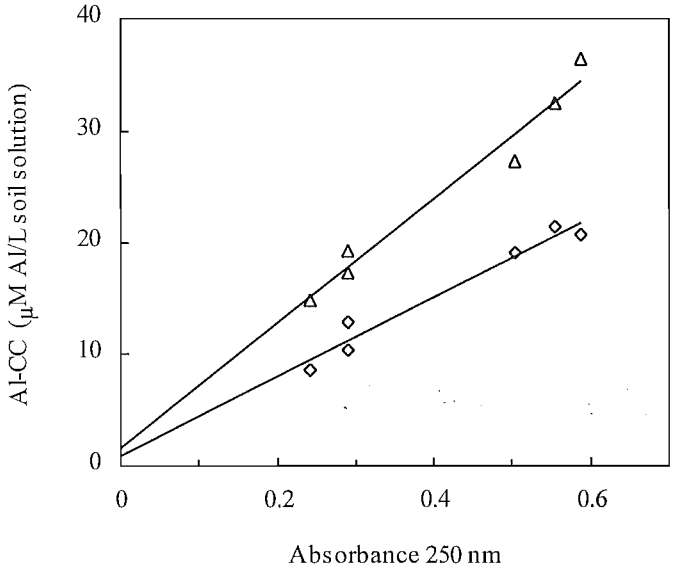

Figure 4.5. Relationship between soil solution aluminium complexation capacity, Al-CC, and UV absorbance at 250 nm (△ pH 5.1, r^2 = 0.97; ◇ pH 4.7, r^2 = 0.96).

The larger slope of the Al-CC *vs.* A_{250} plot at higher pH is consistent with more functional groups being utilised in strong Al binding as the pH increases. For each sample, the measurement of Al-CC at two pH values provides a basis for assessing the effect of acidification on the Al-CC and on the concentration of 'free Al'. For all samples Al-CC decreased by 30-43% on lowering the pH from 5.1 to 4.7.

Humic substances are of primary importance in the complexation of Al in soil solution. The A_{250} values provide an estimate of the concentration of soil solution fulvic and humic substances, which in turn is a consequence of dry matter yield and biological turnover (the

concentrations of soil organic matter are greater on the sunny slopes (McIntosh *et al.* 1994*b*)). However, they are only one fraction of the total NOM present, and therefore A_{250} values alone may underestimate the Al-CC. The fulvic acid concentrations in soil solution, estimated from the A_{250} values, were in the range 8.0-19.6 mg/L (Table 4.3).

The Al-CC value for a standard fulvic acid sample has previously been determined as 10 μmol/L for a 17 mg/L solution at pH 4.7 (Section 3.8). From this, it was possible to compare calculated values for the soil solution Al-CC at pH 4.7 (based on the spectrophotometrically estimated fulvic acid concentrations), with the observed Al-CC values. Calculated values for the soil solution Al-CC ranged from 4.7 to 11.6 μmol/L, and were 53 ± 8% of the respective observed Al-CC values (Table 4.3). This indicates that UV-transparent, NOM fractions also make an important contribution to the Al-CC. This contribution may be ascribed to the presence of low molecular weight aliphatic acids (Hue *et al.* 1986) and polysaccharides (see Chapter 7), both of which are known to bind Al strongly in this pH range. Inorganic Al complexes (*e.g.* AlF_2^+) may also contribute to the Al-CC if they are not included as part of the 'free Al' fraction.

The Al-CC values tend toward zero as A_{250} tends to zero (Figure 4.5) indicating that the UV-transparent organic compounds are present in amounts proportional to species measured at A_{250}. This is consistent with the results of Powell and Hawke (1995) for a series of Canterbury forest soils. However, this relationship does not always hold, as indicated by results obtained for a series of Firm Brown Soils (Waipori silt loam) from tall tussock grassland or *Pinus radiata* forest at a site in the Lammerlaw Range, eastern Otago (Chapter 5). At this site, (in contrast to the soils from Longslip), Al-CC tended to a limiting value of 23 μM at pH 4.7 and 8 μM at pH 4.2 as A_{250} approached zero.

The Al-CC values are much lower than those determined for organic Oa horizons of soils under indigenous upland and lowland forest in Canterbury (34 to 199 μM; Powell and Hawke 1995). The 'organic-bound Al' values (shown by □ in Figure 4.2) are small throughout the titration (<2.5 μM), consistent with the low %C in these soils. As in the example of a soil-extracted fulvic acid (Section 3.13), the limiting value for 'organic-bound Al' represents about 80% of the measured Al-CC. This implies that up to 20% of the complexation capacity involves non-labile coordination sites.

For the two soils from the highest elevation (1190 m), the Al-CC at pH 4.7 was 6-8 times larger than total reactive Al, (as measured by the PCV method). This indicates that only a

small fraction of the total binding capacity is currently utilised. In contrast, for the four soils from lower elevations, the factor was 2-3. These may be considered as safe margins, noting that a soil solution pH of 4.7 (soil slurry pH *ca.* 4.1) is in the range where Al toxicity symptoms may be expected. It may be inferred that any onset of Al toxicity induced by acidification will occur earlier on the lower two sites than on the upper site. Furthermore, shady aspects may be particularly prone to Al toxicity because of their lower absolute Al-CC values. However, such predictions must be tempered with the knowledge that (*a*) any increase in acidification may be accompanied by a build-up of soil organic matter, and (*b*) during the acidification process Al released from minerals would be further 'titrating' the available complexation capacity.

4.4.3 Lucerne root elongation study

Results from the *M. sativa* root elongation experiments are given in Table 4.3. Edmeades *et al.* (1991) classified *M. sativa* as being intermediate in its tolerance to Al, compared to other temperate pasture species. Evidence from Edmeades *et al.* (1991) and Wheeler *et al.* (1992), suggests that the threshold for Al toxicity of *M. sativa* is significantly higher than the concentrations of 'free Al' determined for these soils (≤ 2.1 μM). They also found *M. sativa* to be sensitive to changes in pH from 6.0 to 4.7, however no such effect was observed in this work despite soil solution pH falling within this range.

Except for *M. sativa* seedlings grown in soil from the sunny aspect at 730 m, no significant difference ($\alpha = 0.05$) was determined between seedlings grown in soil from the different sites. At this one site (sunny aspect at 730 m) the root elongations were significantly smaller ($P<0.001$) than those in soil from the other five sites. However, as this soil was neither the most acidic nor contained the highest concentration of 'free Al', it is not clear what caused the observed root growth inhibition.

4.5 CONCLUSION

A series of high country soils were sampled over a range of aspects and altitudes from Longslip Station, South Island, New Zealand. Despite a history of ongoing soil acidification at this site ($\triangle pH_{(H_2O)}$ *ca.* 0.55 since 1978), the current soil solution 'free Al' concentrations are low (0.31 to 0.75 μM), and below reported thresholds for Al toxicity (Edmeades *et al.* 1991; Wheeler *et al.* 1992). Consistent with this, no significant correlations were observed between Wairau lucerne (*M. sativa*) root elongation and either the soil solution pH or the 'free

Al' concentrations. Therefore at current aluminium concentrations, it is unlikely that growth of legumes such as Wairau lucerne would be inhibited by aluminium toxicity in these soils.

Sunny aspects had higher 'organic-bound Al' and lower 'free Al' values. 'Organic-bound Al' correlated strongly with the concentration of humic substances in soil solution, as estimated by the UV absorbance at 250 nm. The values of log $[Al^{3+}]$ calculated from 'free Al' were consistent with control of $[Al^{3+}]$ by an $Al(OH)_3(s)$ phase rather than an organic matter phase.

The ability of soil organic matter to sequester soil solution Al was determined at pH 5.1 and 4.7, by measuring the available aluminium complexation capacity (Al-CC) of the soil solution. The Al-CC decreased with a decrease in soil solution pH, being 30 to 43% lower at pH 4.7. At the highest elevation, the Al-CC at pH 4.7 was 6 to 8 times the total reactive Al, but at the two lower elevations the factor was only 2 to 3. This indicates that with continued soil acidification, the capacity of soil solutions to complex Al (as may be generated by such acidification), is lower for the soils at lower elevations. Hence, there is potential for vegetation at lower elevations to be the first to experience an onset of Al toxicity at these sites.

SECTION B: ALUMINIUM SPECIATION IN HIERACIUM-INFESTED HIGH COUNTRY SOILS

4.6 INTRODUCTION

The species *Hieracium* (hawkweed) is of interest due to its on-going establishment as an invasive weed in the modified short-tussock grasslands of the New Zealand high country. Although the occurrence of some *Hieracium* species in New Zealand was reported as early as 1920, in recent years there has been a dramatic increase in the abundance of some hawkweed species (Makepeace 1985). *Hieracium pilosella* L. (mouse-ear hawkweed) is the dominant *Hieracium* species present in the South Island, however significant populations of *H. praealtum* (king devil hawkweed), *H. caespitosum, H. X stoloniflorum* and *H. lepidulum* also occur.

In dry sub-humid environments, (such as the Mackenzie basin, South Island, New Zealand where much *Hieracium* research has been undertaken), *H. pilosella* grows in approximately circular, or in irregularly-shaped, flat mat-like patches (Figure 4.6). Surrounding these patches is often an area of bare soil, termed the '*halo*'. *Hieracium* species have extensively invaded and displaced high country inter-tussock vegetation, and at some sites have subsequently displaced indigenous tussock species (Makepeace 1985). In doing so, *Hieracium* reduces the herbage available for grazing, and reduces the numbers of native plant species. However, Scott (1993) made the important point that while the perceived problem is of *Hieracium* infestation *per se*, it is actually not a problem due to toxicity or lack of acceptability to stock, but rather due to its habit of growing very close to the ground, limiting direct stock feeding and preventing and excluding the establishment of dietary grass species.

A number of studies have investigated the impacts of *H. pilosella* growth on soil properties. McIntosh and Allen (1993) showed that soils beneath *H. pilosella* patches at a site in the Mackenzie basin were of significantly lower pH (mean pH decrease of 0.5 units) and contained significantly more organic carbon (a relative increase of 40%) than soils under the surrounding grassland. Historical data from this site showed there was little probability of the *H. pilosella* patches being related to a previous vegetation pattern, so rather, it appeared that the *H. pilosella* establishment itself was responsible for the observed changes in soil properties.

Soil acidification may occur as a consequence of organic acid production and/or through a greater rate of cation uptake by *H. pilosella* than by the surrounding flora. McIntosh and Allen (1993) suggest a likely reason for the higher soil C under *H. pilosella* patches arises from it being a perennial plant, which will thus return greater amounts of organic material to the soil through root and leaf death than will the surrounding (predominantly annual) grassland.

Figure 4.6. A typical *H. pilosella* patch. The *halo* area around the centre is evident.

In a later study, McIntosh *et al.* (1995) confirmed these findings of lower topsoil pH and higher organic C under *H. pilosella* compared to surrounding grassland. In the second more detailed study, soils under *H. pilosella* patches were also found to have higher concentrations of exchangeable Ca and Mg than the surrounding soils. Soil in the *halo* area surrounding the *H. pilosella* patches was found to have lower organic C, total N and exchangeable cation values compared to soils under both *H. pilosella* patches and grassland. As the *halo* is underlain by *H. pilosella* roots, McIntosh *et al.* (1995) proposed that the *halo* was an area in which nutrients are depleted to the benefit of the *H. pilosella* itself.

Results from Boswell and Espie (1998) indicate that *H. pilosella* also exploits the halo area for a major part of moisture and nutrient uptake. Moisture is a key limiting factor for plant growth in areas such as the dry sub-humid environment of the Mackenzie basin. In addition to causing increased soil acidity, Boswell and Espie (1998) found *H. pilosella* responsible for increased concentrations of soluble aluminium in the soil directly beneath the patch. For example, 0.01 M $CaCl_2$ extracted Al at field pH was *ca.* 5 ppm beneath a *H. pilosella* patch, compared with *ca.* 1 ppm under grasses (0-5 cm soil depth). The combined effects of reduced

moisture, reduced base cation availability, increased acidity and increased Al concentration in the *halo* soil, clearly makes the immediate environment around *H. pilosella* patches less favourable for the development of competing grassland species.

Part of the reason for *H. pilosella*'s ability to compete effectively in these relatively poor soils may relate to the plant's tolerance to both lower pH and moderately high concentrations of aluminium. *H. pilosella* may be adapted to tolerate the soil conditions which occur through the induced soil acidification by the plant itself. Alternatively, it may be able to promote higher soil Al concentrations directly, by excreting organic chelates or recycling Al through the decay of plant matter (Boswell and Espie 1998). However, Powell *et al.* (1997) found no evidence of elevated concentrations of a 'free Al' fraction, or altered Al complexation properties under *H. pilosella*, in Mackenzie basin soils undergoing contrasting fertiliser treatments. Davis (1997) found that the Al concentration in *H. pilosella* tops was not significantly different from those in clover or grass in pots containing a Mackenzie basin outwash (Orthic Brown) soil. However, lower Al concentrations were reported in roots of *H. pilosella* than in clover or grass, which may be indicative of a greater Al excretion from *H. pilosella* roots, but which could also indicate a mechanism restricting Al uptake by the plant compared with grass and clover.

Makepeace *et al.* (1985) noted the deleterious effect on *Festuca novae-zelandiae* (fescue tussock) in terms of lower N and P biomass concentrations, when grown in areas of dense *H. pilosella* growth. These authors also noted an apparent allelopathic effect on seed germination and root growth of seven different resident grassland species when exposed to leachates from dead *H. pilosella* leaves. These effects were attributed to the presence of phenolic compounds in the leaves, particularly umbelliferone, caffeic acid and chlorogenic acid. Related work in this thesis (Chapter 10) describes a potentiometric study of solution equilibria for the H^+-Al^{3+}-caffeic and H^+-Al^{3+}-chlorogenic acid systems. Polyphenol species have long been known to be important in trace element uptake and, by complexing Al, in reducing potential Al toxicity. Recent studies (*e.g.* Northup *et al.* 1995; Northup *et al.* 1998) have indicated that plant species which occur in poor acidic soils, can excrete similar polyphenol species which immobilise (and effectively monopolise) soil nitrogen into organic forms which competing species are unable to break down.

The objectives of this study were to investigate whether the increase in acidification under *H. pilosella* patches was reflected by an increased concentration of 'free Al' in the soil solution.

Two aluminium complexation capacity titrations were performed, using soil solution extracted from soils from under a *H. pilosella* patch and from surrounding grassland, to determine whether differences in Al-CC values were significant. Root elongation experiments using lucerne (*M. sativa*) were also performed to establish whether Al-induced toxicity and/or an allelopathic effect was operative under conditions of adequate soil moisture.

4.7 MATERIALS AND METHODS

4.7.1 Site description

Samples were taken from a site at Glencairn Station, near Twizel, situated in the Mackenzie basin, New Zealand (Figure 4.1). The site is located on a *ca.* 15° northerly-facing slope at an altitude of *ca.* 440 m. Soils at the site are developed in thin graywacke loess over fan alluvium, and were mapped as a yellow-grey earth, but are now defined as Pallic Soils (Hewitt 1993). The site receives approximately 500-600 mm of annual rainfall, and has never been fertilised. Since 1978 the site has been grazed at an estimated stocking rate of 0.6 ewe equivalents per hectare.

The site has patchy, but significant *Hieracium pilosella* (mouse-ear hawkweed) cover. In addition to *H. pilosella* and significant amounts of bare ground, a range of other vegetation species are present, including *Leontodon taraxacoides* (hawkbit), *Rosa rubiginosa* (sweet briar), *Trifolium arvense* (hare's foot trefoil), *Anthoxanthum odoratum* (sweet vernal), *Muehlenbeckia complexa* (scrub pohuehue), *Melicytus alpinus* (porcupine shrub), *Carex breviculmis* (grassland sedge), *Bromus* spp. (brome), and *Wahlenbergia gracilis* (N.Z. harebell) (McIntosh *et al.* 1995; Nicol 1997).

4.7.2 Soil sampling

Two representative *H. pilosella* patches were selected for sampling. Three bulk soil samples (0-7.5 cm) from each patch were removed for study. The first sample (*centre*) was taken from directly under the centre of the *H. pilosella* patch, the second (*halo*) from the bare soil area (approximately 10 cm width) surrounding each *H. pilosella* patch, and the third (*control*) from under adjoining pasture well removed from the *H. pilosella* patch. Samples were stored in an insulated chest for transit, then refrigerated in the laboratory at 4°C before analysis.

4.7.3 Soil pH measurement

Soil pH was measured using field-moist soil, as described in Section 2.2.2.

4.7.4 Soil solution analyses

Field-moist soils were wetted with TDW to an additional 20% moisture (by weight) and then equilibrated for 24 h at 4°C. Soil solutions were extracted and filtered (0.025 μm) as described in Section 2.2.3. Soil solution pH and UV absorbance at 250 nm (A_{250}) were measured using the methods described in Section 2.2.4. The concentration of fulvic and humic acids in the extracted soil solution was estimated as described in Section 4.2.4. Total reactive Al in soil solution was determined using a 30 s FIA reaction with pyrocatechol violet (PCV), (Section 2.2.7). The concentrations of 'free' and 'organic-bound' Al were determined in soil solutions using the oxine-derivatised Fractogel method (Section 2.2.7.2).

4.7.5 Aluminium complexation capacities

Two aluminium complexation capacity (Al-CC) titrations were performed using soil solution extracted from *centre* and *control* soil samples from a single *H. pilosella* site (Site 1). The Al-CC titrations were performed at pH 4.7 (4.0 mL soil solution diluted to 60 mL), as described in Section 2.2.8. Calculated Al-CC values were obtained by the method described in Section 4.4.2, from the spectrophotometric estimation of fulvic and humic concentrations in soil solution (Section 4.2.4).

4.7.6 Lucerne root elongation experiments

Root elongation of lucerne seeds (*Medicago sativa* cv Wairau) was determined as described in Section 2.2.11. The three soil samples (*centre, halo and control*) were from a single *H. pilosella* site (Site 1). The planted seedlings were placed in the growth chamber for 5 days.

4.8 RESULTS

The analytical results for soil slurry and soil solution pH for the six samples (3 soil samples from two *H. pilosella* sites) are given in Table 4.4. Soil pH values for the six samples were in the range 5.8-6.8. Mean soil pH for the *centre* samples (5.92), was lower than that for both the *halo* samples (mean pH 6.39, $P = 0.09$) and the *control* samples (mean pH 6.72, $P<0.02$).

Soil solution pH values were on average, 0.4 units higher than the respective soil pH values, similar to the results from the Longslip study.

Table 4.4. Analytical results for soil solutions from two *H. pilosella* sites.

Sample		Field-moist pH (± 0.04)[A]	Soil soln pH (± 0.03)[A]	Free Al (μM) (± 0.04)[A]	Org. Al (μM) (± 0.04)[A]	PCV Al (μM) (± 0.08)[A]
Site 1	*centre*	6.02	6.41	0.34	0.78	2.5
	halo	6.59	6.94	0.37	0.25	1.1
	control	6.84	7.31	0.33	0.23	1.9
Site 2	*centre*	5.81	6.23	0.36	2.1	6.0
	halo	6.19	6.60	0.37	0.32	1.2
	control	6.59	6.92	0.32	0.28	1.4

[A] Error associated with instrumental and method precision (1 s.d.).

Concentrations of 'free Al', 'organic-bound Al' and 'PCV-reactive Al' are also given in Table 4.4. The concentrations of 'free Al' were identical (within experimental error) for all samples across the two sites. Concentrations of 'organic-bound Al' ranged from 0.23-2.07 μM Al, and were higher in *centre* samples than in the *halo* or *control* samples ($P = 0.16$). There was no significant difference between 'organic-bound Al' in the *halo* and *control* samples. Concentrations of 'PCV-reactive Al' ranged from 1.1-6.0 μM, and as for the concentrations of 'organic-bound Al' were higher in *centre* samples than in *halo* or *control* samples ($P = 0.16$ and 0.19, respectively).

The experimentally determined and calculated Al-CC values for the diluted soil solutions from selected *centre* and *control* samples are given in Table 4.5. The aluminium complexation capacity curve for diluted soil solution from the *control* soil sample is given below (Figure 4.7). The complexation capacity curve obtained from the *centre* soil solution sample was similar, showing comparable concentrations of 'organic-bound Al', but with a smaller abscissa intercept obtained by fitting a line through the 'free Al' data points. Given that some binding sites on organic species within the soil solution will already be occupied by

Al^{3+} or Fe^{3+}, the complexation capacity value obtained corresponds to the unutilised complexation capacity.

Table 4.5. Lucerne root elongation measurements, A_{250} measurements and the calculated and measured Al-CC values from *H. pilosella* Site 1.

Sample	Mean root length (σ) (mm)	A_{250} (± 0.003)[D]	Estimated [FA][A] (mg/L)	Al-CC_{calc}[B] (μM) pH 4.7	Al-CC_{meas}[C] (μM)
centre	46.5 (23.4)	1.252	41.7	24.5	16.3
halo	46.1 (21.1)	-	-	-	-
control	57.7 (20.0)	0.896	29.9	17.6	24.9

[A] [FA], estimated fulvic acid concentration, see Materials and Methods.

[B] Al-CC_{calc}, calculated using estimated soil solution [FA] and the previously determined Al-CC of an isolated soil fulvic acid.

[C] Al-CC_{meas}, determined by titration.

[D] Error associated with instrumental and method precision (1 s.d.).

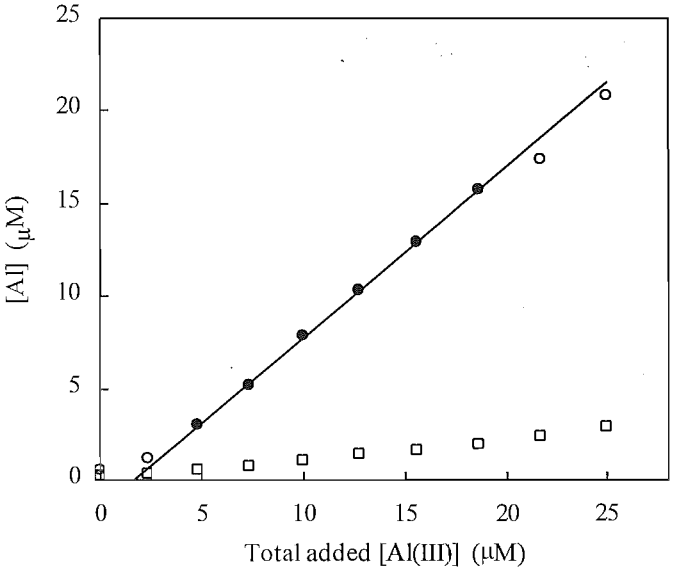

Figure 4.7. Al-CC titration curve at pH 4.7 for *H. pilosella control* soil sample (Site 1). The volume of soil solution was 4.0 mL made up to 60 mL (final composition 0.05 M KCl, 0.005 M acetate buffer). Filled symbols indicate datum points used to fit the line (r^2 = 1.00) to calculate the complexation capacity of the diluted soil solution (○ 'free Al'; □ 'organic-bound' Al). The slope of the fitted line is 0.93, r^2 = 1.00.

Results from the *M. sativa* (lucerne) root elongation experiments are given in Table 4.5. As for the Longslip soils, the standard deviation of root length was high, relative to the value of the mean. Although not significant at the $\alpha = 0.05$ level, root elongation of *M. sativa* was greater in soil from the pasture *control* than in soil from the *centre* and *halo* samples ($P = 0.17$ and 0.14, respectively).

4.9 DISCUSSION

4.9.1 Soil pH and soil solution Al chemistry

The mean field-moist soil pH values from these two *H. pilosella* sites are higher (by 0.1-0.35 pH units) than those noted by McIntosh and Allen (1993) and McIntosh *et al.* (1995) for the same Glencairn site, but who used air-dried soil for pH measurement. As discussed above in relation to results from the Longslip study, the average pH measured using field-moist samples is typically slightly higher than that measured using air-dried samples. As in these two studies, and also in Boswell and Espie (1998), there was a clear transition in soil pH at both sampling sites, with soils becoming progressively more acid when moving from the *control* pasture, through the *halo* area, to under the *centre* of a *H. pilosella* patch. pH values from Site 2 were on average 0.3 pH units more acidic than those from Site 1. As the two sampling locations were similar in terms of both aspect and vegetation, the reason for this difference in pH is unclear. As for the soil pH values, the soil solution pH values also indicated a progressive increase in acidity from the *control* samples to the *centre* samples.

The higher A_{250} measurement in soil solution from the *centre* sample is consistent with the previous observations of greater amounts of organic matter under the centre of *H. pilosella* patches (McIntosh 1993, McIntosh *et al.* 1995).

Concentrations of 'free Al' were low in all samples (<0.4 μM), reflecting the relatively high soil solution pH values (6.2-7.3) from these samples. These concentrations are well below thresholds normally associated with potential Al toxicity for plant species (Edmeades *et al.* 1991; Wheeler *et al.* 1992). Soil solution samples were also analysed by the more aggressive PCV method. This method measures the same 'free Al' fraction determined by the oxine-derivatised Fractogel method, in addition to Al bound in moderately labile Al-organic complexes that can react with PCV during the 30 s reaction in a flow injection analysis

manifold. Results indicated a greater amount of 'PCV-reactive' aluminium under the centre of the *H. pilosella* plot compared to the halo and surrounding pasture. This result is consistent with the work of Boswell and Espie (1998), who found higher concentrations of aluminium under *H. pilosella* patches. In contrast to Boswell and Espie (1998), the present work found no evidence from the 'PCV-reactive Al' results that soil from the halo area also contains higher concentrations of aluminium than soil from surrounding pasture.

4.9.2 Aluminium complexation capacities

Experimentally determined aluminium complexation capacity values for diluted soil solution from *centre* and *control* samples were 16.3 μM and 24.9 μM respectively (Table 4.5). In contrast to results for Longslip soils, these Al-CC values did not correlate with the concentration of humic and fulvic acids, as estimated by the A_{250} measurements (Table 4.5). The A_{250} measurements indicated higher concentrations of humic and fulvic species present in *centre* soil solution, but the unutilised Al-CC determined for the *centre* sample was lower than that determined for the *control*. This suggests that either the organic matter present under the *H. pilosella* already has a large number of the potential binding sites occupied by Al^{3+} (or Fe^{3+}), or that the different types of organic species in the two soils have very different Al complexation properties.

The Al-CC value for a fulvic acid sample extracted from IHSS reference peat has previously been determined as 10 μmol/L for a 17 mg/L solution at pH 4.7 (Section 3.8). Using this result, it was possible to calculate an expected Al-CC value at pH 4.7 (based on the spectrophotometric estimate of soil solution fulvic acid concentrations), and compare this with the measured Al-CC values. Calculated estimates of the two soil solution Al-CC values are given in Table 4.5. The value for soil solution from the *control* pasture sample was 71% of the measured Al-CC value. This is slightly higher than the values obtained from a similar calculation for soils from the Longslip study, where $Al\text{-}CC_{calc}$ was 53 ± 8% of the respective observed Al-CC values. As for the Longslip study, it is clear that in the *control* soil solution, UV-transparent, NOM fractions make an important contribution to the unutilised Al-CC of the soluble organic matter.

For the *centre* sample however, the situation was different. The value of $Al\text{-}CC_{calc}$ was 50% higher than the experimentally determined value of Al-CC. As these Al-CC measurements

reflect the unutilised and not the total complexation capacity of soil solution organic matter, this result suggests that the soluble organic species within the *centre* soil solution are already binding a significant amount of Al. The concentrations of 'organic-bound Al' and 'PCV-reactive Al' are higher in soil solutions from the *centre* samples than in *control* samples (Table 4.4) (which indicates a higher concentration of Al-organic species). However, the concentrations are still relatively low (<6 μM) and do not indicate a large pool of organically-bound Al. Al bound in strong polyphenolic organic complexes would certainly not appear in the oxine-derivatised Fractogel 'organic-bound' Al fraction. It is also questionable whether such strong Al complexes would react quantitatively with PCV during the 30 s reaction time.

4.9.3 Lucerne root elongation study

The very low concentrations of 'free Al' determined for these soils are below the suggested thresholds for *M. sativa* Al toxicity (Edmeades *et al.* 1991; Wheeler *et al.* 1992). It is therefore unlikely that Al-inhibition was responsible for the decreased root elongation observed for the *centre* and *halo* samples, compared with that in the *control* sample. It is possible an allelopathic effect may be partly responsible for the reduced root elongation. As noted previously, Makepeace *et al.* (1985) found the growth of seven grassland species was inhibited when exposed to *H. pilosella* leaf washings. However, given that moisture is a key limiting factor for plant growth in soils from such dry environments (Boswell and Espie 1998), and that these soils were moistened before planting of the *M. sativa* seedlings (15% TDW added by weight), it might be expected that any possible allelopathic effect might be reduced under conditions of adequate soil moisture. Indeed, Makepeace *et al.* (1985) noted the nutrient and moisture status of the soil did modify the observed allelopathic effects of *H. pilosella*.

4.10 CONCLUSION

This study investigated soil solution pH and aluminium speciation in samples taken from three soil zones under, and around *H. pilosella* patches. Despite previous workers noting the ability of *Hieracium* species to induce soil acidification, and the proposal that a tolerance to Al may be a factor in the competitive advantage of *Hieracium* species, the soil solution 'free Al' concentrations were low (<0.4 μM) and well below reported thresholds for Al toxicity (Edmeades *et al.* 1991; Wheeler *et al.* 1992). However, despite the unlikely growth inhibition

of legumes (such as *M. sativa*) by aluminium toxicity in these soils, root elongation was found to be lower in soil from the *centre* and *halo* samples, than in soil from the pasture *control* ($P = 0.17$ and 0.14, respectively). This may be caused by the presence of *H. pilosella* polyphenolic exudates in the soil that cause an allelopathic inhibition of root growth, as observed by Makepeace *et al.* (1985) for a variety of grassland species.

Measurements of the soil solution aluminium complexation capacity for the *centre* and *control* soil samples established there were large differences in the aluminium complexation properties. The Al-CC value obtained for the *control* sample was similar to those obtained for pasture soil samples in the Longslip study, for which UV-transparent species in the soil solution were believed to contribute significantly (*ca.* 30%) to the unutilised Al-CC. In contrast, the Al-CC value obtained for soil solution from the *centre* sample indicated that a significant amount of the total complexation capacity was already utilised, presumably due to the formation of strong Al-polyphenolic complexes.

CHAPTER 5

EFFECTS OF AFFORESTATION ON SOIL AND SOIL SOLUTION ALUMINIUM

5.1 INTRODUCTION

Increasing areas of New Zealand hill and high country grasslands are being converted from pasture to exotic forestry plantations, with radiata pine (*Pinus radiata*) being the dominant plantation species. Sustaining this current planting rate has been given prominence as a possible mechanism for reducing New Zealand's net carbon dioxide emissions (New Zealand Ministry of Environment 1998).

Very few studies have reported the long-term impact on New Zealand soils when converting from pastoral grasslands to forest plantations. However, several short-term studies have observed significant changes in soil properties upon afforestation. Increases in topsoil acidity have been observed under forested sites (Davis and Lang 1991; Giddens *et al.* 1997; Parfitt *et al.* 1997). However, the effect of afforestation on major cations is not generally as consistent. Davis (1998) reported cation concentrations under older stands of pine that were greater than or equal to those from under adjacent grasslands. This was ascribed to the possible cycling of cations from lower horizons into the topsoil horizon. Several studies have also reported increases in measures of available nutrients under conifers, specifically Olsen-P, Bray-2 P, mineralisable N and sulfate-S (Davis and Lang 1991; Davis 1994; Condron *et al.* 1996).

In contrast, Alfredsson *et al.* (1998) reported a general decrease of both total nitrogen and exchangeable cations under two South Island conifer stands compared with adjacent grassland. Giddens *et al.* (1997) and Parfitt *et al.* (1997) reported elevated concentrations of exchangeable Na^+ and Mg^{2+}, (but lower Ca^{2+}) under North Island pine stands compared with grasslands. This increase was attributed to the dry deposition of sea-salt onto the forest canopies, and subsequent transfer to the soil.

It may be expected that the increased acid levels observed with afforestation will be accompanied by increased exchangeable and soil solution Al concentrations. Since Al toxicity is considered to be a major growth limiting factor in acid soils it is important to examine the influence of afforestation on Al in soils. Davis and Lang (1991) and Alfredsson *et al.* (1998) have reported higher exchangeable Al levels in soils under conifers than under adjoining grassland at several South Island sites. In contrast, Giddens *et al.* (1997) reported no significant difference in mean exchangeable Al levels between forest and grassland sites in the North Island, although levels appeared elevated under forest at some sites. There is, however, no information on the influence of afforestation on Al in soil solution.

This chapter reports a detailed analysis and comparison of Al in soil extracts and soil solutions, obtained from three grassland sites and adjacent sites planted in exotic conifer species. These sites had previously been identified as having a range of exchangeable Al concentrations. The oxine-derivatised Fractogel flow injection analysis technique of Simpson *et al.* (1997) was used to investigate the aluminium speciation within soil solutions. The same technique was also used to determine the aluminium complexation capacities (Al-CC) of the soil solutions, a parameter that indicates the capacity of the soluble organic matter to ameliorate Al toxicity.

5.2 MATERIALS AND METHODS

5.2.1 Study area

CP and CF sampling sites were located on terrace and hill slope sites respectively, in the Cragieburn Range, Canterbury, New Zealand (Figure 5.1). The forest at CP consisted of Corsican (*Pinus nigra*) and Ponderosa pine (*P. ponderosa*) with adjacent grassland dominated by moss (*Racomitrium* sp.), club moss (*Lycopodium* sp.), native short tussocks (*Poa* and *Festuca* spp.) and native shrubs (*Dracophyllum*, *Cassinia*, and *Cyathodes* spp.). Forest at CF was planted in Douglas fir (*Pseudotsuga menziesii*), with tall tussock (*Chionochloa macra*) browntop (*Agrostis capillaris*), mountain daisy (*Celmisia spectabilis*) and native shrubs (*Dracophyllum*, *Hebe* and *Cassinia* spp.) dominating the grassland. The third site (LP) was located at Glendhu Forest on a hill slope in the Lammerlaw Range, eastern Otago, New Zealand (Figure 5.1). Forest consisted of Radiata pine (*P. radiata*), with adjacent grassland dominated by narrow-leaved snow tussock (*Chionochloa rigida*). Further site characteristics are summarised in Table 5.1. The soils were developed in humid environments in loess (CP and LP) or greywacke colluvium (CF). Vegetation prior to afforestation consisted of short

(CP) or tall tussock grassland. The sites were grazed prior to afforestation, but grazing was discontinued after planting except at LP where the grassland continues to be lightly grazed by sheep. The sites had not been cultivated or fertilised, and for each pair the forest and grassland sites were similar in terms of soil and topography.

Table 5.1. Characteristics of the sample sites.

Site	Elevation (m)	Rainfall (mm)	Soil group[A]	Soil series	Forest species	Forest age (years)
CP	810	1300	Allophanic Brown Soil	Craigieburn silt loam	*Pinus nigra* + *P. ponderosa*	18
CF	870	1440	Allophanic Brown Soil	Tekoa stony loam	*Pseudotsuga menziesii*	19
LP	460-670	1355	Firm Brown Soil	Waipori silt loam	*P. radiata*	15

[A] Soil classification follows Hewitt (1993).

5.2.2 Sampling

Soils were sampled in November 1997, along three replicate parallel transects. At the forested sites of CP and CF, transects were separated by tree rows, whereas for the adjoining grassland sites the separation between transects was 5 m. The transects at LP were selected at three elevations in the catchment area, at approximately 650 m, 620 m, and 590 m. Five soil cores (6.5 cm internal diameter) were taken along each transect, at intervals of 1 m for CP and CF sites, and 2 m for the LP site. The five sub-samples from each transect were pooled and sealed in plastic bags after collection. CP and CF sites were sampled to a 10 cm depth, the LP site was sampled in 10 cm increments to a depth of 30 cm. Sampling at tussock bases was avoided for the grassland sites. For both forest and grassland sites, overlying vegetation matter was removed to expose the mineral soil before sampling. After transportation, samples were refrigerated at 4°C in the laboratory.

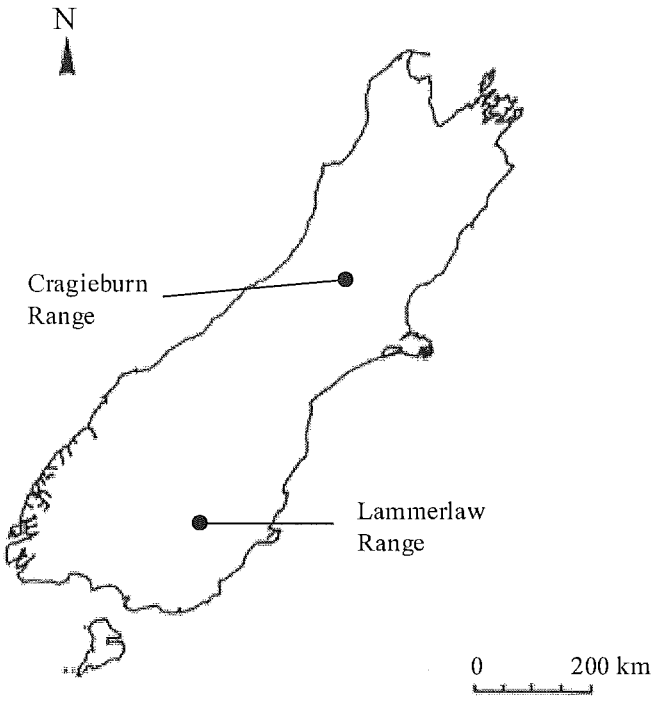

Figure 5.1. Location of the Cragieburn and Lammerlaw Range sampling sites.

5.2.3 Soil analyses

Soil pH was measured on field-moist soil in triply-distilled water (soil:water ratio of 1.0:2.5), as described in Section 2.2.2, except a Russell CMAWL/4/5/S7 micro-combination electrode was used for the measurements.

Soil samples were air-dried, crushed and sieved (<2 mm) before determination of exchange characteristics and exchangeable aluminium. These analyses were performed by the Forest Research Institute, Rotorua, New Zealand. Exchangeable cations and CEC were determined using a 1 M NH_4OAc extract at pH 7 (Nicholson 1984). Aluminium was determined in 1 M KCl and 0.02 M $CaCl_2$ extracts by AAS, as described by Percival *et al.* (1996), except that the extracts were filtered through Whatman No 42 filter paper, not centrifuged.

5.2.4 Soil solution analyses

Forest soils were wetted and equilibrated with TDW to bring them to the same approximate moisture level as the equivalent grassland sites (5-20% TDW by weight added). Soil solutions were extracted and filtered within 24 hours of sampling as described in Section 2.2.3. Soil solution pH was measured on the fresh extract using the Russell micro-

combination electrode described above. Concentrations of fulvic and humic organic matter in soil solution were estimated by measurement of the UV absorbance at 250 nm, using a GBC UV/VIS 918 spectrophotometer. Concentrations of cations in soil solution samples were determined by ICP atomic emission spectroscopy at AgResearch, Grasslands Research Centre, Palmerston North, New Zealand.

5.2.5 Aluminium analyses

Concentrations of 'free Al' and 'organic-bound (moderately-labile) Al' in the fresh soil solutions were determined within 24 h of sampling, using the oxine-derivatised Fractogel method (described in Section 2.2.7). Concentrations of Al^{3+} in soil solution were calculated from the measured concentration of 'free Al' ($[Al^{3+}] + [Al(OH)^{2+}] + [Al(OH)_2^{+}] + [AlF^{2+}]$) using the chemical equilibrium program SOLGASWATER (Eriksson 1979) and stability constants for the hydrolysis of Al^{3+}. The thermodynamic hydrolysis constants of Nordstrom and May (1989) were adjusted to I = 0.005 M (typical for soil solutions from New Zealand topsoils (Edmeades *et al.* 1985)) using the Davies equation, and to 10°C (reflecting approximate soil temperatures) using the temperature-dependence equations of Nordstrom and May (1989) for log *K, as described in Section 2.2.10.

As none of the sampling sites had been fertilised, the concentration of fluoride in soil solution was expected to be low. The total fluoride concentration in freshly extracted soil solutions from the CP site was determined by fluoride ion-selective electrode as part of another study (Chapter 3) and found to be <0.2 μM. The fluoride concentration measured in a representative sample of soil solution from the LP site was of similarly low concentration (0.5 μM). At such low fluoride concentrations, the amount of AlF^{2+} in soil solution (which is quantified as part of the 'free Al' fraction) will be small relative to the sum of the monomeric aluminium-hydroxy species concentrations. Therefore, no adjustment was made to the measured concentration of 'free Al' for the presence of AlF^{2+}.

No correction was made for complexation of Al^{3+} by sulfate. Aluminium sulfate complexes are typically found only in natural systems subject to acidic deposition, where the concentration of SO_4^{2-} is high, and the pH low (Driscoll and Postek 1996). The solubility lines for gibbsite ($Al(OH)_3$) and amorphous $Al(OH)_3$ were calculated using values of log $*K_{s0}$ adjusted for ionic strength and temperature as described in Section 2.2.10.

Al complexation capacity measurements were made on freshly extracted soil solutions, using a representative soil sample obtained by combining subsamples from individual soil replicates. Al-CC experiments were performed at two pH values for each of the two sites at CP and CF (pH 4.7 and 5.1), and for the LP sites at the three sampling depths (pH 4.2 and 4.7). Al-CC experiments involved the incremental addition of Al^{3+} to diluted soil solutions (pH 3.88 to 5.29) buffered (0.005 M acetate buffer, 0.05 M KCl) to the same pH to provide a basis for comparison, as described in Section 2.2.8.

5.2.6 Lucerne root elongation studies

Medicago sativa seeds (Wairau lucerne) were germinated for 72 h on damp filter paper in a growth chamber (16 h light, 8 h dark at 22.5°C), before being planted into pots containing 100 g of moist soil. Six subsamples of LP soil, each derived from five pooled cores from a single transect, were used for the root elongation studies (*i.e.* a forest and grassland soil, each at three depths). Five seedlings were planted per pot, with three replicate pots per soil. The pots were placed in the growth chamber for a further 6 days, after which the seedlings were carefully removed and root elongation measured. Soil and soil solution pH, A_{250}, 'organic-bound Al' and 'free Al' were re-analysed in these soils after completion of the root elongation experiments and were consistent with the results of the original soil analyses.

5.3 RESULTS

5.3.1 Soil acidification: pH

Mean soil pH values for the three sites are given in Table 5.2 and, except at site CF, indicate a lower soil pH at each forest site than at the corresponding grassland site. These differences were significant ($p<0.01$) for topsoils (0-10 cm) at LP ($\triangle$pH = 0.61) and CP ($\triangle$pH = 0.26), but not at CF ($p = 0.11$, $\triangle$pH = 0.18). At LP, pH was also significantly lower under forest at the 10-20 ($p<0.01$) and 20-30 cm ($p<0.05$) depths.

Table 5.3 shows the pH for soil solutions extracted from soils at each site. The changes in pH associated with the change from grassland to forest are again most marked for the base-deficient soils at LP. These differences were large for topsoils (0-10 cm) at LP ($\triangle$pH = 0.73) and CP ($\triangle$pH = 0.42), but not at CF ($\triangle$pH = 0.08). At LP, the pH was significantly lower under forest at the 10-20 ($p = 0.02$) and 20-30 cm ($p<0.01$) depths.

The soil solution absorbance values, A_{250}, (Table 5.3) give an estimate of the soluble humic and fulvic acid components in soil solution. At CP and CF they were higher for forest topsoils. At LP the values were higher for forest soils at 0-10 cm, but were similar or lower at greater depth. The A_{250} values do not indicate the concentration of UV-transparent components, such as low molecular weight organic acids and polysaccharides, that may also contribute to soil solution acidity and complexation capacity. As seen in Table 5.3, the A_{250} values do not parallel the TOC values for soil solutions.

Table 5.2. Acidity and exchange characteristics ($cmol_c/kg$) of soil from grassland and forest at three sites.

Site	Depth (cm)		% Soil moisture	pH	KCl-Al	$CaCl_2$-Al	Na	K	Ca	Mg	ΣBases	ECEC[A]	%BS[B]
CP	0-10	grassland	31.2	5.13	4.00	0.09	0.05	0.48	2.76	0.54	3.84	7.8	48.7
		forest	24.3	4.87	5.66	0.20	0.04	0.16	0.75	0.13	1.09	6.8	16.0
		p (t-test)	<0.01	<0.01	0.01	<0.01	0.71	0.04	0.03	<0.01	0.02	0.12	<0.01
CF	0-10	grassland	32.6	5.28	1.6	0.04	0.07	0.54	4.73	0.97	6.32	7.9	79.9
		forest	23.5	5.46	2.2	0.04	0.01	0.32	3.82	0.71	4.91	7.1	67.9
		p (t-test)	0.01	0.11	0.10	0.41	0.16	0.11	0.37	0.11	0.25	0.38	0.15
LP	0-10	grassland	52.9	4.75	11.67	0.31	0.16	0.55	0.93	0.89	2.27	14.2	17.9
		forest	28.4	4.14	15.06	0.64	0.20	0.29	0.12	0.26	0.87	15.9	5.5
		p (t-test)	<0.01	<0.01	<0.01	<0.01	0.49	0.01	<0.01	<0.01	<0.01	0.06	<0.01

Site	Depth (cm)		% Soil moisture	pH	KCl-Al	$CaCl_2$-Al	Na	K	Ca	Mg	ΣBases	ECEC[A]	%BS[B]
LP	10-20	grassland	35.6	4.81	12.63	0.38	0.10	0.29	0.27	0.42	1.09	13.7	7.9
		forest	28.2	4.29	14.33	0.53	0.12	0.14	0.01	0.15	0.43	14.8	3.0
		p (t-test)	0.04	<0.01	0.26	0.04	0.33	0.04	0.01	0.03	0.02	0.45	0.03
	20-30	grassland	29.0	4.84	11.27	0.36	0.04	0.14	0.10	0.16	0.45	11.7	3.5
		forest	23.8	4.59	12.06	0.42	0.12	0.07	0.01	0.07	0.28	12.3	2.3
		p (t-test)	<0.01	0.04	0.40	0.19	0.11	0.12	0.07	0.04	0.13	0.47	0.09

[A] ECEC (effective cation exchange capacity) = ΣBases + KCl-Al

[B] %BS (percentage base saturation) = ΣBases/ECEC

Table 5.3. Soil solution analyses from grassland and forest at three sites.

Site	Depth (cm)		pH	A_{250}	TOC (μg/mL)	Al (μM) organic	Al (μM) free	ICP analyses (μM) Na^+	K^+	Ca^{2+}	Mg^{2+}	Ca/Al_{free}	Mg/Al_{free}
CP	0-10	grassland	5.63	0.114	26	1.0	0.89	483	153	166	41	191	48
		forest	5.21	0.184	24	2.2	2.4	438	123	112	18	48	8
		p (t-test)	0.24	0.17	0.74	0.10	0.16	0.50	0.23	0.14	0.09	0.04	0.08
CF	0-10	grassland	5.64	0.190	35	1.4	0.60	487	166	165	51	276	85
		forest	5.56	0.264	25	1.8	1.2	413	136	183	63	166	60
		p (t-test)	0.47	0.09	0.12	0.05	0.13	0.19	0.33	0.56	0.44	0.10	0.39
LP	0-10	grassland	4.84	0.227	-	3.3	3.1	409	154	82	48	31	18
		forest	4.11	0.380	-	14.2	36.2	1153	275	111	81	3.2	2.4
		p (t-test)	<0.01	0.26	-	0.18	0.02	0.05	0.21	0.04	0.05	0.07	0.10

Site	Depth (cm)		pH	A_{250}	TOC (µg/mL)	Al (µM) organic	Al (µM) free	ICP analyses (µM) Na^+	K^+	Ca^{2+}	Mg^{2+}	Ca/Al_{free}	Mg/Al_{free}
LP	10-20	grassland	5.02	0.149	-	1.9	2.7	558	126	92	17	37	7.0
		forest	4.37	0.138	-	3.3	13.1	1138	140	108	60	8.4	4.8
		p (t-test)	0.02	0.72	-	0.22	<0.01	0.06	0.79	0.67	0.02	0.23	0.61
	20-30	grassland	5.20	0.155	-	2.2	2.1	804	210	128	21	64	12
		forest	4.62	0.106	-	1.7	5.0	805	86	95	33	35	7.7
		p (t-test)	<0.01	0.04	-	0.32	0.16	0.99	0.03	0.11	0.38	0.01	0.63

5.3.2 Soil acidification: Al^{3+}

The soil properties, exchangeable (1 M KCl) and extractable (0.02 M $CaCl_2$) aluminium, (Table 5.2) both indicate significantly greater ($p<0.01$) Al-acidification in forest topsoils (0-10 cm) at LP and CP. Total Al in 1 M KCl extracts ranged from 1.3 to 16.2 $cmol_c/kg$ for individual soil replicates, and in the corresponding 0.02 M $CaCl_2$ extracts from 0.02 to 1.60 $cmol_c/kg$. There was a strong correlation between the fraction of Al extracted by 1 M KCl and that extracted by 0.02 M $CaCl_2$ (Figure 5.2). With one exception, differences between forest and grassland soils were not significant at greater depth (LP), or in topsoil at CF.

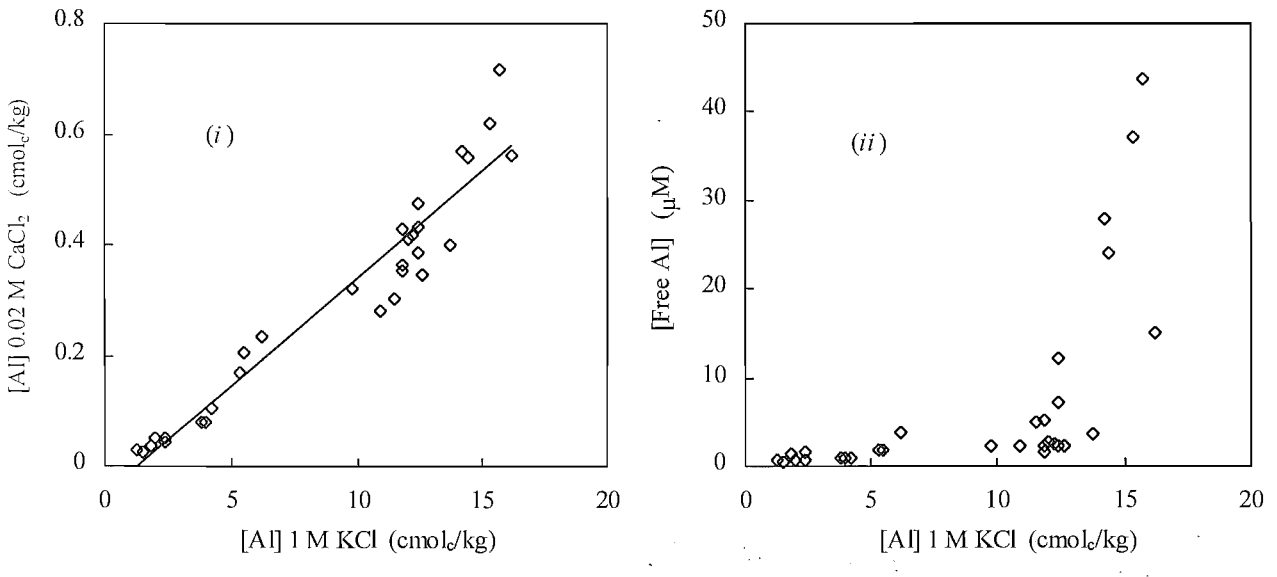

Figure 5.2. Correlations between (*i*) the concentrations of exchangeable 1 M KCl and 0.02 M $CaCl_2$ extractable Al and (*ii*), the concentrations of 1 M KCl exchangeable Al and soil solution 'free Al'. The equation of the regression line in (*i*) is $0.0387x - 0.0486$; $r^2 = 0.93$.

For soil solutions (0-10 cm) from forest sites at CP and CF, the concentrations of 'free Al' were greater (by factors of 2.7 and 2.0 respectively) than those for the respective grassland sites (Table 5.3), but these differences were not significant ($p = 0.16$ and 0.13, respectively). In all cases the concentrations from the individual replicates were less than 3.8 μM, indicating little likelihood of Al-toxicity. Concentrations for 'organic-bound Al' showed a similar trend, with the factors being 2.2 and 1.26 for CP and CF respectively, with these ratios being consistent with the A_{250} values, but not with the TOC values.

For the more acid (H^+) LP soils, the mean 'free Al' concentrations in soil solution for forest sites were 11.5, 6.3 and 2.4 times greater than those for the respective grassland sites at 0-10, 10-20 and 20-30 cm depths. Individual grassland soil replicates had concentrations of 'free

Al' varying to 4.9 μM, whereas for forest soil replicates, concentrations of 'free Al' ranged to a maximum of 43.7 μM. As shown in Figure 5.2, the concentration of 'free Al' in soil solution correlated poorly with the concentration of 1 M exchangeable Al. A similar (poor) correlation was obtained between concentrations of soil solution 'free Al' and Al extracted with 0.02 M $CaCl_2$ (not shown).

Concentrations of $[Al^{3+}]$ were calculated from the relationship 'free Al' = $[Al^{3+}]$ + $[Al(OH)^{2+}]$ + $[Al(OH)_2^{+}]$, using the stability constants for Al^{3+} hydrolysis reactions described in Section 2.2.10. Calculated values for log $[Al^{3+}]$ were in the range -4.4 to -6.9, which correlated strongly with soil solution pH (r^2 = 0.94, n = 30) (Figure 5.3).

5.3.3 Base cations: Ca, Mg, K, Na.

The data in Table 5.2 indicate that, relative to the grassland site at LP, there is a decrease in mean exchangeable K^+, Mg^{2+} and Ca^{2+} at each sampled depth at the forest site. At LP forest and grassland sites, the mean Ca^{2+} topsoil concentrations (0.12 and 0.93 $cmol_c/kg$) were much lower than the respective concentrations at either CP (0.75 and 2.76 $cmol_c/kg$) or CF (3.82 and 4.73 $cmol_c/kg$). Comparison of grassland and forest sites shows no significant trends in exchangeable Na^+ concentrations. Contrasting results were obtained for soil solutions (Table 5.3). For LP, at 0-10 cm and 10-20 cm depths the Na^+, K^+, Mg^{2+} and Ca^{2+} concentrations are all greater in forest soils, but the differences are not significant for K^+, or for Ca^{2+} at the 10-20 cm depth.

5.3.4 Al-complexation capacity

The Al-CC measures the capacity of a soil solution to bind Al in a non-labile or slowly labile form. Results of the Al-CC titrations are given in Table 5.4. Figure 5.4 shows a typical complexation capacity titration curve. Al-CC values at all sites were higher in the forest soils than in the corresponding grassland soils at both pH levels. This result is consistent with the increased amount of humic and fulvic matter (and hence potential Al binding sites) present in these forest soil solutions, as indicated by the higher A_{250} values (Table 5.4). The Al-CC values at pH 4.7 for LP sites correlate well with A_{250} (r^2 = 0.95, n = 6) (Figure 5.6), however, those for sites CP and CF do not. The high mean value for the 'organic-bound Al' in LP topsoil (14.2 μM) is consistent with the high A_{250} values for forest soil solution.

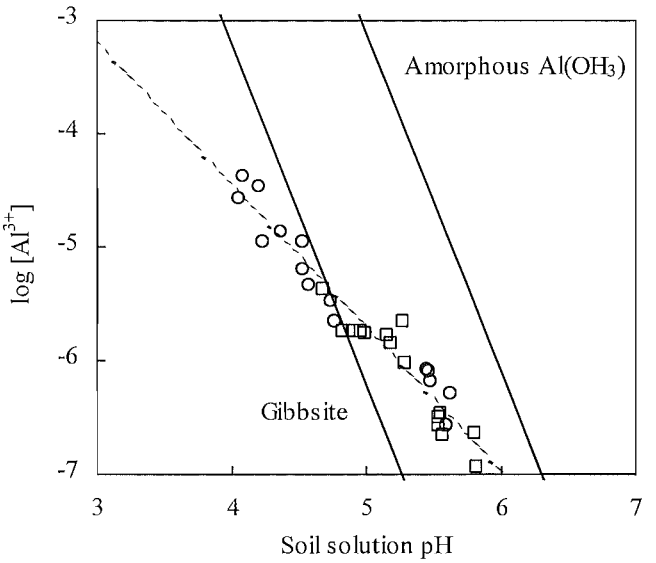

Figure 5.3. Relationship between log $[Al^{3+}]$ and soil solution pH. The solubility line for gibbsite was calculated using log $*K_{s0}$ = 8.79, that for amorphous $Al(OH)_3$ was calculated using log $*K_{s0}$ = 11.9. The dashed least-squares regression line has slope of -1.25 (r^2 = 0.94, n = 30) (○ forest soils; □ grassland soils).

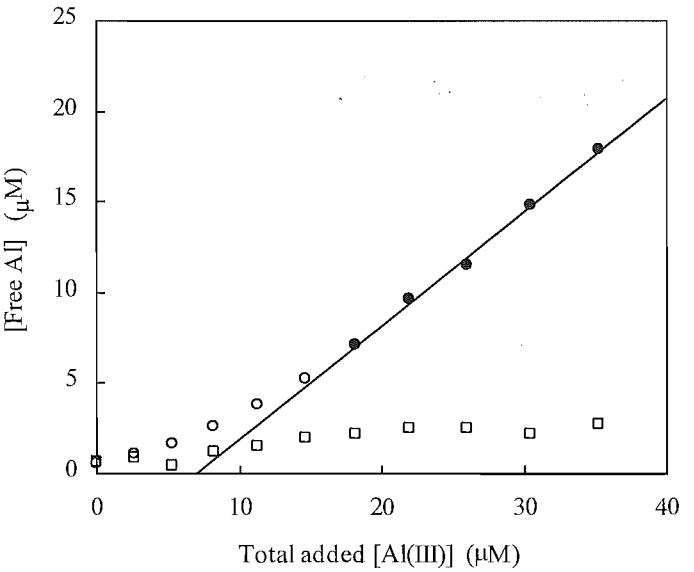

Figure 5.4. Al-CC titration curve at pH 5.5 (for grassland site at CP). The volume of soil solution was 4.0 mL made up to 40 mL (final composition 0.05 M KCl, 0.005 M acetate buffer. Filled symbols indicate datum points used to fit the line (r^2 = 1.00) to calculate the complexation capacity of the diluted soil solution (○ 'free Al'; □ 'organic-bound' Al).

Table 5.4. Aluminium complexation capacities determined on soil solutions from three sites.

Site	Depth (cm)		pH	A_{250}	Al-CC_{meas} (μM)		
					pH 4.2	pH 4.7	pH 5.5
CP	0-10	grassland	5.26	0.113	-	17.3	69.1
	0-10	forest	5.00	0.175	-	43.9	82.4
CF	0-10	grassland	5.13	0.212	-	6.1	23.5
	0-10	forest	4.84	0.221	-	16.3	43.2
LP	0-10	grassland	4.39	0.214	14.4	44.4	-
	0-10	forest	3.88	0.311	19.0	52.1	-
	10-20	grassland	5.27	0.102	10.5	31.1	-
	10-20	forest	4.44	0.171	13.2	40.7	-
	20-30	grassland	5.29	0.135	12.6	33.3	-
	20-30	forest	4.60	0.099	12.7	34.1	-

5.3.5 Lucerne root elongation

The results for the *M. sativa* root elongation experiments are given in Table 5.5. Root lengths from seedlings grown in the forest 0-10 and 10-20 cm soils were significantly shorter ($p<0.01$) than those grown in the corresponding grassland soils. No significant difference was observed for seedlings grown in the 20-30 cm depth soils ($p = 0.24$). In addition to being sensitive to Al^{3+} (*e.g.* Wheeler *et al.* 1992), growth of *M. sativa* has also been found to be sensitive to changes in acidity when grown in solution culture of pH 5.5 and 4.5 (Edmeades *et al.* 1991). Although the forest soils had lower pH and higher concentrations of 'free Al', neither variable, taken singly, correlated strongly with root length. However, ANOVA and multiple regression analyses indicated that, together, soil solution pH (regression coefficient -6.8, $p<0.01$), 'organic-bound Al' (regression coefficient 4.2, $p<0.005$) and 'free Al' (regression coefficient –1.7, $p<0.005$) were best correlated to the observed root elongations ($F_{0.05,3,2} = 196$, $r^2 = 0.997$).

Table 5.5. Root elongation and soil solution analyses at LP.

Depth (cm)		Soil soln. pH	A_{250}	Al (μM) organic	Al (μM) free	Mean root length (σ) (mm)
0-10	grassland	4.95	0.222	1.8	2.2	22.1 (5.4)
0-10	forest	4.15	0.238	10.2	30.8	14.3 (4.0)
p (t-test)		-	-	-	-	<0.01
10-20	grassland	5.06	0.107	1.0	1.6	18.6 (3.3)
10-20	forest	4.60	0.116	1.9	8.7	13.9 (3.7)
p (t-test)		-	-	-	-	<0.01
20-30	grassland	5.46	0.102	0.64	0.38	16.8 (4.0)
20-30	forest	4.85	0.094	0.80	2.1	18.6 (4.2)
p (t-test)		-	-	-	-	0.24

5.4 DISCUSSION

5.4.1 Soil acidification: pH

The decline in pH under forest at CP and LP, and lack of change in pH at CF, confirms earlier observations reported for the study sites (Davis 1994; Alfredsson *et al.* 1998; Yeates and Saggar 1998). However, Davis and Lang (1991) observed no difference in pH between forest and grassland at CP (their Site 1), the forest at that stage being aged 10 years. Declines in soil pH in N.Z. in response to afforestation of grassland have also been reported by Hawke and O'Conner (1993), Belton *et al.* (1995), Giddens *et al.* (1997), and Parfitt *et al.* (1997).

The extent of soil acidification in each forest topsoil can be related to the percentage base saturation at the respective grassland sites: LP (17.9), CP (48.7), CF (79.9); the impact of afforestation is greatest where the largest fraction of colloid exchange sites already carry acid cations (H^+, Al^{3+}). Other factors may have contributed to the different degrees of acidification. The soils at CP and CF are Allophanic Brown Soils, and the buffering capacity provided by large allophane pools may have reduced acidification there (Giddens *et al.* 1997).

In addition, buffering capacity provided by organic matter may have contributed to site differences (Giddens *et al.* 1997; Davis 1998). Alfredsson *et al.* (1998) report higher organic carbon levels in grassland soil for CF (11.9% in the 0-5 cm zone and 6.6% in the 5-15 cm zone) than are reported for the CP and LP sites (*ca.* 7.5% for the 0-10 cm zone (Davis and Lang 1991; Davis 1994)). The different forest species grown at CP (*P. nigra* and *P. ponderosa*) and CF (*Pseudotsuga menziesii*) may be another contributing factor. The increase in soil pH observed with increasing depth at LP is significant ($p<0.01$; $\triangle$pH = 0.45) for the forest site, but not for the corresponding grassland site ($p = 0.35$; $\triangle$pH = 0.09).

On average, the extracted soil solution pH values are 0.20 pH units higher than the corresponding soil pH, a general trend that has been observed in previous work (Chapter 4; Adams *et al.* 1996). Dahlgren *et al.* (1997) noted the loss of CO_2 from soil after sampling and during the extraction of soil solution by centrifugation. Provided the soil solution is in contact with the soil, the degassing should not affect either the soil or soil solution pH, however CO_2 loss from the extracted solution may have contributed to the observed increase in pH. Soil solution pH is important for Al speciation measurements and calculations.

It is clear that, compared with grassland vegetation, forest is able to induce a significant decrease in soil pH. This is most pronounced in topsoils where proton release accompanies cation uptake by roots, and the impact of acidification from oxidation and leaching of organic litter, is greatest. The greater proton release by pines is related to the approximately 10-fold increase in biomass production over grasslands (Davis 1998). The acidification under pine may also be linked to the type of organic matter, *viz.* organic acids and phenols from decomposition of litter, as well as the amount. Forests also have the capacity to intercept greater amounts of potentially acidic species (NH_4^+, SO_2) by dry deposition. However, such deposition is not likely to be a major factor for forests in New Zealand where atmospheric pollution is minimal.

Soil acidification may also be linked to the mobilisation of Al. Proton release from plants promotes weathering of soil (*e.g.* the release of Al^{3+} from aluminosilicates) and the depolymerisation of Al-hydroxy polymers. Both H^+ and Al^{3+} are strongly bound to cation exchange sites on soil colloids, and displace the more weakly bound 'base cations', Ca^{2+} and Mg^{2+}. This is illustrated at CP, and by the three soil horizons at LP (Table 5.2). Relative to the grassland sites, there is an increase in $[H^+]$ and $[Al^{3+}]$ on exchange sites, and a corresponding decrease in $[Ca^{2+}]$ and $[Mg^{2+}]$ for the forest soils.

In the present study, topsoils from the forested sites also had significantly lower moisture contents ($p<0.01$) than topsoils from the grassland sites (Table 5.2). The LP site exhibited the greatest difference, with grassland sites having 70-120% more moisture, whereas the Craigieburn sites had 26-49% more moisture that the respective forest sites. This observation agrees with those of Davis (1994) and Giddens *et al.* (1997), both of whom report lower moisture contents under forest than grassland. The difference in moisture contents is attributed to the interception of rainfall by the forest canopy and the subsequent increased rate of evaporation and transpiration that may occur.

5.4.2 Soil acidification: Al^{3+}

Mobilisation of Al^{3+} is another indicator of soil acidification. At low pH and high soil solution TOC, the weathering of minerals is accelerated, and the release of Al^{3+} (in contrast to $Si(OH)_4$) is enhanced. One result is the competitive adsorption of Al^{3+} onto colloid and humic acid exchange sites, the movement of (complexed) Al^{3+} through the soil profile, and the replacement of H^+-acidity by Al^{3+}-acidity, exemplified by the proton dissociation reactions of the aluminium aqua ion:

$$Al(H_2O)_6^{3+} + H_2O \rightleftharpoons Al(OH)(H_2O)_5^{2+} + H_3O^+ \quad etc.$$

It is clear from the correlation shown in Figure 5.2, that 1 M exchangeable Al is a poor indicator of soil solution 'free Al', and hence will be a poor estimate of soil Al toxicity status. In a study investigating the relationship between soil solution aluminium and exchangeable Al in fourteen New Zealand subsoils, Percival *et al.* (1996) found similar (poor) correlations. The total Al concentrations in 1 M KCl and 0.02 M $CaCl_2$ soil extracts exceeded reported thresholds that indicated potential for Al toxicity (toxicity associated with (*i*) > 1-2 $cmol_c/kg$ of 1 M KCl exchangeable Al or (*ii*) > 3-5 μg Al/g of 0.02 M $CaCl_2$ extractable Al (Edmeades *et al.* 1983)). However, Percival *et al.* (1996) also found that the measured monomeric Al concentrations in soil solution extracted from these soils did not exceed potential Al toxicity concentrations (9-15 μM $\{Al^{3+}\}$ (Edmeades *et al.* 1983)), indicating that exchangeable Al concentrations often provide a less reliable indication of potential Al toxicity than soil solution Al concentrations.

The strong correlation between soil solution pH and the calculated values of log $[Al^{3+}]$ is shown in Figure 5.3. Although forest soils were generally more acidic than the corresponding grassland soils, no pattern in the $[Al^{3+}]$ values was attributable to site, soil depth or vegetation

factors. The single linear relationship between soil solution pH and $[Al^{3+}]$ indicates that a common phase(s) is controlling Al solubility at all sites. The fitted least-squares regression line through all data points has a slope of -1.25, substantially lower than the theoretical slope of -3.00, expected if a solid $Al(OH)_3$ phase was controlling Al solubility in soil solution. At higher soil solution pH (pH > *ca.* 4.8), the calculated values of $[Al^{3+}]$ lie between the solubility lines for gibbsite and amorphous $Al(OH)_3$, consistent with control of $[Al^{3+}]$ by a solid $Al(OH)_3$ phase. However, at lower soil solution pH (pH < *ca.* 4.8) the soil solutions are under-saturated with respect to both $Al(OH)_3(s)$ phases.

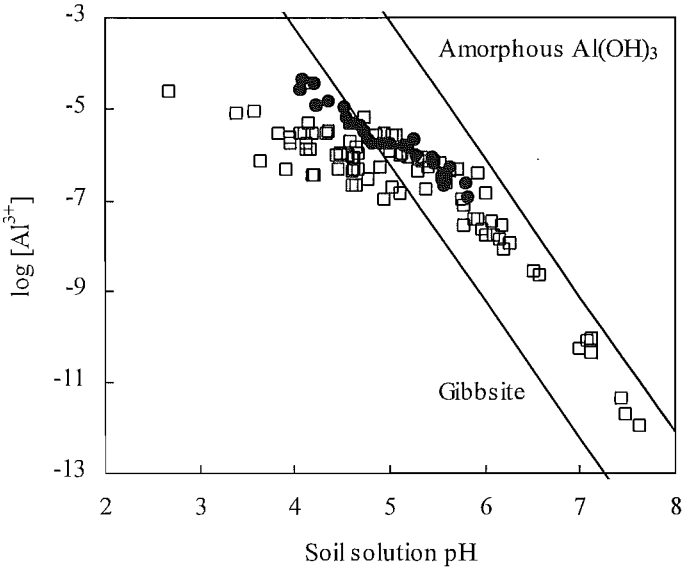

Figure 5.5. Comparison of the relationship between log $[Al^{3+}]$ and soil solution pH for data presented in this chapter, and that from Chapter 3. The solubility line for gibbsite was calculated using log $*K_{s0}$ = 8.79, that for amorphous $Al(OH)_3$ was calculated using log $*K_{s0}$ = 11.9. (● data from this study; □ data presented in Chapter 3).

A similar relationship between soil solution pH and $[Al^{3+}]$ is reported in Section 3.3, and has also been previously reported by others (Cronan *et al.* 1986; Mulder and Stein 1994; Lawrence and David 1997). In these studies it was proposed that solubility of Al^{3+} at acidic pH (< *ca.* 5.5) was controlled by soil organic matter. In Chapter 3, support for an organic phase controlling $[Al^{3+}]$ solubility was provided by the good agreement between a pH-dependent fulvic acid-Al^{3+} binding curve and the experimental soil solution pH *vs.* $[Al^{3+}]$ plot. The data in Figure 5.3 show a degree of scatter, and while some scatter is undoubtedly of natural origin, errors in the analytical measurement of Al and pH, and in assumptions made in the speciation calculations, will also contribute to the observed scatter. A comprehensive discussion of these, and other such potential errors is contained in Section 3.4. Although

these results are spread over a narrower range of soil solution pH than the results presented in Chapter 3, there is nevertheless good agreement between the two sets of results (Figure 5.5). Five soil solutions that contain high concentrations of $[Al^{3+}]$, are noted to lie slightly above the trend established from the results in Chapter 3.

5.4.3 Base cations: Ca, Mg, K, Na.

The data in Table 5.2 indicate there is a decrease in mean exchangeable K^+, Mg^{2+} and Ca^{2+} at each sampled depth at the forest site, relative to the grassland site at LP. However, as there was no evidence for translocation to lower horizons at LP, it may be assumed that the changes indicate cation uptake for inclusion in biomass, rather than acid-induced leaching. Yeates and Saggar (1998) also observed decreased concentrations of K^+, Mg^{2+} and Ca^{2+} under *P. radiata* at their sampling site in the LP catchment. A similar decrease is observed for topsoils at CP. At CF, the site with highest base saturation, the effects are smaller for K^+, Ca^{2+} and Mg^{2+} and not statistically significant. Alfredsson *et al.* (1998) also reported lower levels of all three cations under forest at CF, with the difference for Ca^{2+} not being significant in the upper (0-5 cm) soil.

Contrasting results were obtained for concentrations of cations in soil solutions (Table 5.3). For soil solution from LP soils, Na^+, K^+, Mg^{2+} and Ca^{2+} concentrations are all greater in forest soils at 0-10 cm and 10-20 cm depths. It is noted that these are soil solutions that also have very high concentrations of 'free Al'. For the less acid soils at CP and CF there is no clear pattern, and differences are not significant. For soil solution Na^+ at LP, the higher concentrations in forest soil solution may relate to the canopy interception of dry aerosols derived from sea spray. It may also relate to the high concentrations of Al^{3+} in these soil solutions, as Na^+ will be the least strongly adsorbed cation on colloid exchange sites, and Al^{3+} the strongest.

The [Ca]/[Al] and [Mg]/[Al] ratios are indicators for the possible onset of Al toxicity, or Mg deficiency in soils (Cronan and Grigal 1995). For exchangeable cations the [Ca]/[Al] and [Mg]/[Al] ratios were lower (less favourable) in forest soils than for the respective grassland soils (data not presented). An identical trend was observed for soil solutions, with lower $[Ca]/[Al_{free}]$ and $[Mg]/[Al_{free}]$ ratios in forest soils than in grassland soils (Table 5.3). Of the three sites, LP exhibited the lowest absolute values of the two ratios for grassland and forest soils respectively, with CF having the highest values.

Much literature evidence suggests that low or declining [Ca]/[Al] ratios increase the likelihood and/or severity of Al toxicity. Cronan and Grigal (1995) have published a comprehensive review on the use of soil solution [Ca]/[Al] ratios as ecological risk indicators for tree growth and nutrition. They identified four parameters (of which only the first two pertain to this study) which may be used as potential threshold conditions for measurable forest impacts caused by Al stress: (*i*) a soil base saturation of less than 15% of effective CEC, (*ii*) soil solution [Ca]/[Al] ratio ≤ 1.0 (for a 50% risk of impacts on tree growth or nutrition), (*iii*) fine root tissue [Ca]/[Al] ratio ≤ 0.2 (for 50% risk), and (*iv*) a foliar tissue [Ca]/[Al] ratio ≤ 12.5 (for 50% risk).

In the present study, base saturation was close to or below the suggested threshold in forest soil at CP, and at all soil depths in both forest and grassland at LP (Table 5.2). The lowest soil solution [Ca]/[Al] ratio (total Al determined by ICP spectroscopy) observed in this study was 1.3, in a forest topsoil at LP (mean ratio for LP forest topsoils was 2.0). In contrast, the lowest ratio observed in a grassland topsoil at LP was 6.3 (mean ratio for LP grassland topsoils was 9.4). Both forest and grassland soils at CP had similarly high [Ca]/[Al] ratios (>6.0). Soil solution [Ca]/[Al] ratios were not able to be calculated for the CF site, as total Al in these soil solutions was below the detection limit (<0.1 μg/mL) for the ICP emission technique. However, given the high percentage base saturation for these soils, it is likely that the [Ca]/[Al] ratios will be similar to, or greater, than those calculated for the CP soils. Of the sites sampled, the LP forest sites clearly have the most potential for Al-induced stress to impact upon tree growth and nutrition.

Symptoms of upper mid-crown yellowing, considered to be due to Mg deficiency in *P. radiata* (Beets *et al.* 1993) were evident at LP, while there was no such evidence of Mg deficiency at CP or CF. However, there was no great difference in either exchangeable or soil solution Mg^{2+} concentrations between the three sites. Indeed, the mean soil solution topsoil concentrations of Mg^{2+} under forest and grassland at LP were generally slightly higher than those found at either CP or CF. Ende and Evers (1997) state that Mg deficiency mainly appears on base-poor acidic substrates, where exchangeable Mg^{2+} contents are below 2.0 $cmol_c$/kg soil. All three sampling sites had exchangeable Mg^{2+} concentrations of <1.0 $cmol_c$/kg, but LP exhibited the lowest base saturation of the sites. Root uptake of Mg in forest species may be suppressed by high Al concentrations (Asp *et al.* 1988; Schulze 1989). Mg deficiency observed at LP may have been induced by the development of high soil solution Al concentrations there. Truman *et al.* (1986) reported reduced Mg uptake by

P. radiata roots in the presence of 17 μM Al (the lowest treatment concentration used), well below the concentrations observed in this study for forest topsoil at LP.

5.4.4 Al-complexation capacity

For LP sites the rate of change of Al-CC with A_{250} was 97 μM per absorbance unit at pH 4.7 (Figure 5.6). This value is much greater than that observed for a diverse series of Canterbury indigenous forest soils (15.3 μM) using a kinetically-based FIA technique (Powell and Hawke 1995), and that for a solution of soil-extracted fulvic acid (6.6 μM) (Hawke *et al.* 1996). Furthermore, for the Al-CC values from LP, the least-squares regression line does not pass through the origin at either pH 4.2 or 4.7 (intercept = +8 and +23 μM L^{-1} soil solution respectively) (Figure 5.6). This contrasts with the results of Powell and Hawke (1995) and those from a series of high country pastoral soils (Chapter 4) where, within experimental error, similar plots were observed to pass through the origin.

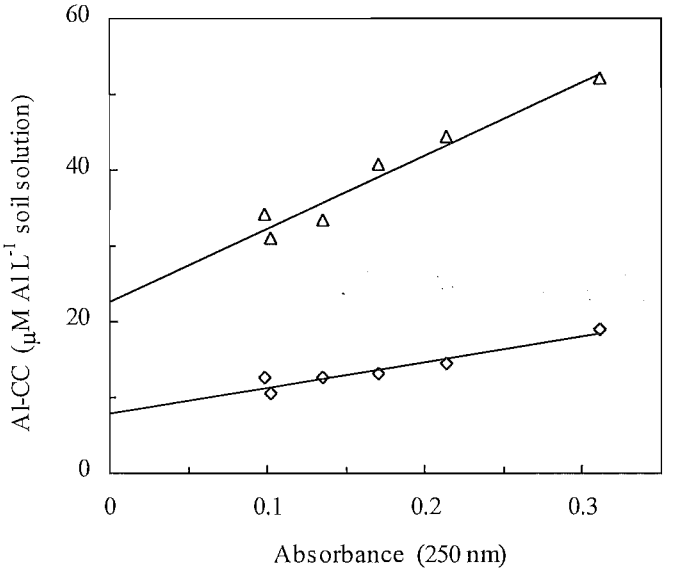

Figure 5.6. Relationship between soil solution aluminium complexation capacity, Al-CC, and UV absorbance at 250 nm at site LP (◇ pH 4.2, $r^2 = 0.90$; △ pH 4.7, $r^2 = 0.95$).

A non-zero intercept, and the large slope are attributed to the presence of non-UV absorbing organic species that contribute significantly to the measured Al-CC. Such organic species may include classes of soil compounds such as low molecular weight aliphatic acids (Hue *et al.* 1986) and polysaccharides (see Chapter 7), both of which are known to bind Al strongly.

Determination of the Al-CC at two pH values allows a general assessment to be made on the ability of the organic substances present to complex and detoxify Al under conditions of increasing $[H^+]$ and $[Al^{3+}]$. At sites CP and CF, the Al-CC decreased by 47 to 75% on lowering the pH from 5.5 to 4.7. At LP, where Al-CC was measured at pH 4.7 and 4.2, the decrease in Al-CC for all soils fell within a narrower range, 62 to 68%. Such large decreases indicate a very marked sensitivity to acidification. The decrease in Al-CC values with pH is consistent with fewer functional groups being able to bind strongly to aluminium as the amount of proton competition increases.

5.4.5 Lucerne root elongation

Edmeades *et al.* (1991) and Wheeler *et al.* (1992) reported that soil solution $\{Al^{3+}\}$ of 3-5 $\times 10^{-6}$ and *ca.* 10 $\times 10^{-6}$ in soil solution, were required to reduce total dry matter (TDM) by 50% of several legume and pasture species, respectively. These activities are equivalent to 'free Al' concentrations of around 6-10 μM and 20 μM, respectively. Edmeades (1983) found that white clover (*Trifolium repens*) was affected (50% reduction in TDM) by Al toxicity associated with (*i*) 1-2 $cmol_c/kg$ of exchangeable Al extracted with 1 M KCl, and (*ii*) 3-5 μg Al/g extracted with 0.02 M $CaCl_2$. Concentrations of exchangeable aluminium in these forest and grassland soils are generally significantly higher than these thresholds (Table 5.2).

As previously noted however, Percival *et al.* (1996) (in addition to this study) found poor correlations between exchangeable and soil solution concentrations of Al. Therefore use of these thresholds as indicators of potential Al toxicity may be misleading. For several soils however, the concentrations of soil solution 'free Al' do exceed the suggested Al toxicity thresholds described above by Edmeades *et al.* (1991) and Wheeler *et al.* (1992). It is therefore very likely that the Al concentration in these soils is sufficient to inhibit the growth of sensitive species.

The results for the *M. sativa* root elongation experiments (Table 5.5) showed seedling root length was significantly shorter ($p<0.01$) in the forest 0-10 and 10-20 cm soils than in the corresponding grassland soils. Although growth of *M. sativa* has been found to be sensitive to both Al and acidity (Edmeades *et al.* 1991), neither variable, when taken singly, correlated well with root length. However, together, soil solution pH, 'organic-bound Al' and 'free Al' did correlate strongly with observed root elongations (root length = -6.8*(soil solution pH) + 4.2*(organic-bound Al) – 1.7*(free Al); Section 5.3.5).

It is interesting to note that 'organic-bound Al' correlates with root elongation with a positive coefficient weighting (*i.e.* beneficial with respect to root elongation). This agrees with the general presumption that organic-bound Al is non-bioavailable and hence non-toxic (*e.g.* Hue *et al.* 1986).

A correlation with a moderately-labile, 'organic-bound Al' fraction has not previously been possible. In much of the earlier work, it is likely that concentrations of inorganic monomeric aluminium were over-estimated. Many reported methods in the literature achieve the analysis of inorganic monomeric Al (Al^{3+}, $Al(OH)^{2+}$ and $Al(OH)_2^{+}$) through a 'selective' reaction between Al^{3+} and a spectrophotometric/fluorimetric reagent (*e.g.* Røyset 1986; Kerven *et al.* 1989*a*), or through capture of the positively-charged unbound Al species on a cation-exchange or chelating resin (*e.g.* Driscoll 1984; Fairman and Sanz-Medel 1996). These methods are commonly overly aggressive towards organically-bound Al, (or the elapsed experimental time is too long) which may cause sample re-equilibration and the subsequent release of Al from organic complexes. This results in an over-estimation of the inorganic monomeric Al. Hence it is quite likely that past analytical results used in correlations between Al and bio-toxicity may have included a small fraction of organically-bound Al as part of the measured 'toxic' inorganic monomeric Al pool.

5.5 CONCLUSION

The impact of land use change from grassland to conifer forest on the aluminium (Al) concentrations in soils and soil solutions was examined. Soils from grassland were compared with those from adjoining 15-19 year old forest stands at three contrasting pairs of sites in the South Island, New Zealand. The results of this study indicated that afforestation of pastoral grassland with conifers may reduce soil pH, with the magnitude of the soil pH change being site specific. Similarly, afforestation may also reduce base cation levels and base saturation. Soil percentage base saturation values were observed to be lower for forest than for grassland soils at all sites. In soil solutions there was a trend for both 'free Al' and Al bound in labile organic complexes to be higher in forest soil at all sites, but site-pair differences were only significant at LP, and only for 'free Al'. The increase in 'free Al' at LP was linked to the low pH and low base saturation at this site.

The effects of afforestation are likely to be most marked in soils with low base saturation, with low buffering capacity, and with tree species that have high uptake rates of base cations.

Where natural base saturation is low (*e.g.* <20%), the increase in 'free Al' concentrations in soil solutions under fast growing tree species such as *Pinus radiata* may be sufficient to interfere with uptake of Mg. Magnesium deficiency symptoms were evident in *P. radiata* at LP, but not at the other sites. Liming or Mg application may be required to ameliorate these effects. The relative importance of base saturation, organic matter and allophane content in buffering the soil against changes in acidity requires further study. Similarly, the influence of tree species on soil acidity development needs to be investigated.

CHAPTER 6

EFFECTS OF AGEING SOIL AND SOIL SOLUTION SAMPLES BEFORE ANALYSIS

6.1 INTRODUCTION

Determination of the nutrient and toxic species in soil solution is often hampered by difficulty not only in extracting the soil solution itself, but by composition changes that may occur during storage or incubation of the field-moist soil prior to extraction (Wolt 1994). Although it is generally recommended that samples be analysed as quickly as possible to obtain data that accurately reflect the *in situ* soil solution composition (Edmeades *et al.* 1985; Ross and Bartlett 1990), in practice this is not always feasible due to transportation considerations or equipment/time limitations. There are a number of studies in the literature which have investigated the effects of sample storage on the chemical composition of the resultant soil solution, soil extract or water samples.

Curtin and Smillie (1995) investigated the effects of incubation on soil solution concentrations of exchangeable cations. As incubation of the field moist soils progressed (up to a period of *ca.* one year) the soil solution concentrations of Ca, Mg, K, and Na increased, together with NO_3^- (and hence also the ionic strength of the soil solution). In contrast to the observed changes in concentrations, the cation ratios (*e.g.* [Ca]:[Mg]) generally remained constant during the incubation period. The concurrent increase in nitrate concentrations tends to suggest the cation changes were microbially mediated.

Increases in the concentrations of base cations during incubation were attributed to their displacement from exchange sites by protons generated during microbially-induced mineralisation of N. Soil solution pH tended to decrease during incubation, and as a result, caused large increases in the concentrations of Al. Storage of unfrozen field-moist soils at low temperatures was subsequently proposed as a protocol to minimise changes in soil solution composition associated with nitrogen mineralisation. Van Miegroet (1995) similarly noted that even sample transportation from the field and the short-term storage of soil

solutions could stimulate turnover of soil inorganic and organic N, and thus affect other soil parameters.

Derome *et al.* (1998) investigated the effect of storage on aluminium fractionation by keeping soil solution samples at 4°C for two weeks. They also investigated the effect of freezing by maintaining the soil samples for two weeks at -20°C. A delay of a few hours to two days between sampling and pre-treatment appeared to have no effect on total Al concentrations in soil solution. The refrigeration of samples at 4°C caused an increase (26%) in the fraction of non-labile Al, suggesting that the fraction of labile monomeric species had decreased during storage. Freezing of samples caused a large reduction (38%) in the concentrations of total Al. Ross and Bartlett (1990) found that freezing for longer periods (36 days) was an inappropriate storage protocol for a series of Spodosol soil samples, as it significantly increased the concentrations of SO_4^{2-}, Cl^-, F^- and total Al in the displaced soil solutions. These authors also found soil solution extraction by a high speed centrifuge method (10 000 r.p.m.) caused significant increases in pH, and F^-, Cl^- and SO_4^{2-} concentrations, compared with two alternative extraction methods.

Berdén (1994) studied the effects of sample storage on a 'quickly-reactive' fraction of Al (Al_{qr}) in soil leachates. As in the study above, samples exhibited a decrease of Al_{qr} with time, but the rate and extent of the decrease varied strongly with the sample type. Samples that contained high concentrations of dissolved organic carbon (DOC) and low concentrations of Al_{qr} were more sensitive to storage than samples with low DOC and high concentrations of Al_{qr}.

For laboratory convenience, air-drying and sieving of soils before long-term storage is a common technique for soil storage. When required, the sample is moistened prior to analysis. Both the drying and moistening steps have the potential to change the chemical composition of the resultant soil solution. Courchesne *et al.* (1995) noted the effects of air-drying on the measurement of soil pH and various soil properties in a number of acidic forest soils. Drying generally resulted in soil acidification for all horizons studied. There was a positive relationship between the pH changes induced by drying, and organic C and exchangeable Al concentrations. The DOC concentrations were always higher in dry soil than in the field-moist soil. The decrease in soil $pH_{(H_2O)}$ (up to 0.50 pH units) was mostly associated with the acidifying effect of an increase in organic matter solubility after drying.

Bartlett and James (1980) published a comprehensive discussion on the potential problems of studying soil samples that have been dried. As was illustrated by the results of Courchesne *et al.* (1995), the air-drying of soils was noted to cause an increase in the surface acidity of soil and increased solubility and likelihood of oxidation of soil organic matter. They also noted that the chemical characteristics of dried soil samples continue to change during dry storage, and that the behaviour of a dried sample immediately after wetting differs from that of the continuously moist soil. Bartlett and James (1980) concluded that while there is not a convenient, simple and suitable alternative to drying soil samples, for short to long term storage the most appropriate protocol is to keep soil samples close to field-capacity moisture, inside thin, breathable polyethylene bags at low (but above freezing) temperatures.

The protocols used in this work were similar to those recommended in several of the studies above. Samples were transported in insulated containers to avoid unnecessary warming of the soil. Where possible, soil solution was extracted as soon as possible after sampling and analysed immediately. If soils were required to be stored before analysis, they were kept in plastic bags at field-moisture and refrigerated (4°C).

The aim of this study was to determine the effects of ageing soil samples (and the extracted soil solutions) on the concentrations of soil solution aluminium, major cations and total organic carbon over a short period (7 days) after sampling. Soils were sampled from two locations, with a grassland and forest soil sampled from each site. Soil solution was extracted from the soil and analysed on day one, and again on day two and day seven after the original extraction. In addition to analyses of the freshly extracted soil solutions, the samples of previously-extracted soil solutions were re-analysed on each occasion to establish the effects of ageing on the soil solution itself. Soil solutions were also obtained from moistened samples of air-dried soils, and the results compared to those obtained from the field moist soils.

6.2 MATERIALS AND METHODS

6.2.1 Site description

The two sampling sites were located on a terrace in the Cragieburn Range, and on Bealey Spur, Canterbury, New Zealand. A grassland and forest soil were sampled from each site. The forested site at Cragieburn consisted of exotic Corsican (*Pinus nigra*) and Ponderosa pine (*P. ponderosa*), with the adjacent grassland site dominated by native short tussocks (*Poa* and

Festuca spp.), moss (*Racomitrium* sp. and *Lycopodium* sp.), and the native shrubs (*Dracophyllum*, *Cassinia*, and *Cyathodes* spp.). The site is at 810 m elevation, and receives *ca.* 1300 mm rainfall annually. The Bealey Spur forested site was predominantly native silver beech (*Northofagus menziesii*) and the grassland consisted of the native short tussocks, and the various mosses and shrubs. Unlike the Cragieburn sampling sites, the two Bealey Spur sites were not adjacent, the grassland site being *ca.* 30 m higher in elevation than the forest site. The approximate elevation of the Bealey Spur forested site was 830 m, and the site receives *ca.* 2000-3000 mm annual rainfall, considerably greater than the more eastern Cragieburn site.

6.2.2 Sampling

Sampling was performed during March 1999. At each of the four sites, approximately 25-30 2.5 cm diameter soil cores (0-10 cm) were taken from random spot samples and pooled. Loose vegetation matter was removed, exposing the top of the mineral soil before sampling. Sampling at tussock bases was avoided at both of the grassland sites. Samples were collected into plastic bags and sealed, before transportation in an insulated chest to the laboratory.

6.2.3 Soil solution analyses

Soils were sampled two days after a significant rainfall event (there had been a total of 380 mm rainfall during the preceding 5 days in the nearby Arthurs Pass township), in order that the soils might be sufficiently moist to allow centrifugation and analysis that same day. However, after sampling it was evident the soil would require wetting (and a subsequent equilibration period) before centrifugation. The field-moist soils were wetted with TDW (15% by weight) and equilibrated for *ca.* 18 hours in the insulated container. After this initial equilibration period at ambient soil temperature, the wetted soils were kept refrigerated at 4°C.

Soil solution was extracted 24 and 48 hours, and 7 days after sampling. Soil solutions were centrifuged and filtered as described in Section 2.2.3. Sufficient soil solution was extracted after 24 hours (Day 1) to allow further analyses to be performed on the two later occasions when soil solution would be extracted. Soil solution samples were stored in centrifuge tubes (*i.e.* head-space existed for possible gas-exchange) and refrigerated, but allowed to return to room temperature before analysis.

Soil solution pH and UV absorbance at 250 nm were measured on the fresh soil solution extracts as described in Section 2.2.4. Concentrations of 'free Al' and organic-bound Al' in

soil solution were obtained using the oxine-derivatised Fractogel method described in Section 2.2.7. The soil solution concentration of the cations (Ca^{2+}, Mg^{2+}, K^+ and Na^+) was determined by ion chromatography (Section 2.2.4.4). As the cation concentrations were not expected to change with storage of the soil solutions, these were analysed in one batch at a later date. Total organic carbon measurements were performed by the Institute of Environmental Science and Research Ltd. (ESR) at the Wellington Science Centre, New Zealand. Samples for TOC analysis were preserved at pH <2.0 (conc. H_2SO_4, BDH AnalaR) and refrigerated until transportation.

A further sub-sample of soil was air-dried at 30°C. The dry soil was subsequently wetted with TDW back to the calculated field water content, and a further 15% TDW added (by weight) as for the original field-moist samples. The wetted samples were refrigerated and equilibrated for 24 hours before centrifugation of the soil solution.

6.3 RESULTS

Experiments were performed to establish the effects of ageing, both soil and soil solutions, on the chemical parameters quantified (soil solution pH, A_{250}, TOC, and concentrations of 'free Al', 'organic-bound Al' and major cations). The results of the soil solution storage experiments (soil solution extracted on Day 1 and re-analysed on later dates) are presented in Table 6.1. Figure 6.1 shows the increase in pH observed with storage of the soil solutions.

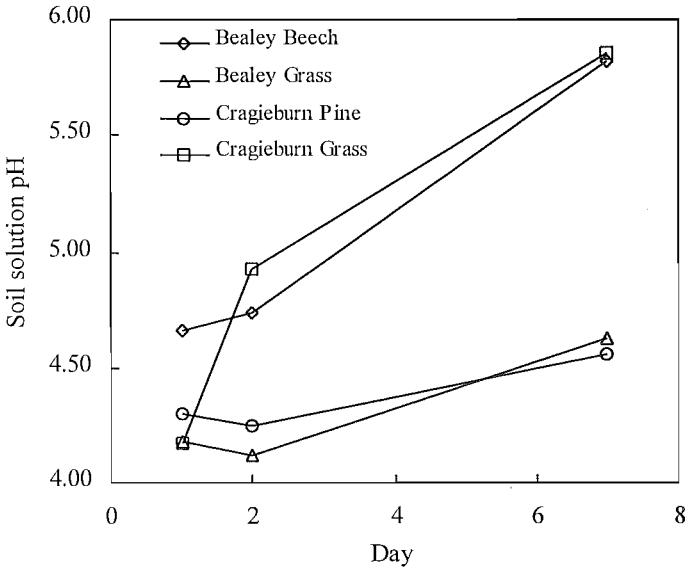

Figure 6.1. The increase in soil solution pH observed with storage of soil solutions (extracted Day 1).

Table 6.1. Mean results of soil solution analyses from soil solution storage experiments.

Site	pH			A_{250}			TOC (mg/L)			'Org.-bound Al' (μM)			'Free Al' (μM)		
	Day 1	Day 2	Day 7	Day 1	Day 2	Day 7	Day 1	Day 2	Day 7	Day 1	Day 2	Day 7	Day 1	Day 2	Day 7
Bealey Beech	4.66	4.74	5.82	0.495	0.489	0.554	260	-	175	4.6	4.3	3.9	1.3	1.2	0.9
Bealey Grass	4.18	4.12	4.63	0.423	0.417	0.476	255	-	285	6.4	6.3	6.5	3.9	4.0	4.4
Cragieburn Pine	4.30	4.25	4.56	0.198	0.197	0.212	210	-	0	4.8	4.7	4. 8	4.4	4.8	5.0
Cragieburn Grass	4.17	4.93	5.85	0.146	0.141	0.198	290	-	140	2.9	2.9	2.9	1.1	1.5	1.2

Table 6.2. Mean results of soil solution analyses from soil incubation experiments.

Site	pH			A_{250}			TOC (mg/L)			'Org.-bound Al' (μM)			'Free Al' (μM)		
	Day 1	Day 2	Day 7	Day 1	Day 2	Day 7	Day 1	Day 2	Day 7	Day 1	Day 2	Day 7	Day 1	Day 2	Day 7
Bealey Beech	4.66	4.87	4.55	0.495	0.383	0.495	260	335	<blank	4.6	3.9	5.2	1.3	1.1	1.8
Bealey Grass	4.18	4.34	4.13	0.423	0.339	0.335	255	130	335	6.4	4.7	5.9	3.9	2.2	4.1
Cragieburn Pine	4.30	4.64	4.55	0.198	0.160	0.169	210	170	395	4.8	3.4	3.5	4.4	1.9	1.8
Cragieburn Grass	4.17	4.44	4.86	0.146	0.095	0.109	290	395	275	2.9	3.1	2.6	1.1	3.4	1.0

Table 6.2 presents the results from the soil incubation experiments (fresh soil solutions extracted and analysed each date). The changes observed for soil solution A_{250} measurements are shown in Figure 6.2.

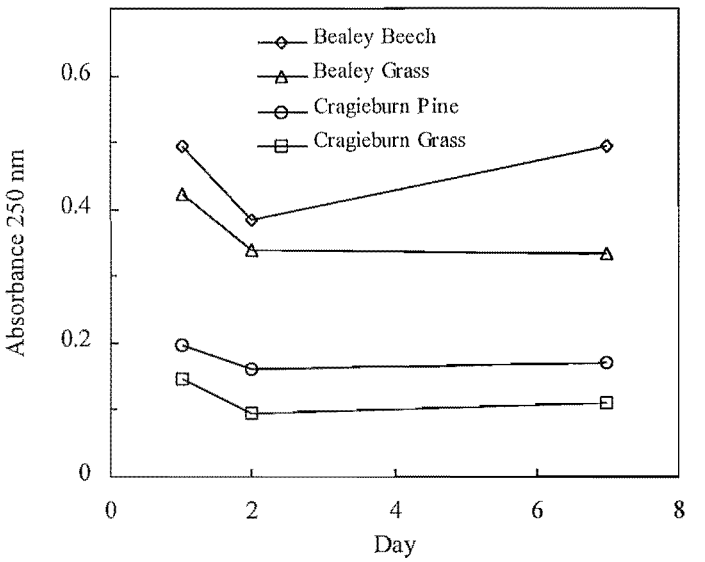

Figure 6.2. Soil solution UV absorbance at 250 nm for incubated soils, showing the initial decrease in A_{250} values.

The results of the determination of base cation concentrations in soil solutions are given in Table 6.3. Large increases in the concentrations of cations were observed when soil solution was extracted from the wetted air-dried soil (Table 6.4). The soil solution pH, A_{250} and TOC values, and Al concentrations for the wetted soils are presented in Table 6.5.

Table 6.3. Concentrations of cations in soil solutions from soil incubation experiments (μM).

Site	Ca^{2+}			Mg^{2+}			K^{+}			Na^{+}		
	Day 1	Day 2	Day 7	Day 1	Day 2	Day 7	Day 1	Day 2	Day 7	Day 1	Day 2	Day 7
Bealey Beech	192	194	189	45	47	37	123	115	94	368	352	289
Bealey Grass	174	157	168	73	72	74	119	150	132	348	392	335
Cragieburn Pine	192	147	112	40	31	23	107	72	48	418	328	263
Cragieburn Grass	137	185	110	35	46	28	119	72	87	262	254	191

Table 6.4. Concentrations of cations in soil solutions from field-moist (Day 1) and air-dried soil samples (μM).

Site	Ca^{2+}		Mg^{2+}		K^{+}		Na^{+}	
	Day 1	Air-Dried	Day 1	Air-Dried	Day 1	Air-Dried	Day 1	Air-Dried
Bealey Beech	192	820	45	256	123	278	368	620
Bealey Grass	174	186	73	117	119	170	348	443
Cragieburn Pine	192	336	40	127	107	230	418	549
Cragieburn Grass	137	344	35	123	119	175	262	385

Table 6.5. Mean results for soil solution extracted from wetted air-dried soil samples.

Site	pH	A_{250}	TOC	'Org.-bound Al' (μM)	'Free Al' (μM)
Bealey Beech	4.30	1.458	480	12.9	6.4
Bealey Grass	4.20	0.660	275	11.7	10.1
Cragieburn Pine	3.90	0.481	225	18.8	32.4
Cragieburn Grass	4.33	0.463	150	6.4	8.8

6.4 DISCUSSION

6.4.1 Soil solution storage

For all samples, soil solution pH rose significantly (mean ΔpH = + 0.89) by Day 7 (Table 6.1; Figure 6.1). Except for one sample (Cragieburn grass) the change in pH 24 hours after the original extraction was minimal. One probable cause for the observed increase in pH (Table 6.1), is CO_2 degassing of the stored soil solutions, a potential problem noted by many authors. Degassing is of particular relevance for solutions having an initial pH of *ca.* 5.0, as it requires high concentrations of CO_2 (a weak acid) to depress the soil solution pH below this.

The concentrations of soluble humic and fulvic acids, which are estimated by the UV absorbance of the soil solution at 250 nm, also increased for all samples during the 7 day storage period (Table 6.1). In contrast to the A_{250} measurements, TOC results had generally decreased by Day 7 (although the 0 mg/L value appears anomalous). There was a poor correlation (r^2 = 0.10) between the A_{250} and TOC values for the four soil solutions, indicating that fulvic and humic species in soil solution did not occur in proportion to the concentrations of low-molecular weight UV-transparent organic compounds.

An increase in soil solution pH, and in the concentration of humic and fulvic species present (as indicated by the A_{250} measurements) might be expected to favour increased levels of 'organic-bound' Al. Nevertheless, concentrations of this fraction of Al generally remained similar throughout the storage period (Table 6.1). The largest change observed was for the Bealey Beech sample, where the concentration of 'organic-bound Al' fell 15% during the

7 day storage period. Larger changes were observed for the concentrations of 'free Al' in the four samples. Despite the observed increase in soil solution pH, three of the four samples had higher concentrations of 'free Al' by day 7. For these three samples, 'free Al' concentrations rose 13%. For the Bealey Beech sample, the concentration of 'free Al' fell 28% (the concentration of 'organic-bound Al' also fell for this sample).

The initial composition of the soil solutions highlight interesting differences between the four sites. As Chapter 5 reports the results of a detailed study of the soil and soil solution chemistry of three forest/grassland site pairs, only a brief discussion of site differences will be made here. At the Cragieburn site, soil solution pH was lower in the forest soil than in the corresponding grassland soil. The concentration of humic and fulvic species (as estimated by the A_{250} measurements) was higher in the forest soils than in the corresponding grassland soils, reflecting the greater return of organic matter (biomass) to the soil surface (although TOC measurements were higher for the Cragieburn grassland site). Afforestation-induced acidification is generally related to the greater input of acidic organic matter at these sites, and/or the greater amount of proton release that occurs due to the increased biomass production of forest over grasslands. Linked to this increase in acidification, concentrations of aluminium at the Cragieburn site were higher in the forest soil solution than in the grassland sample.

In contrast, the grassland site at the Bealey Spur location had lower pH and higher aluminium concentrations than the corresponding beech sampling site. As noted in the site description (Section 6.2.1), the grassland site was not directly adjacent to the forest site (as at the Cragieburn location), but was *ca.* 30 m higher in elevation on an exposed aspect. Differences observed at the Bealey Spur location may arise from the different rates of weathering and leaching that the two sites experience. Given the high annual rainfall at this location (*ca.* 2000-3000 mm), it might be expected that soil weathering and leaching of exchangeable cations will be significantly greater at the more exposed, higher altitude grassland site, than in soil under the shelter of the beech canopy. The higher rates of leaching that occur at higher altitudes (Ruth *et al.* 1998) cause the net removal of exchangeable cations from soil colloids and mineral surfaces, which may be replaced by the acidic ions H^+ and Al^{3+} at exchange sites.

6.4.2 Soil incubation

Results from the soil incubation experiments tended to be more variable than those observed for the soil solution storage experiments (Table 6.2). Comparison of the Day 1 and Day 7 soil solution pH values for the two Bealey samples, shows that the extracted soil solution pH did not change significantly ($\Delta pH \leq 0.1$) during the 7 day soil incubation process (although pH values were *ca.* 0.2 units higher on Day 2). Soil solution pH increased for both the Cragieburn samples. Soil CO_2 degassing is the most likely reason for the pH increase.

Dahlgren *et al.* (1997) found that although significant amounts of degassing occur immediately after a soil is sampled in the field, the cation buffering properties of the soil mean that degassing should not affect either the soil or soil solution pH. However, once the soil solution is removed from contact with the mineral soil, such buffering can no longer occur, and resulting pH changes can be significant (*e.g.* Figure 6.1). The observation that soil solution pH increased for the incubated Cragieburn soils contrasts with the findings of Dahlgren *et al.* (1997). It is unlikely that the pH increase was due to biological activity, as this tends to lower pH as a result of the proton generation that occurs during nitrogen mineralisation.

In contrast to the soil solution storage experiments, the A_{250} readings generally declined during the 7 day incubation period (Table 6.2; Figure 6.2). For all samples a sharp decline had occurred by Day 2, after which the values generally remained constant (except for Bealey Beech, for which the final A_{250} value increased). As observed for the soil storage experiments, there was again a poor correlation between A_{250} and TOC measurements. The TOC values appear very scattered, making interpretation difficult.

Changes in 'organic-bound Al' and 'free Al' levels were also inconsistent, with large variations (>50%) in concentration occurring (Table 6.2). The two fractions of Al did generally change together however, with decreases (or increases) in one, being reflected by a corresponding decrease (increase) in the other. There was no clear correlation between the concentration of the two Al fractions with either soil solution pH or the A_{250} measurements.

In general, concentrations of the four cations decreased over the 7 day soil incubation period (Table 6.3). The percentage decrease in cation concentrations was lower for the two Bealey samples than for the Cragieburn samples. This may be related to a difference in the percentage base saturation of the soils at the respective sites. The Cragieburn Pine sample

exhibited the largest concentration decreases, with Mg^{2+} and K^{+} both decreasing by *ca.* 50%; there was a mean 21% decrease for all cations over the four sites.

6.4.3 Air-dried soil

The air-drying of soil samples, and subsequent wetting before extraction of soil solution caused substantial changes in soil solution composition (Table 6.5), compared with the soil solution initially extracted from the field-moist (+15% TDW) soil (Table 6.1). Large decreases in soil solution pH occurred (mean $\triangle$pH = -0.23), in addition to large increases in the concentrations of fulvic and humic species in soil solution, as estimated by the A_{250} measurements (mean $\triangle A_{250}$ = +0.450).

The higher acidity of these samples was reflected by large increases in the concentrations of both 'organic-bound Al' and 'free Al' fractions (Table 6.5). 'Organic-bound Al' increased by an average 7.8 μM Al; for one sample (Cragieburn Pine) the concentration increased four-fold. Increases in 'free Al' concentrations were even larger (average 11.7 μM Al increase); the concentration measured for the Cragieburn Grass sample was more than seven-fold the initial soil solution 'free Al' concentration.

In addition to the large increases observed for 'organic-bound Al' and 'free Al', the air-drying of soil caused large increases in the cation concentrations for all four soil samples (Table 6.4). Increases ranged from *ca.* 7 to 470%, but were not uniformly consistent across the samples. The mean percentage increase for all cations over the four sites was *ca.* 130%.

As noted by both Bartlett and James (1980) and Courchesne *et al.* (1995), the air-drying of soil caused large changes to occur to the chemical composition of the soil solution. Soil drying resulted in increased soil solution acidity, and large increases in the amount of organic matter present in soil solution. Indeed, TOC values were greater in air-dried soil for three of the four soils studied in this work (Table 6.1; Table 6.5). Courchesne *et al.* (1995) noted that pH decreases observed when drying soils correlated with the TOC present. It follows that oxidation of soil organic matter may be a significant contributing factor to the higher acidity observed.

6.5 CONCLUSION

Soils were sampled from two locations, with a forest and grassland soil being sampled at each. The effects of soil incubation, and soil solution storage on the soil solution pH, A_{250}, aluminium and major cation concentrations was determined. Unfortunately, soils required wetting and equilibration before centrifugation of the soil solution. As a consequence, (potentially significant) changes that may have occurred in the soil solution composition during the first 24 hours after sampling could not be quantified.

The magnitude of changes associated with ageing were site specific. Larger changes were generally observed in soil solutions extracted from incubated soils, than in stored soil solutions, although CO_2 degassing of the stored soil solutions led to large pH increases after 7 days. Excluding pH and TOC values, the magnitude of changes observed in stored soil solution were, somewhat surprisingly, relatively small (< *ca.*10-15%). In general, pH analysis of stored soil solution on Day 2 gave satisfactory agreement with the results obtained immediately after soil solution extraction, and were in better agreement with these original results than were results obtained from re-extracted soil solution from incubated soil on Day 2. However, relatively large changes occurred for concentrations of 'free Al' determined in either stored or freshly-extracted soil solutions (even by Day 2). Therefore, it is clear that Al analyses should ideally be performed as soon as practicable after sampling.

Analysis of air-dried soil samples resulted in large increases in acidity, A_{250} measurements and concentrations of both aluminium and base cations. Although air-drying of soil samples may well be an established protocol for many soil laboratories, the resulting chemical analyses are of questionable worth. It is unlikely that the results represent the true soil solution composition, and therefore will not provide an accurate picture of the chemical conditions experienced by plant root systems.

CHAPTER 7

INTERACTION OF ALUMINIUM WITH POLYELECTROLYTE FLOCCULANTS

7.1 INTRODUCTION

7.1.1 Polyelectrolytes in the water treatment industry

Alum is widely used in the water treatment industry as a coagulant to precipitate soluble natural organic matter (NOM). If not removed from potable water, NOM may react during subsequent chlorination treatment processes, forming a range of potentially carcinogenic chlorinated-organic species (disinfection by-products). Alum alone is not very effective in removing soluble organic species, and so the destabilised colloidal or precipitated matter formed after alum addition (referred to as 'micro-floc') is typically entrapped or bridged by the addition of an anionic polyelectrolyte flocculating agent (Figure 7.1). The large 'macro-flocs' that form during flocculation are more amenable to subsequent settling or filtration processes. A combination of physical and chemical interactions is responsible for macro-floc formation. The dominant interaction will depend upon the nature of the flocculant, the composition of the water, and the operating conditions of the treatment process. The use of polymeric flocculants often results in a substantial reduction in the required alum dose (Bolto 1994).

Synthetic polymeric flocculants are manufactured using a variety of monomer species, allowing properties such as charge, charge density, molecular weight and solubility to be varied. Cationic polymers are sometimes used as an alternative primary coagulant to alum, forming micro-flocs containing destabilised NOM, colloidal and particulate matter (Figure 7.1). Neutral and anionic polymers are then used as flocculants to entrap or bridge these micro-flocs, to form large, robust flocs. The range of available polymers allows treatment protocols to be changed if seasonal or temporary changes in water quality are anticipated. Polymers are also commonly used for sludge de-watering and thickening, but at much higher concentrations than are used in potable water treatment.

'Bridging' is the primary physical mechanism by which polyelectrolyte flocculants overcome the electrostatic repulsive forces between destabilised particles formed during coagulation (Mortimer 1991). Bridging involves adsorption of the polyelectrolyte molecule from solution onto the surface of two or more suspended particles. The physical properties of polyacrylamide flocculants reflect this purpose. Typically they have a low charge density (they are not required to neutralise the net negative charge of the suspended particles) and a high molecular mass (needed to produce large, fast-settling flocs) (AWWA 1990; Mortimer 1991). A strong relationship exists between the charge density of a polyelectrolyte and the optimum flocculation dosage (Kitchener 1972; Wilde and Dexter 1972; Ghosh *et al.* 1985; Leu and Ghosh 1988).

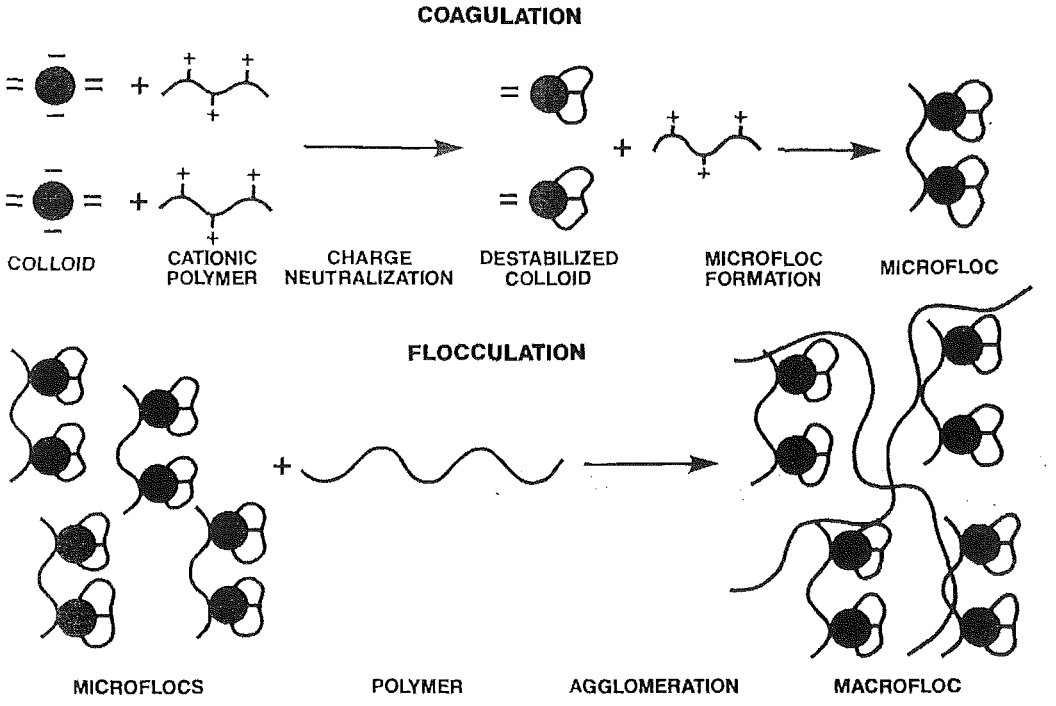

Figure 7.1. Schematic diagram showing the water treatment processes of coagulation and flocculation.

The long-term health effects associated with the use of these polymers are unknown. There are stringent regulations overseas to control the use of synthetic organic polymers in potable water treatment (Letterman and Pero 1990). In New Zealand, acrylamide-based polymers are predominantly used in potable water treatment (Gregor *et al.* 1993). Acrylamide is a cumulative neurotoxin and a genotoxic carcinogen (Letterman and Pero 1990). There is sufficient concern about the health implications of the residual acrylamide monomer, that it appears as an organic determinand of health significance in the Drinking Water Standards for New Zealand (1995). There is a maximum acceptable value of 0.0005 mg/L (the

concentration below which the presence of acrylamide does not result in any significant risk to the consumer over a lifetime of consumption). Nevertheless, health risks from the use of synthetic polymers must be weighed against benefits gained from improving water clarity and removing natural organic matter. The benefits gained by the use of such polymers should however, be greater than those obtainable with alternatives that offer less risk.

Natural polyelectrolytes have come under increasing scrutiny in recent years (especially in developing countries), as cheaper alternatives to the commercial polyacrylamide-based flocculants for water treatment purposes. Chemicals identified as being of potential use for their coagulation and flocculating abilities include seaweed-derived λ-carrageenan and alginates, chitosan, okra, pectins, and carboxy-methyl cellulose (Cohen *et al.* 1958; Kawamura 1991; Al-Samawi and Shokralla 1996; Ganjidoust *et al.* 1997).

The interactions between any alternative flocculant and the various species formed in a coagulated water are important. An alternative flocculant must be capable of forming mixed 'polymer-aluminium-NOM' and mixed 'polymer-aluminium-colloid/particle' entities, without stripping bound aluminium from organic matter. These mixed entities may be chemically and/or physically held together. It is therefore useful to determine the binding interactions (if any) between aluminium and a flocculant, before studying more complicated mixed Al-NOM-flocculant systems. Fundamental studies of this type also provide useful information for elucidating the specific binding interactions within metal-polyelectrolyte systems.

This work investigated the differences in aluminium binding properties between a commercially-available synthetic polymer flocculant (Crystalfloc polyacrylamide B610 PWG) and those of a natural polymer (sodium alginate). Aluminium complexation capacity (Al-CC) titrations were used to probe the binding interactions. Complexation capacity values refer to the maximum amount of non-labile products formed under conditions of excess metal ion. The operational Al-CC value of a ligand is a parameter that describes the amount of aluminium that can be chemically bound to a ligand at a fixed pH, and which is not sequestered during the *ca.* 1.1 s contact time with the oxine-derivatised Fractogel (Section 3.11). Al-CC titrations were performed at three different pH values, using a range of alginate and polyacrylamide concentrations. A brief description of the alginate and polyacrylamide reagents follows.

7.1.2 Alginate

Alginates have previously been used for water treatment in Japan, and have been suggested as a possible substitute for synthetic polymeric flocculants (Kawamura 1991). A brief description of alginate structure, and solution properties, is given. Alginates are hetero-polysaccharides and are widely distributed in nature, occurring in seaweeds, algae and bacteria. They are also used commercially as gelling agents in the food industry, have uses in medicinal and pharmaceutical fields, and are therefore considered safe for human consumption. They have a linear co-polymer structure, comprised of two sugar residues, (1-4) linked β-D-mannuronic and α-L-guluronic acid (Figure 7.2). The constituent monomer units of alginate occur in varying ratios.

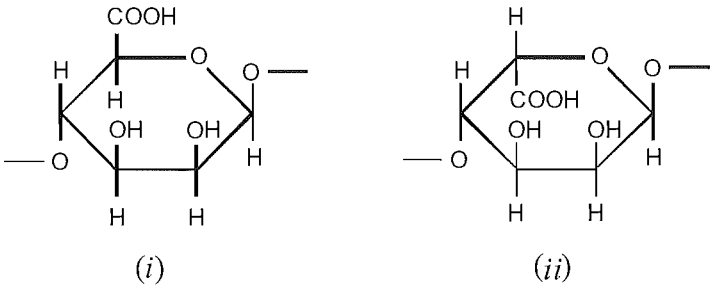

Figure 7.2. Constituent monomer units of alginate (*i*) β-1, 4-D-mannuronic acid unit; and (*ii*) α-1, 4-L-guluronic acid unit.

Several studies, using a variety of techniques, have investigated the solution properties of alginates. Marked changes occur in solution when an alginate interacts with various divalent cations. These changes (*e.g.* increases in viscosity, precipitation and/or gel formation) have been interpreted in terms of the formation of cross-links between the alginate chains and *via* the divalent cations. On the basis of changes in the circular dichroism spectra of polyelectrolyte-calcium species, Grant *et al.* (1973) proposed a cooperative binding mechanism that involved two or more polyelectrolyte chains. The proposed model involved the alignment of alginate chains such that the functional groups formed regular interstices into which cations could bind and pack in a long-range structure. This model was termed 'the egg-box model', (Figure 7.3) with the analogy of a corrugated egg-box being used to represent the way in which cations (eggs) of a particular size could pack into the regular binding clefts formed by the alginate chains (box). Each calcium ion is flanked by four guluronate residues, two from each chain.

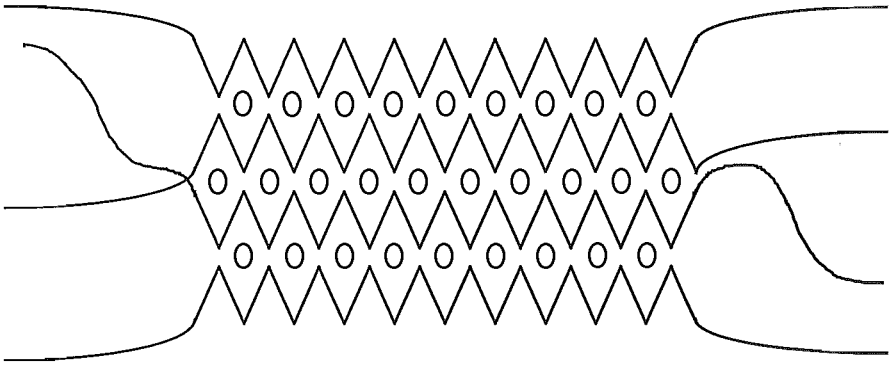

Figure 7.3. A simple representation of the 'egg-box' model proposed by Grant *et al.* (1973).

Wang *et al.* (1993) performed a detailed ^{13}C NMR spectroscopic study on the sol-gel transition of alginate resulting from interactions with the divalent cations Ca, Co, Cu, and Mn. Macroscopic solution properties (such as viscosity) were similar for the four alginate-cation combinations. However, different binding interactions were determined for the Ca-alginate system than for the three transition metal (Co, Cu and Mn)-alginate systems. In the Ca-alginate system, a strong cooperative binding effect occurred between all functional groups of the guluronate residues and the Ca(II) ion. This result was consistent with the "egg-box model" proposed by Grant *et al.* (1973). For the three transition metal ions, 'discrete binding site' complex formation between the metal ions and the alginate involved the carboxyl groups of both guluronate and mannuronate. The other functional groups present, such as hydroxyl groups, were not actively involved in binding.

Reported work in the literature has generally evaluated the water treatment flocculation performance of alginates with respect to physical solution properties such as turbidity removal and adsorption isotherm models (Narayan and Ramasubramanian 1982; Kawamura 1991; Hassan 1993; Jang *et al.* 1995*a* and 1995*b*). Alginate has also been used as a chemical model for extracellular organic matter (EOM). Bernhardt *et al.* (1985) used alginate as a model for algal exudates when investigating the effects these species have on turbidity removal during water treatment. Low doses of alginate were found to cause improvements in both flocculation and filter run-time.

Bernhardt *et al.* (1986) also investigated the effect that calcium ions have on reducing the impairment to turbidity removal caused by high concentrations of EOM. Gregor *et al.* (1996) further investigated the binding interactions of alginate with aluminium and calcium. Alginate was found to have a capacity to bind aluminium similar to that for natural organic

matter. The addition of calcium ions prior to aluminium coagulation was suggested as a method to minimise the effect of high loadings of EOM on coagulation processes.

7.1.3 Polyacrylamide

Synthetic polymers first came into use for water treatment purposes during the mid-1960s. They are now widely used, with a range of polymers being commercially available. Typical synthetic flocculants have a low charge density and are of high molecular weight, properties which allow the formation of a large fast-settling floc (Mortimer 1991). Many studies have illustrated the enhanced flocculation possible through the use of synthetic polymers. The majority of such studies measure flocculant performance by monitoring the colligative and physical properties of solutions (*e.g.* turbidity) (Wilde *et al.* 1972; Ghosh *et al.* 1985; Leu *et al.* 1988) or by determining the residual concentrations of various species after treatment (*e.g.* organic matter) (Haff 1978). The commercially-available flocculant used in this work was Crystalfloc B610 PWG (IChem Ltd), a co-polymer of acrylamide and sodium acrylate. The flocculant has a quoted anionicity of 5% (carboxylate groups).

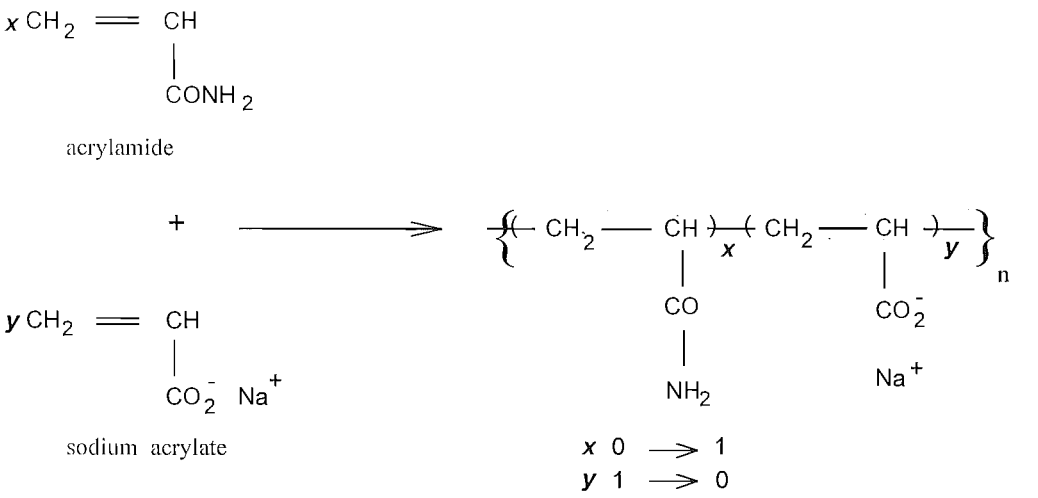

Figure 7.4. The constituent monomer units used in the production of anionic polyacrylamide.

Manufacture of similar high molecular weight polyacrylamide co-polymers was originally performed *via* a base hydrolysis of the amide group at elevated temperatures. This process has now been superseded by co-polymerisation processes using acrylamide monomer with acrylic acid, or one of its alkali metal or ammonium salts (Mortimer 1991) (Figure 7.4).

7.2 MATERIALS AND METHODS

7.2.1 Reagents

Sodium alginate (BDH) had previously been purified using extensive dialysis with EDTA to remove any potential contaminant metal ions (details in Gregor *et al.* 1996). A commercially-available anionic polyacrylamide flocculant Crystalfloc B610 PWG (potable water grade) (IChem Ltd.) was used as supplied. A polyacrylamide stock solution of 500 mg/L was prepared according to the manufacturer's specified 'usual concentration of dissolution', and diluted as required for the aluminium complexation capacity experiments.

7.2.2 Aluminium complexation capacity titrations

Complexation capacity titrations were performed according to the methods described in Section 2.2.8. A sufficient volume of stock alginate or polyacrylamide solution was added to the titration cell to give the desired ligand concentration. Sufficient KCl and buffer (acetic acid for titrations at pH 4.7 and 5.5; MES (2-(N-morpholino)ethanesulfonic acid) at pH 6.5) was included to give final concentrations of 0.05 M and 0.005 M, respectively. Total cell volume was 150 mL. After the addition of Al increments, the titration solution was mixed for 5 minutes, before a 2 mL sample was withdrawn into a plastic syringe. Samples were kept at room temperature for a further 2-3 hours equilibration before analysis. Concentrations of 'free Al' and 'moderately-labile Al' were determined using the oxine-derivatised Fractogel method (Section 2.2.7). The 'moderately-labile Al' is an operationally-defined fraction of Al. It corresponds to complexed Al that is not captured by the resin, but which is sequestered by the colorimetric reagent CAS in the 30 s reaction time in the FIA manifold.

7.2.3 Alginate-aluminium titrations

Complexation capacity titrations were performed using the alginate polymer. This experiment was similar to the Al-CC titrations, but involved the incremental addition of alginate to a solution at pH 4.7, containing a known concentration of Al^{3+}. The solution was mixed for 5 min after each alginate addition, before a 2 mL sample was withdrawn and equilibrated for 2-3 hours. Samples were analysed for aluminium as above.

7.3 RESULTS

The alginate and polyacrylamide polymers were titrated with aluminium at three pH values (pH 4.7, 5.5 and 6.5), over a range of polymer concentrations (0.05 mg/L to 20 mg/L). Performing these titrations at pH 4.7 is relatively straight forward, as hydrolysis of aluminium

in solution is minimal. However, as water treatment plants do not operate at pH 4.7, Al-CC titrations were also performed at higher pH, at which aluminium hydrolysis is extensive.

The Al-CC results for both alginate and polyacrylamide are summarised in Table 7.1, and are expressed as μM Al (as read directly off the complexation capacity curves) and as mg Al/g polymer (for comparison of different polymer concentrations).

Table 7.1. Aluminium complexation capacities (Al-CC) for alginate and polyacrylamide.

pH	Ligand Conc. (mg/L)	Alginate Al-CC (μM)	Alginate Al-CC (mg Al/g polymer)	Polyacrylamide Al-CC (μM)	Polyacrylamide Al-CC (mg Al/g polymer)
4.7	0 (blank)	0	0	0	0
	0.1	0	0	0	0
	1	0	0	-	-
	5	5.3	28.6	0	0
	10	10.9	29.4	-	-
	20	17.8	24.0	-	-
5.5	0 (blank)	0	0	0	0
	0.1	-	-	0	0
	5	-	-	6.6	35.6
	10	36.9	99.6	-	-
6.5	0 (blank)	0	0	0	0
	0.2	-	-	0	0
	1.1	7.4	182		
	5	-	-	14.3	77.2
	10	66.2	179	-	-
Theoretical Maximum Capacity assuming 1:1 Al:COO^- binding			153		19.0

7.3.1 Alginate Al-CC experiments pH 4.7

Al was initially titrated against the 0.005 M acetate buffer in a blank titration at pH 4.7 (0 mg/L alginate). The resulting complexation capacity curve (not shown) was linear with a zero intercept (Al-CC = 0 μM), and a slope close to the theoretical value of 1.00 (slope = 0.96; $r^2 = 1.00$).

Al-CC titrations were performed for a range of alginate concentrations at pH 4.7. At low concentrations of alginate (0.1 to 1 mg/L), alginate-bound aluminium could not be detected (*i.e.* the Al-CC results were identical to those from the blank titration). However, at higher alginate concentrations (5, 10 and 20 mg/L) a distinctive binding interaction with aluminium was observed. Figure 7.5 shows the distinctive complexation capacity curve obtained for the 'free Al' and 'organic bound Al' fractions for the 20 mg/L alginate titration.

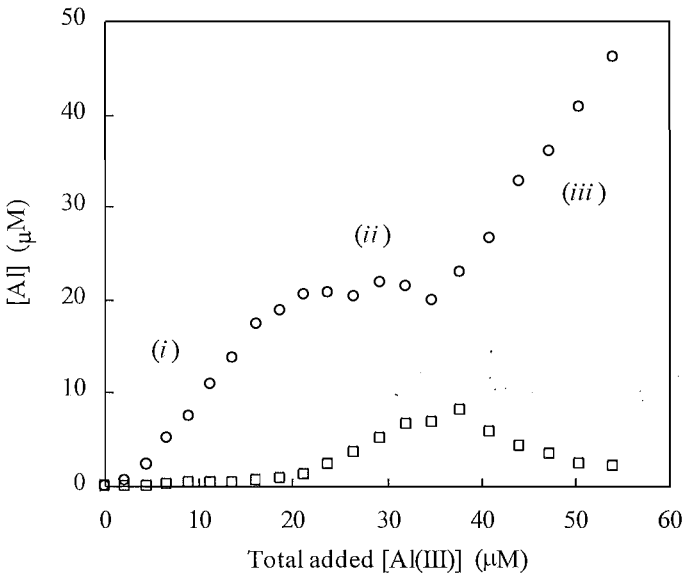

Figure 7.5. Al complexation capacity curve for 20 mg/L alginate (pH 4.7, 0.05 M KCl, 0.005 M acetate) (○ 'free Al'; □ 'moderately-labile Al').

At pH 4.7, alginate Al-CC values were determined from the length of the horizontal 'plateau' region where binding takes place, and not from the intercept of a fitted line with the *x*-axis, as described in Chapter 3 (Section 3.8). For example, the 20 mg/L alginate Al-CC titration had a binding region of 17.8 μM Al (as read off Figure 7.5), equivalent to 24.0 mg Al^{3+}/g of alginate. Determination of the Al-CC by this method is rationalised in Section 7.4.1.

Concentrations of 'moderately-labile Al' for the 20 mg/L alginate Al-CC titration are also shown in Figure 7.5. At low concentrations of added aluminium, insignificant amounts of

'moderately-labile Al' were determined. However, as the binding region started (> *ca.* 18 μM added aluminium), the concentration of 'moderately-labile Al' increased. At high concentrations of added Al, where the Al-CC has been reached and 'free Al' concentrations increase, the concentrations of 'moderately-labile Al' decreased. Titrations performed at the lower alginate concentrations (5 and 10 mg/L alginate) gave similar results.

The length of the observed binding plateau (slope *ca.* 0) was dependent upon the alginate concentration used. As the concentration of alginate increased from 5 to 20 mg/L, the length of the binding region also increased. Figure 7.6 illustrates the observed increase of the binding region for alginate concentrations between 0.1 and 10 mg/L. At 1 mg/L alginate and below, no binding region was apparent (indistinguishable from the blank).

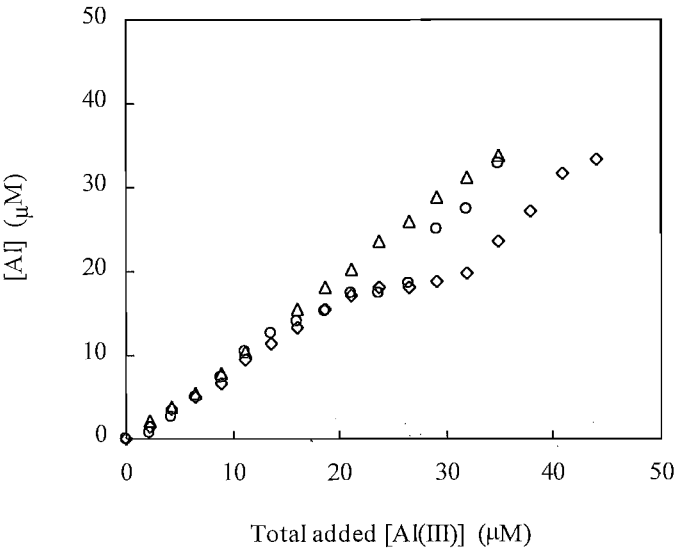

Figure 7.6. Alginate complexation capacity curves showing concentrations of 'free Al' (△ 0.1 mg/L alginate; ○ 5.0 mg/L alginate; ◇ 10 mg/L alginate) (pH 4.7, 0.05 M KCl, 0.005 M acetate).

7.3.2 Alginate-aluminium titrations pH 4.7

Increments of alginate were added to a solution containing a fixed concentration of 30 μM aluminium (Figure 7.7). Initially, 'free Al' concentrations decreased, before a plateau was observed at *ca.* 16 μM 'free Al', the same concentration at which the binding plateau was observed for the aluminium complexation capacity curves (Figure 7.6). Concentrations of 'moderately-labile Al' initially increased, before becoming constant at the same composition at which the plateau was observed for concentrations of 'free Al'.

Similar behaviour was observed for an alginate complexation capacity curve performed using an initial concentration of 20 μM aluminium. As observed for 30 μM aluminium (Figure 7.7), 'free Al' concentrations decreased to a constant value of *ca.* 16 μM. A third binding curve was performed using an initial concentration of 10 μM aluminium. This resulted in a plateau for 'free Al' concentrations at10 μM Al over the entire range of alginate concentration added (0-50 mg/L).

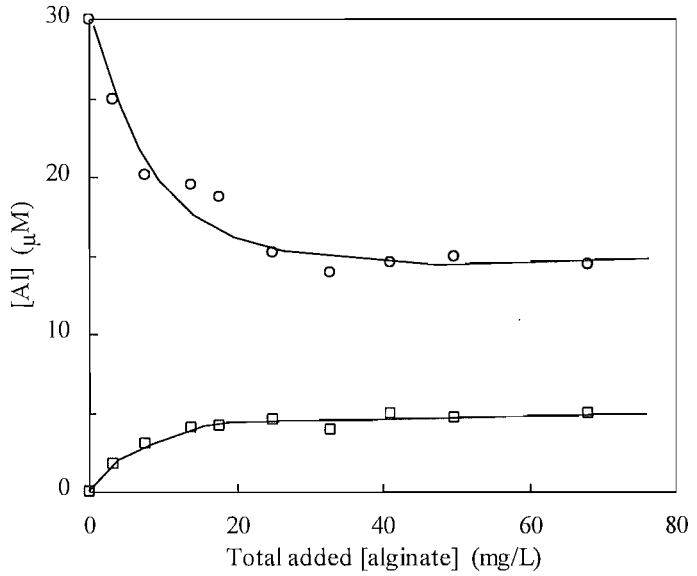

Figure 7.7. Alginate complexation capacity curve for 30 μM aluminium, (pH 4.7, 0.05 M KCl, 0.005 M acetate) (○ 'free Al'; □ 'moderately-labile Al').

7.3.3 Alginate Al-CC experiments pH 5.5 and 6.5

The Al-CC behaviour of 10 mg/L alginate was also studied at higher pH (pH 5.5 and 6.5), a pH of more relevance for water treatment processes. At pH 5.5 and 6.5, hydrolysis and polymerisation of non-complexed aluminium will be extensive. Blank titration curves (no alginate) were performed at pH 5.5 (0.005 M acetate) and pH 6.5 (0.005 M MES). The complexation capacity curves at these pH both had a zero intercept and were linear, with slopes of 0.49 and 0.46, respectively ($r^2 > 0.99$).

The Al-CC titrations performed for 10 mg/L alginate, differed markedly both from the blank titrations, and from the complexation capacity curve obtained at pH 4.7 (Figure 7.8). Unlike the titration performed at pH 4.7, the Al-CC curves at pH 5.5 and pH 6.5 did not exhibit an initial linear region.

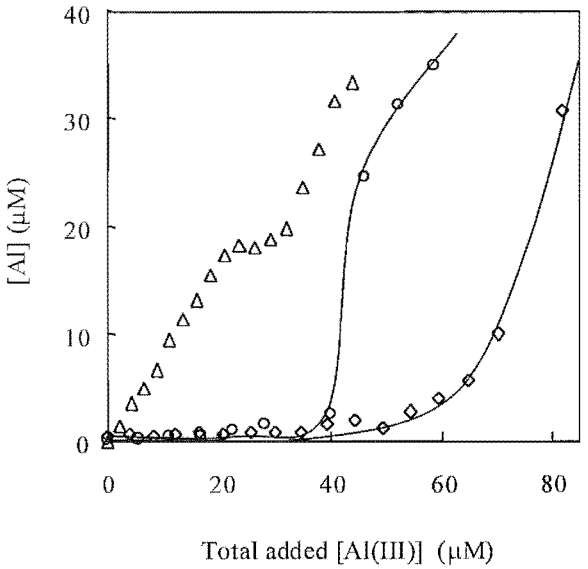

Figure 7.8. Complexation capacity curves for 10 mg/L alginate performed at three pH (△ pH 4.7; ○ pH 5.5; ◇ pH 6.5) (0.05 M KCl, 0.005 M acetate or MES).

7.3.4 Polyacrylamide Al-CC experiments pH 4.7, 5.5 and 6.5

Aluminium complexation capacity measurements were performed at pH 4.7 over a range of polyacrylamide (Crystalfloc B610 PWG) concentrations (0.05-5 mg/L). At low polyacrylamide concentrations, typical of those used in potable water treatment (0.05 to 0.2 mg/L), no binding with aluminium was observed over the pH range 4.7 to 6.5 (Table 7.1) (*i.e.* the Al-CC plots were linear with a slope equivalent to that of the blank at each pH).

At a much higher concentration more typical of sludge conditioning (5 mg/L), binding interactions between polyacrylamide and aluminium were observed at pH 5.5 and 6.5 (Figure 7.9). The Al-CC values obtained from the *x*-axis intercepts from fitted lines through the data at high added aluminium concentrations are given in Table 7.1.

7.4 DISCUSSION

7.4.1 Alginate Al-CC experiments pH 4.7

The IUPAC compilation of stability constants, SCDatabase (Pettit and Powell 1997), does not report values for aluminium-alginate or aluminium-polyacrylamide systems. However, data for simpler Al^{3+}-(hydroxy)-carboxylic acid species (which may be considered as fundamental models for the alginate system) indicate that aluminium may form $AlH_{-1}L$ and $AlH_{-2}L$ complexes (in which ligand hydroxyl groups are deprotonated). The carboxylate groups on

the alginate and acrylate monomer groups are of similar acidity (pK_a values *ca.* 3.5 to 4.7). For Al-CC titrations performed at pH 5.5 and 6.5, proton competition at these sites will be negligible.

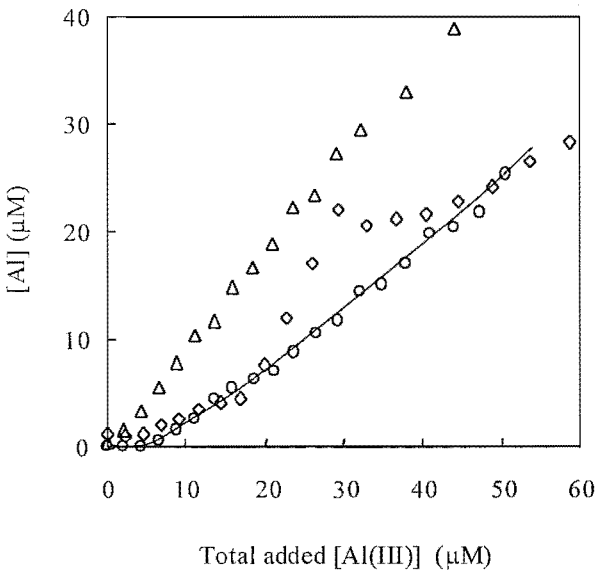

Figure 7.9. Complexation capacity curves for 5 mg/L Crystalfloc B610 PWG (△ pH 4.7; ○ pH 5.5; ◇ pH 6.5) (0.05 M KCl, 0.005 M acetate or MES).

The aluminium complexation capacity curves obtained at pH 4.7 for 5-20 mg/L alginate, contrast with those obtained previously for soil solutions and for natural waters containing NOM. Previously obtained Al-CC curves show an initial binding region ['free Al'] *ca.* 0 μM) until the point at which the available binding sites have been saturated with Al (Al-CC). This is followed by a region with slope *ca.* 0.6-1.0, in which concentrations of 'free Al' increase linearly with total added aluminium (Section 3.8; Powell *et al.* 1995; Hawke *et al.* 1996). The results for the alginate Al-CC titrations clearly contrast with these previous results. The initial linear regions for the alginate Al-CC curves coincide, irrespective of alginate concentration (Figure 7.6). This is followed by a 'plateau' that indicates strong binding. These two effects, together, indicates that cooperative binding is occurring between alginate and Al (as is observed between alginate and Ca (Grant 1973; Steginsky *et al.* 1992; Wang *et al.* 1993)).

For the 20 mg/L alginate Al-CC titration curve (Figure 7.5), the initial linear region (*i*) (slope *ca.* 1.0) indicates that the Al-alginate complex is very labile (sufficiently labile to be measured as part of the 'free Al' fraction). When sufficient 'free Al' is in solution (in this instance *ca.* 18 μM) further added Al is complexed strongly by the alginate, causing the observed plateau

(*ii*). In region (*iii*) the complexation capacity of the alginate is exceeded and 'free Al' concentrations rise again (slope *ca.* 1.4). The increased binding region length observed with increasing alginate concentrations (Figure 7.6) reflects the greater number of binding sites available for complexation to aluminium at higher ligand concentrations.

A possible scenario for a cooperative binding interaction follows. An initial 'coiled' configuration may be thermodynamically stabilised in solution *via* weak hydrogen bonding, solvation, dipole and/or ionic interactions between the carboxylic and hydroxyl groups (Steginsky *et al.* 1992). The alginate then undergoes a stage of conformational changes as increasing amounts of aluminium are added. This aluminium, although weakly associated with the alginate, is sufficiently labile to be sequestered by the oxine-derivatised Fractogel.

At a certain 'threshold' aluminium concentration (*ca.* 18 μM of added aluminium in Figure 7.5), the alginate molecules change from a random or 'coiled' configuration, to a more linear configuration that is receptive to strong Al binding. This may be due to the exposure and availability of strong 'non-labile' (on the experimental time-scale) and 'moderately-labile' binding sites (Figure 7.10). The initial Al may be necessary to promote sufficient ionisation of the alginate to change its conformation from 'coiled' to 'linear'. After all strong non-labile binding sites are saturated, 'free Al' concentrations in solution increase again with increased added aluminium. Although the existence of long-range order in the aluminium-alginate structure is not necessarily implied by these results, the possible formation of a long-range ordered structure (as noted by Wang *et al.* (1991; 1993) for transition metals) cannot be excluded.

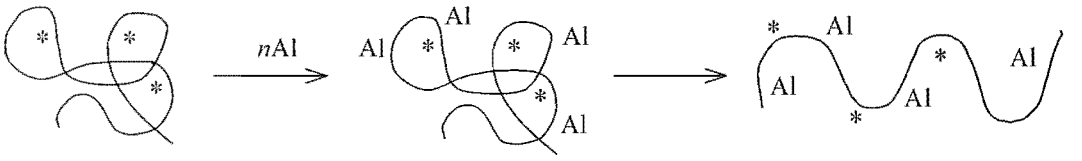

Figure 7.10. A schematic representation of the proposed conformational changes undergone by alginate in the presence of aluminium. The diagram shows the very labile aluminium associated with the alginate (Al), and the increased accessibility of strong binding sites after conformational change (* indicates a strong binding site).

It is apparent that once strong binding occurs, the concentration of labile Al is not reduced *via* a change in its complexation to alginate (*i.e.* a constant concentration of *ca.* 18 μM labile aluminium is always present) (Figure 7.5). This implies that while the conformational change

is induced by the presence of this aluminium, these cations are not available for subsequent strong complexation to the newly available binding sites. It follows that the *ca.* 18 μM Al represents bound, but very labile Al. Although this work proposes that the *ca.* 18 μM aluminium is weakly complexed with the alginate, this labile Al was not included in the complexation capacity values (Table 7.1), as it does not meet the Al-CC operational definition of complexed Al (the amount of aluminium that is chemically bound to a ligand at a fixed pH, and which is not sequestered during the *ca.* 1.1 s contact time with the oxine-derivatised Fractogel (Section 3.11)).

A similarly-shaped Al-CC curve was obtained for alginate by Hawke *et al.* (1996), who used a 7 s reaction between a sample and a chrome azurol S reagent stream in a flow injection manifold to target a 'reactive Al' fraction. The distinctively-shaped Al-CC curve was interpreted as being indicative of a cooperative binding interaction. In contrast, a second study by Gregor *et al.* (1996), did not find similar behaviour for aluminium-alginate complexation curves. However, their method of aluminium analysis involved 24 hours of dialysis equilibration for each datum point. This study, and the work of Hawke *et al.* (1996), distinguished between 'free' and complexed Al by using operationally-defined kinetic-based methods, which may measure Al bound in very labile complexes as part of a 'free Al' fraction. In contrast, the dialysis separation of 'free' and 'complexed Al', in conjunction with an analytical method which measured total Al, meant that labile complexes would not have been measured as part of a 'free Al' fraction.

The final slope of the 'free' aluminium curve (slope *ca.* 1.4; Figure 7.5) exceeds the theoretical value of unity. The release of some of the 'moderately-labile Al' into the 'free Al' fraction would account for this observation. Indeed, the concentrations of 'moderately-labile Al' are observed to decrease, once the Al-CC has been reached (Figure 7.5). This may be associated with aluminium moving from moderately-labile to labile sites, or may indicate that, as non-labile sites become saturated, the moderately-labile sites are indirectly destabilised, or labilised.

Al-CC values for titrations performed at pH 4.7 and 5, 10 and 20 mg/L alginate concentrations are in good agreement, 27 ± 3 mg Al/g alginate (Table 7.1). The calculated theoretical maximum complexation capacity is 153 mg Al/g alginate (assuming an alginate monomer molar mass of 176 g ($C_6H_8O_6$) and 1:1 alginate:monomer (Al:COO^-) complexation). Binding capacities lower than the theoretical values (calculated for a 1:1 complexation model) are consistent with poly-dentate carboxylate-Al binding. At pH 4.7, proton competition at

hydroxyl sites could also decrease the complexation capacity. If the *ca.* 18 μM labile Al is added to the Al-CC values given in Table 7.1, the experimental complexation capacities are still lower than the theoretical capacity of 153 mg Al/g alginate (alginate concentrations of 5, 10 and 20 mg/L yield complexation capacities of 126, 78 and 48 mg Al/g polymer, respectively).

7.4.2 Alginate-aluminium titrations pH 4.7

The results from the titration, in which alginate was incrementally added to a solution containing 30 μM Al^{3+}, are consistent with the cooperative binding scenario presented above. Initially, sufficient 'free Al' is in solution to induce a conformational change in the initial alginate increments. This allows strong and moderately-labile binding to occur (consistent with the observed decrease of 'free Al' concentrations and increase of 'moderately-labile Al' concentrations; Figure 7.7). As more alginate is added, the 'free Al' concentration in solution remains above that required to maintain the conformation required for strong Al^{3+}-alginate binding. The concentration at which this occurs (*ca.* 16 μM) is the same as that observed for the plateau in the aluminium complexation capacity curves. No further strong binding to aluminium occurs.

This suggests that the *ca.* 16 μM Al represents very labile Al bound to the alginate chain, rather than uncomplexed 'free Al'. No binding was observed for a solution initially containing 10 μM Al. The constant plateau observed for 'free Al' concentrations is consistent with there being insufficient 'free Al' in solution to induce a conformational change for the alginate increments, which would allow strong binding to occur.

7.4.3 Alginate Al-CC experiments pH 5.5 and 6.5

For the blank Al-CC titrations (addition of Al^{3+} into a buffer solution), the reduction in slope from unity may be attributed to the formation of polymeric aluminium-hydrolysis products. Although such species may be captured on the column, they are not removed and/or depolymerised by the 0.03 M NaOH eluent, and therefore are not quantified as part of the 'free Al' fraction (Simpson *et al.* 1997). Any interpretation of complexation capacity curves performed at the two higher pH should be compared with the results from these blank titrations.

The Al-CC titration curves at higher pH (Figure 7.8) do not show the initial linear region observed at pH 4.7. This suggests that this region is related to the ionic state of the polymer.

Whereas at pH 4.7 the addition of cationic aluminium is necessary to induce ionisation and a conformational change of alginate (before strong binding to Al can occur), such a change in conformation is evidently also achieved by raising the pH (to pH 5.5 and 6.5). As the pH is increased, a greater percentage of the carboxyl groups on the alginate molecules will be deprotonated. The increased deprotonation (and subsequent increase in intra-molecular electrostatic interactions along the length of the molecule) causes the coiled molecules to unfurl. This gives an extended structure in which strong binding sites are available from the outset (Mortimer 1991).

The alginate complexation capacity (mg Al/g alginate) increases with increasing pH (Table 7.1). This may indicate that strong binding of Al involves alginate hydroxyl groups (in addition to carboxyl groups). As the pH is raised, binding of aluminium at deprotonated hydroxyl groups (to form $AlH_{-1}L$ and $AlH_{-2}L$ species) will be enhanced.

The complexation capacity at pH 6.5 (mean Al-CC = 180.5 mg Al/g alginate) exceeded the calculated theoretical capacity of 153 mg Al/g alginate (Table 7.1) (assuming 1:1 Al-alginate monomer ($Al:COO^-$) complexation and a monomer molar mass of 176 g ($C_6H_8O_6$)). This value may indicate physical surface interactions, such as bridging and/or enmeshment occur, in addition to complex formation. These may occur between the positively-charged polymeric Al-hydroxy species and negatively-charged sites on the alginate, and would contribute to the measured complexation capacity.

At pH 5.5 and 6.5, the complexation curves exhibit a very rapid rise in 'free Al' concentrations (slope *ca.* 2.2) after the point at which the Al-CC is reached (Figure 7.8). The high slopes observed are *ca.* 4 times the value observed for the blank titrations performed at pH 5.5 and 6.5 (*ca.* 0.5). The high slope implies that the Fractogel resin retains alginate that is adsorbed or complexed to colloidal $Al(OH)_3$ (sample aliquots were not filtered before analysis). The sudden increase in 'free-Al' concentrations (once the alginate Al-CC is satisfied) is rationalised on the basis that the alkali eluent solubilises Al from all species that are captured on the resin. Therefore, in addition to captured colloidal $Al(OH)_3$, Al bound to 'moderately-labile' and 'non-labile' sites on alginate will also be solubilised by the eluent, and subsequently react with CAS downline. Landing *et al.* (1986) found columns containing Fractogel resin acted as an efficient colloid and particle filter, and the Fractogel resin was used to confirm the presence of colloidal Al in an unfiltered freshwater sample. Precipitated Al-organic matter captured on the oxine-derivatised Fractogel resin has previously been shown to be solubilised during alkali elution (Nilsson, unpublished).

7.4.4 Polyacrylamide Al-CC experiments pH 4.7, 5.5 and 6.5

A range of polyacrylamide concentrations (0.05-5 mg/L) was used for Al-CC titrations at pH 4.7. No binding was observed. At pH 5.5 and 6.5, the Al-CC values determined for 5 mg/L were 35.6 and 77.2 mg Al/g polyacrylamide, respectively (Figure 7.9; Table 7.1). As observed for alginate, the polyacrylamide Al-CC increases with increasing pH at a given polyacrylamide concentration, and 'free Al' increases with slope >1.0 once the Al-CC is satisfied. The determined capacities are significantly greater than the theoretical complexation capacity of 19.0 mg Al/g for Crystalfloc B610 PWG polyacrylamide (assuming a 5% anionic acrylate monomer composition, a monomer molecular mass of 71 g/mol ($C_3H_3O_2$) and a 1:1 Al:acrylate complex). This indicates that, as for alginate at pH 6.5, chemical binding is not the only means of association between polymer and aluminium. Other surface interactions such as bridging and/or enmeshment between the polymer and hydrolysed polymeric aluminium species may make the dominant contribution to the complexation capacity at high pH.

The proposed binding mechanism for alginate, in which aluminium addition, or ligand deprotonation increases the availability of strong binding sites, is unlikely to be valid for the Crystalfloc B610 PWG polyacrylamide. Alginate has carboxylate binding sites on each monomer unit, as opposed to the sample of polyacrylamide (quoted anionicity of 5% acrylate groups). Both the alginate carboxylate and the acrylate binding groups are of similar acidity, and so at the pH of most water treatment flocculation processes these groups will be deprotonated. Therefore while carboxylate deprotonation is proposed to cause an initial uncoiling of the alginate at higher pH (leading to an increase in the availability of strong binding sites), the significantly lower percentage of such sites on polyacrylamide means that such an electrostatically induced uncoiling is less likely to occur. If uncoiling did occur, then the relative number of exposed binding sites on the polyacrylamide is still likely to be significantly fewer than for the alginate, meaning a reduction in the relative amount of direct chemical complexation possible.

7.5 CONCLUSION

This work has shown that at concentrations of polyacrylamide and pH typical of those used for flocculation in water treatment, anionic Crystalfloc B610 PWG does not chemically bind to aluminium to any significant extent. However, at higher concentrations more typical of those used for sludge conditioning, polyacrylamide does interact with aluminium. The observed complexation capacities are significantly greater than the theoretical values. This

indicates that surface interactions such as bridging and/or enmeshment between the polyacrylamide and hydrolysed polymeric Al-hydroxy species are the dominant contributors to the aluminium complexation capacity.

The different complexation behaviour exhibited towards aluminium by alginate may be due, in part, to its greater number of anionic carboxylate groups. Although the carboxyl groups of the two polymers are of similar acidity, the greater number of carboxyl groups in alginate facilitates the necessary conformational changes that allow easy access of aluminium to potential binding sites. Aluminium may also strongly bind alginate at deprotonated hydroxyl sites. The observed complexation capacity for a 10 mg/L alginate solution at pH 6.5 just exceeded the total calculated complexation capacity, indicating a minor contribution from surface interactions such as bridging and/or enmeshment.

Implications for Water Treatment

The key requirement for any flocculant is that it can bridge Al-NOM without stripping aluminium from the organic matter. Although the ability of alginate to bind chemically to aluminium means that it may sequester residual soluble aluminium in coagulant overdose/underdose situations, it may also result in the detrimental destruction of pre-formed aluminium-NOM micro-flocs. The ability of alginate to compete with natural organic matter for aluminium will depend upon the relative capacities and strengths of binding. Extension of this work to study aluminium-alginate interactions in the presence of natural organic matter would be of relevance. Previous work (Gregor *et al.* 1996) has shown that natural organic matter and alginate have similar capacities for aluminium and that they chemically bind aluminium over the same pH range. Gregor *et al.* (1996) established that for equivalent weights of alginate and fulvic acid, up to twice the concentration of aluminium could be bound by the alginate. Interaction of alginate with Al-NOM may therefore be significant, although both Bernhardt *et al.* (1986) and Gregor *et al.* (1996) proposed that the addition of calcium prior to aluminium coagulation (*e.g.* pH adjustment using lime) may reduce disturbances in the flocculation of waters in the presence of alginate (used in these instances as a model for extracellular organic matter).

CHAPTER 8

IRON FRACTIONATION BY REACTION WITH OXINE-DERIVATISED FRACTOGEL

8.1 INTRODUCTION

Iron is an important trace element in the biosphere. In addition to playing an essential role in many terrestrial microbial and biological processes (*e.g.* photosynthesis), recent evidence also indicates that iron is a limiting growth nutrient for phytoplankton in regions of the open ocean (Martin *et al.* 1994).

Observed concentrations of total dissolved iron in natural water systems vary from 0.2 nM in mid-ocean surface water, up to 400 μM, in polluted urban clouds (Pehkonen 1995). In addition to being present in rock and soil minerals, iron exists in environmental systems in a variety of forms. Fe^{III} is primarily found in aerobic environments, where it may form colloidal species, or be strongly bound to siderophores, humic and fulvic acids. Fe^{II} is present in anoxic environments such as sediments and groundwaters. Measurement of Fe speciation in sea-water (Landing and Westerlund 1988; Waite *et al.* 1995), stream waters (McKnight *et al.* 1988; Kimball *et al.* 1992; Suzuki *et al.* 1992) and atmospheric waters (Zuo 1995; Sedlak *et al.* 1997) have shown that Fe^{II} is also present at significant concentrations in certain oxic environments. Redox cycling between Fe^{III} and Fe^{II} has a significant effect on other redox processes that occur in natural water systems (*e.g.* sulfur redox cycling) (Pehkonen 1995). Determination of the oxidation state of iron in environmental systems is therefore of importance.

The mechanisms by which photo-reduction of Fe^{III} occurs in oxic environments have been extensively studied (Sulzberger *et al.* 1990; Kimball *et al.* 1992; Stumm and Sulzberger 1992; Voelker *et al.* 1997). Photochemical iron reduction may proceed through several pathways, as shown in Figure 8.1. For environments in which low concentrations of dissolved organic carbon are present, formation of dissolved Fe^{II} proceeds through a light-induced reductive dissolution of Fe^{III} hydroxides (Sulzberger *et al.* 1990). In the presence of

organic ligands (*e.g.* carboxylic acids) the photochemical reduction of iron may occur either by a ligand-to-metal charge transfer, or by an oxygen-to-iron charge transfer involving Fe^{III} hydroxide. At constant light intensity (and assuming parameters such as pH, and the quantum efficiency of Fe^{III} photo-reduction are constant), the concentration of Fe^{II} approaches a steady-state. For a given system, the mols of Fe^{II} present will equal the amount of Fe^{II} formed, minus that amount which is lost through subsequent oxidation and precipitation processes (Sulzberger *et al.* 1990). However, if variations in light intensity occur, a steady state approximation is no longer valid. The net concentration of dissolved Fe^{II} at any time will therefore reflect the balance of reduction and oxidation processes, and will tend to parallel the light intensity. Significant diel variations in the concentration of Fe^{II} have been observed for stream, ocean and cloudwater systems (McKnight *et al.* 1988; Waite *et al.* 1995; Sedlak 1997.)

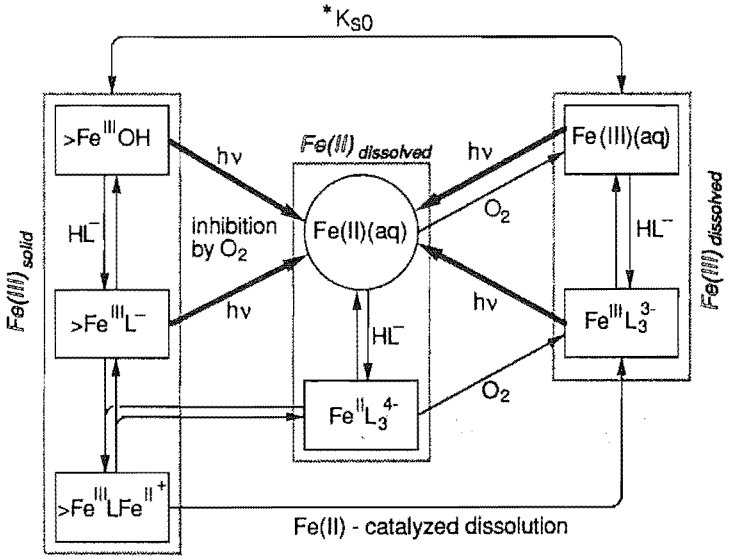

Figure 8.1. Schematic representation of the redox cycles of aquatic iron under the influence of light. The boxes on the left hand side represent the surface species involved in the redox reactions, and the boxes on the right hand side the dissolved Fe^{III} species involved in the redox cycle. Fe(III)(aq) represents soluble Fe^{III} hydrolysis species *e.g.* $Fe(OH)^{2+}$, $Fe(OH)_2^{+}$ and $Fe(OH)_3^{0}$(aq). The diagram is reproduced from Sulzberger *et al.* (1990).

A variety of analytical methods have been used to determine the oxidation state of iron in natural waters. These methods commonly involve a reaction of the sample with a specific chelating agent, with or without prior sample preconcentration *via* solvent exchange methods, or using a chelating resin.

A number of methods have quantified Fe^{II} spectrophotometrically, by monitoring the reaction between Fe^{II} and an Fe^{II}-specific colorimetric reagent. Colorimetric reagents commonly used for Fe^{II} detection include 1,10-phenanthroline, ferrozine, 2-2'-bipyridine, 2,2',2''-tripyridine

and many synthetic derivatives of these (*e.g.* Suzuki *et al.* 1992; Gu and Zhou 1996; Richter and Toral 1996; Pehkonen 1995). Kinetic catalytic spectrophotometric techniques are based on the ability of traces of Fe^{II} (or Fe^{III}) to catalyse the reaction of a species present at much higher concentration than the analyte. For example, Hirayama and Unohara (1988) determined trace concentrations of Fe^{III} in solution by monitoring the Fe^{3+} catalysis of the oxidation of *N,N*-dimethyl-*p*-phenylenediamine (DPD) by hydrogen peroxide. The detection limit of this technique was 4 nM. Measures *et al.* (1995) modified this method by optimising the chemistry for flow injection analysis (FIA) and incorporating on-line preconcentration by using a column containing oxine-derivatised Fractogel. The detection limit of the method was reduced to 0.025 nM.

The preconcentration of analyte from a large sample volume onto a chelating resin is a widely used technique to reduce the detection limit of an analysis. For example, Blain and Tréguer (1995) pumped samples for up to 20 minutes onto a ferrozine-impregnated C_{18} phase column, before a subsequent methanol elution step and spectrophotometric detection. The quoted detection limits for this technique were 0.1 nM for Fe^{II} and 0.3 nM for Fe^{III}.

High sensitivity is required for methods that are used to determine concentrations of iron in open-ocean seawater (typically <1 nM). A number of recently developed FIA methods designed for ship-board use determine sub-nanomolar concentrations of Fe in seawater by using sensitive chemiluminescence detection. Elrod *et al.* (1991) used an FIA method which quantified Fe^{II} from the intensity of light emitted by the chemiluminescent reaction of Fe^{II} with brilliant sulfoflavin and hydrogen peroxide. Samples were preconcentrated on oxine-derivatised Fractogel for 4 minutes, before a stream of HCl was used to elute captured Fe from the resin. The concentration of total dissolved Fe was obtained by adding ascorbic acid to the sample.

Alwarthan *et al.* (1990) and Obata *et al.* (1993) developed FIA systems based on a chemiluminescent reaction between Fe^{II}, luminol and hydrogen peroxide. These methods were more sensitive than that developed by Elrod *et al.* (1991). Obata (1993) quoted a DL (for Fe^{III}) of 0.05 nM for an 18 mL sample of seawater preconcentrated onto an oxine-derivatised, metal alkoxide glass resin. In subsequent work, modification of this technique reduced the detection limit to 0.01 nM (Obata *et al.* 1997). Pehkonen (1995) has published a comprehensive review discussing various methods that have been applied to determination of the oxidation states of iron in natural waters.

In this work the application of the oxine-derivatised Fractogel to fractionation of Fe^{II} and Fe^{III} was examined. In particular, the ability of the resin to sequester Fe^{II} and/or Fe^{III} from organic complexes was studied. Although previous workers have used oxine-derivatised Fractogel to preconcentrate Fe from seawater (Elrod 1991; Measures *et al.* 1995), no information exists on the lability of strongly complexed Fe, when exposed to the oxine-derivatised Fractogel.

In this work it is shown that Fe is present in three fractions. Organically-bound Fe^{II} is labile on the experimental time-scale, and is sequestered by the resin. In the absence of a reducing agent, organically-bound Fe^{III} exists in both 'moderately-labile' and 'non-labile' fractions. The application of the method to monitor the photo-reduction of an Fe^{III} fulvic acid solution was demonstrated. The possible use of a micro-column containing the oxine-derivatised Fractogel as a portable preconcentration device for field measurement of Fe is discussed.

8.2 MATERIALS AND METHODS

8.2.1 Flow injection analysis manifold

The FIA manifold (Figure 8.2), is similar to that used for Al determination with the oxine-derivatised Fractogel, and was constructed using the materials and equipment described in Section 2.1.3. The reagents used in the optimised flow injection analysis manifold are described in the caption to Figure 8.2. The micro-column containing the oxine-derivatised Fractogel had an internal volume of 22 μL.

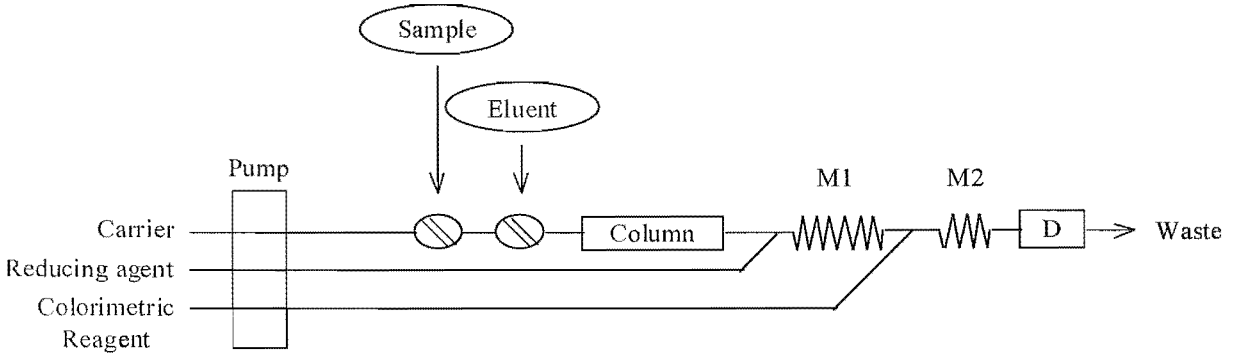

Figure 8.2. Carrier solution = 0.05 M Na-acetate/0.05 M NaCl, pH 4.0 (ENE-10; 0.95 mm i.d. pump tube; 1.0 mL/min); Reducing agent (for Fe^{III} analysis) = 5 % ascorbic acid (ENE-04; 0.44 mm i.d. pump tube; 0.21 mL/min); Colorimetric reagent = 0.05 % 1,10-phenanthroline in 2 M Na-acetate, pH 4.0 (ENE-01; 0.19 mm i.d. pump tube; 0.04 mL/min); Eluent = 0.5 M HCl; D = UV/VIS detector (510 nm); Sample injection loop = 650 μL; Elution injection loop = 65 μL; Pump speed = 40 r.p.m.; Mixing loop M1 is 300 cm in length, M2 is 80 cm.

A second micro-column (15 x 2.5 mm) (not shown in Figure 8.2) containing Chelex 100 resin was placed between the pump and the sample injection valve to capture trace impurities from the carrier, and prevent their accumulation onto the oxine-derivatised Fractogel resin. The Fractogel micro-column was cleaned daily before use, by performing alternate stopped-flow elutions (2 min) using 0.2 M NaOH and 1 M HCl. The direction of flow through the column was periodically reversed to help avoid any build-up in back-pressure due to compaction of the Fractogel resin.

Fe standards and samples were injected into the carrier line using a 650 µL sample loop on the VALCO injection valve. After the sample aliquot had passed through the column, the captured iron was subsequently eluted by using a 65 µL volume of 0.5 M HCl (Rheodyne injection valve). The eluted iron was subsequently reacted with a buffered stream (pH 4.0) of 1,10-phenanthroline, and detected spectrophotometrically as the Fe^{II}(1,10-phenanthroline)$_3$ complex at 510 nm (GBC 918 UV/VIS). Peak heights and areas were determined using the GBC software supplied with the instrument.

Fe^{II} analysis was achieved with a simple two-line manifold, containing the carrier and colorimetric reagent lines shown in Figure 8.2. Fe^{III} was eluted by the 0.5 M HCl eluent simultaneously with Fe^{II}, but did not react with the colorimetric reagent. The addition of a third line to the manifold (containing the ascorbic acid reducing agent; Figure 8.2), allowed an on-line reduction of eluted Fe^{III}. Hence total Fe (Fe^{II} + Fe^{III}) was able to be quantified, and the concentration of Fe^{III} to be determined by difference.

8.2.2 Solutions

Fe^{II} and Fe^{III} stock solutions were prepared as described in Section 2.1.5. Stock solutions of 0.5% 1,10-phenanthroline were prepared in 0.02 M HCl. A 5% ascorbic acid (BP; Pharmaceutical Sales and Marketing Ltd., Auckland, N.Z.) stock solution was prepared daily. Fe^{II} standards (buffered to pH 4.0) were prepared in 0.02 M acetate buffer and 0.1% ascorbic acid.

The effect of possible interferent species on the analytical signal was quantified using solutions that contained 10 µM of Fe^{II} and either 10 µM or 100 µM of a selected interferent cation. Solutions were prepared in 0.02 M acetate and 0.1% ascorbic acid, and were buffered to pH 5.0. Solutions were analysed within 1-2 hours of preparation. Stock solutions of Co, Cr, Cu, Pb, Mn, Ni and Zn were prepared as described in Section 2.1.5.

Model ligand solutions containing 10 μM Fe^{II} and varying concentrations of tartrate, oxalate and citrate were prepared at pH 5.0, in 0.01 M acetate, and 0.2% ascorbic acid. Samples were equilibrated at room temperature for at least 24 hours before analysis. Stability constants (Table 8.1) were selected from the IUPAC Stability Constants Database (Pettit and Powell 1997). Where possible, reliable constants were selected for an ionic strength of 0.1 M, and a temperature of 25°C. The equilibrium composition of these solutions was calculated using the computer program SOLGASWATER (Eriksson 1979). Equilibrium calculations indicated binding of Fe^{II} by ascorbate was negligible in solution at pH 5.0. Fe ascorbate complexes were therefore not included in the equilibrium calculations for H^+-Fe^{2+}-ligand systems.

Table 8.1. Thermodynamic data (I = 0.1 M, 25°C) for the systems H^+-Fe^{2+}-ligand (L), (where L = tartrate, oxalate or citrate) and H^+-Fe^{2+} (iron hydrolysis). The equilibrium constants ($\beta_{p,q,r}$) are given according to the reaction:

$$pH^+ + qFe^{2+} + rL^{2-} \rightleftharpoons H_pFe_qL_r^{(p+2q-2r)+} \quad (H_pFe_qL_r^{(p+2q-3r)+} \text{ for citrate, } L^{3-})$$

Species	$\beta_{p,q,r}$	Log $\beta_{p,q,r}$	Species	$\beta_{p,q,r}$	Log $\beta_{p,q,r}$
Fe^{2+} hydrolysis					
$Fe(OH)^+$	(-1,1,0)	-9.7	*Oxalate cont.*		
$Fe(OH)_2$	(-2,1,0)	-20.81	FeL	(0,1,1)	3.05
$Fe(OH)_3^-$	(-3,1,0)	-31.05	FeL_2^{2-}	(0,1,2)	4.52
$Fe(OH)_4^{2-}$	(-4,1,0)	-45.54			
			Citrate (L^{3-})		
Tartrate (L^{2-})			HL^{2-}	(1,0,1)	5.65
HL^-	(1,0,1)	3.93	H_2L^-	(2,0,1)	9.97
H_2L	(2,0,1)	6.72	H_3L	(3,0,1)	12.88
FeL	(0,1,1)	2.69	FeL^-	(0,1,1)	4.56
FeL_2^{2-}	(0,1,2)	4.68	$FeHL$	(1,1,1)	8.72
			$FeHL_2^{3-}$	(1,1,2)	12.2
Oxalate (L^{2-})			FeH_2L^+	(2,1,1)	11.2
HL^-	(1,0,1)	3.82	$Fe_2H_2L_2^{4-}$	(-2,2,2)	-5.4
H_2L	(2,0,1)	4.86			

Fe-fulvic acid solutions were prepared from a sample of fulvic acid previously isolated from International Humic Substance Society (IHSS) reference peat by the acid pyrophosphate - XAD-7 method (Gregor and Powell 1986). Solutions were prepared in 0.05 M acetate (pH 4.0), and contained either 5 μM Fe^{II} or Fe^{III}, and 35 mg/L fulvic acid.

The rate of reaction between Fe^{III} and 1,10-phenanthroline was compared with that between Fe^{III}, fulvic acid, and 1,10-phenanthroline. Batch experiments were conducted in a 1 cm quartz spectrophotometric cell (GBC 918 UV/VIS; 510 nm), using reagent concentrations of 10 μM Fe^{III}, 0.05% 1,10-phenanthroline and 35 mg/L fulvic acid. Experiments were also performed using a simple two-line FIA manifold. Samples were injected (650 μL sample loop; VALCO injection valve) into a carrier line (ENE-10; 0.95 mm i.d. pump tube) containing H_2O. This line merged with a second line (ENE-04; 0.44 mm i.d. pump tube), containing either H_2O or 50 mg/L fulvic acid solution, before the sample was mixed (300 cm mixing loop; *ca.* 50 s contact time) and the formation of Fe^{II}(1,10-phenanthroline)$_3$ monitored spectrophotometrically at 510 nm (GBC 918 UV/VIS).

Three humic water samples, collected from sites near Ianthe Forest, West Coast, New Zealand, were stored in light-proof bottles, refrigerated (4°C), and filtered before use (as described in Section 2.2.5. To investigate the effect of sunlight on Fe^{II} and Fe^{III} speciation, samples were spiked with *ca.* 10 μM Fe^{III}, and placed in either an open beaker, or a foil-covered light-proof vial. The concentration of Fe^{II} in the samples was determined periodically during the subsequent 60 minutes. Samples in open beakers were exposed to sunlight throughout the 60 minute period. No attempt was made to quantify the respective amount of radiation each sample received.

8.3 RESULTS

8.3.1 Experimental optimisation

In optimising the FIA manifold conditions, a range of reducing agent, and colorimetric reagent concentrations were investigated. In addition, the use of an alternative reducing agent (hydroxyl-ammonium sulfate (BDH CP)) and colorimetric reagent (2-2' bipyridine (dipyridyl) (BDH AnalaR)) was evaluated. As these alternative reagents decreased the signal sensitivity, their use was not continued. A range of eluents was also used to effect the elution of captured iron. Simpson *et al.* (1997) established that Fe^{III} could be eluted from the oxine-derivatised Fractogel by using either a bipyridine/ascorbic acid solution, or a stopped-flow

0.2 M NaOH elution protocol. However, both of these methods were found to give poor recoveries of captured iron, compared with the use of HCl eluent. After evaluation of a range of HCl concentrations, 0.5 M HCl was identified as a suitable eluent, giving a *ca.* 95% recovery of Fe^{II} (Figure 8.4).

The redox stability of Fe^{II} retained on the resin was determined by varying the period between sample injection and elution. When on-line ascorbic acid reduction was not used, the elution signal for a 10 μM Fe^{II} standard significantly decreased with elapsed time (◇; Figure 8.3). However, the results did indicate that Fe^{II} could be eluted from the resin within 60 s of injection, without any signal loss. Elution of bound Fe^{II} in this work was subsequently performed 50 s after sample injection to minimise any signal loss. The likely cause of the signal reduction after the initial period of *ca.* 60 s, is the oxidation of Fe^{II} to Fe^{III} occurring on the oxine-derivatised Fractogel. When the ascorbic acid on-line reduction was included, the elution peak obtained after 60 s was identical to that for an Fe^{II} standard eluted within 60 s (△; Figure 8.3). This result confirms that oxidation of Fe^{II} occurs on the resin after periods of *ca.* 60 s, and indicates that Fe^{III} bound on the resin is readily eluted by the 0.5 M HCl eluent. Furthermore, it is clear that incorporation of the ascorbic acid line into the FIA manifold allows a total Fe analysis to be effected. When measuring total Fe, a decrease in signal height was observed after longer elapsed times (after 600 s the decrease was *ca.* 10% of the initial peak height).

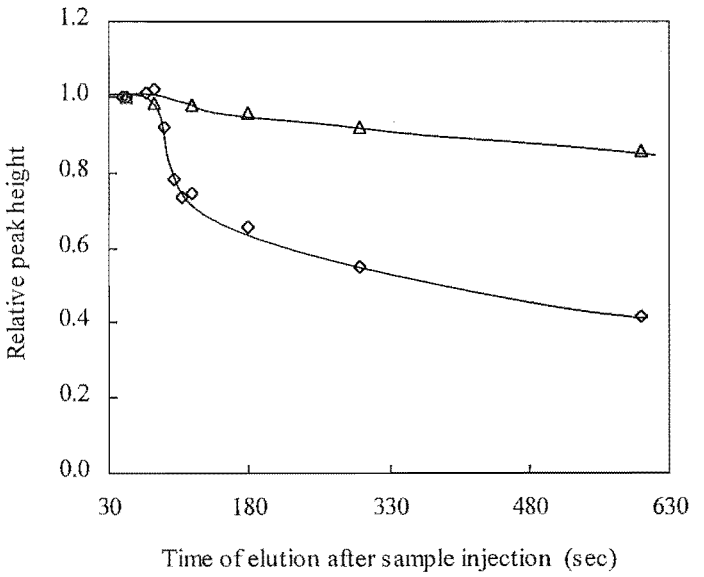

Figure 8.3. Oxidation of Fe^{II} to Fe^{III} on the oxine-derivatised Fractogel under flow conditions (◇ Fe^{II} analysis in the absence of the ascorbic acid line; △ Fe^{II} + Fe^{III} analysis in the presence of ascorbic acid). A concentration of 10 μM Fe^{II} was used.

Typical results for an Fe^{II} calibration are shown in Figure 8.4. At high concentrations, a second elution was required to remove residual Fe from the resin. There was no peak evident before the Fe^{II} elution signal, which indicates that uptake of Fe^{II} by the resin was quantitative over this concentration range.

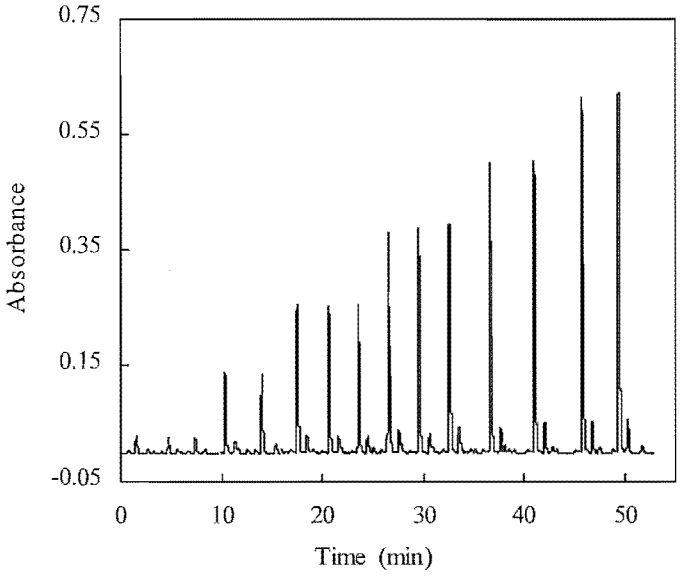

Figure 8.4. Calibration for 1-25 μM Fe^{II}. The major peaks correspond to eluted Fe^{II}, the minor peaks to the elution of residual Fe^{II}.

The RSD for the method was 0.88% at 10 μM Fe^{II} (n = 12; Figure 8.5) and the estimated linear working range was 0.2-25 μM Fe^{II}. A study of the Fe^{II} system also indicated that a five-fold sample preconcentration was achieved. The calculated detection limit (2 s.d. of signals obtained from repeated injections of an Fe^{II} standard close to the blank) was 42 nM.

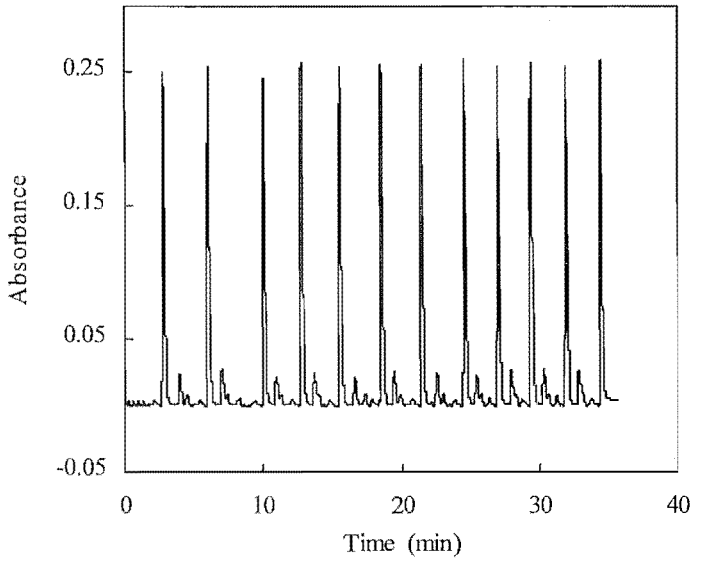

Figure 8.5. Scan showing signals obtained from repeated injections of a 10 μM Fe^{II} solution.

8.3.2 Cation interference

The effect of possible interferent species on the Fe^{II} signal was quantified, by using solutions that contained 10 μM Fe^{II} and either 10 or 100 μM of a selected trace metal. Results are presented in Table 8.2.

Table 8.2. Peak height relative to 10 μM Fe^{II}, for solutions containing 10 μM Fe^{II} and an additional trace metal at two concentrations.

Metal (M)	10 μM [M]	100 μM [M]
Co	0.98	0.47
Cr	0.99	0.95
Cu	0.87	0.74
Pb	0.91	0.90
Mn	1.00	0.95
Ni	1.01	0.94
Zn	1.00	0.70

8.3.3 Studies of Fe^{II} and Fe^{III} organic complexes

(i) Fe^{II} organic complexes

To establish whether the oxine-derivatised Fractogel sequestered Fe^{II} from Fe^{II}-organic species, a series of experiments were performed using Fe^{II} model-ligand solutions. For each solution, the respective equilibrium composition was calculated using the computer speciation program SOLGASWATER. Results from these experiments are shown in Figure 8.6.

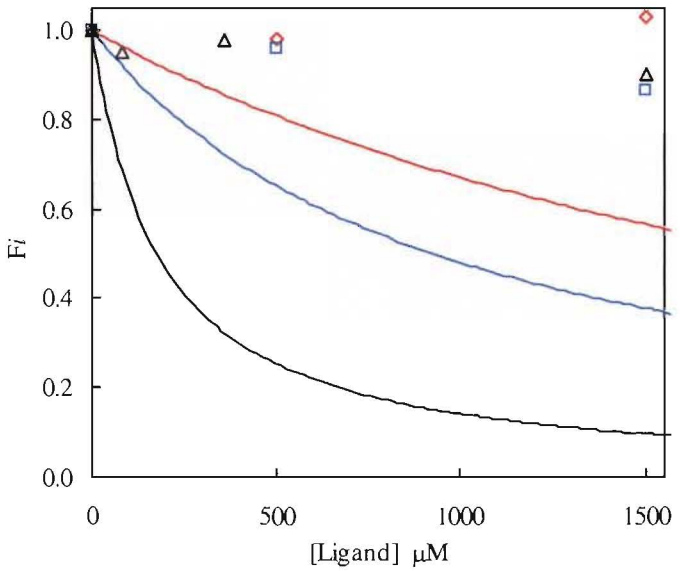

Figure 8.6. The fraction of Fe^{II} measured in solutions containing 10 μM Fe^{II} and 0-1500 μM ligand at pH 5.0. (◊ tartrate, □ oxalate, Δ citrate). The fraction *Fi* was calculated from the response for each solution relative to the response for a 10 μM standard (0 μM ligand). The solid curves (free Fe^{2+}) were calculated from thermodynamic models for each respective H^{+}-Fe^{2+}-ligand system, using the computer program SOLGASWATER.

They indicate that organically-bound Fe^{II} is labile on the experimental time-scale. At a very high ligand to metal ratio, a decrease in peak height was observed for the citrate and oxalate solutions (*ca.* 10% compared with the initial peak height). For these samples a small peak was observed prior to the elution peak, caused by organically-bound Fe^{II} which had passed through the column without being sequestered by the resin, and which subsequently reacted with 1,10-phenanthroline downline.

(ii) Fe^{III} organic complexes

To investigate the characteristics of organically-bound Fe^{III} complexes in the FIA manifold, Fe^{III} fulvic acid solutions were prepared as described in Section 8.2.2. These solutions were analysed in the absence of, and presence of the FIA ascorbic acid line. Typical results are shown in Figure 8.7.

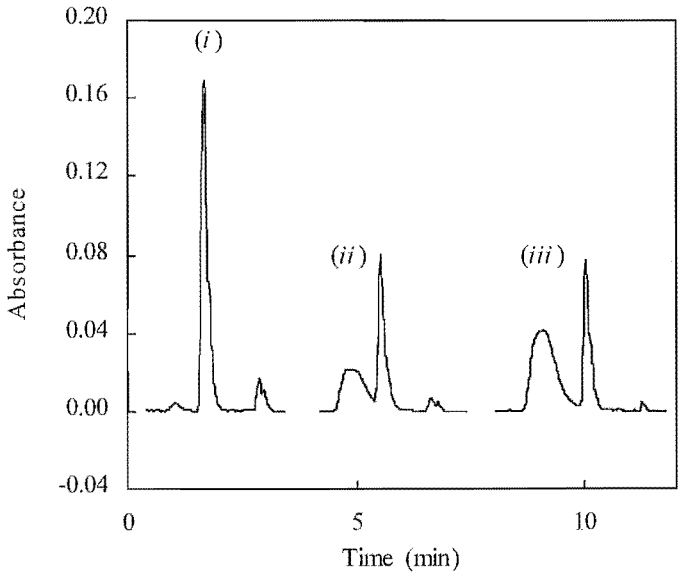

Figure 8.7. Results showing signals for (*i*) a 5 μM Fe^{II} standard; and a 5 μM Fe^{III} – 35 mg/L fulvic acid solution in (*ii*) the absence; and (*iii*) presence of the FIA ascorbic acid line. The relative areas for the three composite signals were 0.394, 0.267 and 0.385, respectively.

(iii) Fe^{II} and Fe^{III} fulvic acid complexes

A second series of experiments further investigated the characteristics of Fe^{II} and Fe^{III} fulvic acid complexes in the FIA manifold. Fulvic acid solutions containing 5 μM Fe^{II} or Fe^{III}, and 35 mg/L fulvic acid were prepared and analysed in the absence (Figure 8.8), and presence (Figure 8.9) of ascorbic acid. A blank peak ((*iii*), Figure 8.8; (*i*), Figure 8.9) was observed for a solution of 35 mg/L fulvic acid. For comparative purposes, in each figure the outline of this blank peak is overlaid on the signals obtained from the two Fe fulvic acid solutions.

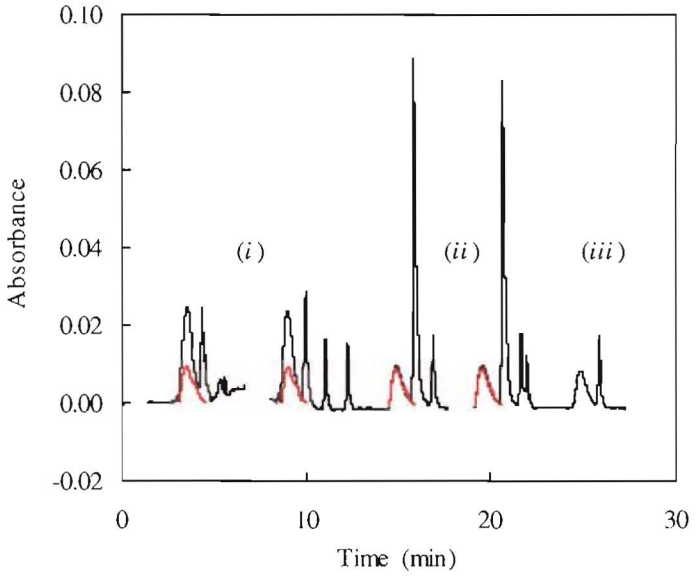

Figure 8.8. Results showing signals obtained for (*i*) Fe^{III} - fulvic acid solution; (*ii*) Fe^{II} - fulvic acid solution; and (*iii*) fulvic acid solution (blank); in the absence of the ascorbic acid line. Solutions contained 5 μM Fe^{II} or Fe^{III}, and 35 mg/L fulvic acid.

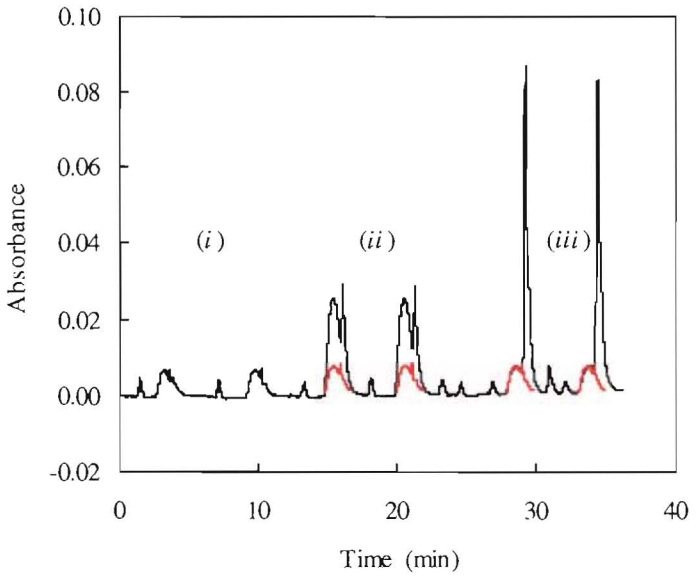

Figure 8.9. Results showing signals obtained for (*i*) fulvic acid solution (blank); (*ii*) Fe^{III} - fulvic acid solution; and (*iii*) Fe^{II} - fulvic acid solution; in the presence of the ascorbic acid line. Solutions contained 5 μM Fe^{II} or Fe^{III}, and 35 mg/L fulvic acid.

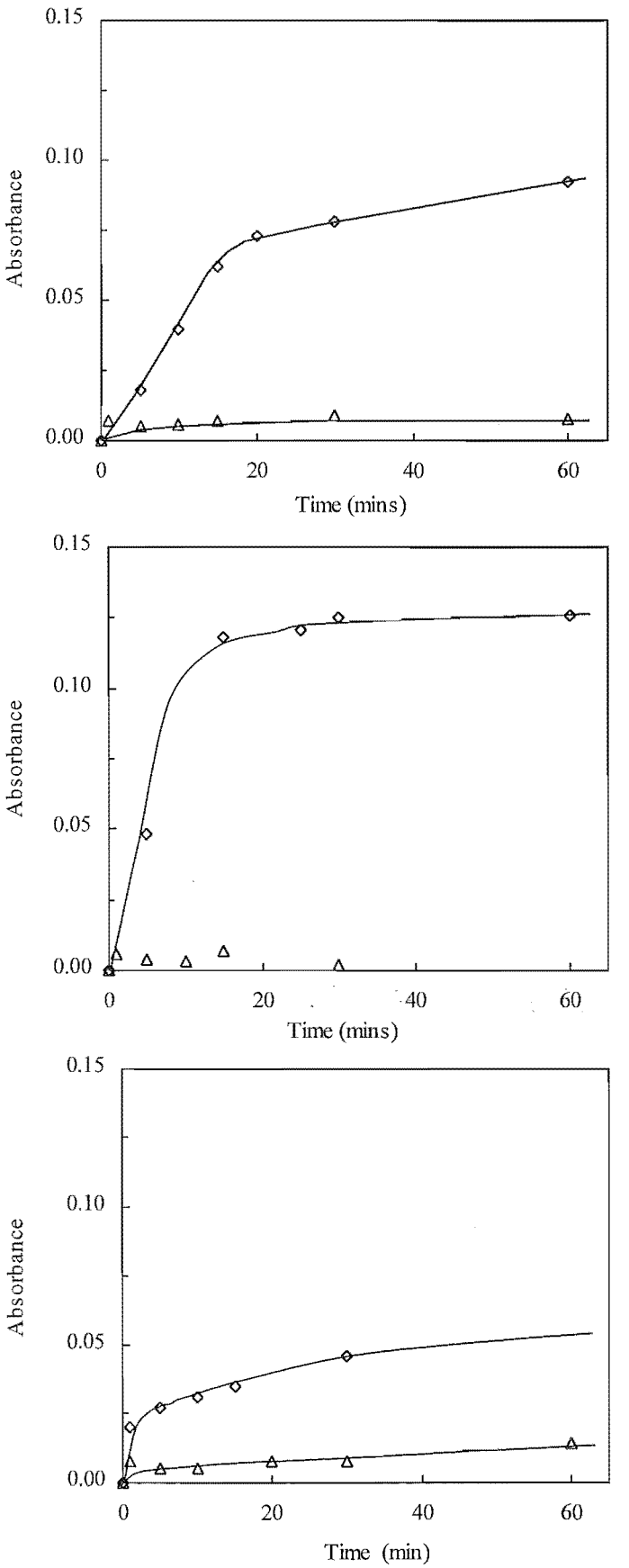

Figure 8.10. The increase in absorbance observed for the concentration of Fe^{II} determined in three humic water samples after spiking with *ca.* 10 μM Fe^{III} (◇ samples exposed to light; △ samples stored in light-proof vials) (initial absorbance has been normalised to 0).

To investigate whether the peaks observed for the Fe^{III} fulvic acid solutions might be caused by photo-reduction of Fe^{III} in the presence of fulvic and humic acids, the effect of sunlight on iron speciation in humic waters was studied. Sub-samples of the three humic water samples were spiked with *ca.* 10 μM Fe^{III} and either exposed to sunlight, or stored in light-proof vials. The concentration of Fe^{II} in each solution was determined periodically during the following 60 minutes. As was observed for Fe^{III}-fulvic acid solutions (Figure 8.7 and Figure 8.8), the humic water samples initially exhibited an elution signal, in the absence of the FIA ascorbic acid line, indicating the presence of Fe^{II}. This initial absorbance was normalised to a value of zero; results are presented in Figure 8.10.

Several experiments were performed to establish whether the peak observed prior to the elution signal for Fe^{III} fulvic acid solutions (in the absence of the FIA ascorbic acid line) was due to Fe^{III} reduction promoted by fulvic acid alone, or promoted by both fulvic acid and 1,10-phenanthroline (Figure 8.7 and Figure 8.8). The rate of formation of Fe^{II} from Fe^{III} in the presence of 1,10-phenanthroline and fulvic acid, was compared with that observed for Fe^{III} and 1,10-phenanthroline alone (Figure 8.11). Absorbance rapidly increased after the addition of fulvic acid to a solution of Fe^{III} and 1,10-phenanthroline. This implies a rapid reduction of Fe^{III}, and formation of the Fe^{II}-(1,10-phenanthroline)$_3$ complex. In contrast, in the absence of fulvic acid, a solution containing Fe^{III} and 1,10-phenanthroline exhibited only a very slight increase in absorbance during the period of the experiment.

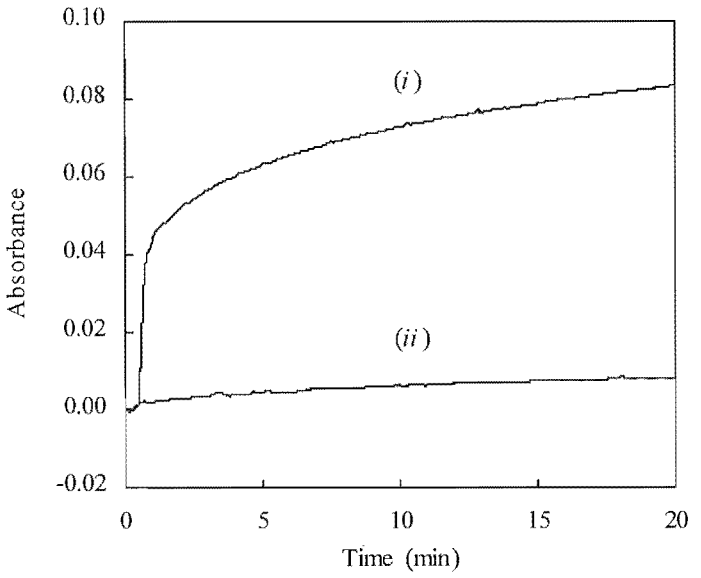

Figure 8.11. Absorbance measured at 510 nm for solutions containing (*i*) 10 μM Fe^{III}, 0.05% 1,10-phenanthroline and 35 mg/L fulvic acid and (*ii*) 10 μM Fe^{III} and 0.05% 1,10-phenanthroline. Reagents were mixed at 30 s.

To establish whether the rapid formation of the Fe^{II}(1,10-phenanthroline)$_3$ complex observed for the spectrophotometric experiments could be reproduced under flow conditions, experiments were performed using the FIA manifold described in Section 8.2.2. Samples containing (*i*) 0.005% 1,10-phenanthroline, and (*ii*) 10 μM Fe^{III} and 0.005% 1,10-phenanthroline were injected into an FIA manifold and merged with a line containing either H_2O (Figure 8.12) or a 50 mg/L fulvic acid solution (Figure 8.13).

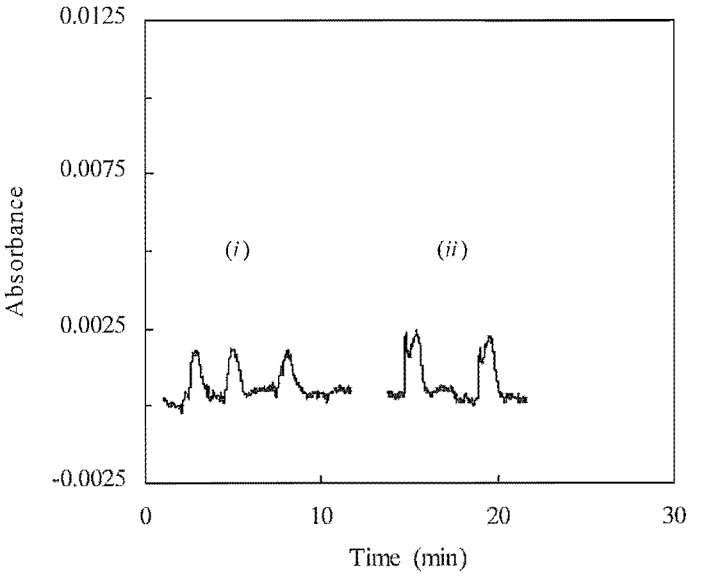

Figure 8.12. Results showing signals obtained for (*i*) 0.005% 1,10-phenanthroline; and (*ii*) 10 μM Fe^{III} and 0.005% 1,10-phenanthroline; injected into an FIA manifold containing H_2O.

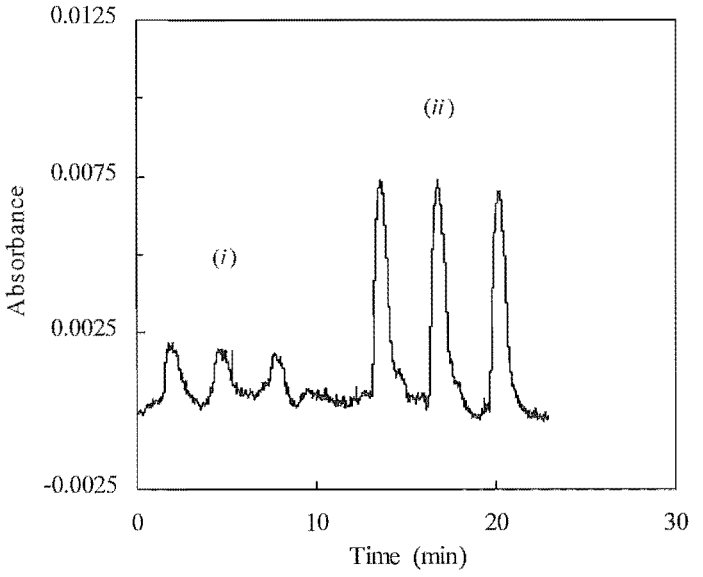

Figure 8.13. Results showing signals obtained for (*i*) 0.005% 1,10-phenanthroline; and (*ii*) 10 μM Fe^{III} and 0.005% 1,10-phenanthroline; injected into an FIA manifold containing 50 mg/L fulvic acid.

8.4 DISCUSSION

8.4.1 Method validation

The developed protocol allows quantification of Fe^{II} by using a simple FIA manifold, with two lines containing a carrier solution and a colorimetric reagent respectively. The addition of a third line to the manifold (containing a reducing agent) allows an on-line reduction of Fe^{III}, and hence total Fe (Fe^{II} + Fe^{III}) to be determined. The sensitivity of the technique was adequate to study the Fe concentrations found in three humic water samples. However, the sensitivity of the technique could be further enhanced to enable the analysis of samples containing lower concentrations of Fe. Preconcentrating large sample volumes onto chelating resins has been used in several studies to achieve low detection limits (<1 nM) (Elrod *et al.* 1991; Obata 1993; Blain and Tréguer 1995). In addition, the use of alternative detection methods (*e.g.* a more sensitive Fe^{II} spectrophotometric reagent, or coupling of the oxine-derivatised Fractogel fractionation step to chemiluminescent detection) would further lower the detection limit.

Figure 8.3 clearly indicates that Fe^{II} is oxidised on the column (after *ca.* 60 s) to Fe^{III}, causing a decrease in the elution peak height (in the absence of ascorbic acid). The amount of oxidation on the column increases with elapsed time. In the presence of ascorbic acid, a total Fe analysis is effected (the elution peak is identical to that of an Fe^{II} injection eluted within 60 seconds). That the oxidised Fe^{II} is able to be quantified *via* incorporation of a line containing ascorbic acid into the FIA manifold, is an important result, as it confirms the ability of the system to differentiate between eluted Fe^{II} and Fe^{III}. Although Fe^{III} and Fe^{II} were simultaneously eluted from the resin by the 0.5 M HCl eluent, it is clear that Fe^{III} did not react downline with the Fe^{II}-specific colorimetric reagent 1,10-phenanthroline. The instability of the Fe^{II} oxidation state is a significant problem if the micro-column was to be adapted for use in the field as a portable pre-concentration device for Fe. Significant changes in the distribution of oxidation states would occur before any subsequent laboratory analysis for Fe could be completed.

The reduction in signal height observed for longer periods between sample injection and elution (when including the on-line reduction) is attributed to the migration of Fe^{III} into inaccessible, strongly binding sites within the Fractogel. A similar signal reduction has previously been noted for aluminium, when elution was attempted after long periods following sample injection (Bridgen 1999). The reduced Fe recovery with elapsed time might be problematic should the micro-column be used as a field sampling device. However,

development of an alternative elution strategy (*e.g.* a stopped-flow elution with a higher concentration of HCl eluent) might allow recovery of a greater percentage of the captured Fe.

The effect of potential interferent species on the Fe^{II} signal was quantified (Table 8.2). A slight reduction in peak height was observed for Cu (-13 %) and Pb (-9 %), when present at the Fe^{II} concentration (10 μM). Significant interference (> 10%) was observed for Co, Cu and Zn when present at ten times the Fe^{II} concentration. These results imply that the cations that give rise to significant interference are retained on the oxine-derivatised Fractogel and eluted concurrently with Fe. It is possible that the cations will compete with Fe^{II} for binding sites on the oxine. However, no pre-elution peaks were observed for these experiments, which indicates that breakthrough of Fe^{II} through the column did not occur. Therefore even in the presence of high concentrations of interferent species, uptake of Fe^{II} on the resin appears quantitative.

The presence of high concentrations of Co, Cu and Zn are recognised as causing interference when Fe^{II} analyses are performed using 1,10-phenanthroline (Pehkonen 1995). However, concentrations of these cations in soil solutions or natural waters from unpolluted environments will be significantly lower than the 10 and 100 μM concentrations used in this study. Therefore it is expected that minimal interference will occur from trace concentrations of these elements in natural samples.

8.4.2 Studies of Fe^{II} and Fe^{III} organic complexes

(*i*) *Fe^{II} organic complexes*

Fe^{II} model-ligand solutions were prepared to establish whether the oxine-derivatised Fractogel sequestered Fe^{II} from Fe^{II}-organic species. Results of analyses performed on the synthetic organic ligand solutions (tartrate, oxalate and citrate) established that even at large excesses of added ligand, Fe^{II} was labile on the experimental time-scale (*ca.* 1.1 s) and was sequestered from the organic complexes by the oxine-derivatised gel (Figure 8.6). Similar results were observed for a prepared solution containing an Fe^{II} fulvic acid complex (Figure 8.8 and Figure 8.9). The relatively high rate constant observed for exchange of inner-sphere water in $Fe(H_2O)_6^{2+}$ (*ca.* 10^7 s^{-1}; Cotton and Wilkinson 1988) is reflected by the observed lability of Fe^{II}-organic complexes. From these results, it is inferred that this method is likely to determine a total Fe^{II} concentration for natural Fe^{II}-organic complexes (having comparable binding strengths to the model-ligand and Fe^{II} fulvic acid complexes).

(ii) Fe^{III} organic complexes

Figure 8.7 presents the results of analyses for an Fe^{III} fulvic acid solution, performed in the absence and presence of ascorbic acid. To avoid the possibility of Fe^{III} precipitation, the initial Fe^{III} fulvic acid solution (buffered to pH 4.0) contained a low ratio of Fe^{III} (5 μM) to fulvic acid (35 mg/L), (the aluminium complexation capacity for this fulvic acid has previously been determined as *ca.* 10 μM for a 17 mg/L solution at pH 4.7 (Section 3.8). A peak prior to elution and an elution peak were observed for the Fe^{III} fulvic acid solution when the FIA ascorbic acid line was not present. These peaks clearly indicate that Fe^{II} is present, either in the Fe^{III} fulvic acid solution prior to analysis, and/or is formed in the manifold prior to detection.

The relative peak areas in Figure 8.7 for the Fe^{II} standard and the Fe^{III} fulvic acid solution (the combined areas of the pre-elution and elution signals), analysed in the presence of the ascorbic acid line, were 0.394 and 0.385, respectively. This agrees with the results presented in Figure 8.3, which indicate that a total recovery of Fe (Fe^{II} + Fe^{III}) occurs when the ascorbic acid line is present. In contrast, the peak area was lower (0.267) for the Fe^{III} fulvic acid solution when the ascorbic acid line was not present. From this, it is inferred that the Fe not accounted for in this signal is present as non-labile Fe^{III}.

(iii) Fe^{II} and Fe^{III} fulvic acid complexes

Unlike the results observed for the Fe^{II} model ligand solutions, the Fe^{II} fulvic acid solution exhibited a small peak prior to the elution signal (Figure 8.8; Figure 8.9). However, as this peak corresponded exactly with the blank peak observed for the fulvic acid solution, it is clear that no contribution to this signal arises from the Fe^{II} fulvic acid complex. These results confirm the results of the Fe^{II} model ligand solutions, establishing that organically-bound Fe^{II} is labile within the experimental time-scale, and hence is quantified in the elution signal.

Two peaks were observed when an Fe^{III} fulvic acid sample was analysed without the ascorbic acid line present (Figure 8.7; Figure 8.8). The observation of an elution peak implies Fe^{II} is present in the sample prior to analysis. The formation of Fe^{II} in solution can only have arisen from a reduction of Fe^{III}, (*e.g.* photo-reduction), a reaction known to readily occur in the presence of fulvic acids (Waite and Morel 1984; Voelker *et al.* 1997). The possibility of this peak being caused by Fe^{III} can be discounted, as Figure 8.3 clearly shows eluted Fe^{III} is not quantified in the absence of ascorbic acid.

A qualitative experiment was performed to investigate whether this technique might be applied to monitor the on-going Fe^{II} formation that occurs as a result of photo-reduction of Fe^{III} fulvic acid samples. Humic waters were spiked with Fe^{III}, and either stored in light-proof vials, or exposed to sunlight. The concentration of Fe^{II} in each solution was subsequently determined at regular intervals during the following 60 minutes.

When samples were stored in light-proof vials, a negligible increase in the concentration of Fe^{II} was observed for each humic water (Figure 8.10). In contrast, when samples were exposed to sunlight, a large increase in Fe^{II} concentration occurred in each sample. The magnitude of the absorbance increase differed for each sample. It is expected that the rate of Fe^{III} photo-reduction will be a function of the number of active reducing sites on organic matter within the sample, and also of the radiation intensity each sample experiences (Sulzberger *et al.* 1990). These results indicate that in the presence of organic matter, the Fe^{III}/Fe^{II} system is very dynamic. The rapid photo-reduction of Fe^{III} alters the iron speciation within natural samples significantly.

The Fe^{III} fulvic acid solutions also exhibited a peak prior to elution, which was significantly greater than that observed for the blank fulvic acid solution (Figure 8.8). Results from the Fe^{II} fulvic acid solution (Figure 8.8) indicate that organically-bound Fe^{II}, if initially present in the sample, would be sequestered by the resin. Therefore this result implies that Fe^{II} formation must be occurring downline of the column in the FIA manifold (*i.e.* Fe^{III} reduction occurring in the presence of fulvic acid and 1,10-phenanthroline).

To establish whether such reduction of Fe^{III} was feasible, the rate of reaction between Fe^{III}, 1,10-phenanthroline and fulvic acid was studied. Figure 8.11 indicates that, in the absence of fulvic acid, formation of the Fe^{II}-(1,10-phenanthroline)$_3$ complex (as monitored at 510 nm) proceeded slowly in a solution containing Fe^{III} and 1,10-phenanthroline. In contrast, in the presence of fulvic acid, the formation of Fe^{II}-(1,10-phenanthroline)$_3$ was rapid (Figure 8.11). This implies that a rapid on-line reduction of Fe^{III}, in the presence of fulvic acid and 1,10-phenanthroline, might well occur in the FIA manifold.

Strong Fe^{II}-specific chelating reagents such as 1,10-phenanthroline, themselves cause a slow reduction of Fe^{III} to Fe^{II} in solution, because of the increase in reduction potential that occurs when the reagents are added to a solution containing both Fe^{II} and Fe^{III} (Pehkonen 1995). For example, the addition of 1,10-phenanthroline to a solution of Fe^{III} increases the reduction potential from 0.76 V (Fe^{3+}/Fe^{2+} half-reaction) to *ca.* 1.1 V (Fe^{3+}-1,10-phenanthroline/Fe^{2+}-1,10-phenanthroline).

To establish whether the rapid formation of the Fe^{II}(1,10-phenanthroline)$_3$ complex occurred under flow conditions, a simple flow manifold was constructed (Section 8.2.2). In the absence of fulvic acid, signals of equal absorbance (Figure 8.12) were obtained from injection of either (*i*) 0.005% 1,10-phenanthroline, or (*ii*) 10 μM Fe^{III} and 0.005% 1,10-phenanthroline, when mixed with a stream of H_2O. When the same samples were injected into the manifold and mixed with a stream of 50 mg/L fulvic acid solution, the signal from an injection of Fe^{III} 1,10-phenanthroline solution was substantially higher than that observed for injection of 1,10-phenanthroline solution alone (Figure 8.13). This result confirms that the 'pre-elution' signal observed for an Fe^{III} fulvic acid solution, corresponds to a fraction of the fulvic-bound Fe^{III}, which being non-labile on the experimental time-scale, is not captured by the column. Downline of the column however, in the presence of both fulvic acid and 1,10-phenanthroline, the Fe^{III} is reduced, thus giving an operationally-defined analytical peak.

8.5 CONCLUSION

An analytical method for speciating Fe^{II} and Fe^{III} was successfully developed, by using a micro-column containing oxine-derivatised Fractogel in an FIA manifold. Experiments using Fe^{II} model ligand and fulvic acid solutions, indicated that Fe^{II} was sufficiently labile on the experimental time-scale to be captured quantitatively by the column. Determination of total Fe^{II} was achieved, after eluting captured Fe^{II} from the resin, by a subsequent reaction with the colorimetric reagent 1,10-phenanthroline in a simple two-line manifold. Incorporation of a third line containing ascorbic acid allowed a quantitative total Fe determination to be obtained. This was established by comparing the peak areas obtained for an Fe^{III}-fulvic acid solution with those obtained from both an Fe^{II} standard and an Fe^{II}- fulvic acid solution (in which all Fe^{II} was labile).

In the presence of fulvic and humic acids, Fe^{III} was shown to readily undergo photo-reduction to Fe^{II}. The ability of Fe^{III} to undergo rapid photo-reduction has implications for sample collection, should quantitative information on iron speciation be required. Samples must be collected and stored in light-proof containers until analysis occurs, to prevent significant changes in speciation.

In the absence of ascorbic acid, an operationally-defined pre-elution peak was observed for an Fe^{III}-FA complex. The apparent presence of Fe^{II} down-line of the column (which if initially present in the fulvic acid solution would have been sequestered by the resin) was rationalised experimentally by establishing that Fe^{III} is rapidly reduced in the FIA manifold, in the

presence of both fulvic acid and 1,10-phenanthroline. The peak therefore corresponded to organically-bound Fe^{III} which was non-labile on the experimental time-scale, but which subsequently underwent reduction in the presence of fulvic acid and 1,10-phenanthroline.

The oxidation of Fe^{II} to Fe^{III} on the resin (which occurred after *ca.* 60 s) would be a problem if the micro-column is to be used in the field to preconcentrate Fe. Large changes in iron speciation will occur before analysis can be effected. Furthermore, the reduced recovery of Fe observed after long time intervals between sample injection and elution, means that an alternative elution protocol will be required if elution of sequestered Fe is to be performed later in the laboratory.

CHAPTER 9

IMINODIACETATE CHELATING RESIN: APPLICATION TO ALUMINIUM ANALYSIS

9.1 INTRODUCTION

Many methods for aluminium analysis have been developed to explore possible correlations between 'reactive Al' fractions in soil solutions and natural waters and observed biological toxicity (Section 1.4). Kinetic-based analysis protocols exploit the relatively slow dissociation and formation of aluminium complexes, and use short reaction times (*ca.* 1-60 s) between the sample and an Al-selective reagent or a stationary adsorbent.

Several authors have determined 'reactive Al' fractions using ion-exchange or derivatised chelating resins, that contain functional groups capable of binding Al. Such methods generally involve separate fractionation and detection steps. By rapidly (and reproducibly) passing samples over such resins, only the most labile Al species are captured. The captured labile fraction of aluminium is subsequently eluted (typically using a strong mineral acid) and quantified using an established analysis method. The use of resins to selectively capture various aluminium species, offers several inherent advantages (*i.e.* on-line sample preconcentration and matrix isolation) compared with traditional methods of aluminium determination. In addition, such techniques offer good analytical selectivity and are often easily automated (*e.g.* by incorporation of micro-columns into flow injection analysis (FIA) manifolds).

A variety of solid polymeric supports have been used to immobilise chelating ligands for batch and column preconcentration methods (*e.g.* Hodges 1987; Persaud and Cantwell 1992; Fairman and Sanz-Medel 1996; Kozûh *et al.* 1997; Pesavento *et al.* 1998*a*). However, one commonly used polymeric resin, Chelex-100 (an iminodiacetate based resin with a polystyrene-divinylbenzene support), has been shown to cause difficulties for on-line operations because of the tendency of the polymeric support to swell as the resin is converted from the acid form to the sodium or ammonium forms (Greenway *et al.* 1996*a*; Fang 1998).

Swelling of oxine-derivatised Fractogel during changes in pH (*i.e.* Al elution with alkali) has also been identified as a problem when the Fractogel micro-column is used in conjunction with on-line electrochemical methods of Al detection (O'Sullivan 1997). Such effects have led to the development of chelating resins based on polymers that are less affected by changes in pH.

Controlled-pore glass (CPG) micro-bead chelating resins are not affected by swelling caused by changes in pH or sample composition (Nelms *et al.* 1995). The chelating reagents 8-hydroxy-quinoline (oxine) and iminodiacetate have both been attached to CPG supports and exploited in on-line matrix separation and preconcentration systems with ETAAS or ICP-MS detection (Nelms *et al.* 1995; Greenway 1996*b*; Nelms *et al.* 1996). However, a significant disadvantage with the oxine-derivatised CPG resin is the low exchange capacity it exhibits compared with oxine-derivatised Fractogel (Landing *et al.* 1996), and a commercially available iminodiacetate-CPG resin (Greenway *et al.* 1996*a*).

A standard method of Al analysis is to extract exchangeable Al from soil using a 1 M KCl matrix (Blakemore *et al.* 1987). It would be informative to be able to determine the aluminium speciation in such samples. However, some evidence from within this research group points to the inability of the oxine-derivatised Fractogel to sequester Al at high ionic strengths. Chelex-100 (iminodiacetate based) is commonly used for preconcentration of trace metals from seawater, but causes problems in on-line systems, as discussed.

In this work the properties of a commercially available iminodiacetate-CPG chelating resin (Prosep) were investigated, to establish whether it could be used in an FIA manifold to determine the speciation of Al in natural samples. This resin was selected as it is able to withstand changes in pH without undergoing changes in volume. It has also been shown to sequester metals from samples of high ionic strength (*e.g.* to preconcentrate metals from synthetic seawater saline matrices (Greenway *et al.* 1996*b*; Nelms *et al.* 1996)). The performance of the resin in sequestering Al from samples of high ionic strength was investigated, and the developed method was tested using model Al-ligand solutions (for which the equilibrium species composition had been calculated), to determine whether the resin sequestered Al from organic complexes. Three humic water samples and four soil sample extracts were analysed, and the results compared with those obtained using other established methods for Al analysis.

9.2 MATERIALS AND METHODS

9.2.1 Samples

Three humic water samples were collected from sites near Ianthe Forest, West Coast, New Zealand. Samples were stored refrigerated (4°C), and filtered before analysis (as described in Section 2.2.5).

Four 0.02 M $CaCl_2$ extracts were obtained from soils sampled from the Cragieburn Range, Canterbury, New Zealand, as part of the study into the effects of afforestation on soil and soil solution aluminium concentrations (described in Chapter 5). Extracts came from soil samples taken from each of the CP and CF grassland and forest sites. A full description of the CP and CF sites, and the soil sampling methods used, is contained in Section 5.2.1.

9.2.2 Total aluminium analyses

The concentration of total aluminium in samples was determined by ETAAS, as described in Section 2.2.7.

9.2.3 Flow injection analysis manifold

The FIA manifold (Figure 9.1) is similar to that used for the oxine-derivatised Fractogel method, and was constructed using the materials and equipment described in Section 2.1.3. The sample of the iminodiacetate-derivatised controlled pore glass chelating resin (PROSEP® Chelating-1) was obtained from Bioprocessing, Consett, Co Durham, England, and used as received. The CPG support is porous glass, with particle size 75-125 μm. The reagents used in the optimised flow injection analysis manifold are described in the caption to Figure 9.1.

The micro-column containing the Prosep was placed in a 65 μL injection loop of a Rheodyne 5020 (6-port) injection valve. Samples were injected using a VALCO (10-port) injection valve (650 μL sample loop). A second micro-column (15 x 2.5 mm) containing Chelex 100 resin (not shown in Figure 9.1), was placed between the pump and the sample injection valve as a precaution against the accumulation of trace impurities from the carrier onto the Prosep resin. The micro-column (20 x 1 mm i.d.) containing the Prosep resin was cleaned daily before use, by performing several stopped-flow elutions (2 min, 1 M HCl). In addition, the direction of flow through the column was periodically reversed to help avoid a build-up in back-pressure due to compaction of the Prosep.

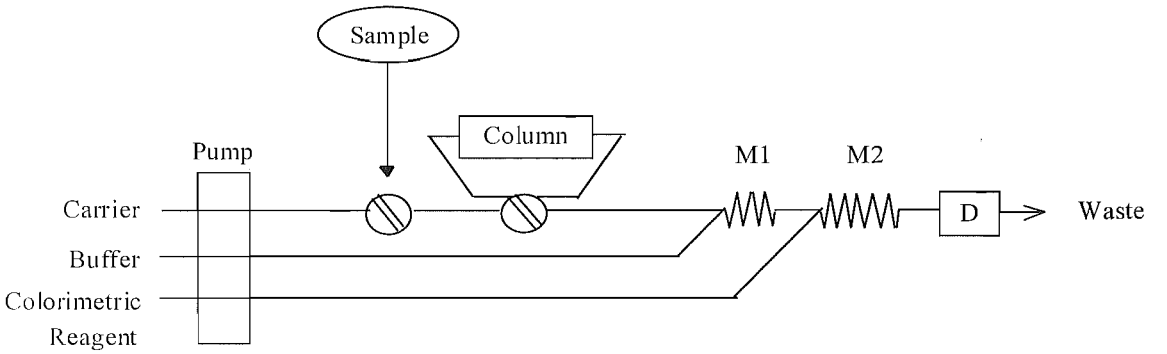

Figure 9.1. Flow injection analysis manifold for the analysis of aluminium using a 16 µL micro-column containing Prosep resin. Pump speed = 40 r.p.m.; Carrier solution = 0.05 M sodium acetate/0.05 M NaCl, pH 5.0 (ENE-12; 1.09 mm i.d. pump tube; 1.23 mL/min); Buffer = 2 M sodium acetate, pH 6.0 (ENE-04; 0.44 mm i.d. pump tube; 0.21 mL/min); Colorimetric reagent = 2 mM CAS (ENE-01; 0.19 mm i.d. pump tube; 0.04 mL/min); Eluent = 0.1 M HCl; D = UV/VIS detector (545 nm); Sample injection loop = 650 µL; Column is placed in a 65 µL injection loop; Mixing loop M1 is 80 cm in length, M2 is 300 cm.

Aluminium standards and samples were injected into the carrier stream using the 650 µL sample loop. 'Free Al' captured on the Prosep was subsequently eluted using 0.1 M HCl in a two minute stopped-flow elution protocol. In this procedure, the column was switched off-line using the injection valve 60 s after injection of the sample, and after the injection loop was filled with the 0.1 M HCl eluent. After the stopped-flow period, the column was switched back on-line, allowing the carrier stream to transport the released Al downline, where it was reacted with chrome azurol S (CAS) and buffered, before spectrophotometric detection (545 nm; GBC 918 UV/VIS). A second stopped-flow elution was also performed to remove any residual Al from the resin, before analysis of the next sample. In samples containing Al and natural organic matter, a peak corresponding to a moderately-labile 'organic-bound Al' fraction is observed prior to elution of the captured 'free Al', similar to the peak observed using the oxine-derivatised Fractogel method.

9.2.4 Method validation

Model ligand solutions containing 15 µM Al and varying oxalate concentrations (0-50 µM), were prepared in 0.01 M acetate (pH 4.5) and 0.1 M KCl. Samples were equilibrated at room temperature for 24 hours before analysis. The equilibrium composition of these solutions was calculated using the computer program SOLGASWATER (Eriksson 1979), using the oxalate constants listed in Table 9.1. Reliable ligand stability constants for the aluminium oxalate system at 25°C are only available at an ionic strength of 0.6 M (Pettit and Powell 1997). While the difference in ionic strength between these constants and the model solutions (*ca.* 0.1 M) was not ideal, the constants were considered adequate for this present study. The

aluminium hydrolysis constants were valid for an ionic strength of 0.1 M (Section 2.2.9). Although aluminium forms a weak complex with acetate, the presence of acetate in Al standards has been shown to be insignificant (Simpson *et al.* 1997). Aluminium acetate complexes were therefore not included in the equilibrium calculations.

Table 9.1. Equilibrium constants ($\beta_{p,q,r}$) for the H^+-Al^{3+}-oxalate (H_2L) system (Pettit and Powell 1997). The equilibrium constants ($\beta_{p,q,r}$) are given according to the reaction $pH^+ + qAl^{3+} + rH_2L \rightleftharpoons H_pAl_qL_r^{(p+3q-2r)+}$.

Species	$\beta_{p,q,r}$	Log $\beta_{p,q,r}$
HL^-	(-1,0,1)	-0.97
L^{2-}	(-2,0,1)	-4.54
$AlHL^{2+}$	(-1,1,1)	1.40
AlL^+	(-2,1,1)	1.43
AlL_2^-	(-4,1,2)	1.85
AlL_3^{3-}	(-6,1,3)	1.26
$Al_3(OH)_3L_3^0$	(-9,3,3)	-4.28
$Al_2(OH)_2L_4^{4-}$	(-10,2,4)	-4.62

Polymeric Al-hydroxy solutions had previously been prepared at 10 or 100 μM total Al in 0.1 M NaCl, over the pH range 4.50-5.70, by the partial neutralisation of acidic Al solutions (Simpson *et al.* 1997). The pH of these solutions was re-measured and compared with the original values. In general, the pH of the solutions was slightly lower than that originally measured for the solutions (mean $\triangle$pH = -0.1). For the analysis of the 100 μM solutions the sample was diluted 10-fold and mixed immediately prior to injection. To establish whether precipitation had occurred with ageing of the hydrolysed Al solutions, the light dispersion of each was checked by performing a wavelength scan (400-200 nm; GBC UV/VIS 918 spectrophotometer) and the results compared with a scan obtained from a freshly prepared solution containing precipitated aluminium-hydroxy species. Except for one sample, there was negligible turbidity, indicating the absence of solid-phase Al species. The sample which may have contained precipitated aluminium was not used for further analyses.

9.3 RESULTS

9.3.1 Experimental optimisation

Preliminary experiments indicated that Al was captured by the Prosep resin, and could be eluted quantitatively using a 250 μL injection of 1 M HCl. However, such high acid concentrations caused unacceptably large blank peaks, due to inadequate buffering within the manifold (the CAS reagent was protonated by excess unbuffered acid, forming a red-coloured species which absorbed strongly at the analytical wavelength of 545 nm). Lower concentrations of HCl, while reducing the height of the blank, did not elute Al quantitatively.

Alternative protocols (including stopped-flow elutions) were investigated. Various concentrations of alkali and a competitive ligand (EDTA) were unsuccessful in removing the captured Al from the resin. However, quantitative elution was found to be possible using a stopped-flow procedure and a relatively low (0.1 M) concentration of HCl. Elution was achieved using a 65 μL eluent loop on the Rheodyne injection valve, significantly smaller than the volume initially used (250 μL); this also assisted in reducing the blank. Initially, the reproducibility of blank stopped-flow elutions was poor. This was found to be caused by the CAS reagent slowly flowing back into the main carrier line when the pump was switched off during the stopped-flow period. This occurred at the confluence point situated before mixing loop M2 in the FIA manifold (Figure 9.1). When the pump was restarted, the backflow of CAS subsequently caused a pulse of concentrated reagent to pass through the detector. To overcome this problem, the Prosep micro-column was placed in the 65 μL injection loop, which allowed it to be removed from the carrier flow by switching the injection valve from the inject position (in-line) to the load position (off-line). The injection loop containing the column could then be filled with the 0.1 M HCl eluent (for a user-defined stopped-flow elution period), before being switched back in-line, to elute the released Al into the carrier stream. A typical scan is shown in Figure 9.2.

The effect of lengthening the stopped-flow elution period was investigated (Figure 9.3). The absorbance of the analytical signal rapidly increased with increased elution time during the first 30 s, but at a slower rate afterward.

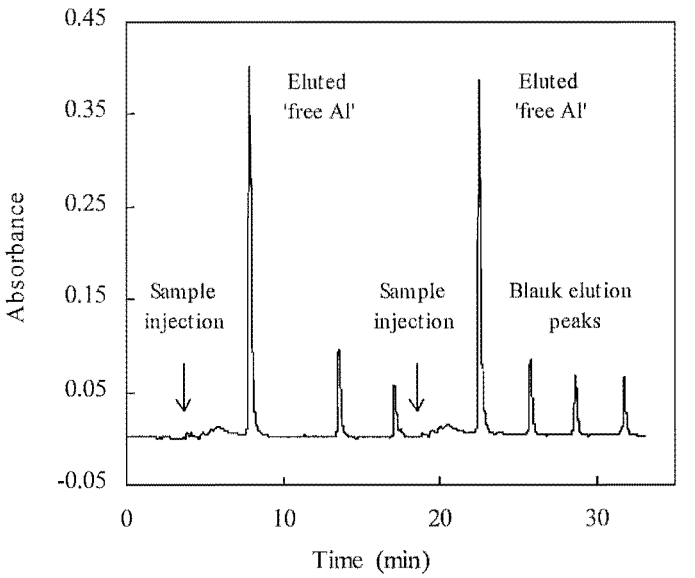

Figure 9.2. Scan showing the signal obtained from a 10 μM Al^{3+} standard. Note the slightly higher peak from the second elution compared with the blank, indicating a small amount of Al carryover.

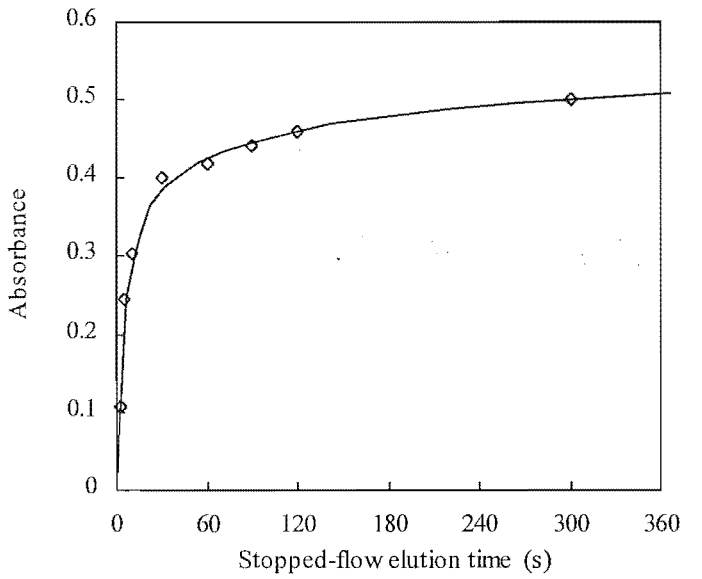

Figure 9.3. Peak height obtained for a 10 μM Al^{3+} solution after different stopped-flow elution periods.

A stopped-flow period of 2 min gave good sensitivity, without being excessively time-consuming, and was therefore used for all subsequent experiments. The calculated detection limit (2 s.d. of signals obtained from repeated injections of an Al^{3+} standard close to the blank) was 0.21 μM. The RSD for the method was 2.0% at 10 μM (n = 8; Figure 9.4), and the estimated linear working range was 1.0-25 μM Al.

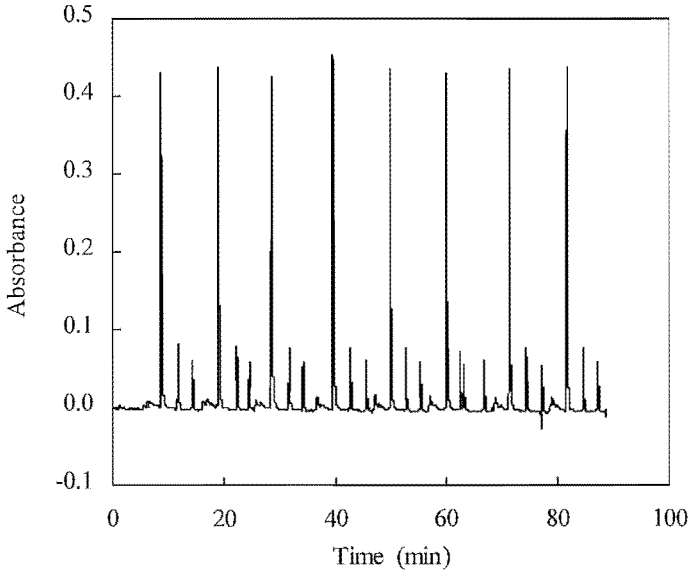

Figure 9.4. Scan showing signals obtained from repeated injections of a 10 μM Al^{3+} standard.

The suitability of the Prosep resin to sequester aluminium from samples with high ionic strength matrices was evaluated by preparing solutions containing 10 μM Al and a range of KCl concentrations (0.0-1.0 M). Experimental results are shown in Figure 9.5.

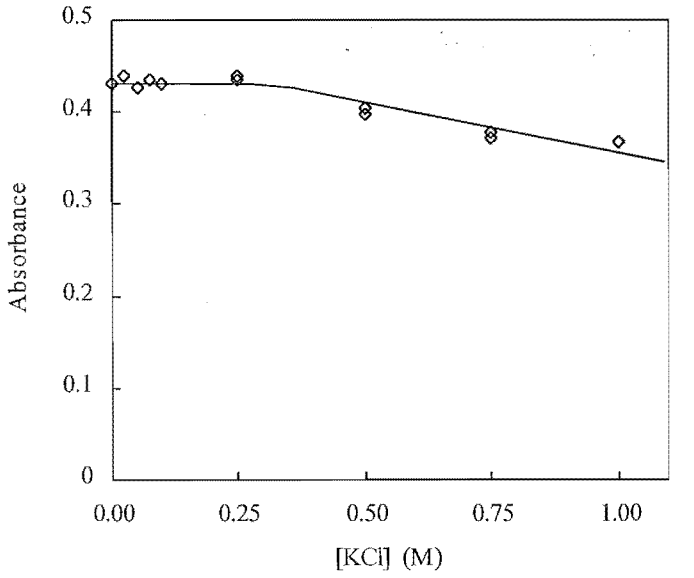

Figure 9.5. Peak height for 10 μM Al^{3+} solutions prepared in a range of KCl concentrations.

Absorbance was constant for Al standards containing up to 0.25 M KCl, but decreased for standards containing higher KCl concentrations. At ionic strengths >0.25 M KCl, where the absorbance of the Al standards decreased, a peak appeared prior to elution of the captured

'free Al'. This peak was caused by breakthrough Al that had passed through the column without binding, and also by the pulse of high ionic strength sample passing through the detector, which for a short period, caused variations in the the refractive index of the carrier solution.

9.3.2 Method validation

The results of the model-ligand solution analyses are shown in Figure 9.6. The measured response from each solution is plotted relative to the response for a 15 μM standard (0 μM oxalate). There was excellent agreement between the experimental results and the calculated curve for $\Sigma\{[Al^{3+}] + [Al(OH)^{2+}] + [Al(OH)_2^+]\}$ derived from the aluminium oxalate thermodynamic model.

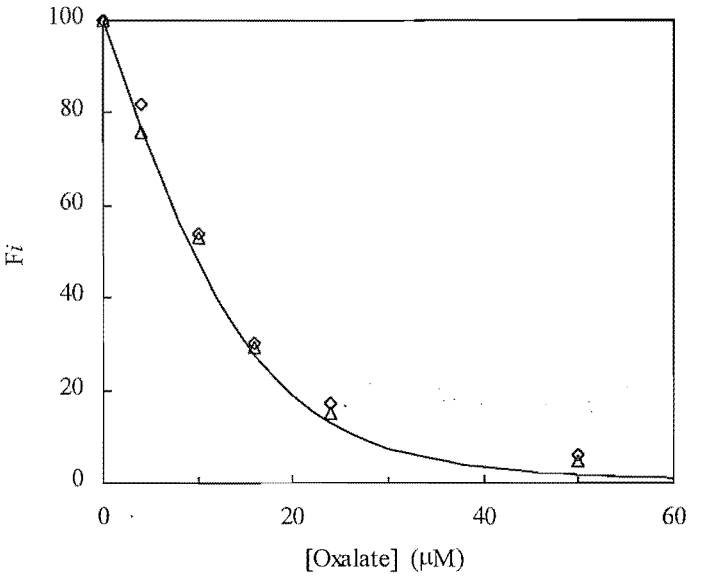

Figure 9.6. The fraction of Al measured in solution containing 15 μM Al and 0-50 μM oxalate at pH 4.7 (△ 40 r.p.m.; ◇ 30 r.p.m. pump speeds). The fraction F*i* was calculated from the response for each solution relative to the response from a 15 μM standard (0 μM oxalate). The solid curve $\Sigma([Al^{3+}] + [Al(OH)^{2+}] + [Al(OH)_2^+])$ was calculated from the thermodynamic model for the H^+-Al^{3+}-oxalate system using the computer program SOLGASWATER.

The model-ligand solutions were analysed at two pump speeds (30 and 40 r.p.m.) to establish if uptake of the 'free Al' fraction was sensitive to changes in carrier flow-rate. There was good agreement between the results obtained at the two pump speeds (Figure 9.6). This indicated that within this flow rate range, an increased contact time (slower pump speed) between the sample and Prosep did not cause significant concentrations of Al to be sequestered from Al-organic complexes by the resin.

A series of aged Al-hydroxy polymer solutions were also analysed, to determine whether aluminium-polymeric species (*e.g.* $Al_{13}(OH)_{32}^{7+}$) were quantified by the experimental protocol. The polymer solutions were initially analysed using a fast reaction with CAS (*ca.* 60 s) in an FIA manifold. The $Al_{13}(OH)_{32}^{7+}$ species does not react with CAS at *ca.* pH 5 on the FIA time-scale (Öhman and Powell unpublished), and so only the monomeric Al-hydroxy species ('free Al') are quantified. The FIA manifold used was identical to that used for the Prosep resin protocol, except that the micro-column was removed, and the 2 M acetate buffer was adjusted to pH 5.3. Good agreement was obtained between the results of these analyses and those from the Prosep resin analyses (Table 9.2).

Table 9.2. Concentrations of 'free Al' (μM) determined in hydrolysed Al solutions by the CAS and Prosep methods. Results for the solutions containing 100 μM Al are for solutions diluted 1:10 before analysis.

Sample	pH	CAS	Prosep
1[A]	4.60	12.4	11.6
4[A]	4.89	9.5	9.9
6[A]	4.95	8.8	8.2
8[A]	5.03	8.0	8.4
11[A]	5.54	1.3	1.3
2[B]	4.79	6.8	6.6
7[B]	5.00	4.3	4.1
9[B]	5.07	3.0	3.1
10[B]	4.98	3.2	3.8

[A] Total [Al] = 10 μM

[B] Total [Al] = 100 μM

The concentrations of 'free Al' measured in the hydrolysed Al solutions using the Prosep method were compared with the sum of the $[Al^{3+}] + [Al(OH)^{2+}] + [Al(OH)_2^{+}]$ concentrations, calculated from a thermodynamic Al-hydrolysis model by using SOLGASWATER (Figure 9.7) (Al hydrolysis constants are given in Section 2.2.9).

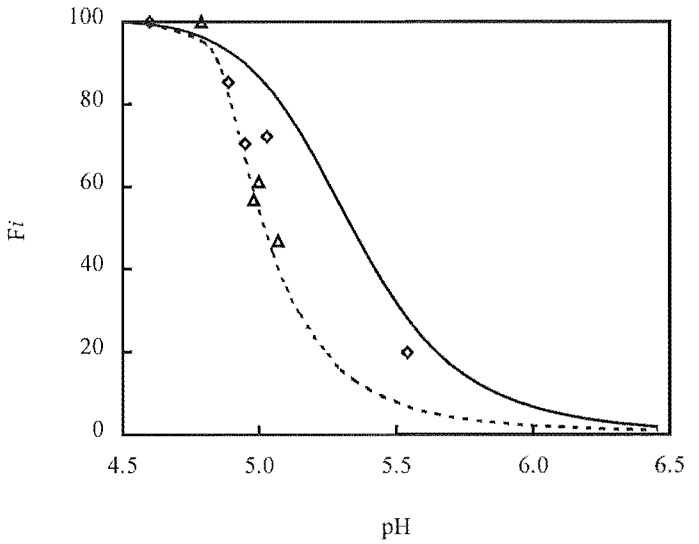

Figure 9.7. The fraction of Al measured in hydrolysed solutions containing 10 (◇) and 100 (△) μM Al. The curves indicate $\Sigma([Al^{3+}] + [Al(OH)^{2+}] + [Al(OH)_2^{+}])$ and were calculated from thermodynamic Al hydrolysis models using the computer program SOLGASWATER (solid curve = 10 μM Al; dotted curve = 100 μM Al).

9.3.3 Sample analyses

Three humic water samples were analysed using the Prosep method, and the results compared with those obtained using the oxine-derivatised Fractogel method. There was good agreement between the concentrations of 'free Al' determined by the two methods (Table 9.3). The Prosep method gave higher concentrations for the 'organic-bound Al' fraction, compared with the concentrations determined by the oxine-derivatised Fractogel method.

The concentration of Al was also determined in four soil sample extracts (0.02 M $CaCl_2$). The concentration of Al in these extracts was sufficiently high to require dilution (10-50-fold) of the samples before analysis. In addition to analysing the samples using the Prosep resin, the fast (*ca.* 60 s) FIA reaction with CAS described above was used to determine the concentration of a 'reactive Al' fraction. Total Al was determined by ETAAS. Analysis results are given in Table 9.4.

Table 9.3. Concentrations of Al (μM) in humic water samples obtained using the Prosep and oxine-derivatised Fractogel methods.

Sample	pH	Prosep		Oxine-Fractogel	
		'org.-bound'	'free Al'	'org.-bound'	'free Al'
Ianthe Rd. Bridge	5.18	7.7	1.5	5.9	1.3
Unnamed Creek	4.82	9.2	1.4	7.2	1.3
Duffer's Creek	4.86	7.0	1.1	5.3	1.0

Table 9.4. Concentration of Al (μM) in 0.02 M $CaCl_2$ extracts of soils from the Cragieburn Range, N.Z.

Sample	Prosep	CAS	ETAAS
	'free Al'	'reactive Al'	'total Al'
CP forest	275	390	616
CP grassland	153	197	329
CF forest	82	102	188
CP grassland	27	41	103

9.4 DISCUSSION

9.4.1 Experimental optimisation

A two minute stopped-flow elution protocol was successfully used to remove captured 'free Al' from the Prosep resin. It is estimated that a throughput of *ca.* 7 samples per hour is possible. The RSD of 2.0% at 10 μM Al shows that adequate precision can be obtained by this method, even though the stopped-flow FIA elution protocol requires a relatively large amount of manipulation (and hence potential error) by the operator. This includes switching the column off-line, filling the injection loop with the eluent for a determined period, and switching the column back on-line. The estimated linear working range (1.0-25 μM Al) could be extended to lower concentrations by reducing the height of the blank (*e.g.* by further optimisation of the buffering within the FIA manifold). However, for the purposes of this

work, which was solely to investigate the potential of the Prosep resin for Al analyses, such refinement was deemed unnecessary.

The Prosep resin was able to sequester Al from standards containing up to 0.25 M KCl, without loss of sensitivity. At concentrations above this, peak height decreased (Figure 9.5). Although the loss in sensitivity for high ionic strength matrices will decrease the linear working range of the method, the decrease is relatively small. Therefore, provided a calibration is performed with standards matching the ionic strength of the samples, the Prosep resin appears suitable for use with samples of high ionic strength. Other workers (Greenway *et al.* 1996*b*; Nelms *et al.* 1996) found calibrations prepared from pure water and seawater matrices were comparable in terms of sensitivity.

Al breakthrough was observed for samples containing high concentrations of KCl. This would cause a significant contribution to the apparent concentration of 'organic-bound Al' for a sample containing aluminium bound to natural organic matter. The amount of breakthrough could possibly be subtracted from the 'organic-bound Al' peak by using data from the calibration scan, but such a correction could lead to further errors and should be attempted with caution.

9.4.2 Method validation

To be suitable as a method for determining 'free Al' ($[Al^{3+}] + [Al(OH)^{2+}] + [Al(OH)_2^{+}]$), it is important that the Prosep resin does not capture significant amounts of Al bound to ligands such as natural organic matter. To establish whether there was a likelihood for the resin to sequester aluminium, Al-oxalate model-ligand solutions were prepared and analysed (Figure 9.6). Good agreement was obtained between the calculated curve for the 'free Al' species and the experimental data. This indicates negligible amounts of Al were sequestered from Al-oxalate complexes by the Prosep resin. Further experiments could be considered to establish whether Al might be sequestered from organic complexes of lower stability than the Al-oxalate system (*e.g.* Al-malonate system). In addition, further work is required to determine whether Al is sequestered from inorganic aluminium species (fluoride and sulfate complexes).

Concentrations of 'free Al' determined in the hydrolysed Al solutions using the Prosep method and a fast (*ca.* 60 s) CAS method were in excellent agreement (Table 9.2). This indicates that only the monomeric 'free Al' species are quantified using the column, and polymeric Al-hydroxy species are not detected. As observed for the model-ligand oxalate

solutions, there was generally good agreement between the experimental data and the sum of the concentrations of the 'free Al' species ($[Al^{3+}] + [Al(OH)^{2+}] + [Al(OH)_2^{+}]$) calculated from an Al-hydrolysis model.

9.4.3 Sample analyses

Good agreement was obtained for 'free Al' analyses of the humic water samples, when comparing the Prosep and oxine-derivatised Fractogel methods (Table 9.3). The concentrations of organic-bound Al were high (> 5 μM), reflecting the acidic pH and high concentration of organic matter in these waters. Higher concentrations of the operationally-defined 'organic-bound Al' fraction were obtained from the Prosep method than from the oxine-derivatised Fractogel method, despite both methods having a similar contact time between the sample and CAS.

This difference in concentrations is caused by differences in the design of the two manifolds (compare Figure 2.1 with Figure 9.1). In the Prosep method, the buffer stream merges with the sample and is mixed before addition of the CAS, whereas in the oxine-derivatised Fractogel method, the CAS is initially buffered before being merged with the sample. Furthermore, the higher pH of the buffer used in the Prosep manifold (pH 6.0 *vs.* 5.3) will increase the rate of reaction between Al and CAS (Hawke and Powell 1994). However, given the recognised operationally-defined nature of the 'organic-bound Al' fraction, the difference between the two methods is not of consequence.

Results from the analysis of the soil sample extracts from four sites in the Cragieburn Range are given in Table 9.4. Samples were diluted immediately prior to analysis, to minimise any change in the speciation of Al. The concentrations of 'reactive Al' determined using a *ca.* 60 s reaction with CAS were, on average, 26% higher than concentrations of 'free Al' determined using the Prosep method. This difference in concentrations is attributed to the presence of Al-organic complexes. These will react significantly with CAS during the *ca.* 60 s time-scale of the FIA experiment (Hawke and Powell 1994), but are not quantified as 'free Al' by the Prosep resin. Total Al concentrations determined by ETAAS were, in turn, greater than the CAS 'reactive Al'. This difference in concentration can be attributed to the presence of stronger Al-organic complexes, which will not react with CAS within the 60 s time-scale of the FIA experiment, but which are quantified by ETAAS.

A second possibility for the higher ETAAS determinations is the presence of polymeric Al species (*e.g.* $Al_{13}(OH)_{32}^{7+}$ - 'Al_{13}') in the extracts. The soils from the Cragieburn sites have relatively high exchangeable concentrations of Al, and pH > *ca.* 5.0 (Chapter 5), conditions which could favour the formation of polymeric aluminium species. However, although a large amount of evidence strongly suggests the formation of the Al_{13} polymer occurs in synthetic solution (Section 1.1.1), the question of whether this species exists in soil and/or soil solution is contentious.

Previous attempts to detect polymeric Al species in soil solution from these Cragieburn sites (using an alkali stopped-flow elution protocol with the oxine-derivatised Fractogel method) were unsuccessful (Nilsson and Adams; unpublished results). It is therefore most unlikely that Al polymeric species contribute to the higher concentrations of Al measured in the soil extracts by ETAAS.

9.5 CONCLUSION

An analytical method to fractionate 'free Al' ($[Al^{3+}] + [Al(OH)^{2+}] + [Al(OH)_2^{+}]$) from natural samples was successfully developed using a commercially available iminodiacetate-CPG resin (Prosep). The method was validated by comparison of the experimentally determined concentrations of 'free Al' with concentrations of 'free Al' calculated from the thermodynamic equilibrium models for Al-oxalate and hydrolysed Al solutions. The results indicated that Prosep did not significantly sequester Al from either oxalate or polymeric Al species. In addition, good agreement was observed between concentrations of 'free Al' determined by the Prosep method and those obtained from other analytical methods, for hydrolysed Al and humic water samples.

Significant advantages of this technique include the ability to analyse solutions of high ionic strength, which may be unsuitable for analysis by other methods (*e.g.* the oxine-derivatised Fractogel method). However, the concentrations of Al obtained from soil sample extractions (typically using 1 M KCl or 0.02 M $CaCl_2$) will generally be far higher than the linear working range of the technique, and large sample dilutions may therefore be required. Such dilutions will decrease sample ionic strength, negating one of the potential advantages of the method.

Further work is required to investigate the interaction between Prosep and polymeric Al hydrolysis products (*e.g.* Al_{13}). Although experimental results indicated that Al_{13} was not quantified as part of the 'free Al' fraction, the fate of such species remains unclear. The Al_{13} species does not react with CAS on the time-scale of the FIA reaction (Öhman and Powell unpublished), and therefore if it passes directly through the chelating resin without retention, it will not contribute to a signal at the detector. Similarly, should it be retained on the resin, and eluted by the stopped-flow protocol without decomposition (depolymerisation) to monomeric Al species, the Al_{13} again will not be detected. It is unlikely however, that Al_{13} species will be present in soil solutions. The interaction of Prosep with inorganic Al species (particularly fluoride and sulfate complexes) requires study, to establish whether such complexes are determined as part of the 'free Al' fraction.

CHAPTER 10

SOLUTION EQUILIBRIUM STUDIES

10.1 INTRODUCTION

10.1.1 Thermodynamic treatment of solution equilibria

Many analytical methods for Al analysis have been developed to explore possible correlations between 'reactive Al' fractions and observed biological toxicity. In order to understand the specific toxicity of Al in any biological system, a knowledge of the aluminium speciation is required. The complete characterisation of an aquatic trace metal system, in terms of its chemical speciation, can be attempted in two significantly different ways (Öhman and Sjöberg 1996). The first approach involves the use of physio-chemical analytical procedures to target specific fractions of Al *e.g.* 'labile monomeric' or 'free Al' (Section 1.4.2). There are several disadvantages with such techniques. Many fractionation schemes are operationally-defined and comparison of results obtained from different methods is difficult, as it is often not clear which specific chemical species are quantified. Samples can also undergo re-equilibration during chemical or physical fractionation processes, which may lead to changes in speciation occurring.

An alternative theoretical approach uses thermodynamic data, together with the measured 'free' or total concentrations of components, to calculate the equilibrium concentrations (or activities) of species in a system. A major advantage of computer speciation modelling is that it has the ability to be predictive *i.e.* in addition to calculating the current speciation of an actual system, the consequences of a change in the input composition can be established. However, the assumption of chemical equilibrium will not be valid for many environmental systems, particularly those where extensive dissolution, precipitation or redox processes occur. Computer speciation modelling is also reliant upon the accuracy of the thermodynamic data used. In addition, identifying all significant components in natural systems (especially organic ligands) is difficult.

Complex formation may be described by a generalised reaction (Equation 10.1). An equilibrium (or stability) constant K may be defined for this system, where the activities of all species are raised to the power of their stoichiometric coefficients (Equation 10.2).

$$aA + bB \rightleftharpoons cC + dD \qquad (10.1)$$

$$K = \frac{\{C\}^c \{D\}^d}{\{A\}^a \{B\}^b} \qquad (10.2)$$

In practice, a concentration-dependent equilibrium constant *K*, is determined. This constant is related to the equilibrium constant K by an activity term Q_γ (Equation 10.3).

$$K = \frac{\{C\}^c \{D\}^d}{\{C\}^a \{D\}^b} = \frac{[C]^c [D]^d}{[A]^a [B]^b} \frac{\gamma_c \gamma_d}{\gamma_a \gamma_b} = K Q_\gamma \qquad (10.3)$$

The activity coefficient (γ) relates the activity of each species to its concentration (Equation 10.4). In most circumstances values of γ are less than 1, and only in infinitely dilute solutions will the activity of a species equal its concentration.

$$\{A\} = \gamma [A] \qquad (10.4)$$

For any given ion in solution, there will be an excess of counter ions surrounding it (Atkins 1990). This leads to a decrease in the effective ion activity as ionic strength increases. Any variation in the activity of species will alter the measured value of the concentration-dependent equilibrium constant. It follows that determination of equilibrium constants in solutions of low ionic strength will be very difficult, as changes in solution composition will affect the activity coefficients of all species.

In practice, concentration-dependent equilibrium constants are determined using a constant ionic medium. This method relies on the principle that for a solution having a constant and high ionic strength (at least *ca.* 100 times greater than that of the reacting species), the formation or disappearance of various species will have a negligible effect on the ionic strength (and hence also a negligible effect on the activity coefficients). The value of the concentration-dependent equilibrium constant will therefore be constant, providing the term describing ion or molecule activity (Q_γ) remains constant under experimental conditions.

Unfortunately, this approach to determining equilibrium constants has a major drawback. The resulting concentration-dependent equilibrium constants are only valid for the ionic medium

in which they were determined. This is caused by the activity term Q_γ being a function of the supporting electrolyte. Medium-independent activity-based equilibrium constants may only be obtained by determining concentration-dependent constants at a variety of ionic strengths, and extrapolating to infinite dilution.

Cumulative formation constants were used in this work to describe the equilibria between protons, Al^{3+}, and ligands. Complexation reactions between the components of the system are described by Equation 10.5. The pqr formalism can be conveniently used to represent the range of reactions that occur in solution (*i.e.* metal-ligand complexation, metal ion hydrolysis, ligand deprotonation and hydrolysis of complexes to formed mixed hydroxo-metal-ligand species).

$$pH^+ + qAl^{3+} + rH_3L^0 \rightleftharpoons H_pAl_q(H_3L)_r^{(p+3q-3r)+} \qquad (10.5)$$

The concentration-dependent formation constant (β_{pqr}) for this system is defined in Equation 10.6.

$$\beta_{pqr} = \frac{[H_p\ Al_q\ H_3L^{(p+3q-3r)+}]}{[H^+]^p\ [Al^{3+}]^q\ [H_3L^0]^r} \qquad (10.6)$$

10.1.2 Ligands investigated in this work

(*i*) *Histidine*

An initial potentiometric study was performed on the $H^+/Cu^{2+}/L^-$-histidine system. The protonation and metal stability constants of this particular system have been critically reviewed by the International Union of Pure and Applied Chemistry (IUPAC) (Pettit 1984). The recommended constants contained within this review therefore allow researchers to test the experimental and computational validity of their own work.

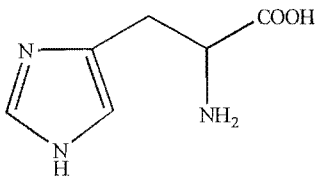

Figure 10.1. Structural formula of histidine.

(ii) Caffeic and chlorogenic acids

The bioavailability to plants of metal ions is influenced by the natural organic complexing agents which may be present in soils. Phenolic compounds are of special interest, as they tend to be exuded by the roots of certain plants which are subject to conditions in which the availability of iron is adversely affected. From this it may be inferred that such species may participate in the transport processes of metal ions from the surrounding soil to the plant roots. Of special interest is caffeic acid (*trans*-3-(3,4-dihydroxy-phenyl)-propenoic acid) (Figure 10.2) which has been identified as an important phenolic compound in the transport of Fe^{III} and the reduction to Fe^{II} in the soil environment (Olsen *et al.* 1982; Römheld and Marschner 1983). Another is chlorogenic acid (1,3,4,5-tetrahydroxy-cyclohexanecarboxylic acid (3,4-dihydroxycinnamate)) (Figure 10.3) which is an important factor in plant metabolism (Lamy *et al.* 1985) and a precursor of caffeic acid. These two species may also form complexes with other metal ions that occur in nutrient and soil solutions (Linder *et al.* 1990).

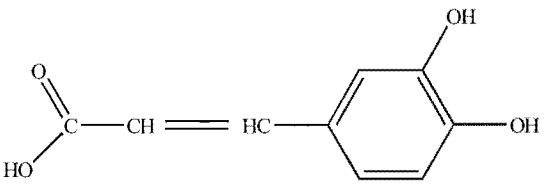

Figure 10.2. Structural formula of caffeic acid.

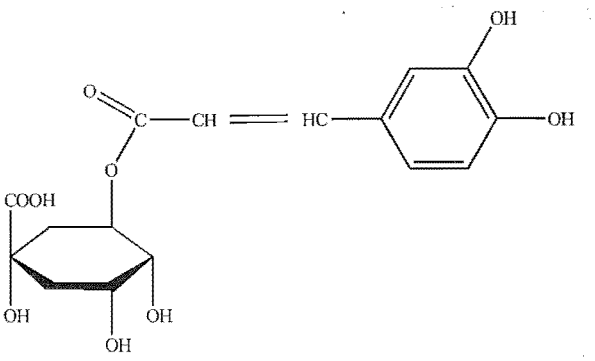

Figure 10.3. Structural formula of chlorogenic acid.

In addition, caffeic and chlorogenic acids have both been identified as exudates from living leaves and roots of *Hieracium pilosella* and *H. praealtum* species (Makepeace *et al.* 1985). These authors noted an apparent allelopathic effect on seed germination and root growth of grassland species when exposed to leachates from *Hieracium* plant matter. It has also been postulated that the exudation of polyphenolic compounds in poor acidic soils may provide

plants with a competitive advantage, by immobilising (*i.e.* complexing toxic free Al^{3+}) or monopolising soil nitrogen and trace elements (Northup *et al.* 1995; Northup *et al.* 1998).

Stability constants for caffeic and chlorogenic acids and various divalent metal ions have previously been reported by several workers (Timberlake 1959; Lamy *et al.* 1985; Linder and Voyé 1987; Kiss *et al.* 1989; Cocks *et al.* 1992; Améziane *et al.* 1996). There is however, no reliable thermodynamic data for these two organic compounds with aluminium. In this work, the solution equilibria between Al and (*i*) caffeic and (*ii*) chlorogenic acids have been studied by potentiometric and spectrophotometric titration in aqueous solution (I = 0.10 M KCl, 25.0°C). Concentration-dependent formation constants for the two systems are reported.

10.2 EXPERIMENTAL

10.2.1 Purity of ligands

L-histidine (L-α-amino-β-imidazolepropionic acid), caffeic acid (trans-3-(3,4-dihydroxy-phenyl)propenoic acid) and chlorogenic acid (1,3,4,5-tetrahydroxycyclohexanecarboxylic acid 3-(3,4-dihydroxycinnamate)) samples were obtained from Sigma. All ligands were dried under vacuum to constant weight before use, and stored in the dark at room temperature. Table 10.1 gives the microanalysis results for each sample (elemental analyses performed at the Campbell Microanalytical Laboratory, University of Otago, New Zealand).

Table 10.1. Microanalysis results.

Ligand	Formula	Carbon %		Hydrogen %		Nitrogen %	
		obs.	calc.	obs.	calc.	obs.	calc.
L-histidine	$C_6H_9O_2N_3$	46.66	46.45	6.08	5.85	26.83	27.08
caffeic acid	$C_9H_8O_4$	60.14	60.00	4.55	4.48	-	-
chlorogenic acid	$C_{16}H_{18}O_9$	53.41	54.24	5.30	5.12	-	-

Satisfactory agreement between observed and calculated results was obtained for the samples of L-histidine and caffeic acid. Chlorogenic acid exhibited a slight difference between observed and calculated values for carbon. This difference however, corresponds to less than half a water of crystallisation and was not considered significant. ^{13}C NMR analyses (Chemistry Department, University of Canterbury) on caffeic and chlorogenic acid samples

showed the expected number of non-equivalent carbons. Excellent agreement was observed between these spectra and reference spectra contained in Pouchert and Behnke (1993). On the basis of these analyses all ligands were used as received, without further purification.

10.2.2 Electrolyte

KCl (BDH AnalaR) was oven-dried (24 hours, 110°C) before storing in a desiccator over anhydrous silica gel. Sufficient dry KCl was added directly to all working and titration solutions to give an ionic strength of 0.10 M.

10.2.3 Preparation of Zn/Hg-V^{2+} oxygen scrubber

Trace amounts of oxygen in the commercial nitrogen gas were removed by bubbling the gas through an acidic vanadium(II) solution, prepared by the reduction of a vanadyl sulfate solution by zinc amalgam (Russell 1977).

A zinc amalgam was prepared by stirring a 2% mercuric chloride solution with zinc pellets for 10 minutes. The amalgam was rinsed three times with triply-distilled water (TDW). A $VOSO_4$ solution was prepared by dissolving 2.5 g $VOSO_4.2H_2O$ (BDH laboratory reagent) in TDW. Concentrated H_2SO_4 (7 mL, BDH AnalaR) was added and the mixture diluted to 250 mL. The amalgam was placed in a gas bottle and covered with the acidic $VOSO_4$ solution. On bubbling N_2 through the zinc amalgam/$VOSO_4$ the colour of the solution was observed to change from blue (VO^{2+}) to green (V^{3+}) to violet (V^{2+}).

10.2.4 Standard Alkali

Standard alkali solutions (approx. 0.25 to 0.35 M) were prepared from KOH pellets (BDH AnalaR). CO_2-free water was prepared by boiling milli-Q® water for *ca.* 25 minutes, before cooling in an ice-bath under oxygen-free nitrogen (BOC Gases, Christchurch). This water was used to rapidly rinse a 2.5-fold excess of KOH pellets to remove any possible carbonate coatings. The first two pellet rinsings were discarded. The remainder of the pellets were dissolved and made up to the appropriate volume with the CO_2-free milli-Q® water. All alkali solutions were stored sealed in plastic under oxygen-free nitrogen. Alkali solutions were standardised by acid-base titration against weighed amounts of the primary standard tris[hydroxymethyl]aminomethane hydrochloride (Trizma® hydrochloride) (SigmaUltra >99% Sigma). Acid solutions were standardised potentiometrically against this alkali. Solutions of

alkali were periodically re-standardised to check for evidence of CO_2 contamination. Fresh alkali solutions were prepared approximately every 4 to 6 weeks.

10.2.5 Ligand Solutions

Ligand solutions were prepared in milli-Q® water with a known amount of standardised HCl (BDH AnalaR) added to prevent ligand oxidiation. Sufficient dry KCl was added to give a total ionic strength of 0.10 M. Solutions of caffeic acid required slight warming for the solid to fully dissolve.

10.2.6 Metal Solutions

The concentration of a previously prepared copper stock solution ($Cu(NO_3)_2.3H_2O$) (BDH AnalaR) in 1 mM HCl (BDH 0.2 N, convol); O'Sullivan (1997)); was re-standardised gravimetrically as the benzoin-α-oximate (cupron) using the method of Vogel (1961) (Appendix I). An acidified aluminium stock solution was prepared as described in (Section 2.1.5), and standardised gravimetrically as the oxinate (Vogel 1961) (Appendix I). The content of Al^{3+} was found to be within 1% of the weighed amount. Excess acidity was determined by titration against standard alkali, using the method of Gran (1952) for endpoint determination. All metal solutions were stored in the dark at 25°C.

10.2.7 Titration Equipment

All titrations were performed in an air-tight water-jacketed glass titration cell (volume *ca.* 120 mL) fitted with a glass lid and sealed by means of ground-glass flanges (Figure 10.4). The titration cell was placed on a magnetic stirrer, with a Teflon-coated magnetic bar used for solution stirring. Two large ground-glass ports located in the lid accommodated the glass-bulb and reference electrodes; smaller ports were used to accommodate the nitrogen gas line and autoburette tip. Water was continuously circulated through the titration cell from a thermostatted water bath (25 ± 0.1°C), with the entire titration assembly being situated in a temperature-controlled room (25 ± 1.5°C).

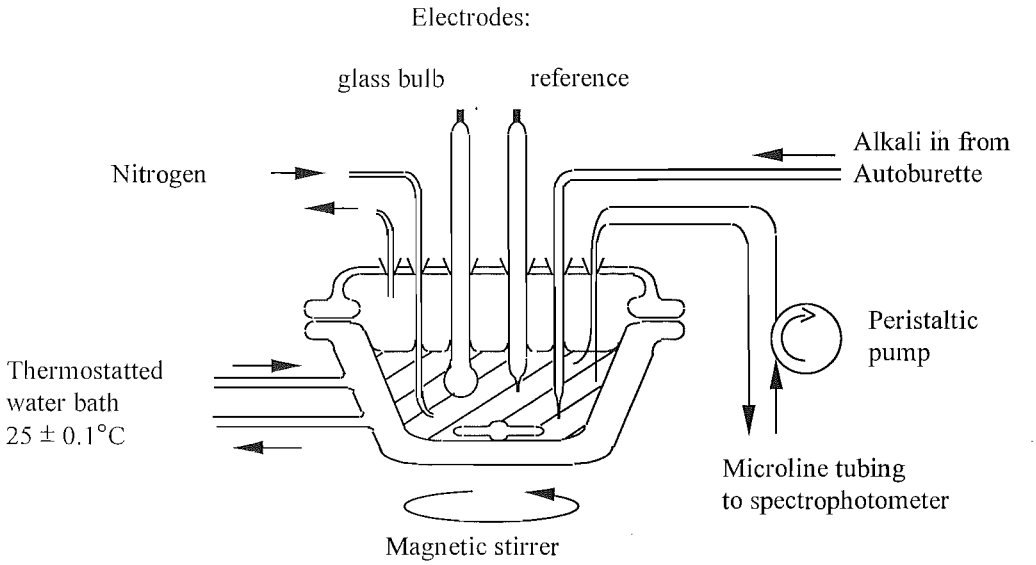

Figure 10.4. Titration apparatus. The tubing to the spectrophotometer was only present for spectrophotometric experiments (from O'Sullivan 1997).

Oxygen-free nitrogen gas was initially bubbled under the surface of the titration solution for *ca.* 120 minutes, and continuously maintained over the surface of the solution for the duration of the titration to prevent the intrusion of oxygen and CO_2 into the titration cell. The gas was initially bubbled through a solution of 0.1 M KOH (to remove trace amounts of CO_2 and acidic impurities) and then passed through a Zn/Hg-V^{2+} oxygen scrubber (Section 10.2.3). Finally, the gas was passed through a solution of 0.1 M KCl, ensuring constant gas humidity. A three-way tap was fitted to the gas supply line allowing gas to be directed either under or over the surface of the titration solution.

Additions of alkali were made using a ABU80 autoburette (Radiometer, Copenhagen). A small length of 0.51 mm i.d. microline™ tubing (Cole-Parmer) was fitted to the end of the glass autoburette tip to minimise diffusion of alkali into the bulk titration solution. pH was determined using a PHM64 pH meter (Radiometer, Copenhagen). Both the autoburette and pH meter were computer-controlled (PC, 08086), using software written within the Chemistry Department. The software allowed control of alkali aliquots, equilibration times and pH measurement. A Russell SWR757 glass bulb electrode was used to measure pH, in combination with a home-built saturated calomel reference electrode (SCE). This had an outer sleeve filled with 0.1 M KCl, preventing the saturated KCl contained in the inner sleeve from coming into contact with the titration solution.

10.2.8 Equilibration

Equilibration conditions, and detection of pH 'drift' or 'noise', were computer-controlled. The system was considered to be at equilibrium after a series of consecutive pH measurements agreed within a specified 'drift limit'. All titration solutions were equilibrated after every addition of alkali. A 1 minute equilibration time was used for titrations not involving Al (*e.g.* ligand protonation titrations). A 20 minute equilibration time was used for titrations involving Al.

After the specified equilibration period, solution pH was measured by the computer, with 20 successive readings taken 1 second apart. A second series of pH measurements were taken after a specified delay time of 10 seconds (or 5 minutes in the presence of Al). If the pH measurements did not agree to within 0.003 pH units, then 'drift' was deemed to be present and the datum point was flagged for later exclusion from equilibrium constant calculations. If readings did not agree to within 0.002 pH in any single pH sweep, then 'noise' was considered to be present, and again the datum point was flagged.

10.2.9 Electrode Calibration

The electrode calibration was performed by titration of standard alkali against strong acid (*ca.* 0.005 M HCl). The acidic calibrant solution was prepared to have an ionic strength of 0.10 M. The titration endpoint was determined using the method of Gran (1952), and the concentration of $[H^+]$ was subsequently calculated at each datum point. Plots of observed $p[H^+]$ *versus* calculated $p[H^+]$ were linear ($r^2 > 0.99999$ or greater, *ca.* 20 datum points) over pH ranges *ca.* 2.5 to 3.4 and 9.9 to 10.8. Calibrations were performed before and after titrations to allow correction for any change in electrode performance with time. Shifts in electrode calibration were assumed to be linear with time over the course of a titration. References to pH in this work therefore refer to $p[H^+]$, the negative logarithm of the hydrogen ion *concentration*, and not to the negative logarithm of the hydrogen ion *activity*.

10.2.10Spectrophotometric titrations

Spectrophotometric titrations were performed using caffeic and chlorogenic acids to determine the protonation constant for the most basic oxygen (K_1). Two 0.56 mm i.d. Teflon™ tubes (Cole Parmer) were passed into the titration cell through a bored rubber stopper fitted into a large ground-glass port in the glass lid of the titration cell. An Alitea XV peristaltic pump was used to circulate the titration solution from the cell through the Teflon™ tubing to a

70 μL flow-cell. Spectrophotometric measurements were obtained with a Hewlett-Packard HP8452a diode-array UV-VIS spectrophotometer using the Hewlett-Packard software supplied with the instrument.

In order to obtain a pH >12 for these experiments, a concentrated solution of alkali (*ca.* 3 M KOH) was prepared using CO_2-free Milli-Q® water. This solution was standardised against Trizma® hydrochloride as described above. The autoburette was controlled manually for these experiments. The titration solution initially contained *ca.* 50 μM ligand, in 0.1 M KCl. For these titrations at high pH, solutions were initially deoxygenated by bubbling the de-oxygenated nitrogen under the surface (180 minutes). Nitrogen was subsequently passed over the solution surface for the duration of the titration. To minimise oxidation of the deprotonated *o*-diphenolic ligand, rapid titrations were performed. After each addition of concentrated alkali, the titration solution was mixed for 20 seconds. The solution was subsequently pumped through the spectrophotometric flow-cell for 40 seconds, before the spectrum was recorded. After switching the pump off a further addition of alkali was made. With this method *ca.* 8 wavelength scans were obtained for each titration, over a pH range of *ca.* 10.6 to 13.4 for each ligand.

10.2.11 Numerical analyses

(*i*) *Potentiometric determination of stability constants*

Potentiometry refers to the investigation of equilibrium systems *via* the use of electrode potential data. The glass bulb electrode gives a linear Nernstian response to hydrogen ion activity, and is commonly used to obtain potentiometric data. The response of this electrode may be related to the hydrogen ion concentration if the activity coefficient of the hydrogen ion remains constant throughout a titration. In practice this is achieved by the use of a supporting electrolyte, having a constant, high ionic strength relative to the concentrations of the various equilibrium system components.

For the glass bulb electrode, reliable pH measurements are effectively limited to a working range of pH 2.4-10.5. At low pH the concentration of the free hydrogen ion is high (pH 1.5 = 0.032 M H^+), and the approximation of a constant activity coefficient for this ion is no longer valid. In addition, the large concentration gradient across the junction between the filling solution of the reference electrode and the titration solution produces a measurable liquid junction potential. This causes the electrode response to deviate from the ideal linear

Nernstian behaviour. At high pH the low concentration of H^+ in solution renders the electrode susceptible to interference from the alkali cations (*e.g.* Na^+, K^+). As these ions are commonly used as the supporting electrolyte, electrode interference at high pH can be severe.

The non-linear least squares computer modelling program SUPERQUAD (Gans *et al.* 1985) was used to determine refined values of the cumulative formation constants (β_{pqr}) from measured potentiometric data. This program determines formation constants by minimisation of an error-square sum based on the calculated and observed electrode potential (pH^+) values (Equation 10.7).

$$U = \Sigma w \left([H^+]^{obs} - [H^+]^{calc} \right)^2 \qquad (10.7)$$

The program applies a weight (w) at each measured titration point, inversely proportional to the variance at that point.

$$w = \left[\left(\frac{\partial E^{obs}}{\partial V} \right)^2 \sigma_V^2 + \sigma_E^2 \right]^{-1} \qquad (10.8)$$

The weights are calculated from the estimated standard deviations in titration volume (σ_V) and EMF (σ_E). The estimate of the slope of the titration curve, $\partial E/\partial V$, is obtained from the titration data, using a first-derivative cubic function. Electrode readings in the region of an end-point are commonly regarded as unreliable, as a small titrant error can have a large effect on the electrode potential. However, using this weighting method, data that occur near an endpoint, where values of $\partial E/\partial V$ are large, are given less weight than other data, thus minimising possible errors. Clearly however, potentiometric work requires careful experimental technique to obtain reliable measurements of $[H^+]$ that are of high precision and accuracy (Öhman and Sjöberg 1996).

(ii) Z_c curves

Experimental data are commonly visualised by the use of Z curves. The function Z gives the average number of protons (or OH^-) bound *per* metal (B), (Z_b), or ligand C (Z_c). For Z_c curves calculated in this work, each titration curve starts at acidic pH with a Z_c value of 3, which corresponds to the protonated ligand H_3L. As the pH increases, the value of Z_c decreases, as ligand deprotonation and aluminium-ligand complexation reactions proceed. Values of Z_c may be calculated from experimental data according to Equation 10.9. Z_c may also be calculated from the refined stability constants over the desired pH range, by using the program SOLGASWATER. Comparison of the experimental and calculated values of Z_c allows the fit

of a proposed model to be inspected visually. Furthermore, the presence of mixed hydroxy metal-ligand species is indicated if the value of Z_c exceeds n in H_nL.

$$Z_c = \frac{H - h + K_w\, h^{-1}}{L_T} \qquad (10.9)$$

where H = total acidity (M)
h = free acidity (M)
K_w = water hydrolysis constant (M^2)
L_T = total ligand concentration (M).

(*iii*) *Spectrophotometric determination of stability constants*

If one, or more of the species in a titration system forms a differently coloured species during the course of a reaction, the solution equilibria may be monitored spectrophotometrically. A widely-used graphical approach to the determination of equilibrium constants from spectrophotometric data was introduced by Ågren (1955), who applied the method to determine protonation constants for a variety of phenolic species. Such an approach is important, as K_1 for a polyphenol will be outside the range for reliable measurement. An equilibrium system for the determination of K_1 may be described by Equations 10.10-10.13. Ågren combined these equations to give a linear relationship (Equation 10.14), from which a value of K may be calculated if the appropriate variables are plotted. Under certain conditions, Ågren's method can also be extended to allow its application to metal-ligand complexation equilibria.

Reaction $$HL^{2-} \rightleftharpoons L^{3-} + H^+ \qquad (10.10)$$

Mass Balance $$T_L = [HL^{2-}] + L^{3-} \qquad (10.11)$$

Equilibrium constant $$K_1 = \frac{[H^+][L^{3-}]}{[HL^{2-}]} \qquad (10.12)$$

Beer-Lambert Law $$A = \varepsilon_{HL^{2-}}[HL^{2-}] + \varepsilon_{L^{3-}}[L^{3-}] \qquad (10.13)$$

where ε_n = molar absorptivity of species n. The pathlength l is taken as unity.

$$\frac{T_L}{A} = \frac{1}{K\varepsilon_{L^{3-}}}\left([H]\frac{A-\varepsilon_{HL^{2-}}T_L}{A}\right) + \frac{1}{\varepsilon_{L^{3-}}} \qquad (10.14)$$

$$y = m \quad x + c$$

However, Ågren's method is not applicable to spectrophotometric data obtained at high pH, as the ionic strength of the titration solution (and hence values of K) do not remain constant. The approach used in this work was based on that described by Kennedy (1984).

Individual values of K_1 were calculated from spectrophotometric data, using the equilibrium expression given in Equation 10.15.

$$K_1 = \frac{[HL^{2-}]}{[H^+][L^{3-}]} \qquad (10.15)$$

For the spectrophotometric titrations the solution pH was higher than could be reliably measured with a glass bulb electrode. As the pH was high and the concentration of ligand low (*ca.* 50 μM), values of $[H^+]$ were calculated from the hydrolysis constant of water and the hydroxide ion concentration arising from the incremental additions of standard alkali (Equations 10.16 and 10.17).

$$pH = pK_w + \log [OH^-] \qquad (10.16)$$

$$[OH^-] = \frac{[alkali]\times[titre]}{\text{total volume}} - 2[T_L] - [\text{initial } H^+] \qquad (10.17)$$

Values of pK_w at each ionic strength were calculated using the empirical relationship given by Harned and Owen (1958) (Appendix IV).

Values of $[L^{3-}]$ were calculated from Equation 10.18, which was derived from the mass balance equation and the Beer-Lambert Law (Equations 10.11 and 10.13, respectively).

$$[L^{3-}] = \frac{Abs - (\varepsilon_{HL^{2-}} \times [T_L])}{(\varepsilon_{L^{3-}} - \varepsilon_{HL^{2-}})} \qquad (10.18)$$

Using the result of Equation 10.18 and the calculated value of $[H^+]$, the value of $[HL^{2-}]$ was calculated from the mass balance equation (Equation 10.11), and a value of log K_1 obtained.

The individual log K_1 values were plotted *vs.* $\left(\frac{I^{0.5}}{(1 + I^{0.5})}\right)$ and the resultant line through these points was extrapolated to give a value of K_1 valid for an ionic strength of 0.1 M.

10.3 RESULTS

10.3.1 Potentiometry of the H^+-Cu^{2+}-histidine (L^-) system

The protonation constants of L-histidine were determined from two titrations for which the ligand concentration was varied 2.0 - 2.8 mM (61 datum points). Complex formation with Cu^{2+} was investigated by performing two titrations (1.9 and 1.0 mM Cu^{2+}) at stoichiometric metal to ligand ratios of 1:1.4, and 1:2.1, respectively (106 datum points). The program SUPERQUAD was used to calculate refined values of the cumulative formation constants β_{pqr}. These values, and the values recommended by the IUPAC critical review (Pettit 1984) are given in Table 10.2. Good agreement was obtained between the formation constant values determined in this work, and the IUPAC recommended values. A closer fit to the recommended stability constants might have been obtained by increasing the size of the data set and by extending the number of titrations with additional metal to ligand ratios. However this was judged unnecessary, as the purpose of these experiments was only to confirm the acceptability of the experimental techniques used.

Table 10.2. Formation constants for the histidine H^+-Cu^{2+}-L^- system. β_{pqr} values are defined according to the equation $pH^+ + qCu^{2+} + rL^- \rightleftharpoons H_pCu_qL_r^{(p+2q-2r)+}$. σ gives the standard deviation for each constant.

pqr	This work		IUPAC recommended		Proposed product
	$\log \beta_{pqr}$	σ	$\log \beta_{pqr}$	σ	
301	16.88	(fixed)	16.88	(0.1)	H_3L^+
201	15.154	(0.010)	15.16	(0.03)	H_2L^0
101	9.109	(0.006)	9.11	(0.02)	HL^-
111	14.11	(0.01)	14.11	(0.02)	$HCuL^+$
011	10.14	(0.004)	10.16	(0.03)	CuL^0
212	27.2	(fixed)	27.2	(0.1)	$H_2CuL_2^0$
112	23.86	(0.01)	23.81	(0.07)	$HCuL_2^-$
012	18.21	(0.02)	18.11	(0.09)	CuL_2^{2-}
-111	1.92	(0.04)	2.0	(0.2)	$(OH)CuL^-$
-222	7.99	(0.02)	7.9	(0.1)	$(OH)_2Cu_2L_2^{2-}$

10.3.2 The H^+-Al^{3+}-caffeic acid (H_3L) system

(*i*) *Potentiometry*

The protonation reactions of caffeic acid were investigated by performing 9 titrations, giving 409 datum points, for which the concentration of caffeic acid was varied over the range 0.72-3.1 mM. Complex formation with Al^{3+} was subsequently investigated by performing 9 titrations (348 datum points) in which the concentrations were varied over the range 0.18-0.39 mM for Al^{3+} and 0.38-1.2 mM for caffeic acid. Stoichiometric metal to ligand ratios were varied over the range 1:1.6-1:4.5. The resultant titration data were analysed numerically with the program SUPERQUAD, to give the formation constants reported in Table 10.3. Values of the aluminium hydrolysis constants used for these calculations are given in Table 2.2 (the species $Al(OH)_{3(aq)}$ was not included).

A selection of titration curves covering a range of metal to ligand ratios is presented in Figure 10.5. The solid curves are plotted as the Z_c function (Equation 10.9), which indicates the average number of protons bound per caffeic acid equivalent. They are calculated from the refined constants in Table 10.3 with the program SOLGASWATER. Values of Z_c below 0.0 obtained for titrations performed at low metal:ligand ratios indicate the significant presence of mixed hydroxo metal-ligand species in these solutions.

Table 10.3. Formation constants for the caffeic acid system H^+-Al^{3+}-H_3L. β_{pqr} values are defined according to the equation $pH^+ + qAl^{3+} + rH_3L \rightleftharpoons H_pAl_q(H_3L)_r^{(p+3q-3r)+}$. σ gives the standard deviation for each constant.

pqr	Log β_{pqr}	σ	Proposed product
-101	-4.382	0.001	H_2L^-
-201	-13.055	0.001	HL^{2-}
-301	-25.7	0.2	L^{3-}
-211	-4.88	0.01	$HAlL^+$
-311	-9.45	0.01	AlL^0
-411	-15.53	0.04	$(OH)AlL^-$
-612	-22.24	0.02	AlL_2^{3-}
-712	-30.73	0.06	$(OH)AlL_2^{4-}$
-913	-39.23	0.04	AlL_3^{6-}

(*ii*) *Spectrophotometric determination of* K_1

The protonation constant for the most strongly basic group of caffeic acid was determined spectrophotometrically, as described in Section 10.2.10. Two titrations were performed, with an initial concentration of caffeic acid of *ca.* 50 μM. Spectra from one of the titrations are shown in Figure 10.6.

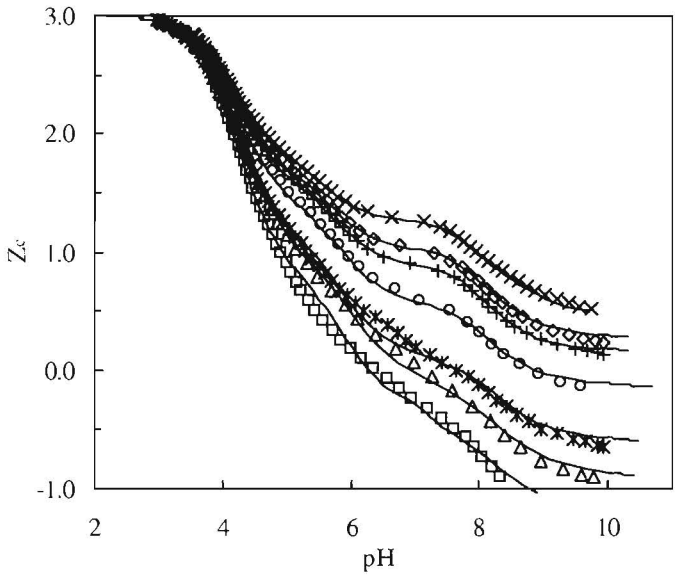

Figure 10.5. Selected Z_c curves for the caffeic acid system H^+-Al^{3+}-H_3L. Symbols show Z_c values calculated from the titration data using Equation 10.9. Solid lines were calculated using the refined constants given in Table 10.3 (metal:ligand ratios: × 1:4.0; Δ 1:3.6; ◊ 1:3.1; ∗ 1:2.4; o 1:2.2; + 1:1.8; □ 1:1.6).

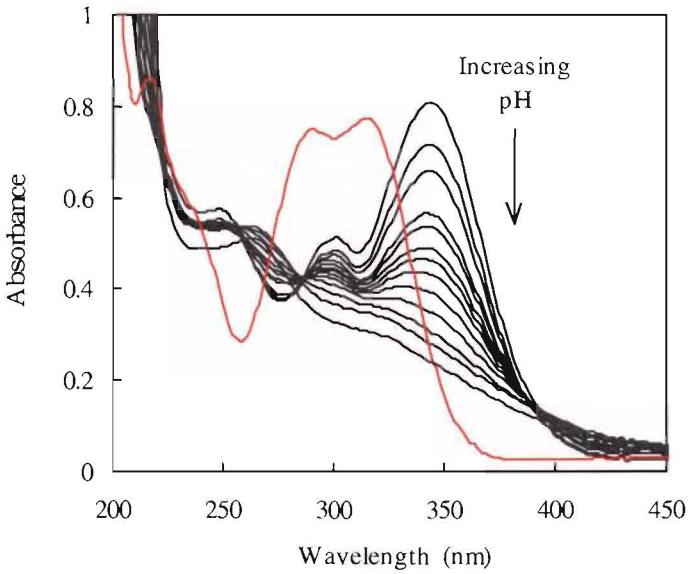

Figure 10.6. Spectra for caffeic acid showing the decrease in absorbance that occurs for the deprotonation reaction of HL^{2-}. The curve for the fully protonated ligand is also shown (red). Note the loss of the two isosbestic points that occurs if air enters the titration cell and ligand oxidation occurs (bottom curve). The initial concentration of caffeic acid was *ca.* 50 μM.

The absorbance maxima occurs at 344 nm, and absorbance data for the calculations were obtained from this wavelength. Two isosbestic points were observed at *ca.* 285 and 390 nm. If the titration was not performed under deoxygenated conditions, the ligand readily underwent oxidation, and loss of both isosbestic points was observed (Figure 10.6).

To calculate the relative concentrations of HL^{2-} and L^{3-} for each of the spectra, molar absorptivity coefficients for both species were required (ε_{HL} and ε_L). The value of ε_{HL} was obtained from a titration in which small increments of alkali were added to the titration cell containing caffeic acid to span the pH range *ca.* 9.5-10.5, and successive spectra recorded. The value of ε_{HL} was subsequently calculated from the spectra having highest absorbance at 344 nm (ε_{HL} = 18861). The molar absorptivity ε_L was determined from the spectra obtained after the dissolution of several NaOH pellets in the titration cell containing caffeic acid. Oxidation of the ligand at high pH occurred rapidly, and although the curve from which the value of ε_L was calculated went through the isosbestic point, a high error will be associated with this value (ε_L = 5285).

Individual values of log K_1 were calculated from each spectrum obtained from the two spectrophotometric titrations, as described in Section 10.2.11. These were plotted as a function of ionic strength, and a value for log K_1 at 0.10 M ionic strength was obtained by extrapolation of a line through the datum points (Figure 10.7). The values for log K_1 calculated from the two titrations were in good agreement (12.62 and 12.55). The mean of these values was used to calculate the value of log β_{-301} given in Table 10.3.

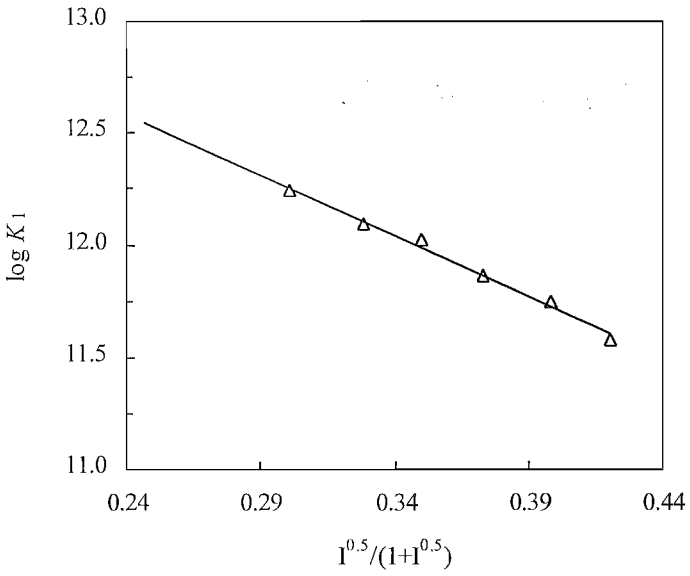

Figure 10.7. Individual values of log K_1 for caffeic acid, calculated from spectrophotometric data and plotted as a function of ionic strength. Outlying values (not shown) occurred at high ionic strength and indicate that ligand oxidation may have occurred at very high pH. The fitted line ($y = -5.41x + 13.88$) has an r^2 value of 0.99.

10.3.3 The H^+-Al^{3+}-chlorogenic acid (H_3L) system

(*i*) *Potentiometry*

The protonation reactions of chlorogenic acid were investigated by performing 8 titrations giving 396 datum points, for which the concentration of chlorogenic acid was varied over the range 0.72-3.1 mM. Complex formation with Al^{3+} was investigated by performing 9 titrations (406 datum points) in which the concentrations were varied over the range 0.20–0.42 mM for Al^{3+} and 0.41-0.83 mM for chlorogenic acid. Stoichiometric ratios of metal to ligand were varied over the range 1:1.5-1:5.5. Titration data were analysed numerically with the program SUPERQUAD, to give the formation constants reported in Table 10.4. Values of the aluminium hydrolysis constants used for these calculations are given in Table 2.2 (the species $Al(OH)_{3(aq)}$ was not included).

Table 10.4. Formation constants for the chlorogenic acid system H^+-Al^{3+}-H_3L. β_{pqr} values are defined according to the equation $pH^+ + qAl^{3+} + rH_3L \rightleftharpoons H_pAl_q(H_3L)_r^{(p+3q-3r)+}$. σ gives the standard deviation for each constant.

pqr	Log β_{pqr}	σ	Proposed product
-101	-3.359	0.004	H_2L^-
-201	-11.610	0.002	HL^{2-}
-301	-23.9	0.3	L^{3-}
-211	-3.91	0.02	$HAlL^+$
-311	-8.17	0.03	AlL^0
-411	-13.79	0.03	$(OH)AlL^-$
-612	-19.28	0.05	AlL_2^{3-}
-712	-27.65	0.15	$(OH)AlL_2^{4-}$
-913	-34.01	0.08	AlL_3^{6-}

Selected Z_e titration curves for chlorogenic acid, covering a range of stoichiometric metal to ligand ratios, are presented in Figure 10.8. The solid lines give the value of Z_e calculated from the refined constants in Table 10.4 with the program SOLGASWATER. As observed

for caffeic acid titrations, the formation of mixed hydroxy metal-ligand complexes at low metal:ligand ratios is significant.

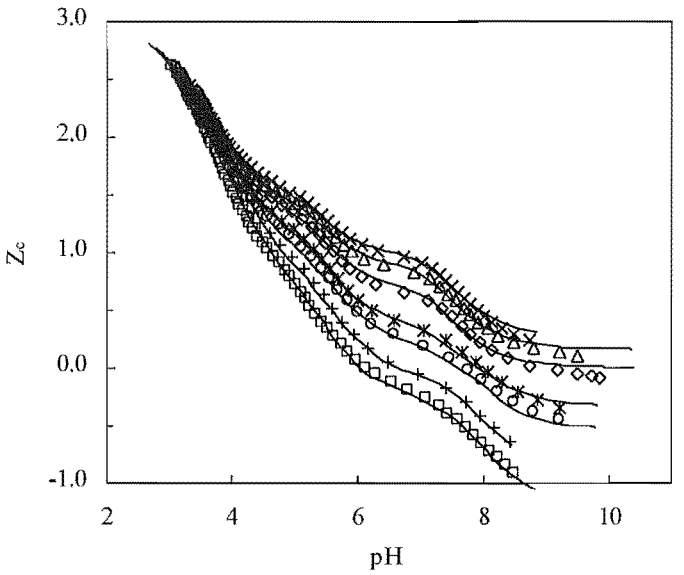

Figure 10.8. Selected Z_c curves for the system H^+-Al^{3+}-H_3L-chlorogenic acid. Symbols show Z_c values calculated from the titration data using Equation 10.9. Solid lines were calculated using the constants given in Table 10.3 (metal:ligand ratios: × 1:4.0; ◇ 1:3.6; + 1:3.1; ○ 1:2.4; ✳ 1:2.2; △ 1:1.8; □ 1:1.6).

(ii) Spectrophotometric determination of K_1

The protonation constant for the most basic group of chlorogenic acid was determined from spectrophotometric data in a similar manner to that described above for caffeic acid (Section 10.3.2). Two titrations were performed using an initial chlorogenic acid concentration of *ca.* 50 μM. Spectra from one titration are shown in Figure 10.9. Three isosbestic points were observed at *ca.* 268, 298 and 400 nm.

A large change in the spectrum was observed when air entered the titration cell and the ligand underwent oxidation. The absorbance maxima occurs at a wavelength of 368 nm, but was observed to increase slightly as the titration proceeded. Data for the calculation of pK_1 was obtained at a wavelength of 356 nm. The molar absorbtivity values ε_{HL} and ε_L were obtained using the methods described above for caffeic acid. Values of ε_{HL} and ε_L were calculated to be 20944 and 8911, respectively.

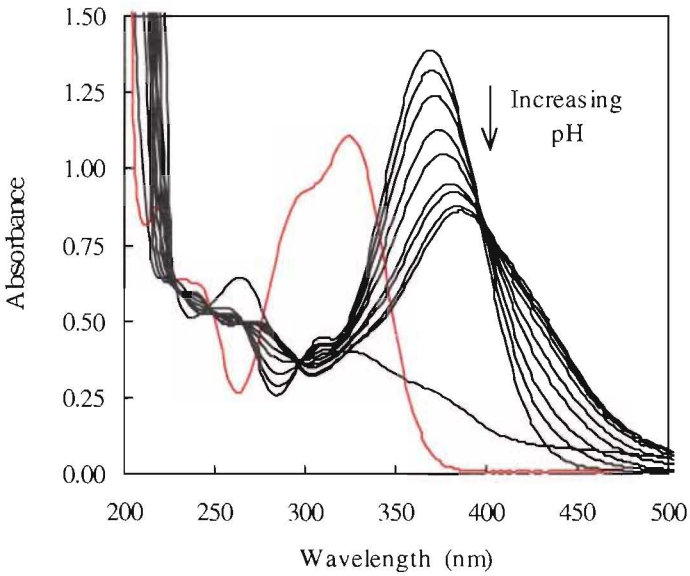

Figure 10.9. Spectra for chlorogenic acid showing the decrease in absorbance that occurs for the deprotonation reaction of HL^{2-}. The curve for the fully protonated ligand is also shown (red), together with the curve obtained if ligand oxidation occurs (bottom curve). The initial concentration of caffeic acid was *ca.* 50 μM.

Individual values of log K_1 were calculated from each spectrum obtained from the two spectrophotometric titrations. The results from one titration are plotted as a function of ionic strength in Figure 10.10. The values for log K_1 (I = 0.10 M) calculated from the two titrations were in reasonable agreement (12.37 and 12.14). The mean of these values was used to calculate the value of log β_{-301} given in Table 10.4.

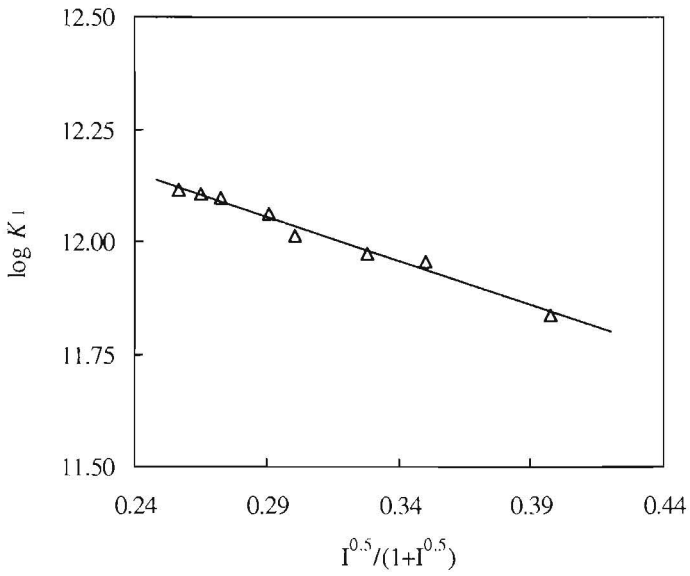

Figure 10.10. Individual values of log K_1 for chlorogenic acid, calculated from spectrophotometric data and plotted as a function of ionic strength. As was observed for caffeic acid, outlying values (not shown) occurred at high ionic strength and indicate that ligand oxidation may have occurred at very high pH. The fitted line ($y = -1.97x + 12.63$) has an r^2 value of 0.98.

10.4 DISCUSSION

(i) Proton complexes

A number of potentiometric titrations were performed over a pH range of *ca.* 3-10. The proton dissociation constants obtained for caffeic and chlorogenic acids (from Table 10.3 and Table 10.4, respectively), are presented in Table 10.5 together with literature values for these and various related ligands .

Table 10.5. Proton dissociation constants for caffeic and chlorogenic acids and for some reference compounds.

Ligand	$pK_{(COOH)}$	$pK_{(OH1)}$	$pK_{(OH2)}$	Reference
Caffeic acid	4.382	8.672	12.6	This work[A]
	4.37	8.55	12.5	Kiss *et al.* (1989)[B]
	4.41	8.72	-	Linder and Voyé (1987)[C]
	4.45	8.66	11.8	Lamy *et al.* (1985)[D]
	4.49	8.76	-	Timberlake (1959)[E]
Chlorogenic acid	3.359	8.251	12.3	This work[A]
	3.35	8.21	12.5	Kiss *et al.* (1989)[B]
	3.37	8.27	11.5	Lamy *et al.* (1985)[D]
	3.35	8.30	12.06	Améziane *et al.* (1996)[F]
Phenylacetic acid	4.12	-	-	Pettit and Powell (1997)[A]
Catechol	-	9.26	13.43	Kennedy and Powell (1985)[A]
3,4-DHPA[G]	4.12	9.33	13.0	Kiss *et al.* (1989)[B]
3,4-DHPP[H]	4.45	9.43	13.7	Kiss *et al.* (1989)[B]

[A] 0.1 M KCl, 25°C.

[B] 0.2 M KCl, 25°C.

[C] 0.1 M NaCl, 25°C.

[D] 0.1 M $NaClO_4$, 25°C.

[E] 0.05 M KNO_3, 25°C.

[F] 1 M KNO_3, 20°C.

[G] 3,4-dihydroxyphenylacetic acid

[H] 3,4-dihydroxyphenylpropionic acid

Inspection of the proton dissociation constants in Table 10.5 shows the values obtained in this work for $pK_{(COOH)}$ and $pK_{(OH1)}$ are in excellent agreement with those obtained previously by other workers. There is poorer agreement between values for the weakly acidic phenolic proton ($pK_{(OH2)}$). The *o*-diphenolate species formed at high pH readily undergo oxidation, which increases the difficulty in obtaining accurate $pK_{(OH2)}$ values for both caffeic and chlorogenic acids. The values reported by Lamy *et al.* (1985) for pK_3 of caffeic and chlorogenic acids are unlikely to be accurate. These values were obtained by potentiometric methods, and fall considerably outside the range for reliable pH measurements imposed by the use of glass bulb electrodes (*ca.* pH 2.3-10.6). The value for pK_3 of caffeic acid reported in this work, is similar to that to that obtained by Kiss *et al.* (1987). However, the pK_3 value obtained for chlorogenic acid fell between values reported by Kiss *et al.* (1987) and Améziane *et al.* (1996). The very weak acidity ($pK>12$) of the third dissociable proton is due to the electrostatic attraction of the adjacent negative charge, and to intra-molecular hydrogen-bond formation between the phenolic hydroxyl proton and phenoxide group (Linder and Voyé 1987; Kiss *et al.* 1989).

The p*K* values of 4.382 and 3.359 for caffeic and chlorogenic acids, respectively, are assigned to the carboxylic acid group. The COOH group of chlorogenic acid is more acidic than that of the other ligands. This has been attributed to the presence of an adjacent alcoholic hydroxyl group on the quinic acid residue of chlorogenic acid (Kiss *et al.* 1989).

The $pK_{(OH1)}$ values in Table 10.5 indicate that phenolic groups in caffeic and chlorogenic acids are slightly more acidic than those in catechol and related ligands. This may suggest that an electron withdrawing effect of the carboxylate group occurs across the double bond of the side chain (Linder and Voyé 1987). This effect is not seen for the two ligands 3,4-DHPA and 3,4-DHPP, both of which have saturated side chains.

(ii) Al^{3+} complexes

Stability constants for the H^+-Al^{3+}-H_3L systems (L = caffeic or chlorogenic acid) have not been reported previously. The range of initial Al^{3+} and ligand concentrations used aided in the identification of protonated and hydroxo species. A computational evaluation of the Al^{3+}-ligand titration curves for both ligands resulted in the proposed formation of six species: $HAlL^+$, AlL^0, $(OH)AlL^-$, AlL_2^{3-}, $(OH)AlL_2^{4-}$, and AlL_3^{6-}. Species distribution diagrams are given in Figure 10.11 and Figure 10.12 for caffeic and chlorogenic acids, respectively.

At low pH, a mono-protonated complex forms ($HAlL^+$). As the pH increases, complex formation proceeds in a step-wise fashion to form the tris-Al-ligand complex, *via* a hydroxo species $(OH)AlL^-$ (presumably formed from the hydrolysis of AlL^0), and a second hydroxo species $(OH)AlL_2^{4-}$ (presumably formed from the hydrolysis of AlL_2^{3-}). The species $HAlL^+$ (-211) could have two possible structures. Al^{3+} may coordinate to the caffeic and chlorogenic ligands either *via* catecholate-type binding where the side-chain carboxylate group is protonated, or *via* the carboxyl site where one of the two phenolic groups is deprotonated.

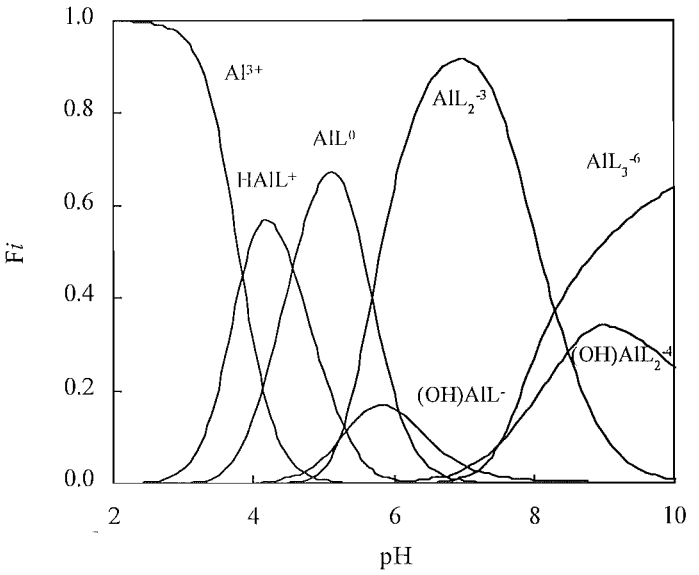

Figure 10.11. Species distribution diagram for the system H^+-Al^{3+}-caffeic acid, calculated with the program SOLGASWATER and using the stability constants given in Table 10.3. [Al] = 1 mM; [caffeic acid] = 2.5 mM.

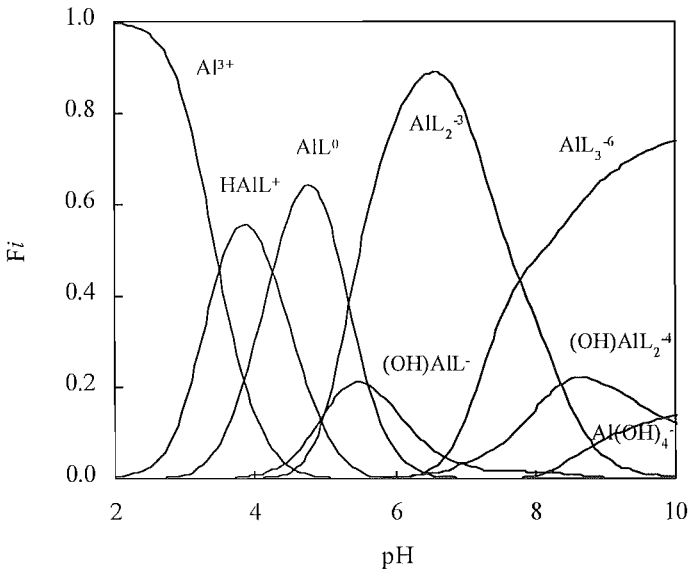

Figure 10.12. Species distribution diagram for the system H^+-Al^{3+}-chlorogenic acid, calculated with the program SOLGASWATER and using the stability constants given in Table 10.4. [Al] = 1 mM; [chlorogenic acid] = 2.5 mM.

For both caffeic and chlorogenic acids, the former structure seems likely. The pH range in which this species is proposed to exist (*ca.* pH 2-6; Figure 10.11 and Figure 10.12) is below the pH for which a phenolic group is expected to be deprotonated ($pK_{(OH1)}$ = 8.672 and 8.251 for caffeic and chlorogenic acids, respectively). For caffeic acid, the equilibrium constant for the reaction $HAlL^{+} \rightleftharpoons AlL^{0} + H^{+}$ is log K = -4.57 (Table 10.3), a value similar to that obtained for the deprotonation of the carboxyl group in the free ligand (log β_{-101} = -4.382). The equivalent logarithmic equilibrium constant for chlorogenic acid (log K = -4.26) is slightly higher than the value observed for deprotonation of the corresponding carboxyl group (-3.359).

Simultaneous metal ion coordination to both carboxyl and catechol sites, and the formation of oligomeric structures, have been observed for the binding of caffeic and chlorogenic acids to various divalent metal ions (Linder and Voyé 1987; Kiss *et al.* 1989; Cocks *et al.* 1992). The possible presence of various Al-ligand oligomeric species was evaluated in this work. However, as inclusion of these species into the speciation model either worsened, or did not improve the goodness of fit, their presence was discounted.

The complexation of Al^{3+} to caffeic and chlorogenic acids was compared to catechol and tiron (a sulfonated catechol derivative) by calculation of pM values (the negative logarithm of the free metal ion) as a function of pH. Values of pM were calculated with the program SOLGASWATER, using the equilibrium constants in Table 10.3 and Table 10.4 for caffeic and chlorogenic acids, respectively. Equilibrium constants for the Al-catechol system were obtained from Kennedy and Powell (1985); those for Al-tiron were obtained from Pettit and Powell (1997). Results are shown in Figure 10.13.

Stable Al-ligand complexation is indicated by low concentrations of free metal, and large values of pM. Below pH *ca.* 4, a pM value of 6 is obtained. This corresponds to 100% of the 1 μM Al being unbound in acidic solution. However, as the pH increases above *ca.* 4, the pM curves rise as complexation proceeds. Tiron clearly forms the strongest complexes with Al; the pM values for caffeic and chlorogenic acid indicate that these ligands have a similar binding strength to catechol.

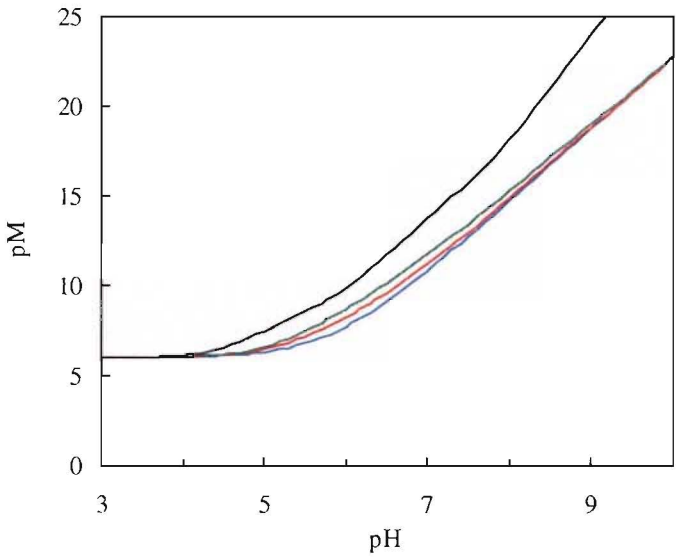

Figure 10.1. Calculated pM values for Al coordination to various catechol derivatives. [Al] = 1 μM; [ligand] = 10 μM. (—— tiron; —— chlorogenic acid; —— caffeic acid; —— catechol).

10.5 CONCLUSION

The solution chemistry of the H^+-Al^{3+}-caffeic acid and H^+-Al^{3+}-chlorogenic acid systems has been examined using potentiometric and spectrophotometric titration techniques. Equilibrium constants for the respective systems have been reported. The values reported in this work for the deprotonation reactions of the two ligands are in good agreement with the results of other workers. The formation of six mononuclear Al-ligand species was proposed in order to adequately rationalise the experimental data. No evidence was found for the presence of oligomeric species, despite previous workers having observed the formation of such complexes for various divalent metal ions.

The refined stability constants indicate that both caffeic and chlorogenic acids bind effectively to aluminium, with a binding strength comparable to that observed for catechol. In natural systems (*e.g.* soils and soil solution) where the presence of caffeic and chlorogenic acid exudates has been demonstrated (Makepeace *et al.* 1985), these ligands have the ability to complex, and detoxify Al^{3+}. In acidic soils of low fertility, the exudation of such organic ligands could be interpreted as being part of an adaptive strategy by a particular plant species to gain a competitive advantage over other rival species.

CHAPTER 11

CONCLUSION

The objective of this thesis was to develop and apply fractionation protocols to investigate aluminium speciation in soil solutions and natural waters. A significant component of this work has involved the application of an established technique for Al speciation to environmental situations where Al is of significance. The remainder of the work has been of a more fundamental nature *i.e.* two method development studies and an investigation of the solution equilibria between Al^{3+} and two organic ligands of environmental relevance.

In soils undergoing acidification, determination of the toxic 'free Al' species is of importance. This thesis has described the development and application of techniques which are able to target 'free Al' within a variety of environmental samples. In particular, studies were performed which investigated aluminium speciation in modified soil environments (soils modified by agriculture and forestry). The data collected in such studies may, in the longer term, be used in the development of models able to predict the effects of land management decisions on aluminium speciation, and hence on soil fertility. The use of such models by land managers in the future will hopefully promote sustainable land management policies.

11.1 ALUMINIUM SPECIATION IN THE ENVIRONMENT

11.1.1 Soil solution chemistry

During the course of this work soil solutions were extracted and analysed from a variety of soils having different vegetation. In the study described in Chapter 3, a number of these results were combined with previously reported data. From the measured concentrations of 'free Al', values of soil solution [Al^{3+}] were calculated. When plotted *vs.* pH, a single curvilinear relationship between log [Al^{3+}] and pH was observed for all soil solutions.

Whereas at low pH (<5.0), values of log [Al^{3+}] were significantly undersaturated with respect to the theoretical gibbsite and amorphous $Al(OH)_3$ solubilities, at higher pH (>5.6), the data were consistent with [Al^{3+}] solubility control being by an $Al(OH)_3$ solid phase. On the basis of these results, two solubility controls were proposed: (*i*) soil organic matter at pH <5.0 and,

(*ii*) a solid $Al(OH)_3$ phase at pH >5.6. The results of a previously-determined Al-fulvic acid binding curve were used to support the proposed control of soil solution Al^{3+} solubility by organic matter at acidic pH. It is relevant to note that under conditions of increased acidity, the concentrations of organic matter in soil generally increase, due to a reduction in the amount of microbial decomposition that occurs (McLaren and Cameron 1996).

Values of $[Al^{3+}]$ in soil solution were readily calculated from the measurements of 'free Al' ($[Al^{3+}] + [Al(OH)^{2+}] + [Al(OH)_2^{+}]$) obtained using the oxine-derivatised Fractogel method of Simpson *et al.* (1997). A major disadvantage of this method however, is that AlF^{2+} is included in the experimental fraction of 'free Al'. Calculation of $[Al^{3+}]$ therefore requires a separate measurement of the total soil solution $[F^-]$ to be made, in addition to a subsequent calculation and correction for the concentration of AlF^{2+} which is present as part of the 'free Al' fraction. Not unexpectedly, concentrations of F^- measured in this work were, in general, only significant (> *ca.* 3 μM) in pastoral soils that had a history of fertiliser use. Nevertheless, for some of these fertilised soils, the calculated concentrations of AlF^{2+} accounted for as much as *ca.* 95% of the measured 'free Al' concentrations, reinforcing the necessity of following the procedure developed in this work.

The impact of land use change from grassland to conifer forest on the Al concentrations in soils and soil solutions was examined at three contrasting pairs of sites in the South Island, New Zealand. Similar trends in the soil chemistry were observed at all three sites, although the magnitude of these changes was site specific. Topsoil pH was significantly lower under forest at two of the three sites, but soil solution pH was only lower under forest at the LP site (the site having lowest percentage base saturation). Soil base saturation values were lower under forest than grassland at all three sites. In soil solutions there was a trend for both 'free Al' and the moderately labile 'organic-Al' fraction to be higher in forest soil at all sites. However, the site-pair differences were only significant at the Lammerlaw Range (LP) site, and only for 'free Al'. The increase in 'free Al' observed at the LP site was linked to the low pH and low soil base saturation.

To establish whether the high 'free Al' concentrations observed at the LP site might impact upon plant growth, root elongation experiments using the Al-sensitive pasture legume *Medicago sativa* were performed. Elongation was significantly smaller in forest than in grassland soil at the 0-10 and 10-20 cm depths, by 35% and 25% respectively, with no significant difference ($p = 0.24$) at 20-30 cm. Interestingly, magnesium deficiency symptoms were evident in *Pinus radiata* at LP, but not at the two other sites, despite all three sites

having similar exchangeable and soil solution Mg concentrations. It is likely that the high concentrations of Al present at the LP site, coupled with the low soil base saturation, are sufficient to interfere with uptake of Mg.

From these results it was clear that the effects of afforestation on soil and soil solution chemistry are likely to be most significant in soils with existing low base saturation values. If sites having low soil buffering capacities are planted with fast growing species such as *P. radiata*, then the rates of base cation uptake by the trees may exceed the rate at which cations are replenished in the soil environment *via* mineral weathering and return of plant biomass. At such sites soil acidification will occur, together with increases in soil Al concentrations and the possibility of cation deficiencies. To avoid these factors impacting upon plant growth, fertilisation and/or liming may be required.

Aluminium speciation was further investigated in a number of high country pastoral soils. Previous workers have established that ongoing soil acidification is occurring at the Longslip Station site. The aim of this work was to establish whether this acidification was reflected by high soil solution aluminium concentrations that might possibly impact upon the growth of pastoral legume species. Despite the history of increasing soil acidity, current soil solution 'free Al' concentrations at the Longslip site were low (0.31 to 0.75 μM), and well below reported toxicity thresholds for legume species (Edmeades *et al.* 1991; Wheeler *et al.* 1992).

A series of aluminium complexation capacity titrations were performed to determine the capacity of the soluble natural organic matter in soil solutions from Longslip, to complex (and hence detoxify) Al. The results of these titrations indicated that with continued soil acidification, the ability of soil solutions to complex Al was lower for the soils at lower elevation. Further acidification might therefore be expected to affect sites at lower elevation first. In general however, for sites at lower altitude the soil processes of cation leaching and plant-induced weathering are more in balance, compared with the net removal of exchangeable cations that occurs at sites of higher elevation (Ruth *et al.* 1998). Therefore soils at these lower elevations are expected to have higher buffering capacity and base saturation than corresponding soils at higher elevations. Hence soil acidification may initially impact at higher altitudes.

A second study investigated soil solution pH and aluminium speciation in samples taken from three soil zones around *Hieracium pilosella* patches. Previous workers have established that *Hieracium* species are able to induce soil acidification, and have proposed that an Al tolerance

mechanism may impart *Hieracium* species with an advantage over competing grassland species (*i.e.* grasses, legumes and tussocks). However, soil solution concentrations of 'free Al' from soil taken from under both *H. pilosella* and adjacent grassland were low (<0.4 μM) and well below suggested thresholds for Al toxicity (Edmeades *et al.* 1991; Wheeler *et al.* 1992).

Interestingly, despite the low soil solution 'free Al' concentrations, and the unlikely growth inhibition of legumes by Al toxicity in these soils, root elongation of *M. sativa* was lower in soil taken from under the centre of a *H. pilosella* patch, and from the surrounding *halo* zone. Makepeace *et al.* (1985) established that *Hieracium* species exude three main polyphenolic species, umbelliferone, caffeic acid and chlorogenic acid. These species were demonstrated by these authors to cause an allelopathic inhibition of root growth for a variety of grassland species. Given the low Al concentrations determined in soil solutions, it is possible that an allelopathic effect may have been at least partly responsible for the observed inhibition of root growth.

11.1.2 Interaction of aluminium with polyelectrolyte flocculants

A series of aluminium complexation capacity titrations were performed to determine whether fundamental differences occurred between the binding of Al with a commercially available synthetic anionic flocculant (polyacrylamide), and its binding to a naturally-derived, anionic, non-toxic flocculant (sodium alginate). Results of this work indicated that at concentrations of polyacrylamide and at pH typical of those used for flocculation in water treatment, the dominant 'binding' with the anionic polyacrylamide sample was *via* surface interactions such as bridging and/or enmeshment between the polymer and hydrolysed polymeric Al-hydroxy species. In contrast, alginate interacted with Al predominantly *via* chemical binding, although a minor contribution to the aluminium complexation capacity from bridging and/or enmeshment was observed at pH 6.5.

A natural progression for this work would be the investigation of the respective binding interactions of polyacrylamide and alginate with Al in the presence of natural organic matter. In particular, the likelihood of alginate competing with natural organic matter for aluminium should be investigated. If alginate should prove to strip aluminium from organic matter, this may well inhibit its usefulness as a flocculant for water treatment purposes. It would also be desirable to characterise more fully the behaviour of the oxine-derivatised Fractogel towards soluble or precipitated hydroxy-Al polymeric species.

11.2 FUNDAMENTAL STUDIES

11.2.1 Development of analytical methods for the speciation of Al and Fe

The use of solid-phase adsorbants (*i.e.* ion-exchange or chelating resins) in flow injection analysis (FIA) manifolds offers several advantages over alternative speciation methods. Analyses may be performed rapidly, using relatively simple and inexpensive equipment, and in addition, on-line analyte preconcentration and separation of the analyte from the sample matrix is achieved. In this work two analytical techniques using FIA methodologies were developed to allow the respective speciation of Al and Fe to be determined in environmental samples.

The development of an FIA technique suitable for determining concentrations of 'free Al' ($[Al^{3+}] + [Al(OH)^{2+}] + [Al(OH)_2^{+}]$) in natural waters, soil solutions and soil extracts was investigated. Al speciation was effected by the selective capture of 'free Al' on an iminodiacetate controlled-pore glass resin ('Prosep'). The 'free Al' captured on the resin was subsequently eluted using 0.1 M HCl with a stopped-flow protocol, and detected spectrophotometrically as the chrome azurol S complex at pH 5.0. The method had a detection limit of 0.21 μM, an estimated linear working range of 1.0-25 μM Al, and an RSD of 2.0% at 10 μM Al.

The method was validated by comparison of the experimentally determined concentrations of 'free Al' with the concentrations of 'free Al' calculated from the thermodynamic equilibrium models for a number of Al-oxalate and hydroxy-Al polymer solutions. The results of these experiments established that the Prosep resin did not significantly sequester Al from either Al-oxalate or hydroxy-Al polymeric species, and was therefore suitable as a method of determining 'free Al'. The method was subsequently applied to the analysis of several humic waters and soil extracts. Good agreement was observed between the concentrations of 'free Al' determined by the Prosep resin method and those obtained from other established analytical methods. Previous work from within this group has established that uptake of Al from samples of high ionic strength is problematic when using the oxine-derivatised Fractogel. In contrast, a significant advantage of the Prosep resin was its ability to capture Al from solutions of high ionic strength. Further application of this Al speciation method to soil extracts might provide interesting information on the relative partitioning of Al between inorganic soil exchange sites and adsorbed organic phases.

The suitability of the oxine-derivatised Fractogel resin as a substrate for speciating Fe^{II} and Fe^{III} in an FIA manifold was investigated. A method was developed in which the Fe^{II} and Fe^{III} captured by the resin was subsequently eluted with 0.5 M HCl. Fe^{II} was quantified spectrophotometrically as the Fe^{II} (1,10-phenanthroline)$_3$ complex at pH 4.0 and total Fe (Fe^{II} + Fe^{III}) by the same method, but including an on-line reduction of Fe(III) with ascorbic acid. The calculated detection limit for the method was 42 nM. The RSD of the technique at 10 μM Fe^{II} was 0.88% and the estimated linear working range was 0.2-25 μM Fe^{II}.

Tests with synthetic organic ligand solutions (tartrate, oxalate and citrate) and fulvic acid solutions established that organically-bound Fe^{II} was labile on the experimental time scale and was therefore sequestered by the oxine-derivatised gel. In contrast, experiments using Fe^{III}-fulvic acid solutions indicated that Fe^{III} was not labile on the experimental time-scale, but did react with the colorimetric reagent downline of the column. Experiments involving the analysis of Fe^{II} and Fe^{III} fulvic acid solutions show that the Fe redox system is very dynamic. Large changes in Fe speciation were observed in solutions that were exposed to sunlight. The ability of Fe^{III} to undergo rapid photo-reduction in the presence of fulvic acid has immediate implications for sampling protocols if Fe speciation information is required from organic-rich water samples.

Potential exists for the application of micro-columns (containing oxine-derivatised Fractogel) for field sampling, where a freshly-extracted soil solution or natural water might be injected to capture the analyte species of interest, which is later analysed in the laboratory. A protocol such as this would be advantageous both in terms of reducing the requirements for bulky sample transportation and storage, and also in eliminating speciation changes that may occur before a transported sample is analysed. Unless analysis could be effected within 60 s, the oxine-derivatised Fractogel would be unsuitable for capturing the speciation of Fe in a field sample due to the oxidation of Fe^{II} to Fe^{III} that occurs on the resin. However, measurement of a labile or 'reactive' Fe^{II} + Fe^{III} fraction would be possible should the problem of reduced Fe (and also Al) recoveries after long time intervals be overcome. Work is continuing in this group to investigate this problem.

11.2.2 Solution chemistry of two Al^{3+}-ligand systems

The toxicity (or conversely the bioavailability) of metals in soils and aquatic ecosystems, is in general, governed by the speciation of the metals concerned. The determination of reliable stability constants is a necessary prerequisite before any computer equilibrium modelling and

subsequent identification of important environmental species can occur. Although computer modelling is inherently reliant upon the reliability of the thermodynamic data used, and on the specific assumptions made regarding the system being modelled, simulations of natural multicomponent systems significantly aid in the understanding of environmental processes (Linder *et al.* 1990).

In this work, the solution equilibria between Al^{3+} and two organic ligands of environmental relevance (caffeic and chlorogenic acids) have been characterised, and equilibrium constants for the respective systems reported. Al complexation by both ligands was found to be similar to that observed for other catechol derivatives, with coordination proceeding *via* a stepwise addition of up to three ligands around the metal ion centre. At low metal:ligand ratios, two hydrolysed species were observed to form ($(OH)AlL^{-}$ and $(OH)AlL_2^{4-}$). Previous workers have observed the formation of oligomeric species between these ligands and various divalent metal ions. However, the incorporation of such species into the present model did not improve the goodness of fit.

A pM plot was used to compare the binding strengths of caffeic and chlorogenic acids with other related ligands. The two ligands bound Al with a strength comparable to that observed for catechol. The high stability of the Al complexes formed by these two ligands suggests that if they were to occur at significant concentrations in soil or hydroponic solutions they would be expected to bind Al strongly, and thus ameliorate any possible Al-induced toxicity.

APPENDIX I

VOGEL'S (1961) METHODS FOR THE GRAVIMETRIC ANALYSIS OF COPPER AND ALUMINIUM

Determination of copper with benzoin-α-oxime (cupron)

Dilute ammonia solution (5%) was added to a neutral solution containing not more than 0.05 g Cu, until a clear blue solution formed. This solution was heated to boiling, and Cu precipitated by the dropwise addition of a 2% ethanolic solution of benzoin-α-oxime (Sigma). Approximately 5.5 mL of 2% benzoin-α-oxime was added *per* 5 mL Cu sample (of concentration *ca.* 0.10 M). Precipitation was complete when the blue colour of the solution disappeared.

The precipitate was collected in a weighed sintered glass filter (porosity 3), and sequentially washed with hot dilute ammonia solution (1%), hot water and warm ethanol. The sample was dried to constant weight at 110°C, and weighed as $Cu(C_{14}H_{11}O_2N)$ ($M_r = 288.50$ gmol^{-1}).

Determination of aluminium with 8-hydroxyquinoline (oxine)

A 5% solution of oxine prepared in 2 N acetic acid is sufficient to precipitate 3 mg of aluminium. An aluminium solution was warmed to 70-80°C, and a 20% excess (calculated for quantitative precipitation) of the oxine reagent (BDH AnalaR) added. 2 N ammonium acetate was added dropwise to the solution until a precipitate just appeared. The solution was then heated to boiling, and a further 25 mL of 2 N ammonium acetate added dropwise, with constant stirring, to ensure complete precipitation (the yellow supernatant of the solution indicated sufficient oxine solution had been added to the sample). After the solution was cooled, the precipitate was collected in a sintered glass filter (porosity 4) and washed well with cold water. The sample was dried to constant weight at 130°C, and weighed as $Al(C_9H_6ON)_3$ ($M_r = 459.44$ gmol^{-1}).

APPENDIX II

(*i*) THE DAVIES EQUATION

The Davies equation relates the activity coefficient (γ) of an ion to solution ionic strength, and is an empirical modification of the Debye-Hückel equation. The limiting form of the Debye-Hückel equation is the most basic expression relating single-ion activity coefficients to ionic strength:

$$\log \gamma_i = -Az_i^2 I^{1/2}$$

where γ_i = single-ion activity coefficient

z_i = charge of ion i

A = constant depending on solvent and temperature (A = 0.509 $M^{1/2}$ for H_2O at 25°C)

I = ionic strength

Experimental measurement of log γ_i shows the Debye-Hückel equation gives good predictions for $I \leq 0.001$ M. However, at higher ionic strengths the equation is inaccurate, as activity in solution becomes increasingly dependent upon additional factors other than coulombic interactions. Although the Davies equation is still based only on coulombic interactions, depending on the ion its predictions are accurate to ionic strengths *ca.* ≤ 0.2 M.

$$\log \gamma_i = -Az_i^2 \left(\frac{I^{1/2}}{1+I^{1/2}} - 0.3I \right)$$

For the reaction $M + L \rightleftharpoons ML$, the Davies equation can be used to relate stability constants at one ionic strength to the value at zero ionic strength (K°).

$$K = \frac{[ML]}{[M][L]} = K^\circ \frac{\gamma_M \gamma_L}{\gamma_{ML}}, \text{ and } \log\left(\frac{\gamma_{ML}}{\gamma_M \gamma_L} \right) = -A \sum z_i^2 \left(\frac{I^{1/2}}{1+I^{1/2}} - 0.3I \right),$$

where the sum $\sum z_i^2$ is taken over all products and reactants.

(*ii*) DERIVATION OF A MASS BALANCE RELATIONSHIP TO CALCULATE THE CONCENTRATION OF ALF^{2+} PRESENT IN SOIL SOLUTION

The purpose of these equations was to derive an expression to allow calculation of the $[AlF^{2+}]$ in soil solution, from the experimental measurements of 'free Al' ($[Al_{meas}]$) and total fluoride ($[F_{tot}]$). The calculated concentration of AlF^{2+} could then be subtracted from $[Al_{meas}]$ to give the sum of the monomeric aluminium-hydroxy species concentrations, from which $[Al^{3+}]$ may be calculated. As $[AlF_2^+]$ is not included as part of the 'free Al' fraction, it is not possible to simply calculate $[Al^{3+}]$ from the known concentrations of 'free Al' and total F^-.

$$[Al_{meas}] = [Al^{3+}] + [Al(OH)^{2+}] + [Al(OH)_2^+] + [Al(OH)_3] + [Al(OH)_4^-] + [AlF^{2+}]$$

$$\Longrightarrow \quad [Al_{meas}] = [Al^{3+}]\left(1 + \frac{{}^*K_1}{[H]} + \frac{{}^*\beta_2}{[H]^2} + \frac{{}^*\beta_3}{[H]^3} + \frac{{}^*\beta_4}{[H]^4}\right) + [AlF^{2+}]$$

$$\Longrightarrow \quad [Al_{meas}] = k\,[Al^{3+}] + [AlF^{2+}]$$

$$\text{where } k = \left(1 + \frac{{}^*K_1}{[H]} + \frac{{}^*\beta_2}{[H]^2} + \frac{{}^*\beta_3}{[H]^3} + \frac{{}^*\beta_4}{[H]^4}\right)$$

$$[Al_{meas}] = k\,[Al^{3+}] + [AlF^{2+}]$$

$$\Longrightarrow \quad [Al_{meas}] = \frac{k\,[AlF^{2+}]}{K_1[F^-]} + [AlF^{2+}] \qquad \left(K_1 = \frac{[AlF^{2+}]}{[Al^{3+}][F^-]}\right)$$

$$\Longrightarrow \quad [F^-] = \frac{k\,[AlF^{2+}]}{K_1([Al_{meas}] - [AlF^{2+}])}$$

$$[F_{tot}] = [F^-] + [AlF^{2+}] + 2[AlF_2^+]$$

(assuming [HF] (pK_a = *ca.* 3.1) will be negligible at the pH of soil solutions)

$$\Longrightarrow \quad [F_{tot}] = [F^-] + [AlF^{2+}] + 2K_2[AlF^{2+}][F^-] \qquad \left(K_2 = \frac{[AlF_2^+]}{[AlF^{2+}][F^-]}\right)$$

and substituting in the expression for $[F^-]$,

$$[F_{tot}] = \left(\frac{k[AlF^{2+}]}{K_1([Al_{meas}] - [AlF^{2+}])}\right) + [AlF^{2+}] + 2K_2[AlF^{2+}]\left(\frac{k[AlF^{2+}]}{K_1([Al_{meas}] - [AlF^{2+}])}\right)$$

$$\Longrightarrow \quad K_1([Al_{meas}] - [AlF^{2+}])[F_{tot}] = k[AlF^{2+}] + K_1([Al_{meas}] - [AlF^{2+}])[AlF^{2+}]$$

$$+ \left(\frac{K_1([Al_{meas}] - [AlF^{2+}])\,2K_2[AlF^{2+}]\,k\,[AlF^{2+}]}{K_1([Al_{meas}] - [AlF^{2+}])}\right)$$

$$\Longrightarrow \quad (K_1[Al_{meas}][F_{tot}]) - (K_1[AlF^{2+}][F_{tot}]) = k[AlF^{2+}] + (K_1[Al_{meas}][AlF^{2+}])$$

$$- K_1[AlF^{2+}]^2 + (2kK_2[AlF^{2+}]^2)$$

$$\Longrightarrow \quad ((2kK_2 - K_1)[AlF^{2+}]^2) + ((k + K_1[Al_{meas}] + K_1[F_{tot}])[AlF^{2+}]) - (K_1[F_{tot}][Al_{meas}]) = 0$$

This final expression is a quadratic, and may be solved for $[AlF^{2+}]$.

(*iii*) CALCULATION OF THE SOLUBILITY OF GIBBSITE (AND AMORPHOUS $Al(OH)_3$)

The dissolution of gibbsite can be expressed as $Al(OH)_{3(s)} \rightleftharpoons Al^{3+}_{(aq)} + 3OH^-_{(aq)}$

for which the solubility product is $K_{sp} = \{Al^{3+}\}\{OH^-\}^3$.

If this is written in terms of negative logarithms: $pK_{sp} = pAl^{3+} + 3pOH^-$

and if $pK_w = 14.0$, and $pK_{sp}(\text{gibbsite}) = 34.0$, then substituting (14 - pH) for pOH^-, and using the pK_{sp} for gibbsite (or amorphous $Al(OH)_3$), produces a pH-dependent Al^{3+} solubility relationship: $pAl^{3+} = 3pH - 8.0$.

APPENDIX III

The following data were used in establishing the relationship between soil solution pH and Al^{3+} concentrations (Chapter 3; Section A). Concentrations of 'reactive Al' obtained using the rapid chrome azurol S (CAS) method of Hawke and Powell (1994) (Al_{7s}) were converted to the resin-based definition of 'free Al' (Al_{resin}) as described in Section 3.2.3. Sites marked by (*) indicate the fluoride concentration was obtained using averaged results from neighbouring sites, or estimated using results obtained for similar sites. Values of $[AlF^{2+}]_{calc}$ were subtracted from the concentration of 'free Al', to give the sum of the monomeric aluminium hydroxy species concentrations ($\Sigma[Al(OH)_x]$), from which log $[Al^{3+}]$ was calculated as described in Section 2.2.10.

Sample code	pH	Free Al (μM)	Total [F] (μM)	$[AlF^{2+}]_{calc}$ (M)	$\Sigma[Al(OH)_x]$ (μM)	Log $[Al^{3+}]$
Cragieburn 1*[A]	5.93	2.81	0.3	2.0E-07	2.61	-6.39
Cragieburn 2	5.59	1.03	0.7	3.7E-07	0.66	-6.61
Cragieburn 3	4.85	3.74	0.4	3.8E-07	3.36	-5.56
Cragieburn 4*	5.18	1.55	0.3	2.4E-07	1.31	-6.06
Edendale KF[A]	5.34	2.21	0.8	6.1E-07	1.60	-6.05
Edendale KP	6.99	0.19	4.5	1.4E-09	0.19	-10.27
Edendale MF	5.02	4.24	0.6	5.6E-07	3.68	-5.56
Edendale MP	5.78	0.88	7.6	7.6E-07	0.12	-7.54
Invermay A[A]	5.78	2.28	11.6	1.9E-06	0.34	-7.09
Invermay B	6.00	1.45	18.1	1.3E-06	0.20	-7.76
Invermay C	6.57	0.40	7.1	8.8E-08	0.31	-8.65
Invermay D	6.08	1.25	7.8	8.7E-07	0.38	-7.46
Invermay E	6.51	0.38	8.8	1.3E-07	0.25	-8.56
Longslip 1 shady[A]	6.16	0.40	2.7	1.8E-07	0.22	-7.84
Longslip 1 sunny	6.09	0.52	3.9	3.1E-07	0.21	-7.74

Sample code	pH	Free Al (μM)	Total [F] (μM)	$[AlF^{2+}]_{calc}$ (M)	$\Sigma[Al(OH)_x]$ (μM)	Log $[Al^{3+}]$
Longslip 5 sunny*	6.25	0.43	3.3	1.8E-07	0.25	-7.95
Longslip 5 shady*	5.96	0.51	3.3	3.4E-07	0.17	-7.61
Longslip 9 sunny*	5.93	0.75	3.3	4.9E-07	0.26	-7.39
Longslip 9 shady*	6.20	0.31	3.3	1.5E-07	0.16	-8.04
Longslip 1a[A]	7.12	0.48	2.3	5.8E-10	0.48	-10.35
Longslip 1b	7.47	0.50	3.6	4.2E-11	0.50	-11.70
Longslip 2a	7.62	1.04	2.9	1.8E-11	1.04	-11.97
Longslip 2b	7.07	0.56	1.7	8.1E-10	0.56	-10.09
Longslip 3a	7.44	0.87	3.9	1.0E-10	0.87	-11.34
Longslip 3b	7.12	0.96	3.6	1.9E-09	0.96	-10.05
Ben Avon*[A]	5.88	0.71	3.3	4.9E-07	0.22	-7.39
Telford forest[A]	6.00	1.41	0.7	2.8E-07	1.13	-6.86
Telford pasture	6.18	1.16	7.1	7.0E-07	0.46	-7.56
Hinewai 1[A]	5.37	0.86	1.2	5.3E-07	0.33	-6.75
Hinewai 3	5.40	1.22	0.3	2.2E-07	1.00	-6.29
Hinewai 4	5.56	1.31	0.6	3.6E-07	0.95	-6.42
Hinewai 5	5.63	1.78	0.7	4.6E-07	1.32	-6.34
Hinewai 6*	4.93	4.46	0.6	5.8E-07	3.88	-5.51
Hinewai 7	5.71	1.84	0.4	2.5E-07	1.59	-6.34
Silcock's Farm 1[A]	4.36	4.30	1.0	8.8E-07	3.42	-5.49
Silcock's Farm 2	4.67	3.24	2.7	2.0E-06	1.27	-5.95
Silcock's Farm 3	4.59	4.59	3.0	2.4E-06	2.18	-5.71
Silcock's Farm 4	4.13	40.16	0.7	7.3E-07	39.43	-4.42
Silcock's Farm 5	4.59	3.16	1.2	1.1E-06	2.10	-5.72
Bealey Oa*[B]	2.67	23.78	0.2	2.0E-07	23.58	-4.63
Bealey E*	3.38	8.52	0.2	2.0E-07	8.32	-5.08
Bealey B*	4.09	3.11	0.2	1.9E-07	2.92	-5.55
Broken River Oa*[B]	4.06	7.36	0.2	1.9E-07	7.17	-5.52

Sample code	pH	Free Al (μM)	Total [F] (μM)	$[AlF^{2+}]_{calc}$ (M)	$\Sigma[Al(OH)_x]$ (μM)	Log $[Al^{3+}]$
Broken River A*	4.57	5.32	0.2	1.9E-07	5.13	-5.33
Broken River B*	5.13	1.77	0.2	1.7E-07	1.60	-5.95
Riccarton Bush Oa[B]	5.53	1.69	0.2	1.5E-07	1.53	-6.19
Riccarton Bush Ag*	4.73	8.16	0.2	1.9E-07	7.97	-5.16
Riccarton Bush Bg*	5.11	1.60	0.2	1.7E-07	1.43	-6.00
Hinewai Oa[B]	3.63	1.24	0.6	4.8E-07	0.76	-6.12
Hinewai B*	4.13	5.86	0.6	6.0E-07	5.26	-5.30
C1*[C]	3.83	4.08	1.1	9.9E-07	3.10	-5.52
C2	3.57	9.58	1.1	1.0E-06	8.54	-5.07
C3*	4.66	1.24	1.1	7.0E-07	0.54	-6.32
C4*	3.95	2.75	1.1	9.3E-07	1.82	-5.75
C5*	4.11	2.75	1.1	9.3E-07	1.82	-5.76
C6*	4.18	3.99	1.1	9.8E-07	3.01	-5.54
A1*[C]	3.96	2.66	0.3	2.8E-07	2.38	-5.64
A2	4.11	1.60	0.3	2.7E-07	1.33	-5.89
A3*	4.16	1.69	0.3	2.7E-07	1.42	-5.87
A4*	4.44	1.33	0.3	2.6E-07	1.07	-6.00
A5*	4.62	1.24	0.3	2.5E-07	0.99	-6.05
A6	4.60	0.71	0.3	2.1E-07	0.50	-6.35
B1[C]	3.91	1.60	1.7	1.1E-06	0.51	-6.30
B2	4.20	1.33	1.7	9.6E-07	0.37	-6.45
B3*	4.19	1.33	1.7	9.6E-07	0.37	-6.45
B4*	4.62	1.60	1.7	1.1E-06	0.53	-6.32
B5	4.46	1.60	1.7	1.1E-06	0.53	-6.31
Tekapo 1 0-5[D]	5.00	2.04	0.5	4.2E-07	1.63	-5.91
Tekapo 1 5-10*	4.89	0.98	0.5	3.5E-07	0.63	-6.29
Tekapo 3 0-5*	5.10	2.31	8.5	2.1E-06	0.20	-6.86
Tekapo 3 5-10*	4.64	2.84	8.5	2.6E-06	0.24	-6.67

Sample code	pH	Free Al (μM)	Total [F] (μM)	$[AlF^{2+}]_{calc}$ (M)	$\Sigma[Al(OH)_x]$ (μM)	Log $[Al^{3+}]$
Tekapo 12 0-5	5.07	4.26	0.7	6.0E-07	3.66	-5.57
Tekapo 12 5-10*	4.60	1.51	0.7	5.1E-07	0.99	-6.05
Tekapo 14 0-5	5.33	1.69	0.5	3.8E-07	1.31	-6.13
Tekapo 14 5-10*	4.65	2.04	0.5	4.2E-07	1.62	-5.84
Tekapo 18 0-5	5.29	2.31	2.9	1.6E-06	0.73	-6.36
Tekapo 18 5-10	4.60	1.77	4.0	1.5E-06	0.24	-6.66
Tekapo 24 0-5*	5.29	1.60	0.7	4.8E-07	1.11	-6.12
Tekapo 24 5-10*	4.48	1.69	0.7	5.3E-07	1.15	-5.97
Tekapo 26 0-5*	5.76	0.98	1.7	5.4E-07	0.43	-6.96
Tekapo 26 5-10	4.55	2.31	1.7	1.3E-06	1.02	-6.03
Tekapo 0-2.5	4.33	3.99	0.8	7.7E-07	3.22	-5.52
Tekapo 2.5-5.0*	4.76	0.83	0.8	4.8E-07	0.35	-6.52
Tekapo 5.0-7.5*	5.02	0.66	0.8	4.0E-07	0.26	-6.71
Tekapo 7.5-10*	4.93	0.43	0.8	2.9E-07	0.14	-6.96

[A] Previously unpublished data.

[B] Powell and Hawke (1995).

[C] Hawke and Powell (1995).

[D] Powell *et al.* (1997).

APPENDIX IV

The empirical method described by Harned and Owen (1958) for the calculation of pK_w as a function of ionic strength is given here.

$$K_w = \frac{\{H^+\}\{OH^-\}}{\{H_2O\}} = [H^+][OH^-]\left(\frac{\gamma_{H^+}\gamma_{OH^-}}{\{H_2O\}}\right)$$

where

$$\log\left(\frac{\gamma_{H^+}\gamma_{OH^-}}{\{H_2O\}}\right) = \frac{-2SI^{0.5}}{1+AI^{0.5}} + BI + CI^{0.5}$$

and $$S = \frac{1.814\times10^6}{(DT)^{1.5}}$$

$$A = \frac{a^0 \times 50.30}{(DT)^{0.5}}$$

$$B = b^0 + b_1 t$$

$$C = c^0 + b_1 t$$

It is assumed B and C vary linearly with temperature, and that a^0 has no temperature dependence. The following parameters are valid for KCl (Harned and Owen 1958).

$(DT) = 2.3147 \times 10^4$ at 25°C

$a^0 = 3.6$ $\quad$ $b^1 = 5.20 \times 10^4$

$b^0 = 0.266$ $\quad$ $c^1 = -4.88 \times 10^4$

$c^0 = -0.0350$ $\quad$ $t = 25°C$

D = dielectric constant $\quad$ T = temperature °K

t = temperature °C

REFERENCES

Adams, M. L., Childs, C., Nilsson, N. and Powell, H. K. J. (1996). Soil pH - what is it? *New Zealand Soil News* 44, 70-74.

Ågren, A. (1955). The complex formation between iron(III) ion and some phenols, IV. The acidity constant of the phenolic group. *Acta Chimica Scandinavica* 9, 49-56.

Ahmed, M., Grant, C. D., Oades, J. M. and Tarrant, P. (1996). Aluminium, soil pH, and the non-phytotoxic disposal of water-clarification sludges (residuals) on land. *Proceedings of the ASSSI and NZSSS National Soils Conference - July 1996* 2, 3-4.

Ahuja, M., Rai, A. K. and Mathur, P. N. (1996). Adsorption behaviour of metal ions on hydroximate resins. *Talanta* 43, 1955-1963.

Al-Samawi, A. A. and Shokralla, E. M. (1996). An investigation into an indigenous natural coagulant. *Journal of Environmental Science and Health, Part A: Environmental Science & Engineering & Toxic & Hazardous Substance Control* 31, 1881-1897.

Alfredsson, H., Condron, L., Clarholm, M. and Davis, M. R. (1998). Changes in soil acidity and organic matter following the establishment of conifers on former grassland in New Zealand. *Forest Ecology and Management* 112, 245-252.

Alva, A. K., Edwards, D. G., Asher, C. J., and Blamey, F. P. C. (1986). Relationships between root length of soybean and calculated activities of aluminum monomers in nutrient solution. *Soil Science Society of America Journal* 50, 959-962.

Alva, A. K., Sumner, M. E., Li, Y. C. and Miller, W. P. (1989). Evaluation of three aluminum assay techniques for extracting aluminum complexed with fluoride or sulfate. *Soil Science Society of America Journal* 53, 38-44.

Alwarthan, A. A., Habib, K. A. J. and Townshend, A. (1990). Flow injection ion-exchange preconcentration for the determination of iron(II) with chemiluminescence detection. *Fresenius' Journal of Analytical Chemistry* 337, 848-851.

Améziane, J., Aplincourt, M., Dupont, L., Heirman, F. and Pierrard, J.-C. (1996). Thermodynamic stability of copper(II), manganese(II), zinc(II) and iron(III) complexes with chlorogenic acid. *Bulletin Societé de Chemie Francais* 133, 243-249.

Anderson, H. A., Berrow, M. L. and Farmer, V.C., Hepburn, A., Russell, J. D. and Walter, A. D. (1982). A reassessment of podzol formation processes. *Journal of Soil Science* 33, 125-136.

Asp, H., Bengtsson, B. and Jensen, P. (1988). Growth and cation uptake in spruce (*Picea abies* Karst.) grown in culture with various aluminium contents. *Plant and Soil* 111, 127-133.

Atkins, P. W. (1990). 'Physical Chemistry.' 4th edition. (Oxford University Press, Oxford.)

AWWA (American Water Works Association), (1990). Chapter 6: Coagulation processes. *In* 'Water Quality and Treatment: A Handbook of Community Water Supplies.' Pontius, F. W. (ed.), (McGraw-Hill Inc., New York.)

Backes, C. A. and Tipping, E. (1987). An evaluation of the use of cation-exchange resin for the determination of organically-complexed Al in natural acid waters. *International Journal of Environmental Analytical Chemistry* 31, 135-143.

Baes, C. F. and Mesmer, R. E. (1976). 'The hydrolysis of cations.' (John Wiley & Sons, New York.)

Baker, T. G. (1988). 'Measurement of Aluminium Toxicity in Acidic Soils.' Department of Agriculture and Rural Affairs, Technical Report series No. 150.

Barnes, R. B. (1975). The determination of specific forms of aluminum in natural water. *Chemical Geology* 15, 177-191.

Bartlett, R. and James, B. (1980). Studying dried, stored soil samples - some pitfalls. *Soil Science Society of America Journal* 44, 721-724.

Bartlett, R. J., Ross, D. S. and Magdoff, F. R. (1987). Simple kinetic fractionation of reactive aluminum in soil 'solutions'. *Soil Science Society of America Journal* 51, 1479-1482.

Beets, P. N., Payn, T. W. and Jokela, E. J. (1993). Upper mid-crown yellowing (UMCY) in *Pinus radiata* forests. *New Zealand Forestry* 38, 24-28.

Belton, M. C., O'Connor, K. F. and Robson, A. B. (1995). Phosphorus levels in topsoils under conifer plantations in Canterbury high-country grassland. *New Zealand Journal of Forestry Science* 25, 265-282.

Benes, P. and Steinnes, E. (1974). *In situ* dialysis for the determination of the state of trace elements in natural waters. *Water Research* 8, 947-953.

Benke, G., Abramson, M. and Sim, M. (1998). Exposures in the alumina and primary aluminium industry - an historical review. *Annals of Occupational Hygiene* 42, 173-189.

Berdén, M., Clarke, N., Danielsson, L.-G. and Sparen, A. (1994). Aluminium speciation: variations caused by the choice of analytical method and by sample storage. *Water, Air and Soil Pollution* 72, 213-233.

Berggren, D. (1989). Speciation of aluminium, cadmium, copper, and lead in humic soil solutions - a comparison of the ion exchange column procedure and equilibrium dialysis. *International Journal of Environmental Analytical Chemistry* 35, 1-15.

Bernhardt, H., Hoyer, O., Schell, H. and Lüsse, B. (1985). Reaction mechanisms involved in the influence of algogenic organic matter on flocculation. *Z. Wasser-Abwasser-Forsch.* 18, 18-30.

Bernhardt, H., Lüsse, B. and Hoyer, O. (1986). The addition of calcium to reduce the impairment of flocculation by algogenic organic matter. *Z. Wasser-Abwasser-Forsch.* 19, 219-228.

Berthon, G. (1996). Chemical speciation studies in relation to aluminium metabolism and toxicity. *Coordination Chemistry Reviews* 149, 241-280.

Bertsch, P. M. and Parker, D. R. (1996). Aqueous polynuclear aluminum species. *In* 'The Environmental Chemistry of Aluminum.' Sposito, G. (ed.) 2nd edition. pp. 117-168, (CRC Press, Boca Raton, Florida.)

Bilba, D., Bejan, D. and Tofan, L. (1998). Chelating sorbents in inorganic chemical analyses. *Croatica Chimica Acta* 71, 155-178.

Birchall, J. D. and Chappell, J. S. (1989). Aluminium, Alzheimer's disease and drinking water. *Lancet I* 953.

Blain, S. and Tréguer, P. (1995). Iron(II) and iron(III) determination in seawater at the nanomolar level with selective preconcentration and spectrophotometric determination. *Analytica Chemica Acta* 308, 425-432.

Blakemore, L. C., Searle, P. L. and Daly, B. K. (1987). 'Methods for Chemical Analysis of Soils.' N.Z. Soil Bureau Scientific Report 80. Department of Scientific and Industrial Research. Lower Hutt.

Bloom, P. R., Weaver, R. M. and McBride, M. B. (1978). The spectrophotometric and fluorimetric determination of aluminum with 8-hydroxyquinoline and butyl acetate extraction. *Soil Science Society of America Journal* 42, 713-716.

Bloom, P. R., McBride, M. B. and Weaver, R. M. (1979). Aluminum organic matter in acid soils: buffering and solution aluminum activity. *Soil Science Society of America Journal* 43, 488-493.

Bloom, P. R. and Erich, M. S. (1996). The quantitation of aqueous aluminium. *In* 'The Environmental Chemistry of Aluminum.' Sposito, G. (ed.) 2nd edition. pp. 1-38, (CRC Press, Boca Raton, Florida.)

Bloxham, M. J., Hill, S. J. and Worsfold, P. J. (1994). Determination of trace metals in sea-wtare and the on-line removal of matrix interferences by flow injection with inductively coupled plasma mass spectrometric detection. *Journal of Analytical Atomic Spectrometry* 9, 935-938.

Boswell, C. C. and Espie, P. R. (1998). Uptake of moisture and nutrients by *Hieracium pilosella* and effects on soil in a dry sub-humid grassland. *New Zealand Journal of Agricultural Research* 41, 251-261.

Bridgen, P. (1999). Fractionation and Amperometric Determination of Reactive Aluminium in Natural Samples. M.Sc Thesis, University of Canterbury, New Zealand.

Brown, P. L., Sylva, R. N., Batley, G. E. and Ellis, J. (1985). The hydrolysis of metal ions. Part 8. Aluminium (III). *Journal of the Chemical Society. Dalton Transcriptions* 1967-1970.

Browne, B. A., McColl, J. G. and Driscoll, C. T. (1990). Aluminum speciation using morin: I. Morin and its complexes with aluminum. *Journal of Environmental Quality* 19, 65-72.

Browne, B. A. and Driscoll, C. T. (1992). Soluble aluminum silicates: stoichiometry, stability and implications for environmental geochemistry. *Science* 256, 1667-1670.

Burba, P., Rocha, J. and Klockow, D. (1994). Labile complexes of trace metals in aquatic humic substances: Investigations by means of an ion exchange-based flow procedure. *Fresenius' Journal of Analytical Chemistry* 349, 800-807.

CAAC (Centre for Advanced Analytical Chemistry - CSIRO) (1998). Aluminium Study puts Drinking Water in the Clear. Media Release. November 2, 1998.

Cameron, R. S., Ritchie, G. S. P. and Robson, A. D. (1986). Relative toxicities of inorganic aluminium to barley. *Soil Science Society of America Journal* 50, 1231-1236.

Campanella, L., Pyrzyńska, K. and Trojanowicz, M. (1996). Chemical speciation by flow-injection analysis. A review. *Talanta* 43, 825-838.

Campbell, P. G. C., Hansen, H. J., Dubreuil, B. and Nelson, W. O. (1992). Geochemistry of Quebec North Shore salmon rivers during snowmelt: organic acid pulse and aluminum mobilization. *Canadian Journal of Fisheries and Aquatic Sciences* 49, 1938-1952.

Chappell, J. S. and Birchall, J. D. (1988). Aspects of the interaction of silicic acid with aluminium in dilute solution and its biological significance. *Inorganica Chimica Acta* 153, 1-4.

Clark, G. D., Hungerford, J. M. and Christian, G. D. (1989). Optimization of confluent mixing in flow injection analysis. *Analytical Chemistry* 61, 973-979.

Clarke, N., Danielsson, L. -G. and Sparen, A. (1992). The determination of quickly reacting aluminium in natural waters by kinetic discrimination in a flow system. *International Journal of Environmental Analytical Chemistry* 48, 77-100.

Clarke, N., Danielsson, L. -G. and Sparén, A. (1996). Analytical methodology for the determination of aluminium fractions in natural fresh waters. *Pure and Applied Chemistry* 68, 1597-1638.

Cocks, S., Linder, P. W. and Voyé, A. (1992). Potentiometric investigations of equilibria between caffeic acid and manganese(II), cobalt(II), nickel(II) and cadmium(II) ions in aqueous solution. *Journal of Coordination Chemistry* 25, 211-220.

Cohen, J. M., Rourke, G. A. and Woodward, R. L. (1958). Natural and synthetic polyelectrolytes as coagulant aids. *Journal of American Waterworks Association* 50, 463-478.

Condron, L. M., Davis, M. R., Newman, R. H. and Cornforth, I. S. (1996). Influence of conifers on the forms of phosphorus in selected New Zealand grassland soils. *Biology and Fertility of Soils* 21, 37-42.

Corain, B., Bombi, G. G., Tapparo, A., Perażzolo, M. and Zatta, P. (1996). Aluminium toxicity and metal speciation: established data and open questions. *Coordination Chemistry Reviews* 149, 11-22.

Cotton, F. A. and Wilkinson, G. (1988). 'Advanced Inorganic Chemistry.' 5th edition. (John Wiley & Sons, New York.)

Courchesne, F., Savoie, S. and Dufresne, A. (1995). Effects of air-drying on the measurement of soil pH in acidic forest soils of Quebec, Canada. *Soil Science* 160, 56-68.

Covington, A. K., Whalley, P. D. and Davison, W. (1983). Procedures for the measurement of pH in low ionic strength solutions including freshwater. *Analyst* 108, 1528-1532.

Cronan, C. S. and Schofield, C. L. (1979). Aluminum leaching response to acid precipitation: effects on high-elevation watersheds in the Northeast. *Science* 204, 304-306.

Cronan, C. S., Walker, W. J. and Bloom, P. R. (1986). Predicting aqueous aluminium concentrations in natural waters. *Nature* 324, 140-143.

Cronan, C. S. and Grigal, D. F. (1995). Use of calcium/aluminium ratios as indicators of stress in forest ecosystems. *Journal of Environmental Quality* 24, 209-226.

Curtin, D. and Smillie, G. W. (1995). Effects of incubation and pH on soil solution and exchangeable cation ratios. *Soil Science Society of America Journal* 59, 1006-1011.

Dahlgren, R. A. and Ugolini, F. C. (1989). Formation and stability of imogolite in a tephretic Spodosol, Cascade Range, Washington, U.S.A. *Geochimica et Cosmochimica Acta* 53, 1897-1904.

Dahlgren, R. A., Percival, H. J. and Parfitt, R. L. (1997). Carbon dioxide degassing effects on soil solutions collected by centrifugation. *Soil Science* 162, 648-655.

David, M. B. and Driscoll, C. T. (1984). Aluminum speciation and equilibria in soil solutions of a Haplorthod in the Adirondack mountains (New York, U.S.A.). *Geoderma* 33, 297-318.

Davis, M. R. and Lang, M. H. (1991). Increased nutrient availability in topsoils under conifers in the South Island high country. *New Zealand Journal of Forestry Science* 21, 165-179.

Davis, M. R. (1994). Topsoil properties under tussock grassland and adjoining pine forest in Otago, New Zealand. *New Zealand Journal of Agricultural Research* 37, 465-469.

Davis, M. R. (1997). Comparative nutrient responses by *Pinus radiata*, *Trifolium repens*, *Dactylis glomerata*, and *Hieracium pilosella* on a Mackenzie Basin outwash plain soil. *New Zealand Journal of Agricultural Research* 40, 9-16.

Davis, M. (1998). Soil impacts of afforestation in the high country. *N.Z. Forestry* 42, 34-38.

Davison, W. (1990). A practical guide to pH measurement in freshwaters. *Trends in Analytical Chemistry* 9, 80-83.

Davison, W. and Zhang, H. (1994). In situ speciation measurements of trace components in natural waters using thin-film gels. *Nature* 367, 546-548.

Delhaize, E. and Ryan, P. R. (1995). Aluminum toxicity and tolerance in plants. *Plant Physiology* 107, 315-321.

Derome, K., Derome, J. and Lindroos, A.-J. (1998). Techniques for preserving and determining aluminium fractions in soil solution from podzolic forest soils. *Chemosphere* 36, 1143-1148.

Dixon, E. and Gardner, M. (1998). Reactive aluminium in UK surface waters. *Chemical Speciation and Bioavailablility* 10, 11-17.

Driscoll, C. T. (1984). A procedure for the fractionation of aqueous aluminium in dilute acidic waters. *International Journal of Environmental Analytical Chemistry* 16, 267-283.

Driscoll, C. T., van Breemen, N. and Mulder, J. (1985). Aluminum chemistry in a forested spodosol. *Soil Science Society of America Journal* 49, 437-444.

Driscoll, C. T. and Postek, K. M. (1996). The chemistry of aluminum in surface waters. *In* 'The Environmental Chemistry of Aluminum.' Sposito, G. (ed.) 2nd edition. pp. 363-418, (CRC Press, Boca Raton, Florida.)

Edmeades, D. C., Smart, C. E. and Wheeler, D. M. (1983). Aluminium toxicity in New Zealand soils: preliminary results on the development of diagnostic criteria. *New Zealand Journal of Agricultural Research* 26, 493-501.

Edmeades, D. C., Wheeler, D. M. and Clinton, O. E. (1985). The chemical composition and ionic strength of soil solution from New Zealand topsoils. *Australian Journal of Soil Research* 23, 151-165.

Edmeades, D. C., Blamey, F. P. C., Asher, C. J. and Edwards, D. G. (1991). Effects of pH and aluminium on the growth of temperate pasture species I. Temperate grasses and legumes supplied with inorganic nitrogen. *Australian Journal of Agricultural Research* 42, 559-569.

Elrod, V. A., Johnson, K. S. and Coale, K. H. (1991). Determination of subnanomolar levels of iron(II) and total dissolved iron in seawater by flow injection analysis with chemiluminescence detection. *Analytical Chemistry* 63, 893-898.

Ende, H.- P. and Evers, F. H. (1997). Visual magnesium deficiency symptoms (coniferous, deciduous trees) and threshold values (foliar, soil). *In* 'Magnesium Deficiency in Forest Ecosystems'. Huttl, R. F. and Schaaf, W. (Eds.) pp 3-22, (Kluwer Academic: Dordrecht.)

Eriksson, G. (1979). An algorithm for the computation of aqueous multi-component, multiphase equilibria. *Analytica Chimica Acta* 112, 375-383.

Exley, C. and Birchall, J. D. (1992). Hydroxyaluminosilicate formation in solutions of low total aluminium concentration. *Polyhedron* 11, 1901-1907.

Fairman, B. and Sanz-Medel, A. (1996). Flow injection-mini-column technique with ICP-AES detection for the isolation and preconcentration of the fast reactive aluminium fraction in waters. *Fresenius' Journal of Analytical Chemistry* 355, 757-762.

Fang, Z.-L. (1998). Trends and potentials in flow injection on-line separation and preconcentration techniques for electrothermal atomic absorption spectrometry. *Spectrochimica Acta Part B* 53, 1371-1379.

Farmer, V. C. (1982). Significance of the presence of allophane and imogolite in podzol Bs-horizons for podzolisation mechanisms: a review. *Soil Science and Plant Nutrition* 28, 571-578.

Farmer, V. C., Adams, M. J., Fraser, A. R. and Palmieri, F. (1983). Synthetic imogolite: properties, synthesis and possible applications. *Clay Minerals* 18, 459-472.

Florence, T. M. and Batley, G. E. (1980). Chemical speciation in natural waters. *Critical Reviews in Analytical Chemistry* 9, 219-296.

Furrer, G., Trusch, B. and Müller, C. (1998). The formation of polynuclear Al_{13} under simulated natural conditions. *Geochimica et Cosmochimica Acta* 56, 3831-3838.

Ganjidoust, H., Tatsumi, K., Yamagishi, T. and Gholian, R. N. (1997). Effect of synthetic and natural coagulant on lignin removal from pulp and paper wastewater. *Water Science and Technology* 35, 291-296.

Ganrot, P.-O. (1986). Biochemistry and metabolism of Al^{3+} and similar ions. A review. *Environmental Health Perspectives* 65, 363-441.

Gans, P., Sabatini, A. and Vacca, A. (1985). SUPERQUAD: An improved general program for computation of formation constants from potentiometric data. *Journal of the Chemical Society. Dalton Transcriptions* 6, 1195-1200.

Ghosh, M. M., Cox, C. D. and Prakash, T. M. (1985). Polyelectrolyte selection for water treatment. *Journal of American Waterworks Association* 77, 67-73.

Giddens, K. M., Parfitt, R. L. and Percival, H. J. (1997). Comparison of some soil properties under *Pinus radiata* and improved pasture. *New Zealand Journal of Agricultural Research* 40, 409-416.

Grant, G. T., Morris, E. R., Rees, D. A., Smith, P. J. C. and Thom, D. (1973). Biological interactions between polysaccharides and divalent cations: the egg-box model. *Febs Letters* 32, 195-198.

Greenway, G. M., Nelms, S. M., Skhosana, I. and Dolman, S. J. L. (1996*a*). A comparison of preconcentration reagents for flow injection analysis flame atomic spectrometry. *Spectrochimica Acta Part B* 51, 1909-1915.

Greenway, G. M., Nelms, S. M. and Koller, D. (1996*b*). Application of a novel iminodiacetate chelating material to automated matrix separation for inductively coupled plasma mass spectrometry. *Analytical Communications* 33, 57-59.

Gregor, J. E., and Powell, H. K. J. (1986). Acid pyrophosphate extraction of soil fulvic acids. *Journal of Soil Science* 37, 577-585.

Gregor, J. E. (1987). Metal Organic Complexing in Soil Systems. Ph.D Thesis, University of Canterbury, New Zealand.

Gregor, J. E., Simpson, S. and Andrew, C. (1993). Institute of Environmental Health and Forensic Sciences, Health Risks of Synthetic Polymers and Monomers, and Methods of Monitorinig and Control. Confidential Client Report to Department of Health.

Gregor, J. E., Fenton, E., Brokenshire, G., Van Den Brink, P. and O'Sullivan, B. (1996). Interactions of calcium and aluminium ions with alginate. *Water Research* 30, 1319-1324.

Gu, X. and Zhou, T. (1996). Determination of iron(II) in water by a spectrophotometric method after preconcentration on an organic solvent-soluble membrane filter. *Analytical Letters* 29, 463-476.

Haff, J. D. (1978). Removal of humic acid using alum and synthetic polyelectrolytes. *Journal of American Waterworks Association* 70, 520-521.

Hassan, R. M. (1993). Alginate polyelectrolyte ionotropic gels. XIII geometrical aspects for chelation in metal alginate complexes related to their physico-chemical properties. *Polymer International* 31, 81-86.

Hawke, D. J. and Hunter, K. A. (1992). Dissolved trace metal speciation in the Manuherikia River, Central Otago, New Zealand. *Australian Journal of Marine and Freshwater Research* 43, 1381-1391.

Hawke, D. J. and Powell, H. K. J. (1994). Flow-injection analysis applied to the kinetic determination of reactive (toxic) aluminium: comparison of chromophores. *Analytica Chemica Acta* 299, 257-268.

Hawke, D. J. 'Activity, and activity coefficients.' Lecture notes. 1995.

Hawke, D. J., Powell, H. K. J. and Gregor, J. E. (1996). Determination of the aluminium complexing capacity of fulvic acids and natural waters, with examples from five New Zealand rivers. *Marine and Freshwater Research* 47, 11-17.

Hawke, M. F., and O'Connor, M. B. (1993). Soil pH and nutrient levels at Tikitere agroforestry research area. *New Zealand Journal of Forestry Science* 23, 40-48.

Heinrichs, H., Böttcher, G., Brumsack, H.-J. and Pohlman, M. (1996). Squeezed soil-pore solutes - a comparison to lysimeter samples and percolation experiments. *Water, Air and Soil Pollution* 89, 189-204.

Henshaw, J. M. and Lewis, T. E. (1988). A semi-automated colorimetric method for the determination of monomeric aluminum species in natural waters by flow injection analysis. *International Journal of Environmental Analytical Chemistry* 34, 119-135.

Hewitt, A. E. (1993). 'New Zealand Soil Classification.' Landcare Research Science Series No. 1. (Manaaki Whenua Press: Lincoln, Canterbury, N.Z.)

Hill, J. M. (1973). Silica gel as an insoluble carrier for the preparation of selective chromatographic adsorbents. The preparation of 8-hydroxyquinoline substituted silica gel for the chelation chromatography of some trace metals. *Journal of Chromatography* 76, 455-458.

Hiradate, S., Taniguchi, S. and Sakurai, K. (1998). Aluminum speciation in aluminum-silica solutions and potassium chloride extracts of acidic soils. *Soil Science Society of America Journal* 62, 630-636.

Hirayama, K., Sekine, T. and Unohara, N. (1994). Determination of trace aluminium in natural waters by ICP-AES after separation and preconcentration using Chrome Azurol S immobilized silica gel (Japanese). *Bunseki Kagaku* 43, 1065-1070.

Hodges, S. C. (1987). Aluminum speciation: a comparison of five methods. *Soil Science Society of America Journal* 51, 57-64.

Hue, N. V., Craddock, G. R. and Adams, F. (1986). Effect of organic acids on aluminum toxicity in subsoils. *Soil Science Society of America Journal* 50, 28-34.

Hunter, D. and Ross, D. S. (1991). Evidence for a phyto-toxic hydroxy-aluminum polymer in organic soil horizons. *Science* 251, 1056-1058.

Jallah, J. K. and Smyth, T. J. (1998). Assessment of rhizotoxic aluminum in soil solutions by computer and chromogenic speciation. *Communications in Soil Science and Plant Analysis* 29, 37-50.

Jang, L. K., Nguyen, D. and Geesey, G. G. (1995*a*). Selectivity of alginate gel for Cu *vs* Co. *Water Research* 29, 307-313.

Jang, L. K., Nguyen, D. and Geesey, G. G. (1995*b*). Effect of pH on the absorption of Cu(II) by alginate gel. *Water Research* 29, 315-321.

Johnson, N. M. (1979). Acid rain: neutralization within the Hubbard Brook ecosystem and regional implications. *Science* 204, 497-499.

Jones, P. and Schwedt, G. (1989). Dyestuff-coated high-performance liquid chromatographic resins for the ion-exchange and chelating-exchange separation of metal ions. *Journal of Chromatography* 482, 325-334.

Jones, D. L. and Kochian, L. V. (1996). Aluminium-organic acid interactions in acid soils - I. Effect of root-derived organic acids on the kinetics of Al dissolution. *Plant and Soil* 182, 221-228.

Kawamura, S. (1991). Effectiveness of natural polyelectrolytes in water treatment. *Journal of American Waterworks Association* 83, 88-91.

Kennedy, J. A. (1984). Metal-organic complexing in natural soil systems. Ph.D Thesis, University of Canterbury, New Zealand.

Kennedy, J. A. and Powell, H. K. J. (1985). Aluminium(III) and iron(III) 1,2 diphenolato complexes: a potentiometric study. *Australian Journal of Chemistry* 38, 659-667.

Kerven, G. L., Edwards, D. G., Asher, C. J., Hallman, P. S. and Kokot, S. (1989*a*). Aluminium determinations in soil solution. II. Short-term colorimetric procedures for the measurement of inorganic monomeric aluminium in the presence of organic acid ligands. *Australian Journal of Soil Research* 27, 91-102.

Kerven, G. L., Edwards, D. G., Asher, C. J., Hallman, P. S. and Kokot, S. (1989*b*). Aluminium determinations in soil solution. I. Evaluation of existing colorimetric and separation methods for the determination of inorganic monomeric aluminium in the presence of organic acid ligands. *Australian Journal of Soil Research* 27, 79-90.

Kimball, B. A., McKnight, D. M., Wetherbee, G. A. and Harnish, R. A. (1992). Mechanisms of iron photoreduction in a metal-rich, acidic stream (St. Kevin Gulch, Colorado, U.S.A.). *Chemical Geology* 96, 227-239.

Kinraide, T. B. (1991). Identity of the rhizotoxic aluminium species, ' *In* 'Plant-soil Interactions at Low pH.' Wright, R. J. *et al.* (eds.) pp. 717-728, (Kluwer Academic Publishers, Netherlands.)

Kiss, T., Nagy, G. and Pécsi, M. (1989). Complexes of 3,4-dihydroxyphenyl derivatives - X. Copper(II) complexes of chlorogenic acid and related compounds. *Polyhedron* 8, 2345-2349.

Kitchener, J. A. (1972). Principles of action of polymeric flocculants. *British Polymer Journal* 4, 217-229.

Kozuh, N., Milacic, R. and Gorenc, B. (1996). Comparison of two methods for speciation of aluminium in soil extracts. *Annali di Chimica* 86, 99-113.

Kozuh, N., Milacic, R., Gorenc, B., Abollino, O. and Sarzanini, C. (1997). Speciation of aluminium in environmental water samples employing microcolumn chelating ion-exchange chromatography - ETAAS. *International Journal of Environmental Analytical Chemistry* 67, 27-40.

Lalande, H. and Hendershot, W. H. (1986). Aluminum speciation in some synthetic systems: comparison of the fast-oxine, pH 5.0 extraction and dialysis methods. *Canadian Journal of Fisheries and Aquatic Sciences* 43, 231-234.

Lamy, I., Seywert, M., Cromer, M. and Scharff, J.-P. (1985). Simple and mixed ligand complexes of copper(II) with polyfunctional phenolic compounds as models of natural substances. *Analytica Chemica Acta* 176, 201-212.

Landing, W. M., Haraldsson, C. and Paxéus, N. (1986). Vinyl polymer agglomerate based transition metal cation chelating ion-exchange resin containing the 8-hydroxyquinoline functional group. *Analytical Chemistry* 58, 3031-3035.

Landing, W. M. and Westerlund, S. (1988). The solution chemistry of iron(II) in Framvaren Fjord. *Marine Chemistry* 23, 329-343.

Lawrence, G. B. and David, M. B. (1996). Chemical evaluation of soil solution in acid forest soils. *Soil Science* 161, 298-313.

Lawrence, G. B. and David, M. B. (1997). Response of aluminum solubility to elevated nitrification in soil of a red spruce stand in eastern Maine. *Environmental Science and Technology* 31, 825-830.

LaZerte, B. D. (1984). Forms of aqueous aluminum in acidified catchments of central Ontario: a methodological analysis. *Canadian Journal of Fisheries and Aquatic Science* 41, 766-776.

Letterman, R. D. and Pero, R. W. (1990). Contaminants in polyelectrolytes used in water treatment. *Journal of American Waterworks Association* November 1990, 87-97.

Leu, R.- J. and Ghosh, M. M. (1988). Polyelectrolyte characteristics and flocculation. *Journal of American Waterworks Association* 80, 159-167.

Linder, P. W. and Voyé, A. (1987). Potentiometric investigations of the equilibria between caffeic acid and copper(II), zinc(II), iron(II) and hydrogen ions in solution. *Polyhedron* 6, 53-60.

Linder, P. W., Voyé, A. and Cocks, S. (1990). The effect of caffeic acid on the speciation of metal ions in plant nutrient solutions. *In* NATO ASI Series, Volume G23, 'Metal Speciation in the Environment.' Broekaert, J. A. C., Güçer, Ş. and Adams, F. (eds.) pp. 91-104, (Springer-Verlag, Berlin Heidelberg.)

Lindsay, W. L. and Walthall, P. M. (1996). The solubility of aluminum in soils. *In* 'The Environmental Chemistry of Aluminum.' Sposito, G. (ed.), 2nd edition. pp. 363-418, (CRC Press, Boca Raton, Florida.)

Lundström, U. S. (1993). The role of organic acids in the soil solution chemistry of a podzolised soil. *Journal of Soil Science* 44, 121-131.

MacFall, J. S., Ribeiro, A. A., Cofer, G. P., Dai, K.- H. G., Labiosa, W., Faust, B. C. and Richter, D. D. (1995). Design and use of background-reduced ^{27}Al NMR probes for the study of dilute samples from the environment. *Applied Spectroscopy* 49, 156-162.

Mahmoud, M. E. (1996). Comparison of metal uptake properties of silica gel-bound ion exchangers and some amine derivatives. *Analytical Letters* 29, 1791-1804.

Makepeace, W., Dobson, A. T. and Scott, D. (1985). Interference phenomena due to mouse-ear and king devil hawkweed. *New Zealand Journal of Botany* 23, 79-90.

Martín-Esteban, A., Fernández, P., Pérez-Conde, C., Gutiérrez, A. and Cámara, C. (1995). On-line preconcentration of aluminium with immobilized Chromotrope 2B for the determination by flame atomic absorption spectrometry and inductively coupled plasma mass spectrometry. *Analytica Chemica Acta* 304, 121-126.

Martyn, C. N., Osmond, C., Edwardson, J. A., Barker, D. J. P., Harris, E. C. and Lacy, R. F. (1989). Geographical relationship between Alzheimer's disease and aluminium in drinking water. *Lancet I* 59-62.

McIntosh, P. D., Sinclair, A. G. and Enright, P. D. (1985). Responses of legumes to phosphorus and sulphur fertilizers on two toposequences of North Otago soils, New Zealand. *New Zealand Journal of Agricultural Research* 28, 501-515.

McIntosh, P. D. and Allen, R. B. (1993). Soil pH declines and organic carbon increases under hawkweed (*Hieracium pilosella*). *New Zealand Journal of Ecology* 17, 59-60.

McIntosh, P. D., Allen, R. B., Patterson, R., Aubrey, B. and McGimpsey, P. (1994*a*). Monitoring the effects of pastoral use on upland and high country soils in South Island, New Zealand. *Proceedings of the New Zealand Grasslands Association* 56, 233-237.

McIntosh, P. D., Allen, R. B. and Patterson, R. G. (1994*b*). Temporal changes of vegetation and soil carbon, nitrogen, and pH on seasonally dry high country, South Island, New Zealand. *The Rangeland Journal* 16, 3-15.

McIntosh, P. D., Loeseke, M. and Bechler, K. (1995). Soil changes under mouse-ear hawkweed (*Hieracium pilosella*). *New Zealand Journal of Ecology* 19, 29-34.

McIntosh, P. (1997). Nutrient changes in tussock grasslands, South Island, New Zealand. *Ambio* 26, 147-151.

McKnight, D. M., Kimball, B. A. and Bencala, K. E. (1988). Iron photoreduction and oxidation in an acidic mountain stream. *Science* 240, 637-640.

McLaren, R. G. and Cameron, K. C. (1996). 'Soil Science. Sustainable production and environmental protection.' 2nd edition. (Oxford University Press, Auckland.)

Measures, C. I., Yuan, J. and Resing, J. A. (1995). Determination of iron in seawater by flow injection analysis using in-line preconcentration and spectrophotometric detection. *Marine Chemistry* 50, 3-12.

Menzies, N. W., Bell, L. C. and Edwards, D. G. (1991). Characteristics of membrane filters in relation to aluminium studies in soil solutions and waters. *Journal of Soil Science* 42, 585-597.

Millero, F. J. and Schreiber, D. R. (1982). Use of the ion pairing model to estimate activity coefficients of the ionic components of natural waters. *American Journal of Science* 282, 1508-1540.

Miyasaka, S. C., Buta, J. G., Howell, R. K. and Foy, C. D. (1991). Mechanism of Al tolerance in snapbeans: root exudation of citric acid. *Plant Physiology* 96, 737-743.

Molina-Diaz, A., Herrador-Mariscal, J. M. and Pascual-Reguera, M. I. (1993). Determination of traces of aluminium with Chrome Azurol S by solid-phase spectrophotometry. *Talanta* 40, 1059-1066.

Molodovan, Z. and Vlãdescu, L. (1996). Preparation, characterization and sorption studies of a chrome-azurol-S-loaded anion-exchange resin. *Talanta* 43, 1573-1577.

Mookherji, S. and Floyd, M. (1991). The effect of aluminium on growth of and nitrogen fixation in vegetable soybean germplasm. *Plant and Soil* 136, 25-29.

Mortimer, D. A. (1991). Synthetic Polyelectrolytes - a review. *Polymer International* 25, 29-41.

Mulder, J., and Stein, A. (1994). The solubility of aluminium in acidic forest soils: long-term changes due to acid deposition. *Geochimica et Cosmochimica Acta* 58, 85-94.

Narayan, K. S. and V. R. (1982). Rheological properties of polysaccharide gums. *Indian Journal of Technology* 20, 333-338.

Nelms, S. M., Greenway, G. M. and Hutton, R. C. (1995). Application of multi-element time-resolved analysis to a rapid on-line matrix separation system for inductively coupled plasma mass spectrometry. *Journal of Analytical Atomic Spectrometry* 10, 929-933.

Nelms, S. M., Greenway, G. M. and Koller, D. (1996). Evaluation of controlled-pore glass immobilized iminodiacetate as a reagent for automated on-line matrix separation for inductively coupled plasma mass spectrometry. *Journal of Analytical Atomic Spectrometry* 11, 907-912.

Nelson, D. J. (1996). Aluminum complexation with nucleoside di- and triphosphates and implication in nucleoside binding proteins. *Coordination Chemistry Reviews* 149, 95-111.

New Zealand Ministry for the Environment. (1998). 'Technical design issues for a domestic emissions trading regime for greenhouse gases: a working paper.' (Ministry for the Environment: Wellington.)

Nicol, E. R. (1997). 'Common Names of Plants in New Zealand.' (Manaaki Whenua Press, Lincoln, Canterbury, New Zealand.)

Nordstrom, D. K., and May, H. M. (1989). Aqueous equilibrium data for mononuclear aluminium species. *In* 'The Environmental Chemistry of Aluminum.' G. Sposito. (ed.) pp. 29-53. (CRC Press: Boca Raton, Florida.)

Nordstrom, D. K. and May, H. M. (1996). Aqueous equilibrium data for mononuclear aluminum species. *In* 'The Environmental Chemistry of Aluminum.' Sposito, G. (ed.) 2nd edition. pp. 39-80, (CRC Press, Boca Raton, Florida.)

Northup, R. R., Yu, Z., Dahlgren, R. A. and Vogt, K. A. (1995). Polyphenol control of nitrogen release from pine litter. *Nature* 377, 227-229.

Northup, R. R., Dahlgren, R. A. and McColl, J. G. (1998). Polyphenols as regulators of plant-litter-soil interactions in northern California's pygmy forest: A positive feedback? *Biogeochemistry* 42, 189-220.

Obata, H., Karatani, H. and Nakayama, E. (1993). Automated determination of iron in seawater by chelating resin concentration and chemiluminescenece detection. *Analytical Chemistry* 65, 1524-1528.

Obata, H., Karatani, H., Matsui, M. and Nakayama, E. (1997). Fundamental studies for chemical speciation of iron in seawater with an improved analytical method. *Marine Chemistry* 56, 97-106.

O'Connor, K. F. and Harris, P. S. (1991). Biophysical and cultural factors affecting the sustainability of high country pastoral land uses. *In* 'The Proceedings of the International Conference on Sustainable Land Management, Napier, Hawke's Bay, New Zealand, 17–23 November 1991'. Henriques, P. R. (ed.) pp. 304-313, (Hawke's Bay Regional Council: Napier, New Zealand.)

Öhman, L.-O. and Edlund, U. (1996) Aluminium-27 NMR of solutions. *In* 'Encyclopedia of NMR.' Grant, D. M. and Harris, R. K. (eds.) pp. 742-751, (John Wiley & Sons, New York.)

Öhman, L.- O. and Sjöberg, S. (1996). The experimental determination of thermodynamic properties for aqueous aluminium complexes. *Coordination Chemistry Reviews* 149, 33-57.

Olsen, R. A., Brown, J. C., Bennett, J. H. and Blume, D. (1982). Reduction of Fe^{3+} as it relates to Fe chlorosis. *Journal of Plant Nutrition* 5, 433-445.

O'Sullivan, B. (1997). Electroanalysis of Aluminium. Ph.D Thesis, University of Canterbury, New Zealand.

Palmer, D. A. and Wesolowski, D. J. (1992). Aluminium speciation and equilibria in aqueous solutions: II. The solubility of gibbsite in acidic sodium chloride solutions from 30 to 70°C. *Geochimica et Cosmochimica Acta* 56, 1093-1111.

Parfitt, R. L., Percival, H. J., Dahlgren, R. A. and Hill, F. F. (1997). Soil and solution chemistry under pasture and radiata pine in New Zealand. *Plant and Soil* 191, 279-290.

Parker, D. R., Kinraide, T. B. and Zelazny, L. W. (1988). Aluminum speciation and phytotoxicity in dilute hydroxy-aluminum solutions. *Soil Science Society of America Journal* 52, 438-444.

Parker, D. R., Kinraide, T. B. and Zelazny, L. W. (1989). On the phytotoxicity of polynuclear hydroxy-aluminum complexes. *Soil Science Society of America Journal* 53, 789-796.

Pehkonen, S. (1995). Determination of the oxidation states of iron in natural waters. A review. *Analyst* 120, 2655-2663.

Percival, H. J., Giddens, K. M., Lee, R. and Whitton, J. S. (1996). Relationships between soil solution aluminium and extractable aluminium in some moderately acid New Zealand soils. *Australian Journal of Soil Research* 34, 769-779.

Persaud, G. and Cantwell, F. F. (1992). Determination of free magnesium ion concentration in aqueous solution using 8-hydroxyquinoline immobilized on a nonpolar adsorbent. *Analytical Chemistry* 64, 89-94.

Pesavento, M., Profumo, A., Riolo, C. and Soldi, T. (1989). Separation of trace amounts of aluminium on a strong anion-exchange resin loaded with a sulphonated azo dye. *Analyst* 114, 623-626.

Pesavento, M., Alberti, G. and Biesuz, R. (1998*a*). Investigation of the speciation of aluminium in drinking waters by sorption on a strong anionic-exchange resin AG1X8. *Analytica Chemica Acta* 367, 215-222.

Pesavento, M., Biesuz, R. and Palet, C. (1998*b*). Study of aluminium speciation in freshwaters by sorption on a chelating resin. *Analyst* 123, 1295-1301.

Pettit, L. (1984). Critical survey of formation constants of complexes of histidine, phenylalanine, tyrosine, L-dopa and tryptophan. *Pure & Applied Chemistry* 56, 247-292.

Pettit, L. D. and Powell, H. K. J. (1997). 'SC-Database: Stability Constant Database.' IUPAC. (Academic Software, Oxford.)

Poléo, A. B. S., Lydersen, E., Rosseland, B. O., Kroglund, F., Salbu, B., Vogt, R. and Kvellstad, A. (1994). Increased mortality of fish due to changing Al-chemistry of mixing zones between limed streams and acidic tributaries. *Water, Air and Soil Pollution* 75, 339-351.

Poléo, A. B. S., Østbye, K., Øxnevad, S. A., Andersen, R. A., Heibo, E., and Vøllestad, L. A. (1997). Toxicity of acid aluminium-rich water to seven freshwater fish species: a comparative laboratory study. *Environmental Pollution* 96, 129-139.

Pouchert, C. J. and Behnke, J. (eds.) (1993). 'The Aldrich Library of 13C and 1H FT NMR Spectra.' (Aldrich Chemical Company, Milwaukee.)

Powell, H. K. J. and Hawke, D. J. (1995). Free aluminium and aluminium complexation capacity of natural organic matter in acidic forest soil solutions from Canterbury, New Zealand. *Australian Journal of Soil Research* 33, 611-620.

Powell, A. K. and Heath, S. L. (1996). X-ray structural analysis of biologically relevant aluminium(III) complexes. *Coordination Chemistry Reviews* 149, 59-80.

Powell, H. K. J., Hawke, D. J. and Scott, D. (1997). Free aluminium and related parameters in soil solution from a South Island (New Zealand) high country site under contrasting S and P fertilisation. *Australian Journal of Soil Research* 35, 175-181.

Powell, K. J. (1998). Application of flow injection analysis adsorption-elution protocols for aluminium fractionation. *Analyst* 123, 797-802.

Quintela, J., Gallego, M. and Valcarcel, M. (1993). Flow injection spectrophotometric method for the speciation of aluminium in river and tap waters. *Analyst* 118, 1199-1203.

Rajwanshi, P., Singh, V., Gupta, M. K., Kumari, V., Shrivastav, R., Ramanamurthy, M. and Dass, S. (1997). Studies on aluminium leaching from cookware in tea and coffee and estimation of aluminium content in toothpaste, baking powder and paan masala. *Science of the Total Environment* 193, 243-249.

Rao, C. R. M. (1995). Selective preconcentration of gallium using Muromac A-1 ion exchange column. *Analytica Chemica Acta* 318, 113-116.

Reuss, J. O. and Johnson, D. W. (1985). Effect of soil processes on the acidification of water by acid deposition. *Journal of Environmental Quality* 14, 26-31.

Reynolds, B. (1984). A simple method for the extraction of soil solution by high speed centrifugation. *Plant and Soil* 78, 437-440.

Richter, P. and Toral, M. I. (1996). Flow injection with an integrated retention/photometric detection unit for the determination of iron in water. *Microchemical Journal* 53, 413-419.

Römheld, V. and Marschner, H. (1983). Mechanism of iron uptake by peanut plants. I. Fe^{III} reduction, chelate splitting and release of phenolics. *Plant Physiology* 71, 949-954.

Ross, D. S. and Bartlett, R. J. (1990). Effects of extraction methods and sample storage on properties of solutions obtained from forested Spodosols. *Journal of Environmental Quality* 19, 108-113.

Rosseland, B. O., Eldhuset, T. D. and Staurnes, M. (1990). Environmental effects of aluminium. *Environmental Geochemistry and Health* 12, 17-27.

Rosseland, B. O., Blakar, I. A., Bulger, A., Kroglund, F., Kvellstad, A., Lydersen, E., Oughten, D. H., Salbu, B., Staurnes, M. and Vogt, R. (1992). The mixing zone between limed and acidic river waters: complex aluminium chemistry and extreme toxicity for salmonids. *Environmental Pollution* 78, 3-8.

Røyset (1986). Flow-injection spectrophotometric determination of aluminium in water with pyrocatechol violet. *Analytica Chemica Acta* 185, 75-81.

Russell, J. M. R. (1977). A thermodynamic study of transition metal oxime complexes. Ph.D Thesis, University of Canterbury, New Zealand.

Russell, E. J. (1988). 'Russell's soil conditions and plant growth.' 11th edition. (Longman Scientific and Technical, Harlow, England.)

Ruth, A., Johnson, J. J. and Fowler, T. J. (1998). Geomorphic controls on aluminium in acid soils of the Axe Creek catchment, Victoria. *Australian Journal of Soil Research* 36, 951-962.

Saxena, R., Singh, A. K. and Sambi, S. S. (1994). Synthesis of a chelating polymer matrix by immobilizing Alizarin Red-S on Amberlite XAD-2 and its application to the preconcentration of lead(II), cadmium(II), zinc(II) and nickel(II). *Analytica Chemica Acta* 295, 199-204.

Schulze, E.- D. (1989) Air pollution and forest decline in spruce (*Picea abies*) forest. *Science* 244, 776-783.

Scott, D. (1993). Response of *Hieracium* in two long term manipulative agricultural trials. *New Zealand Journal of Ecology* 17, 41-46.

Sedlak, D. L., Hoigné, J., David, M. M., Colville, R. N., Seyffer, E., Acker, K., Wiepercht, W., Lind, J. A. and Fuzzi, S. (1997). The cloudwater chemistry of iron and copper at Great Dun Fell, U.K. *Atmospheric Environment* 31, 2515-2526.

Shann, J. R. and Bertsch, P. M. (1993). Differential cultivar responses to polynuclear hydroxo-aluminum complexes. *Soil Science Society of America Journal* 57, 166-120.

Simpson, S. L., Powell, H. K. J. and Nilsson, N. H. S. (1997). Flow injection determination of Al^{3+} and $Al_{13}(OH)_{24}(H2O)_{12}^{7+}$ species using a 1.3-s reaction with 8-quinolinol-derivatised Fractogel. *Analytica Chemica Acta* 343, 19-32.

Singh, A. K. and Dhingra, S. K. (1992). Application of Dowex-2 loaded with sulfonephthalein dyes to the preconcentration of copper(II) and cadmium(II). *Analyst* 117, 889-891.

Steginsky, C. A., Beale, J. M., Floss, H. G. and Mayer, R. M. (1992). Structural determination of alginic acid and the effects of calcium binding as determined by high-field n.m.r. *Carbohydrate Research* 225, 11-26.

Stumm, W. and Morgan, J. J. (1981). 'Aquatic Chemistry.' 2nd Edition. (J. Wiley and Sons: New York.)

Stumm, W. and Sulzberger, B. (1992). The cycling of iron in natural environments: Considerations based on laboratory studies of heterogeneous redox processes. *Geochimica et Cosmochimica Acta* 56, 3233-3257.

Suarez, D. L. (1987). Prediction of pH errors in soil-water extractors due to degassing. *Soil Science Society of America Journal* 51, 64-67.

Sullivan, T. J. and Seip, H. M. (1986). A comparison of frequently used methods for the determination of aqueous aluminum. *International Journal of Environmental Analytical Chemistry* 26, 61-75.

Sulzberger, B., Schnoor, J. L., Giovanoli, R., Hering, J. G. and Zobrist, J. (1990). Biogeochemistry of iron in an acidic lake. *Aquatic Sciences* 52, 56-74.

Sumner, M. E. (1994). Measurement of soil pH: problems and solutions. *Communications in Soil and Plant Analysis* 25, 859-879.

Suzuki, Y., Kuma, K., Kudo, I., Hasebe, K. and Matsunaga, K. (1992). Existence of stable Fe(II) complex in oxic river water and its determination. *Water Research* 26, 1421-1424.

Takahashi, T., Fukuoka, T. and Dahlgren, R. A. (1995). Aluminum solubility and release rates from soil horizons dominated by aluminum-humus complexes. *Soil Science and Plant Nutrition* 41, 119-131.

Taylor, D. B., Kingston, H. M., Nogay, D. J., Koller, D. and Hutton, R. (1996). On-line solid-phase chelation for the determination of eight metals in environmental waters by inductively coupled plasma mass spectrometry. *Journal of Analytical Atomic Spectrometry* 11, 187-191.

Timberlake, C. F. (1959). Complex formation between copper and some organic acids, phenols and phenolic acids occurring in fruit. *Journal of the Chemical Society* 2795-2798.

Truman, R. A., Humphreys, F. R. and Ryan, P. J. (1986). Effect of varying solution ratios of Al to Ca and Mg on the uptake of phosphorus by *Pinus radiata*. *Plant and Soil* 96, 109-123.

van Miegroet, H. (1995). Inorganic nitrogen determined by laboratory and field extractions of two forest soils. *Soil Science Society of America Journal* 59, 549-553.

Vance, G. F., Stevenson, F. J. and Sikora, F. J. (1996). Environmental chemistry of aluminum-organic complexes. *In* 'The Environmental Chemistry of Aluminum.' Sposito, G. (ed.) 2nd edition. pp. 169-220, (CRC Press, Boca Raton, Florida.)

Verbost, P. M., Berntssen, M. H. G., Krogland, F., Lydersen, E., Witters, H. E., Rosseland, B. O., Salbu, B. and Bonga, S. E. W. (1995). The toxic mixing zone of neutral and acidic river water - acute aluminium toxicity in brown trout (*Salmo trutta* L). *Water, Air and Soil Pollution* 85, 341-346.

Voelker, B. M. and Sulzberger, B. (1996). Effects of fulvic acid on Fe(II) oxidation by hydrogen peroxide. *Environmental Science & Technology* 30, 1106-1114.

Vogel, A. I. (1961). 'A Textbook of Quantitative Inorganic Analyses including Elementary Instrumental Analysis.' 3rd edition. (Longmans, London.)

Wagatsuma, T. and Kaneko, M. (1987). High toxicity of hydroxy-aluminum polymer ions to plant roots. *Soil Science and Plant Nutrition* 33, 57-67.

Waite, T. D., Szymczak, R., Espey, Q. I. and Furnas, M. J. (1995). Diel variations in iron speciation in northern Australian shelf waters. *Marine Chemistry* 50, 79-91.

Walker, W.J., Cronan, C.S. and Bloom, P.R. (1990). Aluminum solubility in organic soil horizons from northern and southern forested watersheds. *Soil Science Society of America Journal* 54, 369-74.

Wang, Z.-Y., Zhang, Q.-Z., Konno, M. and Saito, S. (1991). Sol-gel transition of alginate solution by additions of various divalent cations: critical behavior of relative viscosity. *Chemical Physics Letters* 186, 463-466.

Wang, Z.-Y., Zhang, Q.-Z., Konno, M. and Saito, S. (1993). Sol-gel transition of alginate solution by the addition of various divalent cations: 13C-NMR spectroscopic study. *Biopolymers* 33, 703-711.

Wheeler, D. M., Edmeades, D. C., Christie, R. A. and Gardner, R. (1992). Effect of aluminium on the growth of 34 plant species: a summary of results obtained in low strength solution culture. *Plant and Soil* 146, 61-66.

Wilde, P. F. and Dexter, R. W. (1972). Parameters affecting the performance of polyelectrolytes as aids to water clarification. *British Polymer Journal* 4, 239-250.

Wilson, M. J. (1986). Mineral weathering processes in podzolic soils on granitic materials and their implications for surface water acidification. *Journal of the Geological Society, London* 143, 691-697.

Witters, H. E. (1998). Chemical speciation dynamics and toxicity assessment in aquatic systems. *Ecotoxicology and Environmental Safety* 41, 90-95.

Wolt, J. D. (1994). 'Soil Solution Chemistry: Applications to Environmental Science and Agriculture.' (John Wiley & Sons, New York.)

Wright, R. J. and Wright, S. F. (1987). Effects of aluminum and calcium on the growth of subterranean clover in Appalachian soils. *Soil Science* 143, 341-348.

Yeates, G. W. and Saggar, S. (1998). Comparison of soil microbial properties and fauna under tussock-grassland and pine plantation. *Journal of the Royal Society of New Zealand* 28, 523-535.

Yuchi, A., Sato, T., Morimoto, Y., Mizuno, H. and Wada, H. (1997). Adsorption mechanism of trivalent metal ions on chelating resins containing iminodiacetate acid groups with reference to selectivity. *Analytical Chemistry* 69, 2941-2944.

Zabowski, D. and Sletten, R. S. (1991). Carbon dioxide degassing effects on the pH of Spodosol soil solutions. *Soil Science Society of America Journal* 55, 1456-1461.

Zhang, H. and Davison, W. (1995). Performance characteristics of diffusion gradients in thin films for the in situ measurement of trace metals in aqueous solution. *Analytical Chemistry* 67, 3391-3400.

Zuo, Y. (1995). Kinetics of photochemical/chemical cycling of iron coupled with organic substances in cloud and fog droplets. *Geochimica et Cosmochimica Acta* 59, 3123-3130.